# Radiocarbon

An International Journal of Cosmogenic Isotope Research

VOLUME 42 / NUMBER 3 / 2000

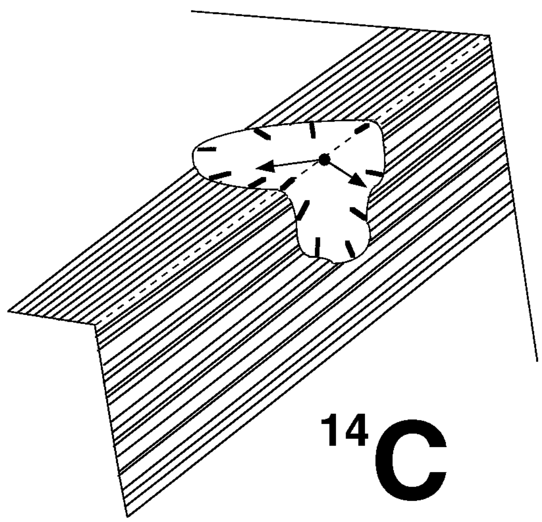


**Varve/Comparison Issue**



Department of Geosciences
The University of Arizona
4717 East Fort Lowell Road
Tucson, Arizona 85712-1201 USA

ISSN: 0033-8222

**RADIOCARBON**
An International Journal of Cosmogenic Isotope Research



Published by
Department of Geosciences
The University of Arizona

Published three times a year at The University of Arizona, Tucson, AZ 85712-1201 USA.



*Subscription rates* (2001): $150.00 (for institutions), $80.00 (for individuals). Foreign postage is $10. All subscriptions now include free access to our online journal at http://www.catchword.com/titles/00338222.htm. A complete price list, including proceedings of international conferences, special publications, and back issues, appears on the inside back cover of this issue. Advertising rates are also listed at the back of this issue and on our website at http://www.radiocarbon.org/adrates.html.

*Missing issues* will be replaced without charge only if a claim is made within three months (six months for India, New Zealand and Australia) after the publication date. Claims for missing issues will not be honored if non-delivery results from failure by the subscriber to notify the Journal of an address change.

*Authors:* See our "Information for Authors" document at http://www.radiocarbon.org/Authors/ for guidelines concerning manuscript submission and format. All correspondence and manuscripts should be addressed to the Managing Editor, *RADIOCARBON*, Department of Geosciences, The University of Arizona, 4717 East Fort Lowell Road, Tucson, AZ 85712-1201 USA. Tel.: +1 520 881-0857; Fax: +1 520 881-0554; Internet: editor@radiocarbon.org.

*List of laboratories*. Our comprehensive list of laboratories is published annually, and is also available on the WWW at http://www.radiocarbon.org/Info/lablist.html. We ask all laboratory directors to provide their laboratory code designation, as well as current telephone and fax numbers, and e-mail addresses. Changes in names or addresses, additions or deletions should be reported to the Managing Editor. Conventional and AMS laboratories are now arranged in alphabetical order by country, and we include laboratories listed by code designation.

*RADIOCARBON* on the World Wide Web: http://www.radiocarbon.org/

*RADIOCARBON* is indexed and/or abstracted by the following sources: *Anthropological Index; Anthropological Literature; Art and Archaeology Technical Abstracts; Bibliography and Index of Geology* (GeoRef); *British Archaeological Bibliography; Chemical Abstracts; Chemistry Citation Index; Current Advances in Ecological and Environmental Sciences; Current Contents* (ISI); FRANCIS (Institut de l'Information Scientifique et Technique – CNRS); *Geographical Abstracts; Geological Abstracts; Oceanographic Literature Review; Science Citation Index; Social Sciences Citation Index*.

14C **RADIOCARBON**

*An International Journal of Cosmogenic Isotope Research*

The University of Arizona
Department of Geosciences
4717 E. Fort Lowell Rd, Rm. 104
Tucson, AZ 85712-1201 USA

Phone +1 520 881-0857
Fax: +1 520 881-0554

E-mail: orders@radiocarbon.org
http://www.radiocarbon.org/

# 2001 PRICE LIST*

| | |
|---|---|
| **Proceedings of the 16th International Radiocarbon Conference** (Vol 40, Nrs 1 and 2, 1998) | $50.00 |
| **INTCAL98** (1998 Calibration issue; Vol 40, Nr 3, 1998) | 40.00 |
| **Proceedings of the 15th International Radiocarbon Conference** (Vol 37, Nr 2, 1995) | 50.00 |
| **Liquid Scintillation Spectrometry 1994** (ISBN: 0-9638314-3-7; 1996) | 20.00 |
| **Liquid Scintillation Spectrometry 1992** (ISBN: 0-9638314-0-2; 1993) (ISBN: 0-9638314-0-2; 1993) | 10.00 |
| *Special offer*—**LSC 92** and **LSC 94** package—save $5.00 | 25.00 |
| **Late Quaternary Chronology and Paleoclimates of the Eastern Mediterranean** (ISBN: 0-9638314-1-0; 1994) | 30.00 |
| **Tree Rings, Environment and Humanity** (ISBN 0-9638314-2-9; 1996) (Proceedings of the International Tree-Ring Conference, Tucson, Arizona, 1994) | 20.00 |

**SUBSCRIPTION RATES VOLUME 43, Nrs 1–3, 2001** *Now with free online access!*

| | |
|---|---|
| **Institution** | **150.00** |
| **Individual** | **80.00** |
| Lifetime Subscription—Institutional | 2500.00 |
| Lifetime Subscription—Individual | 1000.00 |

**BACK ISSUES** (except conference proceedings and special issues) — Single issue 40.00

| | | |
|---|---|---|
| VOLUMES 1–9 | each volume | 40.00 |
| VOLUMES 10–21 | each volume | 65.00 |
| VOLUMES 22–41 | each volume | 100.00 |
| Radiocarbon Conference Proceedings | | 50.00 |

**SPECIAL FULL-SET OFFER—Volumes 1–42 (1959–2000)** 1000.00

Big savings. Includes 11 out-of-print issues. Take $50.00 off for each additional set.

**POSTAGE AND HANDLING CHART**

| | U.S. | Foreign |
|---|---|---|
| Subscription | -- | $10.00 |
| Book or Proceedings | $2.75 | $5.00 |
| Single back issue | $1.25 | $2.00 |
| Full set | $65.00 | $100.00 |

Postage rates are for surface mail. Please contact us for airmail or express delivery rates.

Orders must be prepaid. We accept payments by Visa and MasterCard, or by check or money order payable in $US to *Radiocarbon*.

*Postage will be added; see above chart. Subscription rates and book prices are subject to change.

Online access via CatchWord, Ltd. See http://www.catchword.com/titles/00338222.htm.

Vol 42, Nr 3 **Radiocarbon** 2000

## CONTENTS

## EDITORIAL BOARD

RADIOCARBON, Vol 42, Nr 3, 2000, p 313–322 

# INTRODUCTION

## THE 2000 RADIOCARBON VARVE/COMPARISON ISSUE

Johannes van der Plicht, guest editor

Centre for Isotope Research, Radiocarbon Laboratory, Groningen University, Nijenborgh 4, 9747 AG Groningen, the Netherlands. Email: plicht@phys.rug.nl.

*For radiocarbon calibration, the arrow of time is pointing backwards but the entropy does not necessarily decrease in this direction…*

At the 16th International Radiocarbon Conference in Groningen, June 1997, it was decided to publish the 3rd calibration issue (Stuiver and van der Plicht, editors 1998). Upon amending and extending previous calibration issues (Stuiver and Kra 1986; Stuiver et al. 1993), a new and recommended calibration curve INTCAL98 has been constructed (Stuiver et al. 1998).

Calibration is the conversion of radiocarbon ages (BP) into historical ages (cal BC, cal AD, or cal BP). The $^{14}$C content of the atmosphere is not a natural constant throughout the ages, but depends on factors such as geomagnetic field intensity and solar fluctuations (directly influencing the cosmic ray flux and thus the $^{14}$C production rate in the atmosphere), and carbon reservoir reorganizations (mainly $CO_2$ exchange ocean/atmosphere) (Bard 1998). Past atmospheric $^{14}$C fluctuations are known by measuring the $^{14}$C content of samples which are dated by other means, i.e. independent of $^{14}$C, and preferably absolute.

The INTCAL98 calibration curve is based on the following such records:

**a**). tree rings measured by both $^{14}$C and dendrochronology (absolute);
**b**). tree rings measured by both $^{14}$C and dendrochronology (floating);
**c**). corals dated by both $^{14}$C and U-series decay;
**d**). high resolution marine varves dated by $^{14}$C.

The following remarks can be made concerning the selection of these records:

**Ad a**). Strictly speaking, only this part is a true calibration curve since dendrochronology is the only dating method which is absolute. This part of the calibration curve is the product of high-resolution $^{14}$C measurements on mainly German Oak, Irish Oak, US Bristlecone and US Douglas Fir. These measurements have been performed during the last decennia by several laboratories (Belfast, Heidelberg, Pretoria, Seattle, Tucson, and Groningen), using high precision conventional dating and mutual cross-checking. The absolute tree ring chronology yields a calibration curve, now reaching back to 8329 cal BC (Kromer and Spurk 1998; Stuiver et al. 1998).

**Ad b**). A 1900-yr-long floating chronology for German pine trees is matched (using the $^{14}$C measurements) to the absolute tree ring chronology, extending the calibration record back to 9908 cal BC (Kromer and Spurk 1998). The uncertainty of the match is about 20 calendar years.

**Ad c**). For the Late Glacial and Deglaciation periods, beyond the tree-ring limit, corals are used for calibration purposes. The record consists of paired measurements $^{14}$C vs. U-series dating (Bard et al. 1998; Burr et al. 1998). This record extends the INTCAL98 calibration curve back to 15,585 cal BP. Contrary to tree rings which are atmospheric, the coral record is marine so the calibration curve beyond the tree ring limit is “marine derived”.

One has to be aware of the following constraints using these data:

1. Concerning $^{14}$C dating: Because the coral part of the curve is marine, there is a "reservoir effect" correction. For INTCAL98, this reservoir age is taken as 400 and 500 yr for times younger and older than 10,000 cal BP, respectively. These are very reasonable numbers, but it remains an assumption. Furthermore, reservoir ages are now known to be significantly larger during Late Glacial and Glacial times, at least in the Southwest Pacific (Sikes et al. 2000). As another additional possible complication, rapid atmospheric $^{14}$C fluctuations are damped by the ocean.
2. Concerning U/Th dating: the U-series dates are a result of a measurement, which is different from dendrochronology which is simply based on tree-ring counting. The measurements are considered reliable and understood, but are by definition not absolute.

**Ad d**). $^{14}$C measurements for material from laminated sediments (varves) yield floating chronologies, which have to be matched to the calibration curve. Such measurements from the Cariaco basin (Hughen et al. 1998a, 1998b), as an exception to the rule, are included in INTCAL98 because it did strengthen the tree-ring/coral link considerably. The assumptions here are again 1) the marine reservoir correction for $^{14}$C, and 2) the accuracy of varve counting.

All together, INTCAL98 was and is the calibration curve recommended for general use until further notice, taking the above mentioned constraints into account. The INTCAL98 curve covers the time from the present back to 13,635 cal BC (15,585 cal BP). Back to 24,000 cal BP there are more paired $^{14}$C/U-series datapoints from the corals available (Bard et al. 1998). Also, the coral record includes two datapoints at around 30,000 and 40,000 cal BP. This resolution, however, is too low in order to call the part beyond 15,585 cal BP a "calibration curve". In addition, there are conflicting records for this time range (as discussed below and in several papers of the present issue).

Calibration information is based on paired measurements of $^{14}$C versus another independent dating method. Apart from the tree rings and corals which form the basic dataset for INTCAL98, there are several other dating methods which can be compared with $^{14}$C, and which are not included in INTCAL98 for a variety of reasons discussed below. We can make the following inventory:

**a**). Laminated ("varved") sediments which contain $^{14}$C datable material
**b**). Speleothems dated by both $^{14}$C and U-decay series
**c**). Radiocarbon versus Thermoluminescence (TL)
**d**). Radiocarbon versus $^{40,39}$Ar isotope dating, ESR, OSL, AAR
**e**). Isolated (Late Glacial) floating trees measured by $^{14}$C
**f**). Reconstructions, i.e. not the comparison $^{14}$C versus another dating measurement but versus a reconstructed timescale.

These records have not been included in INTCAL98. The reason is—in general—conflicts between records which are not (yet) resolved. Several "calibration curves" could be constructed, differing up to many millennia during Glacial times. Nevertheless there is a wealth of important information on $^{14}$C variations in the past available in these records, several now covering the complete $^{14}$C dating range. Therefore it was decided to dedicate a special issue of the Radiocarbon Journal to these datasets (Stuiver and van der Plicht 1998).

The following remarks can be made concerning these datasets:

**Ad a**). *Varved records.* Laminated sediments yielding varve chronologies are only absolute when they extend to the present and when the laminations are truly annual. But all varve chronologies are floating and thus have to be matched to the calibration curve; counting of laminations is quite often problematic. Revisions had to be made quite often in the past (see e.g. Wohlfarth 1996). Annual layer identification can be a personal affair, and there can be hiatuses in the sediment. Individual chronologies are not internally checked like tree rings, where missing or double rings can be identified by cross-dating. In addition, reservoir effects have to be reconciled for marine or lacustrine sediments.

**Ad b**). *Speleothems.* Calibration work based on dating speleothems depends on assumptions for both methods. For $^{14}C$ there is the reservoir effect: the initial conditions of fossil carbon has to be known, and this reservoir correction is assumed constant throughout time. For U/Th, the initial $^{230}Th$ present during speleothem growth has to be known (Beck et al. 2000). Furthermore there can be periods of reduced growth (Vogel and Kronfeld 1997).

**Ad c**). *TL.* The practical use of TL for calibration purposes is limited because of the large error bars for this method. Nevertheless, for the Glacial part useful $^{14}C$/TL comparisons were made (Barbetti 1980).

**Ad d**). *Other.* These techniques have been used only incidental, and the use is limited for the same reason as TL (large errors). Only mentioned here for completeness reasons. Details concerning Electron Spin Resonance (ESR) dating, Optically Stimulated Luminescence (OSL) dating and dating by Amino Acid Racemization (AAR) are described in textbooks like Aitken 1990.

**Ad e**). *Floating trees.* Isolated trees beyond the present INTCAL98 limit (9908 cal BC) are known, and in some cases $^{14}C$ measurements are done. These data can be matched to the calibration curve (the marine derived coral part), or to a high resolution laminated sediment. This might yield information on past atmospheric $^{14}C$ levels, or on the magnitude of the marine reservoir effect. Examples are Kromer et al. (1998) using tree ring sections around 11,500 BP (Allerød) and 15,000 BP, and Miramont et al. (this issue).

**Ad f**). *Reconstructions.* $^{14}C$ "calibration curves" can be reconstructed by linking series of $^{14}C$ measurements to archives such as ice cores and pollen sequences.

Voelker et al. (1998; this issue) use $^{14}C$ and $^{18}O$ from marine sediment foraminifera. The $^{18}O$ shows D/O cycles which could be linked to the same signals in the GISP2 ice core, so that the GISP2 timescale can be used as a "calibrated timescale" for the $^{14}C$ measurements.

Sediments with a $^{14}C$ time/depth relation have been used to reconstruct "calibration curves". This can be done when (absolute) time markers are identified, like clear boundaries between pollen zones. As an example for the Late Glacial/Early Holocene, see Zbinden et al. 1989. This is not further discussed in this issue.

The records not included in INTCAL98 are brought together in this issue, except some records which have been published recently before in this journal (Geyh and Schlüchter 1998; Vogel and Kronfeld 1997) or which will be published elsewhere (Beck et al. 2000). At the Groningen Radiocarbon conference, there was the question *"to varve or not to varve"* for the construction of INTCAL98. It was decided to bring together the varve chronologies and the calibration related information from these records. Later, it was decided to expand the issue in order to include also non-varved records (as mentioned in the list above), so that a more appropriate name now is "comparison issue".

The first varve chronologies used for $^{14}C$ calibration purposes where the Swedish varves (Tauber 1970) and varves from Lake of the Clouds in Minnesota, USA (Stuiver 1970). At that time, dendrochronologically based $^{14}C$ calibration curves were limited in timescale, and the varved records gave unique information on Late Glacial atmospheric $^{14}C$ variations (Stuiver et al. 1986). The $^{14}C$ measurements were conventional, and not very detailed. After the introduction of AMS it became possible to obtain detailed varve chronologies by measuring material from individual laminations—including pollen, macrofossils, branches and insects. During the last decade, new or revised varve/$^{14}$C chronologies were obtained for Sweden/Scandinavia (Wohlfarth 1996), Holzmaar/Germany (Hajdas 1995), Soppensee/Switzerland (Hajdas 1993), Lake Gościąż/Poland (Goslar 1998) and Lake Suigetsu/Japan (Kitagawa and van der Plicht 1998a, 1998b). All these records are represented in this issue with either an overview of existing data, revisions and/or new measurements added. A new varve/$^{14}$C record from Meerfelder Maar (Germany) is presented in this issue as well.

There are no new additional data for the coral records constituting INTCAL98 (Bard et al. 1998; Burr et al. 1998). A new dataset for corals measured by both $^{14}$C and U/Th is presented by Yokoyama et al. (this issue).

Finally, a few remarks concerning terminology. First there is the mystery of the word "calibration". Calibration per definition is the conversion of a measurement (in our case, the measurement of a $^{14}$C date expressed in BP) into something absolute—truly absolute, thus actually only dendrochronology qualifies for this purpose. The end product of calibration is then a historical date (or better, a probable date range as produced by the calibration software) in cal BC or cal AD (Mook 1986). Sometimes cal BP is used, being calibrated (or calendar) years before the $^{14}$C standard year 1950 AD: cal BP = 1950 – cal AD = 1949 + cal BC. Unfortunately, this time unit is also commonly used for chronologies like ice-cores (both the ice layer counted parts and the modeled age part), for U/Th dating, varve counting, TL dating, etc. But actually this "calibrated" timescale is not truly absolute, but the result of a measurement or a match. In addition, cal BP is not well defined—for example, it is not clear whether the U-series dates are corrected for decay (using $T_{measurement}$ – 1950); and sometimes the reference year is not chosen as 1950. This is not unlike the "absolute ages aren't exactly" discussion in geochronology (Renne et al. 1998). Throughout this issue, we use BP for the $^{14}$C timescale (or ka BP, meaning thousands BP) and cal BP (or ka cal BP) for the calendar time scale.

In many plots of BP ($^{14}$C method) versus cal BP (other method) the errors or assumptions in cal BP are not shown. Such errors can be quite significant (see Figure 1). One has to be aware that this can be misleading since cal BP suggests an absolute scale. Moreover, confusion is prone to emerge when the BP/cal BP numbers are transferred into $^{14}\Delta$. Increased atmospheric $^{14}$C levels show up as peaks in $^{14}\Delta$. Such peaks can easily appear or disappear when the cal BP number is changed: excursions in $^{14}\Delta$ strongly depend on the absolute value. Since the chronologies for the Glacial period discussed in this issue differ considerably (by several millennia towards the end of the $^{14}$C time range), one has to be careful stating conclusions. For instance, in Archaeological discussions about the Upper/Middle Paleolithic chronologies, it seems that everybody is looking for a proposed synchronization between $^{14}$C and TL or other dating technique (Bar Yosef 2000; van Andel 1997). This plays a role in the Neanderthal/human interference discussion (Mellars et al. 1999).

I would also advocate more respect for the term "calibration curve". Given the fact that by the strict definition the $^{14}$C calibration curve is based on absolute dates, calibration curves cannot be different in principle. Nevertheless, very different "calibration curves" are produced—see e.g. Vogel and Kronfeld (1997), and as is apparent in this issue alone. Perhaps it is better to use the term "comparison curve".

A survey of comparison measurements other than varves, new (this issue) and old (literature survey), shows large variations—up to many millennia for the Glacial part (>≈20 ka). It is illustrative to plot paired $^{14}$C/"other method" (BP vs. cal BP) for all data available to date. For clarity, the data are divided into two figures (Figures 1a, 1b) and compared with the "equiline" (cal BP = 1950 – cal AD).

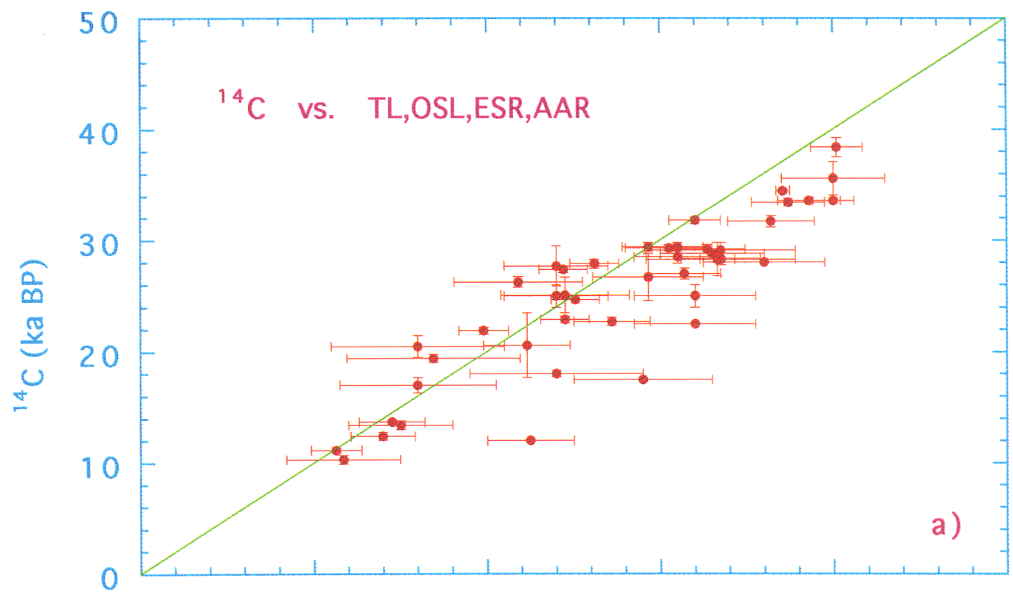


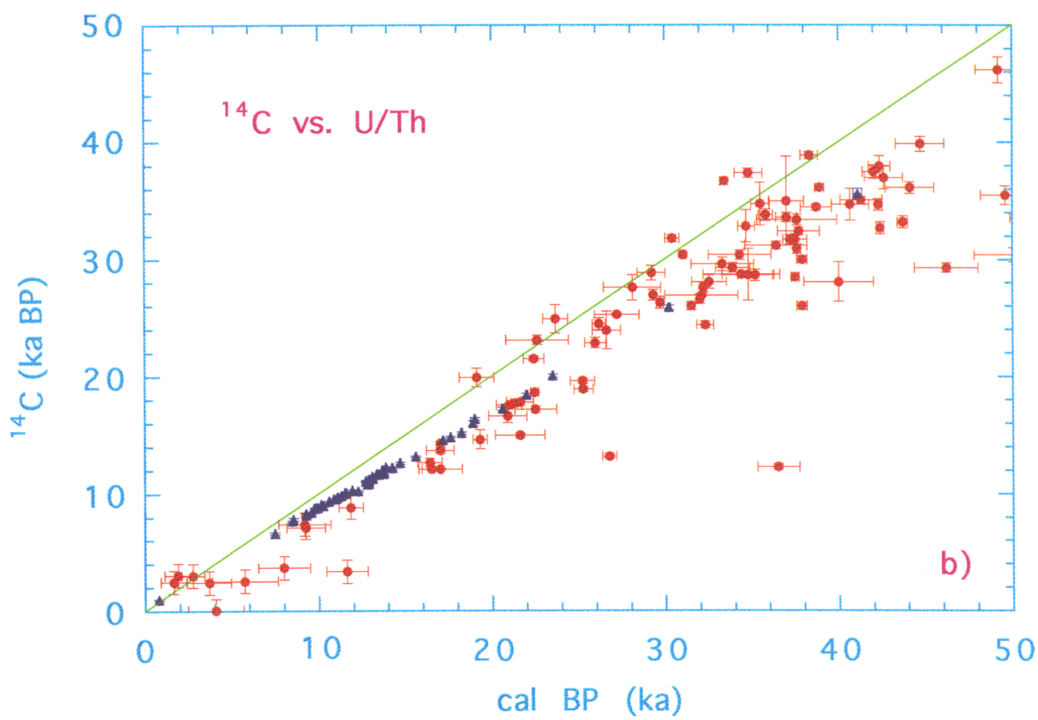


Figure 1 Compilation: comparison of $^{14}C$ versus other dating methods. a: TL, OSL, ESR, and AAR. b: U/Th dating.

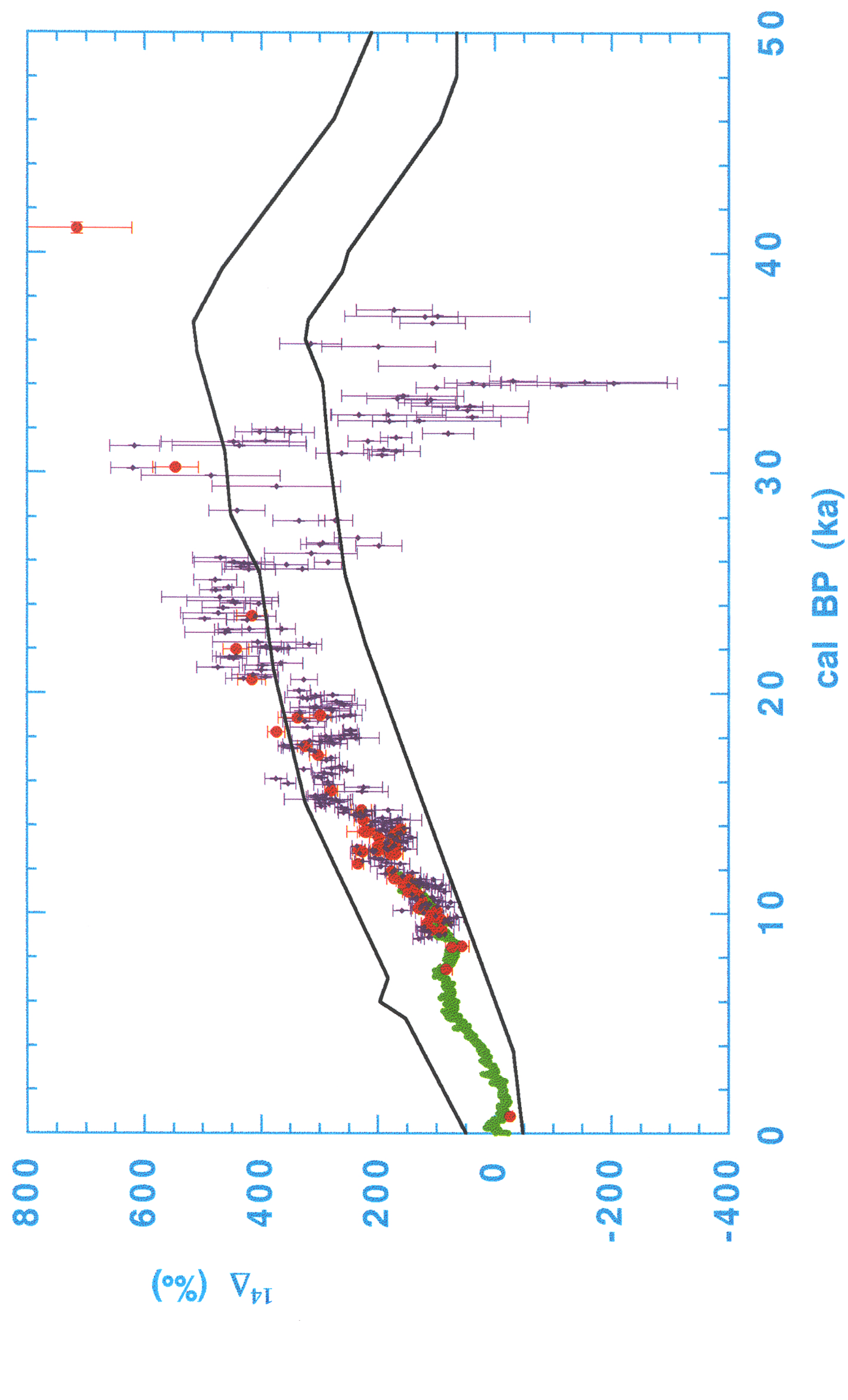


Figure 2 Atmospheric $^{14}C$ content (in $^{14}\Delta$, ‰) for the complete dating range of 50 ka, derived from paleomagnetism (Guyodo and Valet 1996; 2σ range), INTCAL98 (green, tree-ring part only), U/Th for corals (red, 1σ error) and Lake Suigetsu (purple, 1σ error).

Figure 1a shows $^{14}C$ versus (mostly) TL as published over the years in a variety of studies (Barbetti 1980; Mellars 2000; Richter et al. 2000; Huxtable and Aitken 1977; Prescott and Smith 1993; Bell 1991; Zhu et al. 1999; Readhead 1988; Roberts et al. 1990). Single datapoints for OSL (Abeyratne et al. 1997), ESR (Mellars 2000), AAR (Farrand 1994) and $^{39/40}Ar$ (Geyh and Schlüchter 1998) are shown here as well.

Figure 1b shows $^{14}C$ versus U/Th taken from: a). the literature (Bischoff et al. 1994; Chappell and Veeh 1978; Geyh and Schlüchter 1998; Holmgren et al. 1994; Lin et al. 1996; Lin et al. 1998; Lomitschka and Mangini 1999; Vogel and Kronfeld 1997), b). this issue (Goslar et al.; Stein et al.; Yokoyama et al.) and c). the "reference dataset" of coral calibration data (Bard et al. 1998). We note that in Figure 1b, measurements with quoted errors >2500 yr (1$\sigma$) are omitted. The only conclusion one can draw from this compilation is that (apart from the coral dataset) the records deviate to strongly from each other to yield anything like a "calibration/comparison curve". Clearly, the assumptions underlying each particular method (as discussed above) has to be further investigated. In any case, calibration can not be done by interpolating between a few coral datapoints (Bard et al. 1998).

Figure 2 shows a comparison plot in terms of $^{14}\Delta$. The "band" (between the two black solid lines) shows the range of atmospheric $^{14}C$ values calculated from paleomagnetic stack measurements (Guyodo and Valet 1996). Note that the two black solid lines correspond to 2$\sigma$ errors. Similar $^{14}\Delta$ yields result from calculations of cosmogenic radionuclide production, derived from stacked $^{10}Be$ deposition rates (Frank 2000). Bard (1997) discusses these cosmic trends.

A selection of calibration/comparison data is shown in Figure 2; the errors for these data are 1$\sigma$. In green, the dendrochronological part of INTCAL98 (Stuiver et al. 1998) is plotted, in red, the coral dataset of Bard et al. (1998), and in purple, the updated dataset for the Lake Suigetsu varves (Kitagawa and van der Plicht, this issue). Perhaps this figure can be regarded as the present state-of-the-art. The mean geomagnetic field intensity describes the general trend of the atmospheric $^{14}C$ variations very well. The tree rings (green), corals (red) and Japanese varves (purple) back to about 20 ka cal BP follow this trend. Going to older ages no detailed "calibration curve" conclusions can be made. In this figure only the varves from Lake Suigetsu are shown because it is the only detailed terrestrial (atmospheric) record available to date in this time range. Note that the error in cal BP (not shown) is estimated as 2000 years (Kitagawa and van der Plicht 1998a). Beyond 30 ka cal BP, fluctuations in $^{14}\Delta$ are shown in conflict with the general geomagnetic trend. The large peak at 31 ka cal BP is attributed to a magnetic excursion (Kitagawa and van der Plicht 1998a). Such excursions (known as Mono Lake and/or Laschamp; see also the discussion by Voelker et al. in this issue) have also been observed in other cosmogenic isotope records: $^{10}Be$ in the ice cores Vostok (at 35 ka, Raisbeck et al. 1987) and GRIP (at 41 ka, Yiou et al. 1997), $^{10}Be$ in marine sediments from the Mediterranean Sea (at 37 ka, Castagnoli et al. 1995), Gulf of California (at 32 ka, McHargue et al. 1995) and Caribbean Sea (at 37 ka, Aldahan and Possnert 1998), and $^{36}Cl$ in the GRIP ice core (at 38 ka, Baumgartner et al. 1998; at 32 ka, Wagner et al. 2000). Obviously there is a lot of room for discussion here concerning the "absolute" timescale cal BP, and the caution mentioned above concerning the influence of this timescale on peaks in the $^{14}\Delta$ signal is repeated here. Also new records show cosmogenic peaks, at different times and sometimes with extremely large amplitudes (Beck et al. 2000).

The work presented in this issue should be qualified as "work in progress". It is obvious that this is in particular true for the Glacial period >25 ka, where records strongly deviate from each other. What is needed is a new record, independent, terrestrial and with high resolution, to provide true atmospheric $^{14}\Delta$ values.

No recommendations can yet be made as to the use of a particular calibration (comparison) curve at this stage beyond INTCAL98. However, consensus seems to be emerging for the Deglaciation and Late Glacial parts of the $^{14}$C dating range. For example, with new data from the Cariaco basin, a 400-yr reservoir correction seems better now than the 500 used for INTCAL98 (Southon et al. 2000). This results in an excellent agreement between Cariaco and Lake Suigetsu for the Deglaciation.

We expect small revisions of INTCAL for this time period sometime in the near future. We may look forward to proposals or decisions at the next Radiocarbon conference in Wellington.

*… time flies! …*

## NOTES

1. Compiled from textbooks and encyclopedia:

*varve*: a distinctive, thin annual sedimentary layer, the lower part consisting of coarser, lighter colored clay and silt that was deposited in summer, and the upper of a finer-grained, darker clay deposited in winter. Numerous successive varves accumulated in temporary lakes near melting glaciers. Thicker and thinner varves at different places can be matched like tree rings.

Glacial melting is not the only cause of varves; in non-glacial lakes seasonal variation in accumulation of organic detritus may also give rise to annual laminations, as well as seasonal variation in sedimentation and chemical precipitation.

The word "varve" comes from Sweden—*varv* means as well a circle as a periodical iteration of layers (de Geer 1912).

2. Perhaps superfluous but useful for reasons of clarity we give here the definition of $^{14}\Delta$ (expressed in BP and cal BP)

$$^{14}\Delta = [\exp(-BP/8033)\times\exp(\text{cal } BP/8267)-1]\times 1000\ (‰)\ .$$

Note that this corresponds to $^{14}\delta^{i}_{N}$ as proposed by Mook and van der Plicht (1999).

- BP = conventional $^{14}$C age, i.e. activity measured relative to the Oxalic Acid standard and corrected for isotopic fractionation to $^{13}\delta = -25$ ‰.
- cal BP = historical date with respect to 1950 AD
- physical half-life 5730 year: $T_{1/2}/\ln 2 = 8267$
- conventional half-life 5568 year: $T_{1/2}/\ln 2 = 8033$

3. From Webster's Dictionary:

*calibrate*: to fix, check or correct the graduations of a measuring instrument.
*compare*: to examine, in order to observe or discover similarities or differences.

## REFERENCES

Abeyratne M, Spooner NA, Grün R, Head J. 1997. Multidating studies of Batadomba cave, Sri Lanka. *Quaternary Science Reviews* 16:243–55.

Aitken M. 1990. *Science based dating archaeology.* UK: Longman House.

Aldahan A, Possnert G. 1998. A high resolution $^{10}$Be profile from deep sea sediment covering the last 70 ka: indication for globally synchronized environmental events. *Quaternary Geochronology* 17:1023–32.

Barbetti M. 1980. Geomagnetic strength over the last 50,000 years and changes in atmospheric $^{14}$C concentration: emerging trends. *Radiocarbon* 22(2):192–9.

Bard E. 1997. Nuclide production by cosmic rays during the Last Ice Age. *Science* 277:532–3.

Bard E. 1998. Geochemical and geophysical implications of the radiocarbon calibration. *Geochimica et Cosmochimica Acta* 62:2025–38.

Bard E, Arnold M, Hamelin B, Tisnerat-Laborde N, Cabioch G. 1998. Radiocarbon calibration by means of mass spectrometric $^{230}$Th/$^{234}$U and $^{14}$C ages of corals: an updated database including samples from Barbados, Mururoa and Tahiti. *Radiocarbon* 40(3):1085–92.

Bar-Yosef O. 2000. The impact of radiocarbon dating on old world Archaeology: past achievements and future expectations. *Radiocarbon* 42(1):23–39.

Baumgartner S, Beer J, Masarik J, Wagner G, Meynadier L, Synal HA. 1998. Geomagnetic modulation of the $^{36}$Cl flux in the GRIP ice core. *Science* 279:1330–2.

Beck W, Richards D, Herrera S, Calsoyas L, Donahue D, Edwards L, Smart P, Burr G, Jull AJT. 2000. $^{230}$Th and $^{14}$C dating of speleothems from the Bahamas: implications for calibration of the Radiocarbon timescale to 45 ka BP. Abstract. 17th International Radiocarbon Conference, Israel. June 2000.

Bell WT. 1991. Thermoluminescence dates for the Lake Mungo Aboriginal fireplaces and the implications for radiocarbon dating. *Archaeometry* 33:43–50.

Bischoff JL, Ludwig K, Garcia JF, Carbonell E, Vaquero M, Stafford TW, Jull AJT. 1994. Dating of the basal Aurignacian sandwich at Abric Romani (Catalunya, Spain) by radiocarbon and uranium-series. *Journal of Archaeological Science* 21:541–51.

Burr GS, Beck JW, Taylor FW, Récy J, Edwards RL, Cabioch G, Corrège T, Donahue DJ, O'Malley JM. 1998. A high resolution radiocarbon calibration between 11,700 and 12,400 calendar years BP derived from $^{230}$Th ages of corals from espiritu Santo Island, Vanuatu. *Radiocarbon* 40(3):1093–105.

Castagnoli CG, Albrecht A, Beer J, Bonino G, Shen C, Callegari E, Taricco C, Ditrich-Hannen B, Kubik P, Suter M, Zhu GM. 1995. Evidence for enhanced $^{10}$Be deposition in Mediterranean sediments 35 kyr BP. *Geophysical Research Letters* 22:707–10.

Chappell J, Veeh HH. 1978. $^{230}$Th/$^{234}$U age support of an interstadial sea level of –40m at 30,000 yr BP. *Nature* 276:602–4.

de Geer G. 1912. A geochronology of the last 12,000 years. *C R 11th International Geological Congres 1910.* Stockholm. p 241–53.

Farrand WR. 1994. Confrontation of geological stratigraphy and radiometric dates from Upper Pleistocene sites in the Levant. In: Bar-Yosef O, Kra RS, editors. *Late Quaternary Chronology and Paleoclimates of the Eastern Mediterranean.* Tucson: Radiocarbon. p 33–53.

Frank M. 2000. Comparison of cosmogenic radionuclide production and geomagnetic field intensity over the last 200,000 years. *Phil. Trans. Royal Society of London* A358:1089–107.

Geyh MA, Schlüchter C. 1998. Calibration of the $^{14}$C time scale beyond 22,000 BP. *Radiocarbon* 40(1):475–82.

Goslar T. 1998. Floating varve chronology of Lake Gosciaz. In: Ralska-Jasiewiczowa M, Goslar T, Madeyska T, Starkel L, editors. *Lake Gosciaz, central Poland, a monographic study.* Polish Academy of Sciences. p 97.

Guyodo Y, Valet JP. 1996. Relative variations in geomagnetic intensity from sedimentary records: the past 200 thousand years. *Earth and Planetary Science Letters* 143:23–36.

Hajdas I, Zolitschka B, Ivy-Ochs SD, Beer J, Bonani G, Leroy SAG, Negendank JW, Ramrath M, Suter M. 1995. AMS radiocarbon dating of annually laminated sediments from lake Holzmaar, Germany. *Quaternary Science Reviews* 14:137–43.

Hajdas I, Ivy SD, Beer J, Bonani G, Imboden D, Lotter AF, Sturm M, Suter M. 1993. AMS radiocarbon dating and varve chronology of Lake Soppensee: 6000 to 12000 $^{14}$C years BP. *Climate Dynamics* 9:107–16.

Holmgren K, Lauritzen SE, Possnert G. 1994. $^{230}$Th/$^{234}$U and $^{14}$C dating of a Late Pleistocene stalagmite in Lobatse II cave, Botswana. *Quaternary Geochronology* 13:111–9.

Hughen KA, Overpeck JT, Lehman SJ, Kashgarian M, Southon J, Peterson LC, Alley R, Sigman DM. 1998a. Deglacial changes in ocean circulation from an extended radiocarbon calibration. *Nature* 391:65–8.

Hughen KA, Overpeck JT, Lehman SJ, Kashgarian M, Southon J, Peterson LC. 1998b. A new $^{14}$C calibration dataset for the Last Deglaciation based on marine varves. *Radiocarbon* 40(1):483–94.

Huxtable J, Aitken MJ. 1977. Thermoluminescent dating of Lake Mungo geomagnetic polarity excursion. *Nature* 265:40–1.

Kitagawa H, van der Plicht J. 1998a. Atmospheric radiocarbon calibration to 45,000 yr BP: Late Glacial fluctuations and cosmogenic isotope production. *Science* 279:1187–90.

Kitagawa H, van der Plicht J. 1998b. A 40,000 year varve chronology from Lake Suigetsu, Japan: extension of the $^{14}$C calibration curve. *Radiocarbon* 40(1):505–15.

Kromer B, Spurk M, Remmele S, Barbetti M, Toniello V. 1998. Segments of atmospheric $^{14}$C change as derived from Late Glacial and Early Holocene floating tree-ring series. *Radiocarbon* 40(1):351–8.

Kromer B, Spurk M. 1998. Revision and tentative extension of the tree-ring based $^{14}$C calibration, 9200–11,855 cal BP. *Radiocarbon* 40(3):1117–25.

Lin JC, Broecker WS, Anderson RF, Hemming S, Rubenstone JL, Bonani G. 1996. New $^{230}$Th/U and $^{14}$C Ages from lake Lahontan carbonates, Nevada, USA, and a discussion of the origin of initial Thorium. *Geochimica et Cosmochimica Acta* 60:2817–32.

Lin JC, Broecker WS, Hemming SR, Hajdas I, Anderson RF, Smith GI, Kelley M, Bonani G. 1998. A reassessment of U-Th and $^{14}$C ages for Late Glacial High-Frequency Hydrological Events at Searles Lake, California. *Quaternary Research* 49:11–23.

Lomitschka M, Mangini A. 1999. Precise Th/U-dating of small and heavily coated samples of deep sea corals. *Earth and Planetary Science Letters* 170:391–401.

McHargue LR, Damon PE, Donahue DJ. 1995. Enhanced cosmic-ray production of $^{10}$Be coincident with the Mono Lake and Laschamp geomagnetic excursions. *Geophysical Research Letters* 22:659–62.

Mellars P. 2000. Châtelperronian chronology and the case for the Neanderthal/modern human 'acculturation' in western europe. *Current Anthropology*. Forthcoming.

Mellars P, Otte M, Straus L, Zilhao J, D'Errico F. 1999. The Neanderthal problem, continued. CA forum on theroy in Anthropology. *Current Anthropology* 40(3):341–64.

Mook WG. 1986. Business meeting (12th International Radiocarbon Conference). *Radiocarbon* 28(2A):799.

Mook WG, van der Plicht J. 1999. Reporting $^{14}$C activities and concentrations. *Radiocarbon* 41(3):227–39.

Prescott JR, Smith MA. 1993. Comparison of thermoluminescence and $^{14}$C dates as an indicator of cosmic ray intensity variations. *Papers of the 23rd International Cosmic Ray Conference*. Calgary. p 838–41.

Raisbeck GM, Yiou F, Fruneau M, Loiseaux JM, Lieuvin M, Ravel JC, Lorius C. 1981. Cosmogenic $^{10}$Be concentrations in Antartic ice during the past 30,000 years. *Nature* 292:825–6.

Readhead ML. 1988. Thermoluminescence dating study of quartz in aeolian sediments from Southeastern Australia. *Quaternary Science Reviews* 7:257–64.

Renne PR, Karner DB, Ludwig KR. 1998. Absolute ages aren't exactly. *Science* 282:1840–1.

Richter D, Waiblinger J, Rink WJ, Wagner GA. 2000. Thermoluminescence, electron spin resonance and $^{14}$C-dating of the Late Middle and Early Upper Palaeolithic site of Geissenklösterle Cave in southern Germany. *Journal of Archaeological Science* 27:71–89.

Roberts RG, Jones R, Smith MA. 1990. Thermoluminescence dating of a 50,000 year old human occupation site in northern Australia. *Nature* 345:153–6.

Sikes EL, Samson CR, Guilderson TP, Howard WR. 2000. Old Radiocarbon ages in the southwest Pacific Ocean during the last glacial period and deglaciation. *Nature* 405:555–9.

Southon J, Hughen K, Herring C, Lehman S, Overpeck J. 2000. A detailed $^{14}$C calibration for the Bølling-Allerød-Younger Dryas. Abstract. 17th International Radiocarbon Conference, Israel. June 2000.

Spurk M, Friedrich M, Hofmann J, Remmele S, Frenzel B, Leuschner H, Kromer B. 1998. Revisions and extensions of the Hohenheim Oak and Pine chronologies: new evidence about the timing of the Younger Dryas/ Preboreal transition. *Radiocarbon* 40(3):1107–16.

Stuiver M. 1970. Long term $^{14}$C variations. In: Olsson IU, editor. Radiocarbon Variations And Absolute Chronology. Proceedings of the 12th Nobel Symposium; 1970; Uppsala University, Sweden. p 197–213.

Stuiver M, Kromer B, Becker B, Ferguson CW. 1986. Radiocarbon age calibration back to 13,300 years BP and the $^{14}$C age matching of the German Oak and US Bristlecone Pine chronologies. *Radiocarbon* 28(2B):969–79.

Stuiver M, Kra RS, editors. 1986. Calibration issue. *Radiocarbon* 28(2B):805–1030.

Stuiver M, Long A, Kra RS, editors. 1993. Calibration issue. *Radiocarbon* 35(1):1–244.

Stuiver M, van der Plicht J, editors. 1998. INTCAL98, Calibration issue. *Radiocarbon* 40(3):1041–164.

Stuiver M, Reimer PJ, Bard E, Beck JW, Burr GS, Hughen KA, Kromer B, McCormac G, van der Plicht J, Spurk M. 1998. INTCAL98 radiocarbon age calibration, 24,000–0 cal BP. *Radiocarbon* 40(3):1041–84.

Tauber H. 1970. The Scandinavian varve chronology and C14 dating. In: Olsson IU, editor. Radiocarbon variations and absolute chronology. Proceedings of the 12th Nobel Symposium; 1970; Uppsala University. p 173–96.

van Andel TH. 1998. Middle and Upper Paleolithic environments and the calibration of $^{14}$C dates beyond 10,000 BP. *Antiquity* 72:26–33.

Voelker AHL, Sarnthein M, Grootes PM, Erlenkeuser H, Laj C, Mazaud A, Nadeau MJ, Schleicher M. 1998. Correlation of marine $^{14}$C ages from the Nordic seas with the GISP2 isotope record: implications for the $^{14}$C calibration beyond 25 ka BP. *Radiocarbon* 40(1):517–34.

Vogel JC, Kronfeld J, 1997. Calibration of radiocarbon dates for the Late Pleistocene using U/Th dates on stalagmites. *Radiocarbon* 39(1):27–32.

Wagner G, Beer J, Laj C, Kissel C, Masarik J, Muscheler R, Synal HA. 2000. Chlorine-36 evidence for the Mono Lake event in the Summit GRIP ice core. *Earth and Planetary Science Letters* 181:1–6.

Wohlfarth B. 1996. The chronology of the Last Termination: a review of high-resolution terrestrial stratigraphies. *Quaternary Science Reviews* 15:267–84.

Yiou F, Raisbeck GM, Baumgartner S, Beer J, Hammer C, Johnsen S, Jouzel J, Kubik P, Lestringuez J, Stievenard M, Suter M, Yiou P. 1997. Beryllium 10 in the Greenland Ice Core Project ice core at Summit, Greenland. *Journal of Geophysical Research* 102(C12):26,783–94.

Zbinden H, Andree M, Oeschger H, Ammann B, Lotter A, Bonani G, Wölfli W. 1989. Atmospheric radiocarbon at the end of the Last Glacial: an estimate based on AMS radiocarbon dates on terrestrial macrofossils from lake sediments. *Radiocarbon* 31(3):795–804.

Zhu R, Pan Y, Liu Q. 1999. Geomagnetic excursions recorded in Chinese loess in the last 70,000 years. *Geophysical Research Letters* 26(4):505–8.

RADIOCARBON, Vol 42, Nr 3, 2000, p 323–333 

# AMS RADIOCARBON MEASUREMENTS FROM THE SWEDISH VARVED CLAYS

Barbara Wohlfarth

Department of Quaternary Geology, Lund University, Tornavägen 13, SE-22363 Lund, Sweden.
Email: Barbara.Wohlfarth@Geol.lu.se.

Göran Possnert

Ångström Laboratory, Uppsala University, Box 534, SE-75121 Uppsala, Sweden

**ABSTRACT.** The Swedish varve chronology, or Swedish Time Scale, is an annual chronology based upon the successive correlation of more than 1000 varve-thickness diagrams. The Late Glacial-Early Holocene varved clays were deposited as glaciolacustrine sediments in the Baltic Sea during the recession of the Scandinavian ice sheet. Formation of varved clays continued throughout the Holocene and is still going on in the estuary of River Ångermanälven in northern Sweden. Accelerator mass spectrometry (AMS) radiocarbon measurements, which have been performed on terrestrial plant macrofossils extracted from the varved clays, show—in comparison with other annual chronologies—that several hundreds of varve years are missing in the varve chronology. These findings are supported by, among others, pollen stratigraphic investigations on time-equivalent varve year intervals. If an effort were undertaken to evaluate the erroneous parts, the Swedish Time Scale would have the potential of becoming a continuous annual chronology.

## INTRODUCTION

Since De Geer's (1912) famous publication, where he introduced the Swedish Time Scale (STS) to an international audience and presented the first annual (varve) chronology based upon glaciolacustrine and estuarian sediments, the interest in the Swedish varved clays has varied considerably. Initially, De Geer's (1912) chronology was greatly acknowledged (see e.g. Zeuner 1950). But later, when radiocarbon dating became more and more common, several errors became obvious (Olsson 1970), which gradually led to a decreasing international interest in the STS. In Sweden, however, large efforts were undertaken to revise the varve chronology and to firmly connect it to present time (Strömberg 1983, 1985a, 1985b, 1994; Cato 1987; see e.g. also the summaries in Björck et al. 1992 and Wohlfarth et al. 1995, 1993).

In general, the STS is composed of two different types of clastic, varved sediments (see Figure 1). The older "gotiglacial" and "finiglacial" varves are glacio-lacustrine varved clays with distinct couplets of thin fine sand/silt and thicker clay layers (Wohlfarth et al. 1993, 1995). They were deposited in the Baltic basin during the retreat of the inland ice and reflect the melting of the ice during summer as well as the gradual settling of clay particles during winter, when the Baltic was ice covered. The younger postglacial varves are delta sediments, which were and still are deposited in the estuary of River Ångermanälven in northern Sweden (Cato 1987, 1998; Wohlfarth et al. 1997). They are composed of thick and fairly coarse silt or sand and thin clay, to fine silt couplets and mirror river discharge variations in spring/summer and calmer conditions during winter.

The STS is based on a visual correlation of more than 1000 successively overlapping varve-thickness diagrams, which have been established based upon varve thickness measurements in open sections (e.g., De Geer 1912, 1940; Lidén 1913; Cato 1998) or on sediment cores (e.g. Cato 1987; Ringberg 1991; Strömberg 1989, 1994; Brunnberg 1995; Wohlfarth et al. 1998a). The dense net of investigated varved clay sites in many of the local chronologies (Figure 1) facilitates the correlation between single varve diagrams and provides several replicate time series. Therefore, if varves are missing or disturbed due to local processes at one site, the problematic time interval can easily be covered by varve measurements at a neighboring locality (see e.g. Figure 2). The same holds true for erroneous measurements due to an over- or underestimation of varves, although this is a rarely encountered problem because the boundaries between summer and winter layers are very distinct. In

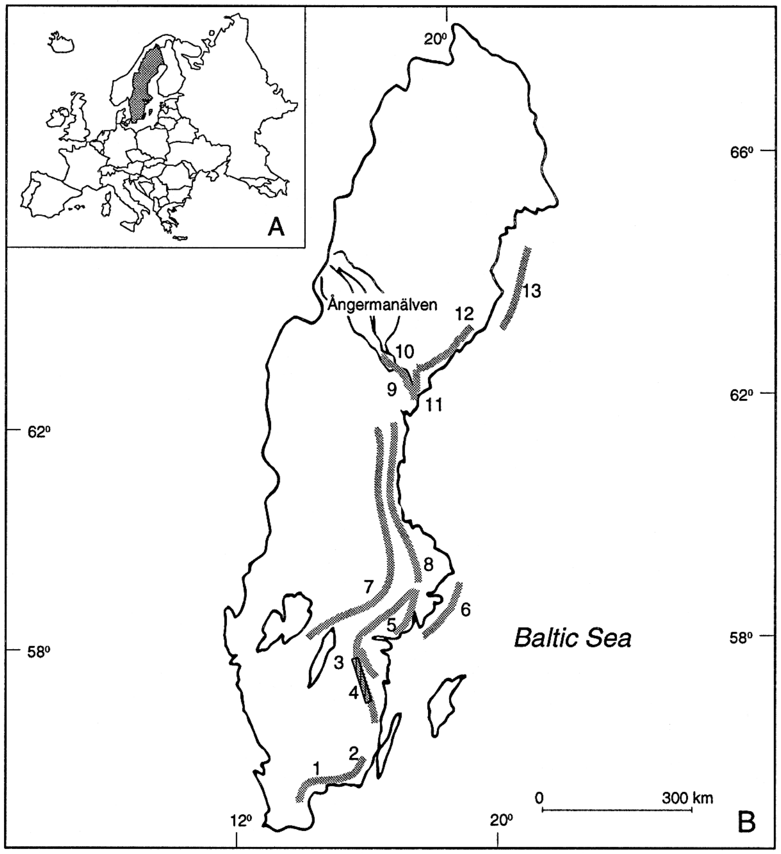


Figure 1 Europe and Sweden (A) and geographical location of the different local varve chronologies which are part of the Swedish Time Scale (B). Modified after Andrén et al. (1999) and Cato (1998). The different local chronologies were established by: 1) Ringberg (1991), 2) Ringberg and Rudmark (1985), 3) Kristiansson (1986), 4) Wohlfarth et al. (1998a), 5) Brunnberg (1995), 6) Andrén et al. (1999), 7) Strömberg (1989; 1994), 8) De Geer (1940), 9) Cato (1998), 10) Hörnsten and Olsson (1964), 11) Cato (1987), 12) Bergström (1968), and 13) Andrén (forthcoming). The gotiglacial varved clays are covered by the local chronologies 1–6 and by the older part of chronologies 7 and 8. The finiglacial varved clays are contained in the younger part of chronologies 7 and 8 and in chronologies 10, 12, and 13. The postglacial part of the STS is represented in the youngest part of chronologies 7 and 8 and in chronologies 9 and 11. Links between the gotiglacial and finiglacial parts of the STS were made according to varve-diagram correlations in chronologies 7 and 8 and between the finiglacial and postglacial parts of the STS according to correlations presented in chronologies 7–9. The link to the present is made through chronology 11 (Cato 1987). The AMS $^{14}C$ measurements shown in Table 1 were obtained on varve sequences from chronologies 4, 7, and 9.

general, the structure of the STS has more resemblance with a tree-ring chronology than with a varve chronology established upon sediment cores in a single lake basin. For the gotiglacial and finiglacial varves the correlations follow the receding ice margin, i.e. the varved clays/varve-thickness diagrams become younger from south to north (e.g. Strömberg 1983; Holmquist and Wohlfarth 1997). In the case of the postglacial varves, the correlation is from northwest to southeast, i.e. following the isolation of the delta surfaces (Cato 1987, 1998).

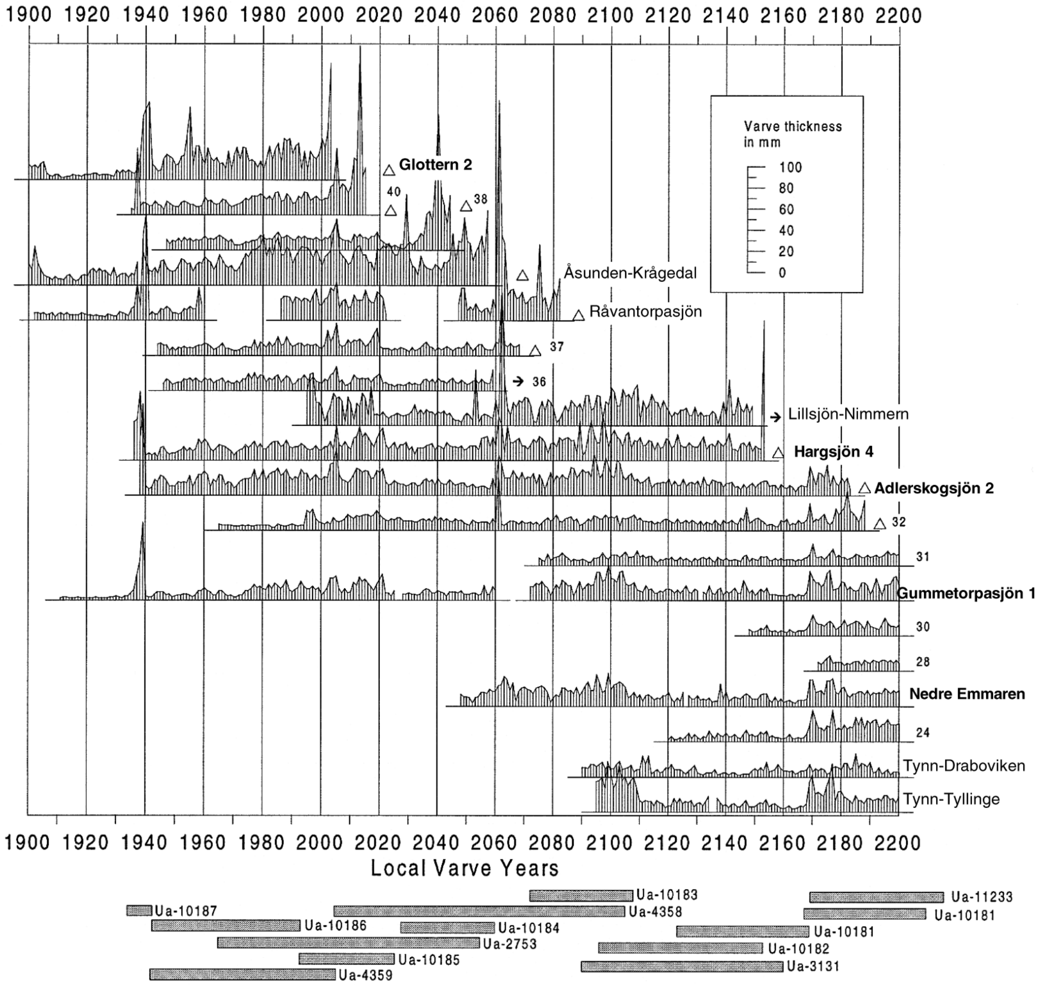


Figure 2 Example of a varve-diagram correlation from chronology 4 (Wohlfarth et al. 1998a). The varve-year intervals covered by the AMS $^{14}C$ measurements from southeastern Sweden (see Table 1) are marked. The localities from which the $^{14}C$-dated varve sequences were obtained are shown in bold letters.

According to the most recent revisions of the varve chronology (summarized in Wohlfarth et al. 1993 and Björck et al. 1992), it was assumed that the STS covers about the last 13,300 calendar years (Wohlfarth et al. 1995). However, based among others on AMS $^{14}C$ measurements on terrestrial macrofossils extracted from the varved clays, it became gradually clear that the chronology is still not complete and that several hundreds of years are missing, both in the older (Björck et al. 1996; Wohlfarth 1996; Wohlfarth et al. 1998a) and in the younger part (Wohlfarth et al. 1997; Andrén et al. 1999; Björck et al. forthcoming) of the time scale. Consequently, the STS cannot yet be regarded as a continuous annual chronology. Here we present these $^{14}C$ dates, their varve ages (according to the Swedish varve chronology) and their estimated calendar-year ages and show where likely errors in the time scale may be situated.

## METHODS

The methodological approach for obtaining the AMS $^{14}C$ measurements has been in detail described in Wohlfarth et al. (1995; 1998a) and is only shortly summarized here:

1. Coring for varved clays in areas where varve chronologies have already been established. Thickness measurements of the individual summer and winter layers, establishment of computer-drawn varve-thickness diagrams for each coring site, visual and statistical correlations to close-by varve-thickness diagrams (Figure 2), which are part of the STS, assignment of local varve years.
2. Sampling of 25–100 varve-year segments from the obtained clay-varve cores, sieving the samples under running water (mesh width 0.5 mm), selecting suitable terrestrial plant macrofossil remains (e.g. leaves, fruits, seeds and flowers of *Betula nana*, *Dryas octopetala*, *Salix polaris*, and *Salix* sp.) for AMS $^{14}C$ measurements.
3. The first set of samples was stored in distilled water, to which several drops of 2% HCl were added to attain a pH of ~2. The samples were kept in a cold room for 1 month to 1 year prior to the AMS measurements. After realizing that bacteria and/or fungi easily attack wet-stored samples, the samples were submitted immediately to the $^{14}C$ laboratory following sieving and identification. Although this procedure largely reduced the errors, the dating results were still not completely satisfactory. Therefore, and based on results from a parallel study (Wohlfarth et al. 1998b), the selected plant macrofossils were immediately dried after sieving and determination on aluminium foil overnight at 50–60 ºC.
4. Sample preparation at the $^{14}C$ laboratory included acid-alkali-acid (AAA) chemical pre-treatment (1% HCl and 0.5% NaOH at 80 ºC for 4 h) followed by combustion with CuO, Fe-catalytic graphitization (Vogel et al. 1984) and AMS measurements with the Uppsala EN-tandem accelerator (Possnert 1990).

All together, 74 samples were measured, but only the 32 samples presented in Table 1 are considered reliable. All other samples provided measurements that were several thousand years younger than expected. Replicate AMS $^{14}C$ samples covering the same varve year intervals (Wohlfarth et al. 1998a) and experiments with plant macrofossil samples (Wohlfarth et al. 1998b) showed that bacteria and/or fungi had affected the samples, which gave erroneously young ages (see above). The too young $^{14}C$ age of the samples could furthermore be confirmed by pollen stratigraphic investigations over the $^{14}C$ dated varve year intervals.

## RESULTS

Following the arguments outlined in Björck et al. (1996), Wohlfarth (1996), Wohlfarth et al. (1997; 1998a), Andrén et al. (1999), and Björck (1999, 2000), major correlation problems still exist in the Swedish varve chronology. Although several of the individual local and regional chronologies are fairly well established (Figure 1), problematic areas with weak varve-diagram correlations remain. It is, therefore, at present not possible to assign calendar-year ages based upon a continuous varve chronology to the AMS $^{14}C$ dates presented below. Alternative approaches, such as wiggle-matching and calibration of the $^{14}C$ dates with the OxCal Program (Ramsey 1999), comparisons with the $^{14}C$/varve curve presented by Kitagawa and van der Plicht (1998), correlations of pollen stratigraphic zones to the GRIP Event stratigraphy (Björck et al. 1998; Walker et al. 1999) or the synchronization of the AMS $^{14}C$ dates with Lake Gościąż presented in Goslar et al. (1999), allow circumventing some of the problems (Table 1). In the following, the ages that were obtained through wiggle-matching/calibration (Ramsey 1999) and through a visual correlation with the curve presented by Kitagawa and van der Plicht (1998) are expressed as cal BP and those obtained from the synchronization with Lake

Table 1 AMS $^{14}C$ measurements on terrestrial plant macrofossils from the Swedish varve chronology and the local varve years covered by each sample; the years were obtained through a correlation of the varve diagrams to the local varve chronologies in each area. See below for details.[a]

| Lab nr (Ua-) | $^{14}C$ AMS age (BP) ±1 σ | Local varve years | Cal BP ±2 σ[b] | Estimated cal BP[c] | Estimated cal GZ BP[d] | GRIP Events | Adjusted varve BP[e] |
|---|---|---|---|---|---|---|---|
| *Southernmost Sweden* | | | | | | | |
| 4247 | 12,595 ± 360 | +108 – +170 | 14,950 ± 600 | ca. 15,150 | | GI-1e | |
| 2469 | 12,740 ± 150 | +142 – +226 | 14,850 ± 600 | ca. 14,700 | | GI-1e | |
| 4245 | 12,330 ± 370 | +167 – +181 | 14,850 ± 600 | ca. 14,820 | | GI-1e | |
| 4248 | 12,310 ± 145 | +171 – +214 | 14,850 ± 600 | ca. 14,620 | | GI-1e | |
| 4246 | 12,590 ± 130 | +182 – +216 | 14,850 ± 600 | ca. 14,580 | | GI-1e | |
| 3132 | 12,090 ± 185 | +266 – +299 | 13,950 ± 500 | ca. 13,750 | | GI-1d | |
| *Southeastern Sweden* | | | | | | | |
| 2725 | 11,820 ± 150 | Correlation not possible | 13,850 ± 500 | | | | |
| 2750 | 11,520 ± 225 | | 13,550 ± 600 | | | | |
| 4945 | 11,539 ± 130 | | 13,500 ± 500 | | | | |
| 11233 | 10,740 ± 240 | 2273–2169 | —[f] | | 12,871 | GI-1a | |
| 10181 | 11,450 ± 240 | 2231–2167 | — | | 12,849 | GI-1a | |
| 11234 | 10,885 ± 250 | 2169–2123 | 13,058 ± 40 | | 12,769 | GI-1a | |
| 10182 | 11,470 ± 130 | 2153–2093 | — | | 12,788 | GI-1a | |
| 3131 | 10,890 ± 120 | 2160–2090 | 13,038 ± 38 | | 12,775 | GI-1a | |
| 10183 | 11,030 ± 120 | 2108–2072 | 13,003 ± 38 | | 12,740 | GI-1a | |
| 4358 | 10,980 ± 100 | 2105–2005 | 12,968 ± 38 | | 12,705 | GI-1a | |
| 10184 | 10,970 ± 90 | 2060–2028 | 12,958 ± 38 | | 12,694 | GI-1a | |
| 2753 | 10,480 ± 150 | 2055–1965 | — | | 12,660 | GI-1a | |
| 10185 | 11,230 ± 100 | 2025–1993 | — | | 12,659 | GI-1a | |
| 4359 | 10,610 ± 110 | 2004–1942 | — | | 12,623 | GS-1 | |
| 10186 | 11,040 ± 110 | 1993–1943 | — | | 12,618 | GS-1 | |
| 10187 | 10,420 ± 220 | 1942–1934 | — | | 12,588 | GS-1 | |
| 4496 | 10,585 ± 465 | 1906–1806 | 12,768 ± 38 | | 12,506 | GS-1 | |
| *Eastern Middle Sweden* | | | | | | | |
| 4217 | 10,330 ± 175 | 11,485–11,457 | 12,210 ± 200 | | | GS-1 | 12,346 |
| 4216 | 10,620 ± 155 | 11,456–11,418 | — | | | GS-1 | 12,312 |
| 2742 | 9945 ± 115 | 11,381–11,331 | — | | | GS-1 | 12,231 |
| 4215 | 10,140 ± 155 | 11,228–11,128 | 11,915 ± 195 | | | GS-1 | 12,053 |
| 4214 | 10,170 ± 195 | 11,126–11,104 | 11,850 ± 200 | | | GS-1 | 11,990 |
| 2741 | 9640 ± 190 | 11,081–10,973 | 11,745 ± 205 | | | GS-1 | 11,902 |
| 4212 | 10,160 ± 115 | 11,020–11,000 | — | | | GS-1 | 11,885 |
| 11829[g] | 9970 ± 120 | 10,618–10,546 | 11,320 ± 200 | | | Holocene | 11,457 |
| *Northeastern Sweden* | | | | | | | |
| 11230 | 4720 ± 135 | 4710 ± 5 | 5350 ± 350 | | | Holocene | |

[a]Calibrated BP are based on:
[b]Wiggle-matching with the OxCal Program (Ramsey 1999), except for samples 2725, 2750, and 4945, which were only calibrated.
[c]Visual matching to the $^{14}C$/varve curve presented by Kitagawa and van der Plicht (1998).
[d]Synchronization with Lake Gościąż presented in Goslar et al. (1999) and Wohlfarth et al. (1998), correlation of pollen-stratigraphic zones to the GRIP Event stratigraphy (Björck et al. 1998; Walker et al. 1999).
[e]Adjusted varve BP are according to Andrén et al. (1999), who suggest that 875 years are missing in the STS.
[f]— indicates that wiggle-matching did not produce statistically significant results.
[g]Radiocarbon date published in Björck et al. (forthcoming). See text for further explanation.

Gościąż (Goslar et al. 1999) as cal GZ BP, in order to differentiate between the different approaches. "Local varve yr" refer to local varve years in each separate (local) varve chronology and "varve BP" to the chronology suggested for the STS (e.g., Strömberg 1994; Brunnberg 1995).

### AMS $^{14}$C–Varve Chronology in Southernmost Sweden

The varve chronology in southernmost Sweden was established by Ringberg (1991) and Ringberg and Rudmark (1985) and covers the local varve yr –325 to +314 (chronologies 1 and 2 in Figure 1). Later, additional clay-varve diagram correlations allowed prolonging the varve chronology to the year +368 (Ising 1998; Wohlfarth et al. 1994). The local varve chronology in southernmost Sweden has thus a total length of 694 varve yr. The tentative link between this and the local varve chronology in southeastern Sweden (chronology 3 in Figure 1), which had been suggested by Björck and Möller (1987), led Wohlfarth et al. (1995) to assume an age of around 12,650–13,300 varve BP for chronologies 1 and 2.

Based on pollen-stratigraphic investigations in varved clays by Björck (1981), Wohlfarth et al. (1994) placed the transition between the Bølling and Older Dryas pollen zones at the local varve year +220. The varved clays deposited between the years +108 to +220 would accordingly correlate with the Bølling pollen zone, while those between +220 and +299 would correspond to the Older Dryas pollen zone. Compared to the event stratigraphy suggested by Björck et al. (1998) and Walker et al. (1999) varve yr +108 to +220 would then relate to the youngest part of GI-1e (14,050–14,160 GRIP BP), while varve yr +220 to +299 would fall within GI-1d (14,050–13,970 GRIP BP) (see Table 1). Wiggle-matching (Ramsey 1999) and the visual correlation (to Kitagawa and van der Plicht's [1998] curve) of the AMS $^{14}$C measurements presented in Table 1 (corresponding to the local varve yr +108 to +216), give considerably older ages, ranging at around 14,950–14,850 and 15,150–14,580 cal BP, respectively (Table 1). The cal yr age of the youngest AMS $^{14}$C date, however, seems to be in good agreement with the GRIP age estimate for the Older Dryas/GI 1d (Table 1). The discrepancy between the two age estimates could be an artifact and explained by the fairly large standard error of some of the $^{14}$C measurements, which makes their exact $^{14}$C age highly uncertain. Furthermore, $^{14}$C calibration during this time period is still weak due to the large $^{14}$C plateau at around 12,600 BP. This, together with the standard error of our $^{14}$C dates, makes cal yr age attributes very imprecise.

In accordance with other lake-sediment studies in this area (pollen stratigraphy, lake isolation, shore displacement curves) by e.g. Björck (1981) and Björck and Möller (1987) and based on the above outlined arguments, we assume that the AMS $^{14}$C dated part of the varved clays was deposited between the end of the Bølling and during the early part of the Older Dryas pollen zone or, during the youngest part of GI-1e and during GI-1d according to Björck et al. (1998) and Walker et al. (1999). Although the cal BP attribution remains uncertain, except for the youngest sample, it is clear that the varves in southernmost Sweden are between 1200 and 2400 years older than earlier assumed by Wohlfarth et al. (1995) (Figure 3).

### AMS $^{14}$C–Varve Chronology in Southeastern Sweden

The varve chronology for southeastern Sweden had been established by Kristiansson (1986) (chronology 3 in Figure 1). It was partly revised by Brunnberg (1995), who tentatively connected it to his chronology (chronology 5 in Figure 1), which in turn is connected to the main part of the STS. Chronology 3 covers the local varve yr 2825–515, i.e. a total length of 2310 varve yr. Following Brunnberg's (1995) correlations, this part would correspond to 12,830–10,520 varve BP. However, detailed cross-correlation analyses of all varve diagrams in Kristiansson's (1986) chronology (Holmquist and Wohlfarth 1997) made it evident that many of the visual correlations are statistically

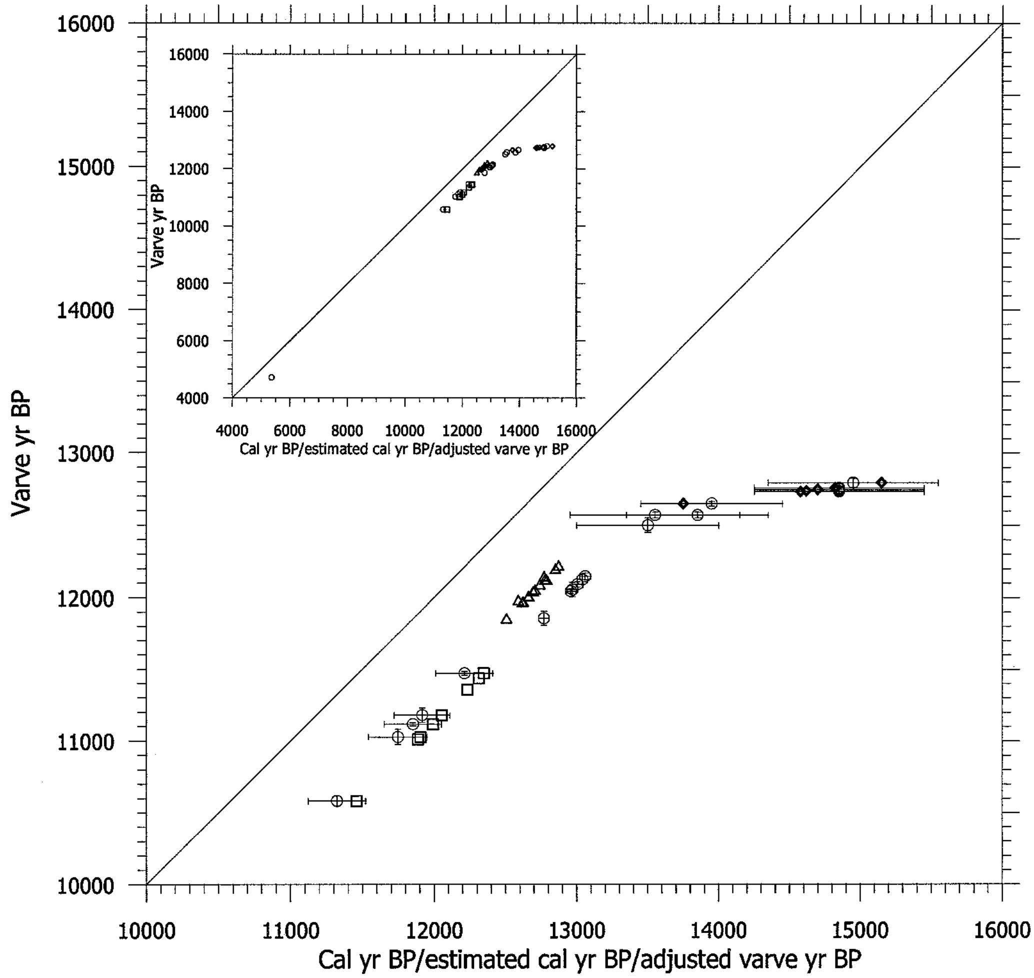


Figure 3 Comparison between varve BP (according to the STS, see Wohlfarth et al. 1995, Table 1) and different cal yr estimates for the AMS $^{14}C$ measurements (see text for discussion) shown in Table 1. Open circle = cal BP according to INTCAL98, open diamonds = cal BP according to Kitagawa and van der Plicht (1998), open triangles = calendar BP obtained through a comparison with Lake Gościąż (Goslar et al. 1999), open squares = adjusted varve BP according to Andrén et al. (1999).

not significant. New clay-varve measurements (chronology 4 in Figure 1), combined with AMS $^{14}C$ dates (Wohlfarth et al. 1998a) and pollen-stratigraphic investigations (Björck 2000), suggested that only the part between 2475–1700 varve yr should be regarded as a reliable chronology.

The AMS $^{14}C$ measurements obtained between 2457 and 1700 local varve yr (Table 1, Figure 2) were compared to the AMS $^{14}C$-dated laminated lake-sediment sequence from Lake Gościąż (Goslar et al. 1999). The best fit between the two sequences was obtained by paralleling the varve yr 2000 with 12,650 cal GZ BP or the Allerød/Younger Dryas boundary. Pollen stratigraphic investigations by Björck (2000) on the same clay-varve sequences later gave clear evidence for an Allerød/Younger Dryas pollen zone boundary at around the local varve year 2000. Based on the best fit with Lake Gościąż, calendar years (cal GZ BP) were calculated for each $^{14}C$-dated varve segment (Goslar et al. 1999) (Table 1), as well as for the entire 775-yr long varve chronology (chronology 4) (Wohlfarth et al. 1998a). Accordingly, this chronology covers the time period between 13,125–12,350 cal GZ BP. The resulting offset of 200–300 yr between the calculated cal yr estimates and those obtained by matching the sequence to Lake Gościąż (Table 1) is easily explained by different estimates for the length of the Younger Dryas. In Lake Gościąż, the length of Younger Dryas is given at around 1150 yr (Goslar et al. 1995), which is in accordance with the GRIP ice core (e.g. Björck et al. 1998). However, in the calibration program (Stuiver et al. 1998) as well as in the GISP isotope stratigraphy (Alley et al. 1997), the length of Younger Dryas is about 1300 yr. Based on the pollen-stratigraphic investigations, the AMS $^{14}$C dates and on their corresponding cal yr estimates, the reliable part of the local varve chronology would correspond to GI-1b, GI-1a and to parts of GS-1 in the event stratigraphy presented by Walker et al. (1999) and Björck et al. (1998). Independent of the divergence between the different cal yr estimates presented in Table 1, it is clear that an offset of >650–1000 yr exists between these and Brunnberg's (1995) and Wohlfarth et al.'s (1995) varve yr estimate for the same time period (i.e. 12,475–11,700 varve BP) (Figure 3).

### AMS $^{14}$C–Varve Chronology in Eastern-Middle Sweden

Strömberg (1994) established the varve chronology for central Sweden and connected it to the main part of the STS (chronology 7 in Figure 1). The varved sequence, from which the AMS $^{14}$C dates were obtained, could be correlated to Strömberg's (1994) chronology (Table 1) and covers 11,471–11,010 varve BP in the STS. Based on pollen stratigraphic investigations of varved clays corresponding to 10,735–10,430 varve BP, Björck et al. (forthcoming) concluded, that these varves were deposited during the early Holocene. Andrén et al. (1999) could show that the distinct increase in varve thickness (in chronology 6) at 10,650 varve BP, coincides with the Younger Dryas/Holocene transition and that it compares nicely with the GRIP isotope stratigraphy. The tentative match to the GRIP ice core, led the authors to correlate 10,650 varve BP with 11,525 cal BP (according to GRIP). Björck et al. (forthcoming), on the other hand, based on pollen stratigraphy, correlated 10,740 varve BP (in chronology 7) with 11,525 GRIP cal BP. Despite the slight differences in defining the Younger Dryas/Holocene transition in the varved clays, both comparisons give evidence for an error amounting to 800–900 varve yr.

The adjusted varve yr presented in Table 1 were calculated following Andrén et al.'s (1999) estimate of 875 missing varves. The obtained years correspond well to the cal yr estimates obtained through wiggle-matching (Table 1, Figure 3). Compared to the GRIP Event stratigraphy (Björck et al. 1998; Walker et al. 1999), the time period covered by the AMS $^{14}$C dates shown in Table 1 would thus correspond to parts of GS-1 and to the earliest part of the Holocene.

### AMS $^{14}$C–Varve Chronology in Northeastern Sweden

The postglacial varve chronology in northeastern Sweden is based on about a 2000-yr-long chronology from the estuary of River Ångermanälven, AD 1978–50 BC (Cato 1987) and a connection of this chronology to Lidén's (1913) old chronology (Cato 1998) (chronologies 11 and 9, respectively in Figure 1). The latter varve chronology had been established upon varve thickness measurements in bluffs along River Ångermanälven. Cato's (1998) recent revisions and correlations show that the whole postglacial chronology extends back to 9000 varve BP. A link between this chronology and the glaciolacustrine varved clays, which can be found along the east coast up to Ångermanälven, has been attempted by Strömberg (1989). Cato's (1987) 2000-yr long varve chronology has been validated by cross-correlation analyses (Holmqvist and Wohlfarth unpublished) and all varve-diagram correlations have been found to be statistically significant. One AMS $^{14}$C measurement performed on terrestrial plant macrofossils extracted from the postglacial varves at the varve year 4710 ± 5 gave a calibrated age of 4720 ± 135 BP (5350 ± 400 cal BP, 2 σ) (Table 1, Figure 3). Wohlfarth et al. (1997) suggested that the offset between the varve age and the calibrated age of the sample may point to an error or parts of an error in the varve chronology between 2000 and 5000 varve BP. Unfortunately, due to the scarcity of plant material in the postglacial varves, this AMS $^{14}C$ date could so far not be supported by replicate $^{14}C$ measurements.

### Where are the 'Missing' Varve Years?

The above outlined arguments make it clear that the STS, despite the many efforts during the last decades, can still not be regarded as a continuous annual chronology. However, the obtained AMS $^{14}C$ dates combined with pollen stratigraphic investigations and new clay-varve measurements allow pointing to areas where these errors could be found and corrected.

The first package of "missing" varves (>800 yr) shows up at the beginning of the Holocene and/or in the middle part of the postglacial varves (Figure 3). Since Strömberg's (1989) and Brunnberg's (1995) chronologies (7 and 5 in Figure 1) are generally regarded as reliable, two possibilities remain for finding the weak points: within the postglacial chronology (chronology 9) or at the link between chronologies 9 and 7. A re-evaluation of some of the postglacial varve-diagram connections and new varve measurements in the area between chronology 7 and 9 would easily solve this problem.

Only 650 varves are missing at the Allerød/Younger Dryas boundary, if we adopt the match between the AMS $^{14}C$ dated varve sequence and Lake Gościąż (Goslar et al. 1999). However, if we follow the estimated cal BP obtained from wiggle-matching, the missing varves amount to about 1000 (Figure 3), which is more in agreement with the 875 missing years suggested by Andrén et al. (1999). But, since the younger part of chronology 3 is characterized by insignificant varve-diagram correlations (Holmqvist and Wohlfarth 1997), the link between chronology 3 and chronologies 7 and 5 is fairly weak, and Andrén et al.'s (1999) chronology does not reach as far back as the Allerød/Younger Dryas boundary, we do not know how many varve years are contained in the STS between the Allerød/Younger Dryas transition and the Younger Dryas/Holocene boundary. One important task would, therefore, be to reinvestigate the varve-diagram correlations in the younger part of chronology 3 in order to obtain a firm link between chronologies 3 and 5. Another possibility would be to prolong chronology 5 by new clay varve measurements and to link it to the well established chronology 4.

At the Bølling/Older Dryas boundary, which has been defined in varve chronology 1, the offset between estimated cal BP and the earlier assumption of 12,700–12,800 varve BP (Wohlfarth et al. 1995; Table 1) amounts to approximately 1200–2400 yr. This would mean that the number of "missing" varves has increased additionally as compared to the Allerød/Younger Dryas and Younger Dryas/Holocene transition. No valid link exists between chronology 2 and chronology 3, and the older part of chronology 3 is, furthermore, highly uncertain (Holmqvist and Wohlfarth 1997). The additional error may, therefore, very likely be found if new clay-varve measurements could be performed in the area between chronologies 2 and 3 and in the older part of chronology 3.

## CONCLUSION

The Swedish varve chronology or STS is based upon the successive matching of more than 1000 varve-thickness measurements performed in open sections or on sediment cores. Deposition of the older glacio-lacustrine varved clays occurred in the Baltic basin during the recession of the Scandinavian inland ice. The younger postglacial varves are delta sediments, which are now exposed along the bluffs in River Ångermanälven and which are still deposited today in the estuary of River Ångermanälven in northeastern Sweden.

Although the Swedish varve chronology had been regarded as a continuous annual chronology, several independent lines of evidence have pointed to major errors. These errors may be found by re-evaluating older varve-diagram correlations and by establishing firm links between the different local varve chronologies through new clay-varve measurements. Until these errors are resolved, the STS remains a floating varve chronology, without a possibility to assign calendar years BP to its AMS $^{14}$C dated and pollen stratigraphic investigated parts. Through wiggle-matching, calibration and/or synchronization of the AMS $^{14}$C-dated intervals in combination with pollen stratigraphic investigations, tentative cal yr could be obtained, which allow estimating the number of "missing" varves within the varve chronology. The offset between the STS and the tentative cal BP presented in Table 1 can be assumed to be in the order of >800 yr at the Younger Dryas/Holocene boundary, of around either 650 yr or 900–940 yr at the Alleröd/Younger Dryas transition, of around 1300 yr at the Bölling/Older Dryas boundary and of >2000 yr in the oldest part of the chronology (Figure 3).

## ACKNOWLEDGMENTS

The Swedish Natural Science Research Council (NFR) is currently financing BW's position ("sediments as environmental archives"). The results presented above were obtained within research projects financed by the Swiss National Science Foundation (SNF) (1991–1993), the Swedish Natural Science Research Council (NFR) (1991–1997) and the Geological Survey of Sweden (SGU) (1993–1998).

## REFERENCES

Alley RB, Shuman CA, Meese DA, Gow AJ, Taylor KC, Cuffey KM, Fitzpatrick JJ, Grootes PM, Zielinski GA, Ram M, Spinelli G, Elder B. 1997. Visual-stratigraphic dating of the GISP2 core: basis, reproducibility, and application. *Journal of Geophysical Research* 102(C12):26,370–81.

Andrén T. The last Weichselian deglaciation of the Bothnian Bay, northern Scandinavia. *Boreas*. Forthcoming.

Andrén T, Björck J, Johnsen S. 1999. Correlation of the Swedish glacial varves with the Greenland (GRIP) oxygen isotope stratigraphy. *Journal of Quaternary Science* 14:361–71.

Bergström R. 1968. Stratigrafi och isrecession i södra Västerbotten. *Sveriges Geologiska Undersökning* C634:1–76.

Björck J. 1999. Event stratigraphy for the Last Glacial-Holocene transition in eastern middle Sweden. *Quaternaria*, Series A, Nr 6:1–48.

Björck J. 2000. The Alleröd-Younger Dryas pollen zone boundary in an 800 year varve chronology from southeastern Sweden. *GFF.* Forthcoming.

Björck J, Possnert G, Schoning K. Early Holocene deglaciation chronology in Västergötland and Närke, Sweden—biostratigraphy, clay varve, $^{14}$C and calendar year chronology. *Quaternary Science Reviews*. Forthcoming.

Björck S. 1981. A stratigraphic study of Late Weichselian deglaciation, shore displacement and vegetation history in south-eastern Sweden. *Fossils and Strata* 14:1–93.

Björck S, Cato I, Brunnberg L, Strömberg B. 1992. The clay-varve based Swedish Time Scale and its relation to the Late Weichselian radiocarbon chronology. In: Bard E, Broecker WS, editors. *The last deglaciation: absolute and radiocarbon chronologies*. NATO ASI Series I, Volume 2. Berlin: Springer Verlag. p 25–44.

Björck S, Kromer B, Johnsen S, Bennike O, Hammarlund D, Lemdahl G, Possnert G, Rasmussen TL, Wohlfarth B, Hammer CU, Spurk M. 1996. Synchronized terrestrial-atmospheric deglacial records around the North Atlantic. *Science* 274:1155–60.

Björck S and Möller P. 1987. Late Weichselian environmental history in southeastern Sweden during the deglaciation of the Scandinavian ice sheet. *Quaternary Research* 28:1–37.

Björck S, Walker MJC, Cwynar LC, Johnsen S, Knudsen K-L, Lowe JJ, Wohlfarth B, INTIMATE members. 1998. An event stratigraphy for the Last Termination in the North Atlantic region based on the Greenland ice-core record: a proposal by the INTIMATE group. *Journal of Quaternary Science* 13:283–92.

Brunnberg L. 1995. Clay-varve chronology and deglaciation during the Younger Dryas and Preboreal in the easternmost part of the Middle Swedish Ice Marginal Zone. *Quaternaria,* Series A, 2:3–94.

Cato I. 1987. On the definitive connection of the Swedish Time Scale with the present. *Sveriges Geologiska Undersökning* Ca68:1–55.

Cato I. 1998. Ragnar Liden's postglacial varve chronology from the Ångermanälven valley, northern Sweden. *Research Papers SGU series* Ca88:1–82.

de Geer G. 1912. A geochronology of the last 12,000 years. *Congrès de Geologie International, Comptes Rendues*. p 241–253.

de Geer G. 1940. Geochronologia Suecica, principles. *Kungliga Svenska Vetenskapsakademiens Handlingar* 18:1–367.

Goslar T, Arnold M, Bard E, Kuc T, Pazdur M F, Ralska-Jasiewiczowa M, Rozanski K, Tisnerat N, Walanus A, Wicik B, Wieckowski K. 1995. High concentration of atmospheric $^{14}C$ during the Younger Dryas cold episode. *Nature* 377:414–7.

Goslar T, Wohlfarth B, Björck S, Possnert G, Björck J. 1999. Variations of atmospheric $^{14}C$ concentrations over the Alleröd-Younger Dryas transition. *Climate Dynamics* 15:29–42.

Holmquist B, Wohlfarth B. 1997. An evaluation of the Late Weichselian Swedish varve chronology based on cross-correlation analysis. *GFF* 120:35–46.

Hörnsten Å, Olsson I. 1964. En $C^{14}$-datering av glaciallera från Lugnvik, Ångermanland. *Geologiska Föreningens i Stockholm Förhandlingar* 86:206–10.

Ising J. 1998. Late Weichselian pollen stratigraphy, clay-varve chronology, radiocarbon chronology and palaeomagnetic secular variations at Farslycke, Blekinge, southern Sweden. *GFF* 120:321–32.

Kitagawa H, van der Plicht J. 1998. A 40,000-year varve chronology from Lake Suigetsu, Japan: extension of the radiocarbon calibration curve. *Radiocarbon* 40(1): 505–15.

Kristiansson J. 1986. The ice recession in the southeastern part of Sweden. A varve-chronological time scale for the latest part of the Late Weichselian. *University of Stockholm, Department of Quaternary Research report* 7:1–132.

Lidén R. 1913. Geokronologiska Studier öfver det Finiglaciala Skedet i Ångermanland. *Sveriges Geologiska Undersökning* 9:1–39.

Olsson I, editor. 1970. *Radiocarbon variations and absolute chronology*. Stockholm: Almqvist & Wiksell. p 1–230.

Possnert G. 1990. Radiocarbon dating by the accelerator technique. *Norwegian Archaeological Review* 23:30–7.

Ramsey BC. 1999. OxCal Program version 3.3.

Ringberg B. 1991. Late Weichselian clay varve chronology and glaciolacustrine environment during deglaciation in southeastern Sweden. *Sveriges Geologiska Undersökning* 79:1–42.

Ringberg B, Rudmark L. 1985. Varve chronology based upon glacial sediments in the area between Karlskrona and Kalmar, southeastern Sweden. *Boreas* 14:107–10.

Strömberg B. 1983. The Swedish varve chronology. In: Ehlers J, editor. *Glacial deposits in northwest Europe*. Rotterdam: Balkema. p 97–105.

Strömberg B. 1985a. New varve measurements in Västergötland, Sweden. *Boreas* 14:111–5.

Strömberg B. 1985b. Revision of the lateglacial Swedish varve chronology. *Boreas* 14:101–5.

Strömberg B. 1989. Late Weichselian deglaciation and clay varve chronology in east-central Sweden. *Sveriges Geologiska Undersökning* Ca73**:**1–70.

Strömberg B. 1994. Younger Dryas deglaciation at Mt. Billingen, and clay varve dating of the Younger Dryas/Preboreal transition. *Boreas* 23:177–93.

Stuiver M, Reimer PJ, Bard E, Beck JW, Burr GS, Hughen KA, Kromer B, McCormac G, van der Plicht J, Spurk M. 1998. INTCAL98 radiocarbon age calibration, 24,000–0 cal BP. *Radiocarbon* 40(3):1041–83.

Vogel JS, Southon JR, Nelson DE, Brown TA. 1984. Performance of catalytically condensed carbon for use in accelerator mass spectrometry. *Nuclear Instruments and Methods in Physics Research* B5:289–93.

Walker MJC, Björck S, Lowe JJ, Cwynar LC, Johnsen S, Knudsen K-L, Wohlfarth B, INTIMATE group. 1999. Isotopic "events" in the GRIP ice core: a stratotype for the Late Pleistocene. *Quaternary Science Reviews* 18: 1143–50.

Wohlfarth B. 1996. The chronology of the Last Termination: a review of high-resolution terrestrial stratigraphies. *Quaternary Science Reviews* 15:267–84.

Wohlfarth B, Björck S, Cato I, Possnert G. 1997. A new middle Holocene varve diagram from river Ångermanälven, Northern Sweden: indications for a possible error in the Holocene varve chronology. *Boreas* 4: 347–54.

Wohlfarth B, Björck S, Lemdahl G, Ising J. 1994. Ice recession and depositional environment in the Blekinge archipelago of the Baltic Ice Lake. *GFF* 116:3–12.

Wohlfarth B, Björck S, Possnert G. 1995. The Swedish Time Scale—a potential calibration tool for the radiocarbon time scale during the Late Weichselian. *Radiocarbon* 37(2):347–60.

Wohlfarth B, Björck S, Possnert G, Holmquist B. 1998a. A 800-year long, radiocarbon-dated varve chronology from south-eastern Sweden. *Boreas* 27:243–57.

Wohlfarth B, Björck S, Possnert G, Lemdahl G, Brunnberg L, Ising J, Olsson S, Svensson N-O. 1993. AMS dating Swedish varved clays of the last glacial/interglacial transition and the potential/difficulties of calibrating Late Weichselian "absolute" chronologies. *Boreas* 22:113–28.

Wohlfarth B, Possnert G, Skog G, Holmquist B. 1998b. Pitfalls in the AMS radiocarbon-dating of terrestrial macrofossils. *Journal of Quaternary Science* 13:137–45.

Zeuner FE. 1950. *Dating the past*. London: Methuen & Co. Ltd. 474 p.

RADIOCARBON, Vol 42, Nr 3, 2000, p 335–348 

# RADIOCARBON CALIBRATION BY MEANS OF VARVES VERSUS $^{14}$C AGES OF TERRESTRIAL MACROFOSSILS FROM LAKE GOŚCIĄŻ AND LAKE PERESPILNO, POLAND

Tomasz Goslar[1] • Maurice Arnold[2] • Nadine Tisnerat-Laborde[3] • Christine Hatté[3] •
Martine Paterne[3] • Magdalena Ralska-Jasiewiczowa[4]

**ABSTRACT.** This paper presents radiocarbon dates of terrestrial macrofossils from Lakes Gościąż and Perespilno, Poland. These data agree very well with most of the German pine calibration curve. In the Late Glacial, they generally agree with the data from Lake Suigetsu, Japan, and indicate constant or even increasing $^{14}$C age between 12.9 and 12.7 ka BP, rapid decline of $^{14}$C age around 12.6 ka BP, and a long plateau 10,400 $^{14}$C BP around 12 ka BP. Correlation with corals and data from the Cariaco basin seems to support the concept of site-speficic, constant values of reservoir correction, in contradiction to those introduced in the INTCAL98 calibration. Around the Allerød/Younger Dryas boundary our data strongly disagree with those from the Cariaco basin, which reflects large discrepancy between calendar chronologies at that period. The older sequence from Lake Perespilno indicates two periods of rapid decline in $^{14}$C age, around 14.2 and 13.9 ka BP.

## INTRODUCTION

Radiocarbon dating of terrestrial macrofossils from Lake Gościąż (Goslar et al. 1995) demonstrated that annually laminated sediments can be suitable material for $^{14}$C calibration. The most severe drawback of such material, the possibility of missing varves in the sequence (cf. Hajdas et al. 1995), has been minimized by varve-to-varve correlation of seven sediment cores from three different lake depths (e.g. Goslar 1998a). The Gościąż data clearly disagreed with those from the German pine chronology (Kromer and Becker 1993), an effect which disappeared (Goslar and Mądry 1998) after the revision of the link between the German pine and oak chronologies (Kromer and Spurk 1998). Beyond the range of long pine chronology, our data roughly agreed with coral $^{14}$C calibration (Bard et al. 1998; Burr et al. 1998), but they poorly covered the time scale before 11.6 ka BP and their one-sigma uncertainty was quite large.

Recently, our data set (Tables 1 and 2) has been supplemented with 47 $^{14}$C dates from the oldest section of Lake Gościąż (LG) sediments, and 51 dates from the annually laminated sediments of Lake Perespilno (LP) in eastern Poland (Goslar et al. 2000). The new Gościąż samples come from three additional cores, perfectly replicating the LG varve chronology. The chronology of Lake Perespilno sediments (Goslar et al. 1999a) is based on seven cores. However, all of them show a 6–10 cm thick disturbance about 10 cm below the AL/YD boundary. According to $^{14}$C dates, this disturbance splits the LP sequence in two separate sections.

### Radiocarbon Dating

$^{14}$C dating was performed on terrestrial macrofossils collected from a few precisely synchronized cores. Only a few well-defined and easy to identify types of macrofossils were used (bud scales, seeds, needles and peridermis fragments of pine, as well as fruit scales and nutlets of birch). We selected only large macrofossils, not destroyed mechanically, and with no traces of decomposition. This lowered the probability of dating reworked material, and material contaminated with foreign

[1]Institute of Physics, Silesian University of Technology, ul. Krzywoustego 2, 44-100 Gliwice, Poland.
Email: goslar@zeus.polsl.gliwice.pl.
[2]UMS 2004 (CNRS-CEA), Tandetron Bat. 30, Avenue de la Terrasse, 91198 Gif sur Yvette, France
[3]Laboratoire des Sciences du Climat et de l'Environnement, CNRS-CEA, Avenue de la Terrasse, 91198 Gif sur Yvette, France
[4]W. Szafer Institute of Botany, Polish Academy of Sciences, ul. Lubicz 46, 31-512 Kraków, Poland

carbon. To minimize contamination with modern carbon (e.g. of biological origin), the surface of each macrofossil was thoroughly scraped with a plastic brush before chemical pretreatment. The AMS $^{14}C$ dating was performed at the Tandetron facility at Gif sur Yvette (Arnold et al. 1989). Usually, two targets were measured, and the results averaged. For all the small samples dated between 1993 and 1998, we used the correction for mass-dependence of background introduced after measurements of "infinitely" old wood samples (Goslar et al. 1993). However, further improvements in the cleaning preparation of samples and glass containers lowered the background in 1999 to about one third of that occurring in 1993. Therefore, although a blank lowering of similar amplitude was also obtained on the C1 marble at the same time by changing sample preparation, it would be possible that the $^{14}C$ ages of the second set (Tables 1 and 2) are slightly younger than quoted here. This has been checked very recently, by dating Lake Perespilno samples from nearly the same varves as those dated in 1996. Comparison of these dates (Figure 2, Table 2) indicates that the change in the mass-dependence of the background correction was not significant.

Most of the Gościąż dates fit one another quite well (Figures 2, 4). Few $^{14}C$ dates for the very small samples from the older set appear too young, possibly due to contamination with modern carbon. In the new set, two dates are obviously too old, probably due to redeposition of older material. They occur in the earlier half of Younger Dryas (12.65–12 ka BP), when vegetation cover around the lake was the thinnest (Ralska-Jasiewiczowa 1998), and the sediments contain some amount of material rebedded from the littoral zone (Goslar 1998a). Similar redeposition is revealed by one sample from Lake Perespilno.

### Uncertainty of Varve Counting and Absolute Age Determination

The varve chronologies have been constructed using several cores (10 for LG and 7 for LP) varve-to-varve synchronized with one another. Therefore, difficulties with some varves being not clear enough in one core could be overcome by using other cores. The accuracy of the varve chronology is limited by varves that appear unclear in all analyzed cores. The methods of the varve counting method and construction of the LG varve chronology are described in detail elsewhere (Goslar 1998a, 1998b).

The uncertainty in the 2937-varve-long section of the LG sediments between the bottom of lamination and 10,000 cal BP (total 2937 ± 55 varves) is not uniformly distributed in time (Figure 1). Most of the uncertainty appears in the Younger Dryas (YD) part (1140 ± 40 varves), while accuracy of varve counting in the early Holocene is excellent (1496 ± 10 varves). Similarly, worse quality of lamination in the YD part (1125 ± 70 varves) is the reason why the number of varves in the younger section of the LP sediments (2158 ± 100) is less accurate than in the older section (936 ± 35).

The absolute age of the LG varve sequence has been determined (Goslar and Mądry 1998) by wiggle-matching $^{14}C$ dates from the younger parts of sediments to the revised oak $^{14}C$-calibration curve (Kromer and Becker 1998). Since the link between German pine and oak chronologies has been found (Spurk et al. 1998), we now rely also on the match with the pine curve (Figure 2). This suggests an adjustment of the age of LG sediments (Goslar et al. 2000) by 15 yr. However, as the age of German pines is still uncertain (± 20 yr; Kromer and Spurk 1998), taking into account the pine data improved the accuracy of our dating only very slightly. The absolute age of the Lake Gościąż varve chronology is expressed by the age of varve nr. 1072 (11,496 ± 36 cal BP), a midpoint of rapid rise of $\delta^{18}O$ at the YD/Holocene boundary (Goslar et al. 1995). It is worth noting that the rise of $\delta^{18}O$ in LG perfectly coincides with the increase of tree-ring width of German pines (Spurk et al. 1998), both marking climatic warming at the onset of Holocene (Figure 3).

Table 1 Calendar and $^{14}C$ ages of terrestrial macrofossils from the laminated sediments of Lake Gościąż. All errors are 1σ. References: 1. Goslar et al. (1995); 2. Goslar et al. (2000); 3. outliers, not included in the discussion.

| Cal BP | $^{14}C$ BP | mg C | Ref. |
|---|---|---|---|
| 12,927 ± 55 | 11,310 ± 90 | 0.65 | 2 |
| 12,907 ± 55 | 11,120 ± 90 | 0.97 | 2 |
| 12,877 ± 54 | 11,250 ± 90 | 0.86 | 2 |
| 12,847 ± 54 | 11,150 ± 90 | 0.94 | 2 |
| 12,827 ± 54 | 11,130 ± 70 | 2.69 | 2 |
| 12,807 ± 53 | 11,140 ± 70 | 1.38 | 2 |
| 12,787 ± 52 | 10,990 ± 60 | 2.58 | 2 |
| 12,767 ± 51 | 11,140 ± 70 | 3.03 | 2 |
| 12,747 ± 50 | 11,190 ± 70 | 1.59 | 2 |
| 12,727 ± 49 | 11,280 ± 70 | 2.34 | 2 |
| 12,718 ± 49 | 10,920 ± 90 | 0.56 | 1 |
| 12,707 ± 48 | 11,170 ± 80 | 0.92 | 2 |
| 12,687 ± 48 | 11,180 ± 70 | 1.65 | 2 |
| 12,668 ± 48 | 10,890 ± 80 | 1.68 | 1 |
| 12,667 ± 48 | 10,990 ± 60 | 1.84 | 2 |
| 12,637 ± 47 | 10,770 ± 90 | 0.63 | 2 |
| 12,597 ± 46 | 10,780 ± 70 | 1.22 | 2 |
| 12,573 ± 47 | 10,440 ± 110 | 0.84 | 1, 3 |
| 12,567 ± 45 | 10,930 ± 70 | 1.71 | 2 |
| 12,527 ± 45 | 10,890 ± 120 | 0.51 | 2 |
| 12,467 ± 44 | 10,950 ± 190 | 0.16 | 2 |
| 12,427 ± 43 | 10,620 ± 70 | 1.66 | 2 |
| 12,387 ± 43 | 11,070 ± 70 | 1.44 | 2, 3 |
| 12,337 ± 43 | 10,560 ± 70 | 1.33 | 2 |
| 12,307 ± 42 | 10,640 ± 80 | 0.83 | 2 |
| 12,277 ± 42 | 10,550 ± 120 | 0.54 | 2 |
| 12,247 ± 42 | 10,390 ± 80 | 0.81 | 2 |
| 12,227 ± 41 | 10,530 ± 100 | 0.38 | 2 |
| 12,194 ± 41 | 11,230 ± 130 | 0.39 | 2, 3 |
| 12,188 ± 41 | 10,300 ± 100 | 0.56 | 1 |
| 12,183 ± 41 | 10,200 ± 100 | 0.51 | 1 |
| 12,178 ± 41 | 10,030 ± 250 | 0.17 | 1 |
| 12,169 ± 41 | 10,450 ± 120 | 0.76 | 1 |
| 12,167 ± 41 | 10,450 ± 80 | 0.62 | 2 |
| 12,135 ± 40 | 10,860 ± 180 | 0.20 | 2 |
| 12,107 ± 40 | 10,400 ± 90 | 0.65 | 2 |
| 12,087 ± 40 | 10,410 ± 160 | 0.85 | 2 |
| 12,057 ± 39 | 10,660 ± 110 | 0.44 | 2 |
| 12,027 ± 39 | 10,710 ± 220 | 0.15 | 2 |

| Cal BP | $^{14}C$ BP | mg C | Ref. |
|---|---|---|---|
| 12,012 ± 38 | 10,330 ± 110 | 0.34 | 2 |
| 12,007 ± 39 | 10,440 ± 80 | 1.44 | 2 |
| 11,987 ± 38 | 10,650 ± 100 | 0.52 | 2 |
| 11,963 ± 37 | 10,420 ± 90 | 1.19 | 1 |
| 11,957 ± 37 | 10,550 ± 80 | 1.16 | 2 |
| 11,948 ± 37 | 10,170 ± 100 | 0.96 | 1 |
| 11,927 ± 37 | 10,410 ± 70 | 2.00 | 2 |
| 11,907 ± 37 | 10,560 ± 100 | 0.52 | 2 |
| 11,887 ± 37 | 10,470 ± 100 | 0.69 | 2 |
| 11,884 ± 37 | 9600 ± 280 | 0.15 | 1 |
| 11,857 ± 37 | 10,450 ± 80 | 0.83 | 2 |
| 11,827 ± 37 | 10,390 ± 70 | 2.01 | 2 |
| 11,802 ± 37 | 10,470 ± 90 | 0.55 | 2 |
| 11,778 ± 36 | 9950 ± 120 | 0.59 | 1, 3 |
| 11,773 ± 36 | 9440 ± 80 | 1.00 | 1, 3 |
| 11,768 ± 36 | 10,340 ± 80 | 0.93 | 2 |
| 11,763 ± 36 | 10,510 ± 70 | 1.18 | 2 |
| 11,747 ± 36 | 10,310 ± 90 | 0.57 | 2 |
| 11,732 ± 36 | 9870 ± 150 | 0.36 | 1 |
| 11,717 ± 36 | 10,300 ± 80 | 0.73 | 2 |
| 11,708 ± 36 | 9870 ± 330 | 0.17 | 1 |
| 11,688 ± 36 | 10,320 ± 80 | 0.77 | 2 |
| 11,638 ± 36 | 10,040 ± 240 | 0.23 | 1 |
| 11,604 ± 36 | 9830 ± 100 | 0.52 | 1 |
| 11,538 ± 36 | 10,360 ± 160 | 0.33 | 1 |
| 11,524 ± 36 | 9970 ± 100 | 1.30 | 1 |
| 11,484 ± 36 | 10,050 ± 100 | 2.21 | 1 |
| 11,469 ± 36 | 9900 ± 90 | 1.84 | 1 |
| 11,443 ± 36 | 10,050 ± 90 | 0.80 | 1 |
| 11,411 ± 36 | 9750 ± 210 | 0.23 | 1 |
| 11,393 ± 36 | 9920 ± 90 | 0.84 | 1 |
| 11,393 ± 36 | 10,030 ± 100 | 0.56 | 1 |
| 11,361 ± 36 | 10,050 ± 120 | 0.83 | 1 |
| 11,343 ± 36 | 10,100 ± 80 | 2.06 | 1 |
| 11,303 ± 36 | 9950 ± 90 | 1.24 | 1 |
| 11,268 ± 36 | 10,020 ± 100 | 1.10 | 1 |
| 11,228 ± 36 | 9680 ± 80 | 0.86 | 1 |
| 11,183 ± 36 | 9760 ± 80 | 0.96 | 1 |
| 11,163 ± 36 | 9550 ± 120 | 0.35 | 1 |

| Cal BP | $^{14}C$ BP | mg C | Ref. |
|---|---|---|---|
| 11,113 ± 36 | 9700 ± 100 | 1.01 | 1 |
| 11,113 ± 36 | 9740 ± 90 | 1.24 | 1 |
| 11,063 ± 36 | 9600 ± 90 | 0.97 | 1 |
| 11,063 ± 36 | 9650 ± 110 | 2.60 | 1 |
| 11,021 ± 36 | 9410 ± 70 | 1.20 | 1 |
| 11,003 ± 36 | 9410 ± 120 | 0.31 | 1 |
| 10,983 ± 36 | 9600 ± 110 | 0.40 | 1 |
| 10,953 ± 36 | 9340 ± 100 | 0.78 | 1 |
| 10,943 ± 36 | 9560 ± 90 | 0.57 | 1 |
| 10,943 ± 36 | 9770 ± 120 | 0.66 | 1 |
| 10,913 ± 36 | 9730 ± 90 | 2.63 | 1 |
| 10,883 ± 36 | 9560 ± 90 | 1.69 | 1 |
| 10,843 ± 36 | 9670 ± 110 | 1.46 | 1 |
| 10,833 ± 36 | 9490 ± 90 | 0.88 | 1 |
| 10,783 ± 36 | 9430 ± 100 | 2.77 | 1 |
| 10,783 ± 36 | 9400 ± 100 | 0.77 | 1 |
| 10,743 ± 36 | 9590 ± 90 | 1.47 | 1 |
| 10,733 ± 36 | 9450 ± 90 | 2.40 | 1 |
| 10,683 ± 36 | 9420 ± 100 | 2.09 | 1 |
| 10,653 ± 36 | 9330 ± 100 | 1.40 | 1 |
| 10,648 ± 36 | 9410 ± 80 | 0.85 | 1 |
| 10,603 ± 36 | 9360 ± 80 | 0.69 | 1 |
| 10,598 ± 36 | 9210 ± 90 | 1.51 | 1 |
| 10,558 ± 36 | 9100 ± 110 | 0.69 | 1 |
| 10,548 ± 36 | 9280 ± 90 | 1.93 | 1 |
| 10,513 ± 36 | 9300 ± 80 | 1.02 | 1 |
| 10,503 ± 36 | 9190 ± 110 | 0.74 | 1 |
| 10,373 ± 36 | 9340 ± 110 | 1.24 | 1 |
| 10,328 ± 36 | 9160 ± 90 | 2.27 | 1 |

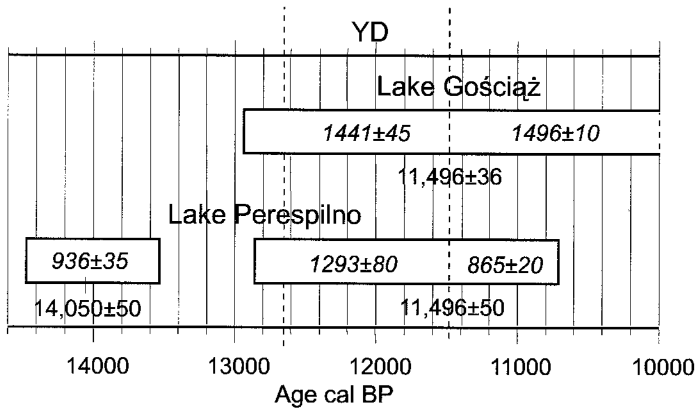


Figure 1 Range of the varve chronologies of Lake Gościąż and Lake Perespilno. Numbers of varves in the Late Glacial and early Holocene parts of sediments have been given within the bars. The numbers below the bars denote calendar ages of characteristic levels (YD/Holocene boundary and varve nr. 415 in the older Perespilno section) of separate sections.

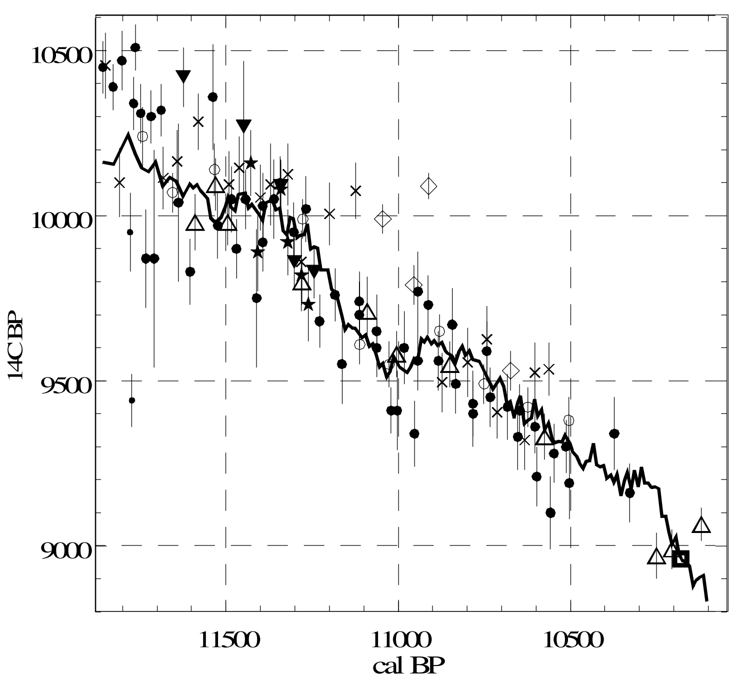


Figure 2 Comparison of $^{14}C$ ages from Lake Gościąż and Perespilno with the tree-ring $^{14}C$ calibration and other relevant data. $^{14}C$ ages are conventional ages in yr BP with statistical errors given at the 1σ level. — = the data from German pines (Kromer and Spurk 1998), ● = data from Lake Gościąż, ▼ = data from Lake Perespilno, ★ = data from Lake Perespilno, obtained in 2000, Δ = data from Barbados, Tahiti and Mururoa (Bard et al. 1998), ◊ = data from New Guinea (Edwards et al. 1993), O = data from Cariaco basin (Hughen et al. 1998), × = data from Lake Suigetsu, Japan (Kitagawa and van der Plicht 1998). □ denotes calendar and $^{14}C$ age of Saksunarvatn ash (Grönvold et al. 1995; Birks et al. 1996). The outlying Gościąż and Perespilno dates (Goslar et al. 2000) have been denoted by smaller symbols.

Table 2 Calendar and $^{14}C$ ages of terrestrial macrofossils from the laminated sediments of Lake Perespilno. All errors are 1σ. References: 1. Goslar et al. (1999a); 2. Goslar et al. (2000); 3. Outliers, not included in the discussion; 4. Samples used for comparison of mass-dependence of background correction, dated in 1996 (4a) and in 2000 (4b).

| Older section | | | | Younger section | | | |
|---|---|---|---|---|---|---|---|
| Cal BP | $^{14}C$ BP | mg C | Ref. | Cal BP | $^{14}C$ BP | mg C | Ref. |
| 14,455 ± 53 | 12,640 ± 110 | 0.69 | 2 | 12,852 ± 85 | 11,350 ± 200 | 0.79 | 2 |
| 14,435 ± 52 | 12,440 ± 130 | 0.36 | 2 | 12,832 ± 85 | 11,390 ± 100 | 0.66 | 2 |
| 14,415 ± 52 | 12,660 ± 130 | 0.38 | 2 | 12,812 ± 84 | 11,190 ± 70 | 1.14 | 1 |
| 14,395 ± 51 | 12,580 ± 120 | 0.73 | 2 | 12,792 ± 84 | 10,970 ± 100 | 0.70 | 2 |
| 14,375 ± 51 | 12,670 ± 110 | 0.43 | 2 | 12,772 ± 83 | 11,150 ± 80 | 0.88 | 2 |
| 14,355 ± 51 | 12,490 ± 110 | 0.63 | 2 | 12,772 ± 83 | 11,440 ± 130 | 0.32 | 2 |
| 14,335 ± 50 | 12,470 ± 70 | 1.37 | 1 | 12,753 ± 83 | 11,250 ± 70 | 2.40 | 1 |
| 14,315 ± 50 | 12,620 ± 110 | 0.45 | 2 | 12,734 ± 83 | 11,190 ± 100 | 0.53 | 2 |
| 14,295 ± 50 | 12,510 ± 90 | 0.77 | 1 | 12,715 ± 82 | 11,170 ± 90 | 0.55 | 2 |
| 14,265 ± 50 | 12,660 ± 130 | 0.41 | 2 | 12,715 ± 82 | 11,220 ± 100 | 0.45 | 2 |
| 14,265 ± 50 | 12,610 ± 110 | 0.54 | 2 | 12,685 ± 82 | 11,260 ± 100 | 0.70 | 2 |
| 14,225 ± 50 | 12,350 ± 110 | 0.44 | 2 | 12,654 ± 82 | 11,060 ± 90 | 0.96 | 1 |
| 14,215 ± 50 | 12,080 ± 90 | 0.74 | 2 | 12,294 ± 75 | 10,820 ± 70 | 1.38 | 1, 3 |
| 14,175 ± 50 | 12,260 ± 120 | 0.41 | 2 | 12,101 ± 45 | 10,560 ± 70 | 2.13 | 1 |
| 14,115 ± 50 | 12,180 ± 120 | 0.59 | 2 | 11,906 ± 45 | 10,510 ± 70 | 1.27 | 1 |
| 14,095 ± 50 | 12,330 ± 80 | 1.61 | 1 | 11,624 ± 45 | 10,420 ± 90 | 0.91 | 1 |
| 14,075 ± 50 | 12,350 ± 140 | 0.25 | 2 | 11,448 ± 45 | 10,270 ± 200 | 1.34 | 1, 4a |
| 14,075 ± 50 | 12,230 ± 140 | 0.29 | 2 | 11,428 ± 45 | 10,160 ± 100 | 0.64 | 4b |
| 14,055 ± 50 | 12,050 ± 90 | 0.79 | 2 | 11,408 ± 45 | 9890 ± 120 | 0.41 | 4b |
| 14,035 ± 50 | 12,120 ± 70 | 1.53 | 1 | 11,341 ± 46 | 10,090 ± 80 | 2.09 | 1, 4a |
| 13,995 ± 50 | 12,170 ± 100 | 0.58 | 2 | 11,341 ± 46 | 10,080 ± 80 | 1.76 | 4b |
| 13,975 ± 50 | 12,100 ± 100 | 0.51 | 2 | 11,321 ± 47 | 9920 ± 100 | 0.87 | 4b |
| 13,955 ± 50 | 12,140 ± 120 | 0.36 | 2 | 11,301 ± 47 | 9860 ± 80 | 1.72 | 1, 4a |
| 13,935 ± 50 | 12,030 ± 90 | 0.84 | 1 | 11,281 ± 47 | 9820 ± 110 | 0.36 | 4b |
| 13,831 ± 50 | 11,720 ± 110 | 0.60 | 2 | 11,261 ± 48 | 9730 ± 11 | 0.34 | 4b |
| 13,809 ± 50 | 11,860 ± 120 | 0.44 | 2 | 11,244 ± 48 | 9830 ± 80 | 1.09 | 1, 4a |
| 13,787 ± 51 | 12,110 ± 160 | 0.25 | 2 | | | | |
| 13,765 ± 52 | 11,710 ± 110 | 0.43 | 2 | | | | |
| 13,754 ± 52 | 11,790 ± 200 | 0.73 | 1 | | | | |
| 13,715 ± 52 | 11,620 ± 120 | 0.48 | 2 | | | | |
| 13,685 ± 52 | 11,780 ± 90 | 0.73 | 1 | | | | |

The younger section of LP sediments has been dated by synchronizing sharp changes of pollen spectra at the YD boundaries with those in the LG sediments (Goslar et al. 1999a). The uncertainty of synchronization, connected with time resolution of pollen data (± 25 yr), makes dating of LP sediments (11,496 ± 50 cal BP) less accurate than of the LG. The absolute age of the older LP section has been determined (Goslar et al. 2000) by wiggle-matching $^{14}C$ dates to the coral calibration data.

## RESULTS AND COMPARISON WITH OTHER CALIBRATION DATA

### Holocene Section (10,000–11,500 cal BP)

In the Holocene section, our data agree very well with the tree-ring calibration, and confirm the plateaux of the calibration curve at 10,000 and 9500 BP (Figure 2). The mean uncertainty of the $^{14}C$ age of the LG macrofossils can be assessed from the mean-square deviation of $^{14}C$ dates from the tree-ring $^{14}C$-calibration curve, which between 11.65 and 10.3 ka BP is 1.32 times the standard error (i.e. 130 yr on average). Systematic bias of the LG dates can be determined as a mean deviation from the calibration curve at the 10,000 and 9500 BP plateaux. These deviations (–25 yr for 11.65–11.3 ka BP and –10 yr for 11.1–10.8 ka BP) show that the systematic error of the LG dates is negligible.

In general, agreement between calibration data from different archives (tree rings—Kromer and Spurk 1998; Barbados corals—Bard et al. 1998; New Guinea corals—Edwards et al. 1993; sediments from Cariaco Basin, Atlantic—Hughen et al. 1998; and sediments from Lake Suigetsu, Japan —Kitagawa and van der Plicht 1998) is reasonable (except for two New Guinea dates around 11 ka BP, and one date from Suigetsu at around 11.1 ka BP), and the calibration curve in this section seems well established.

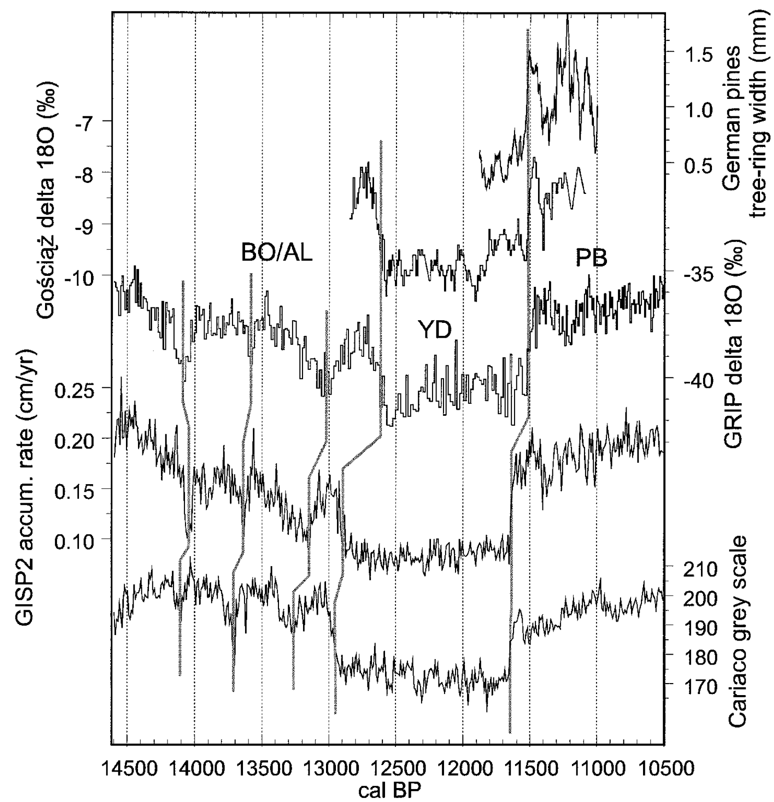


Figure 3 Comparison of calendar time scales of the records discussed in the text. The climatic events during the Late Glacial, common to all the records (e.g. boundaries of YD) have been marked by vertical lines.

### Late-Glacial Section of Lake Gościąż and Younger Lake Perespilno Sequence (11,500–13,000 cal BP)

In this section, the Gościąż and Perespilno dates indicate constant or even increasing $^{14}C$ age between 12.9 and 12.7 ka BP, rapid decline of $^{14}C$ age after the beginning of Younger Dryas (at 12.65 ka BP), and around 12 ka BP a long plateau at around 10,400 BP.

### *Comparison with Tree-Ring Calibration*

Before 11,650 cal BP, the LG data offset the pine curve significantly, much beyond the uncertainty of $^{14}C$ age. This might be due to some varves missing from the LG sequence, which seems difficult to accept as the LG chronology is replicated in several cores from three separate lake basins (e.g. Goslar 1998a). An alternative explanation is perhaps inadequate cross-correlation of the pine tree-ring sequences in the period, where few trunks are available, the tree-rings are very thin, and frequently missing (Spurk et al. 1998).

### *Comparison with Lake Suigetsu Data*

The LG and LP dates agree with those obtained on sediments from Lake Suigetsu (LS), Japan (Kitagawa and van der Plicht 1998). Most LS data (except one date at around 11.8 ka BP) fit the plateau at 10,400 BP, documented by our data between 12.2 and 11.8 ka BP (Figure 4), and show a similar slope of the calibration curve between 12.5 and 12.2 ka BP. Also before 12.5 ka BP, only one LS date (at around12.75 ka BP) is distinctly younger than those from LG and LP, and the group of LS dates between 12.9 and 13.2 ka BP continues the trend indicated by the LG and LP data. The deviation between the LS and LG/LP (Table 3) dates is insignificant during the millennium 12.5–11.5 ka BP, while before 12.5 ka BP, the LG/LP $^{14}C$ dates appear too old by about 150 years. However, both data sets may be reconciled within error limits of varve chronologies, e.g. shift of the LG/LP curve by 50 calendar years cancels that deviation almost completely (cf. Table 3). Another reason for the deviation could be systematic error of $^{14}C$ dates, because of admixture of rebedded macrofossils in the LG/LP samples, and partly because of problems (uncertainties?) with the background correction (cf. “Radiocarbon Dating” section). The systematic bias, however, seems constrained by the comparison of Cariaco and LG/LP dates, which agree quite well when synchronized (cf. further paragraph).

Table 3 Comparison between the Gościąż/Perespilno and other calibration data in the section 11,500–13,000 cal BP. The numbers give mean deviations of $^{14}C$ dates of given data set from the spline curve fitted to the LG/LP data (Goslar et al. 2000). Numbers of samples from each set and period have been denoted in parentheses. The values obtained when one date from LS (with LS-LG/LP = –460 yr) is omitted, are given in italics. All uncertainties are 1σ. Cor. = corals.

| Period (ka BP) | LS-LG/LP | LS-LG/LP[a] | Cor.-LG/LP | Cor.-LG/LP[a] | CB-LG/LP | CB[b]-LG/LP |
|---|---|---|---|---|---|---|
| Original values of reservoir correction[c] | | | | | | |
| 11.5–12.0 | −50 ± 75 (6) | 14 ± 74 (6) | −100 ± 89 (3) | −64 ± 96 (3) | −147 ± 90 (4) | −114 ± 51 (5) |
| 12.0–12.5 | −38 ± 67 (6) | 17 ± 72 (6) | −176 ± 100 (4) | −161 ± 96 (4) | −193 ± 64 (4) | −44 ± 33 (4) |
| 12.5–13.0 | −179 ± 71 (6)<br>*−134 ± 63 (5)* | −132 ± 66 (6)<br>*−97 ± 65 (5)* | −164 ± 52 (8) | −117 ± 64 (8) | −454 ± 70 (5) | −37 ± 56 (8) |
| INTCAL98 value of reservoir correction[d] | | | | | | |
| 11.5–12.0 | −50 ± 75 (6) | 14 ± 74 (6) | −241 ± 125 (3) | −205 ± 137 (3) | −241 ± 98 (3) | −194 ± 51 (5) |
| 12.0–12.5 | −38 ± 67 (6) | 17 ± 72 (6) | −201 ± 113 (4) | −186 ± 104 (4) | −260 ± 39 (5) | −124 ± 33 (4) |
| 12.5–13.0 | −179 ± 71 (6)<br>*−134 ± 63 (5)* | −132 ± 66 (6)<br>*−97 ± 65 (5)* | −323 ± 58 (8) | −276 ± 64 (8) | −524 ± 64 (5) | −117 ± 56 (8) |

[a]LG/LP curve shifted by 50 yr towards the older age

[b]CB and LG/LP chronologies synchronized at the AL/YD and YD/PB boundaries

[c]Reservoir correction of marine $^{14}C$ dates as in original publications (300 yr for Tahiti and Mururoa, 400 yr for Barbados, 420 yr for Cariaco, 500 yr for New Guinea)

[d]Reservoir correction according to the INTCAL98 calibration (Stuiver et al. 1998)

### *Comparison with Corals from Barbados, Tahiti, Mururoa and New Guinea*

The quality of agreement with coral $^{14}$C-calibration data depends on the "reservoir age" correction of coral $^{14}$C dates. Bard et al. (1998) used different corrections for corals from different sites (300 yr for Tahiti and Mururoa, and 400 yr for Barbados). A constant correction (400 yr) was also applied by Edwards et al. (1993) for the corals from New Guinea. On the other hand, in the INTCAL98 paper (Stuiver et al. 1998), the same coral data were used with the correction uniform over the whole tropical ocean, but variable in time (500 yr for samples older than 10,000 cal BP vs. 400 yr for younger samples).

The variation of reservoir correction (R) has been derived from comparison of coral and tree-ring $^{14}$C ages (Stuiver et al. 1998). Indeed, R—when averaged for all the sites—seems higher before than after 10,000 cal BP (Table 4). However, reservoir ages differ significantly between sites (except for the millennium 8–9 ka BP), which disagrees with the assumption of uniform R. The site-specific data show also that there is no reason to suspect that the reservoir ages in Barbados and Tahiti varied in the period considered. With the INTCAL98 value of R, all $^{14}$C ages from Barbados and Tahiti between 12 and 10 ka BP (11 points; cf. Figures 3 and 5 in Stuiver et al. 1998) appear younger than those of tree rings, which is an indication of a systematic error in the reservoir correction.

Table 4 Mean reservoir ages of corals from Barbados and Tahiti (Bard et al. 1998) and New Guinea (Edwards et al. 1993) derived from comparison with the tree-ring $^{14}$C calibration. Numbers of samples from each site and period are in parentheses. The values obtained when one outlying date from New Guinea (R = 900 ± 60 yr) is omitted, are given in italics. All uncertainties are 2σ.

| Period (ka BP) | Barbados | Tahiti | New Guinea | Whole |
|---|---|---|---|---|
| 8–9 | 360 ± 160 (1) | 370 ± 200 (1) | 360 ± 130 (2) | 360 ± 90 (4) |
| 9–10 | 430 ± 100 (2) | 220 ± 70 (4) | 500 ± 45 (3) | 420 ± 35 (9) |
| 10–11 | — | 290 ± 60 (5) | 700 ± 50 (4) | 530 ± 40 (9) |
| | | | *520 ± 70 (3)* | *380 ± 45 (8)* |
| 11–12 | 400 ± 100 (3) | 230 ± 90 (3) | 790 ± 170 (1) | 360 ± 60 (7) |
| Whole 8–12 | 400 ± 65 (6) | 260 ± 40 (13) | 580 ± 30 (10) | 450 ± 25 (29) |
| | | | *500 ± 40 (9)* | *400 ± 25 (28)* |

The LG and LP data do not differ much from those from the Barbados, Mururoa, and Tahiti corals when the original reservoir correction (Bard et al. 1998) is applied (Figure 4 and Table 3a), but deviate clearly from the coral data with R=500 yr (Figure 5 and Table 3b). This would support a site-specific, constant R, at least for the period after 13,000 cal BP. This converges with the earlier suggestion of low R (325 instead of 500 yr), derived from comparison between corals and Lake Suigetsu (Stuiver et al. 1998).

Further support for the original reservoir correction is given by dating of the Vedde ash layer, which has been identified in the GRIP core at 11,980 cal BP (Grönvold et al. 1995). This layer has been independently dated by $^{14}$C to 10,330 ± 30 BP (based on 11 AMS $^{14}$C ages from Bard et al. 1996 and Birks et al. 1996), which agrees with the coral date from Tahiti (at 11,930 cal BP) only when R=300 yr is applied (Figures 4 and 5).

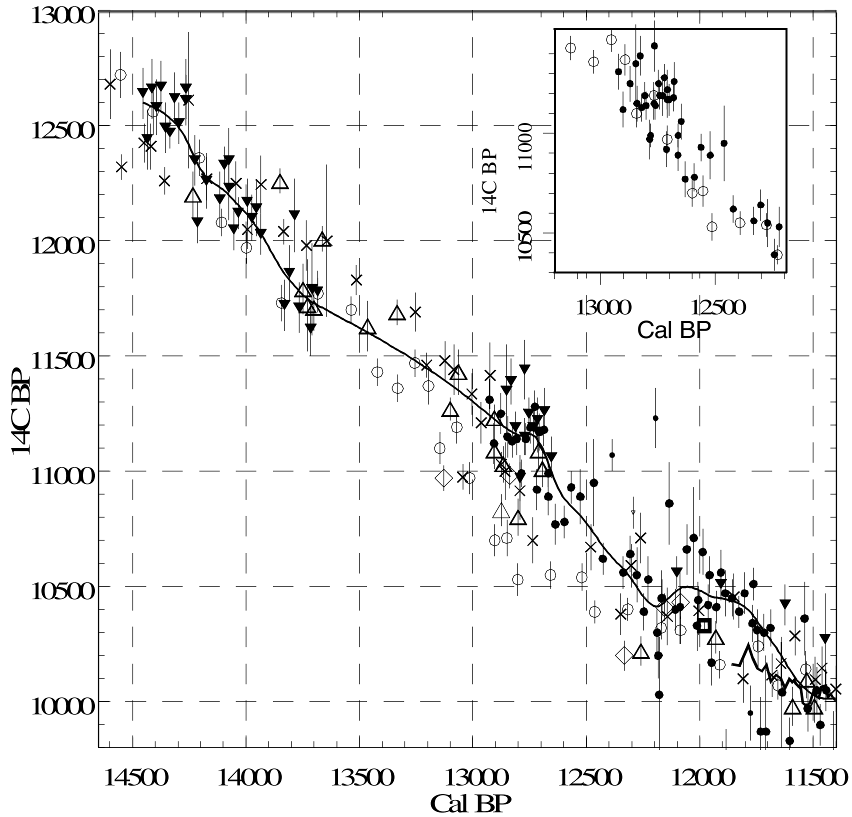


Figure 4 Comparison of $^{14}$C ages from Lake Gościąż and Perespilno with the $^{14}$C calibration data in the Late Glacial. For oceanic samples (corals and Cariaco basin sediments), values of reservoir correction published originally (i.e. by Bard et al. 1998, Edwards et al. 1993 and Hughen et al. 1998) were used. □ denotes calendar and $^{14}$C age of Vedde Ash (Grönvold et al. 1995; Birks et al. 1996), other symbols are as in Figure 2. Thin smooth line represents the spline function fitted to the LG and LP data (Goslar et al. 2000). The inset figure illustrates good correspondence of the $^{14}$C dates from Gościąż and Perespilno with Cariaco basin, when the Cariaco Allerød/YD transition (cf. Figure 3) is synchronized with that recorded in the LG sediments.

### *Comparison with Data from the Cariaco Basin*

Independent of the value of reservoir correction (Figures 4 and 5), $^{14}$C dates from the Cariaco basin (Hughen et al. 1998; Stuiver et al. 1998) in the period between 13 and 12.5 ka BP are significantly younger than the LG and LP dates. As indicated elsewhere (Goslar et al. 2000) this disagreement reflects the large difference between absolute ages of the AL/YD boundary in both archives (Figure 3) and disappears when the Cariaco and LG/LP chronologies are synchronized at the AL/YD transition (inset to Figure 4).

Chronologies of the LG and the Cariaco basin (CB) sediments are supported by those of the GRIP (Johnsen et al. 1992) and GISP2 (Alley et al. 1993, 1997) ice cores (Figure 2), respectively, which show distinct time lags between several events, too. Probably, some of the considered chronologies (either GRIP/LG or GISP2/CB) need an adjustment.

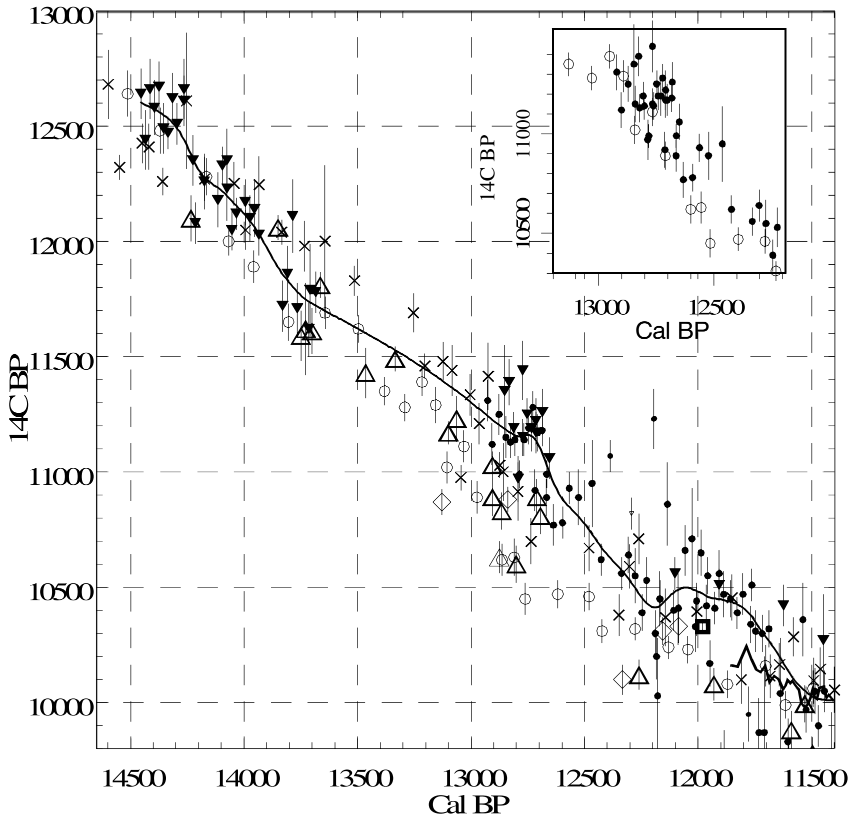


Figure 5 Comparison of $^{14}C$ ages from Lake Gościąż and Perespilno with the $^{14}C$ calibration data in the Late Glacial. For oceanic samples (corals and Cariaco basin sediments), the INTCAL98 version of reservoir correction (Stuiver et al. 1998) was used. Symbols are as in Figure 2. The inset figure illustrates correspondence of the $^{14}C$ dates from Gościąż and Perespilno with Cariaco basin, when the Cariaco Allerød/YD transition (cf. Figure 3) is synchronized with that recorded in the LG sediments.

The YD/Holocene boundaries in GRIP and Gościąż are synchronous with that found in German pines, while those in Cariaco and GISP2 are about 100 years older. The discrepancy between GISP2 and tree-ring chronologies is supported by the GISP2 $^{10}Be$ record (Finkel and Nishiizumi 1997) between 8 and 5 ka BP, which lags the dendro-dated record of atmospheric $^{14}C$ by about 100 years, too. As noted by Bard et al. (1998), the GRIP timescale is also confirmed through the Saksunarvatn ash layer, which has been identified in the GRIP core and dated to 10,180 (Grönvold et al. 1995). This layer has been independently dated by $^{14}C$ to 8960 ± 70 BP (based on three AMS $^{14}C$ ages from Birks et al. 1996), which perfectly fits the pine calibration curve (Figure 2).

In the Late Glacial, reliability of the GRIP and LG time scales is supported by the data from Lake Perespilno and German Maar lakes (Brauer et al. 1999 and this issue), all revealing significantly shorter duration of the Younger Dryas period (about 1150 years) than in the GISP2 and CB archives (about 1300 years). Moreover, $^{14}C$ dates of the oldest samples from LG agree with most of the dates from Lake Suigetsu (Figure 4, Table 3), while in the same period, and also in the preceding millennium, all the Cariaco dates are much younger than those of LS. On the other hand, comparison with the coral data is not too conclusive, as the deviations between LG/LP and coral and CB data distinctly depend on the model of reservoir age correction (cf. Tables 3a, 3b).

The arguments above seem to suggest that the GISP2 and CB time scales might be not adequate. This would imply that the maximum of atmospheric $^{14}C$ concentration at the beginning of Younger Dryas was smaller than previously believed (e.g. Goslar et al. 1999b; Hughen et al. 1998; Broecker 1997), and as argued by Goslar et al. (2000), it is explicable without ocean circulation changes. However, the reasons that could produce a too-long CB chronology, are difficult to imagine.

Synchronization of the CB and LG/LP records at the AL/YD transition completely cancels the discrepancy between $^{14}C$ dates from these archives, when the original value of reservoir correction for the CB (R=420 yr; Hughen et al. 1998) is applied (inset to Figure 4; Table 3a). With R=500 yr (Stuiver et al. 1998) the agreement is worse (inset to Figure 5; Table 3b), but still much better than without synchronization. This constrains the marine reservoir correction in the range between 500 yr (INTCAL98 value) and 400 yr (if the LG/LP $^{14}C$ ages are free of systematic bias), and the systematic bias of the LG/LP $^{14}C$ dates between 0 (no rebedded macrofossils) and about 100 years (if the INTCAL98 value of R is correct). It is worth noting that this finding is independent of whichever calendar (either the CB or LG/LP) is incorrect.

*Comparison with Vanuatu Corals*

The Lake Gościąż data document rather constant $^{14}C$ ages between 11.7 and 12.2 ka BP, which disagrees with data from Vanuatu corals (Figure 6). Surprisingly, variations of atmospheric $^{14}C$ suggested by the data from Vanuatu, are comparable or even stronger than that documented at the beginning of YD. The Vanuatu sequence is broken by three hiatuses, when the coral died off for some period. It is remarkable that $^{14}C$ declined rapidly in periods of coral growth, and in all four sections it was minimum just prior to the end of the growth period. It is improbable that the alternation of coral growth and die-off was in phase with $^{14}C$ variations by chance. One possible link between those two signals would be large changes of vertical oceanic circulation, but such changes are visible neither in paleoceanographic nor in paleoclimatic data. An alternative possibility is that the Vanuatu data are affected by changes of apparent $^{14}C$ age. As stated by Burr et al. (1998), the hiatuses could be an effect of emergence, which would raise the $^{14}C$ content of the coral due to recrystallization. However, no evidence of recrystallization was found (Burr et al. 1998).

The Vanuatu and LG data could be also reconciled if >300 varves were missing from the LG sequence at around 11.65 ka BP. However, adding 300 yr would make the Gościąż YD section 1450 yr long, in disagreement with what is known from any other archives. At any rate, an independent calibration data set with time resolution comparable to those from Vanuatu and LG is needed to resolve the problem.

**Older Lake Perespilno Sequence (>13,500 cal BP)**

The older LP section has been dated (Goslar et al. 2000) by the wiggle-match of $^{14}C$ dates to coral calibration data (Bard et al. 1998). The small uncertainty for that date (varve nr. 415 at 14,050 ± 50 cal BP) may be surprising, regarding that only a few coral dates in the period of overlap are available. However, the absolute age of LP section is tightly constrained by matching both ends of 12,150 BP plateau in the middle part of that section, with two coral points at around 13.8 and 14.2 ka BP (Figure 4).

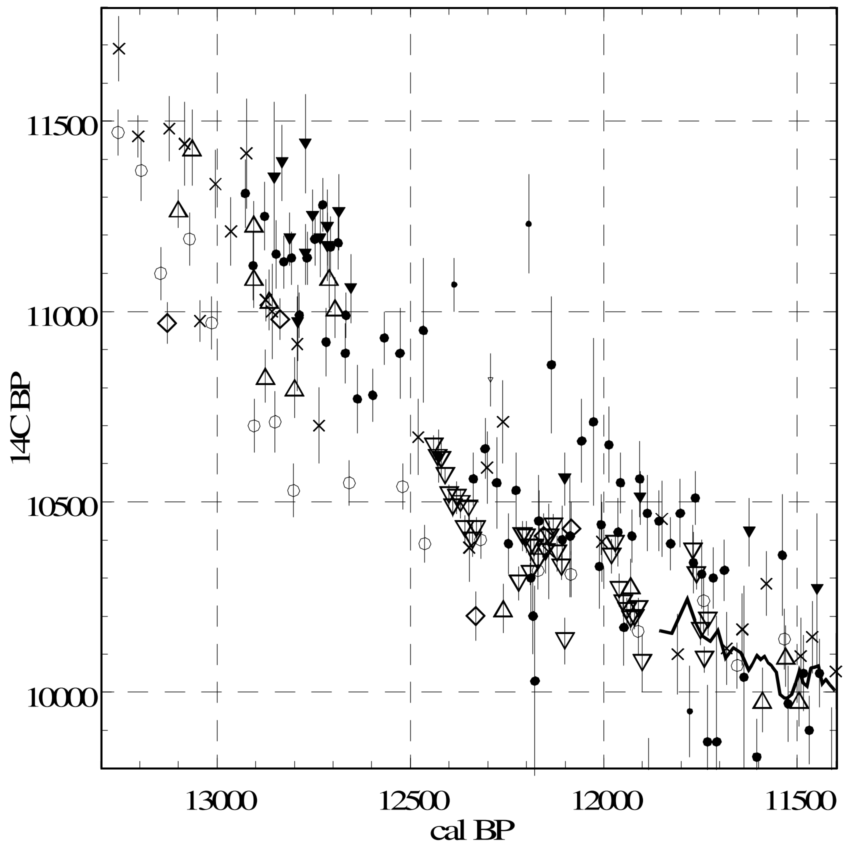


Figure 6 Comparison of $^{14}C$ ages from Lake Gościąż and Perespilno with the $^{14}C$ calibration data from Vanuatu corals. ∇ = data from Vanuatu (Burr et al. 1998), other symbols as in Figure 2.

An additional uncertainty of that match is introduced by the not exactly known reservoir age of the corals. Indeed, the match to the coral data with R=500 yr (Stuiver et al. 1998) makes the age of LP younger by 95 yr, but as argued above the R=500 yr model seems problematic.

An independent check of the LP dating is possible through the match to the Lake Suigetsu data, which makes the LP 55 years younger, and to the Cariaco Basin dates, which makes it 65 or 60 yr (depending on whether the R=420 or R=500 yr model is used) older than 14,050 cal BP. Both matches appear more precise than those with corals, since more data points were involved in the match. On the other hand, accuracy of absolute dating through those matches is limited by uncertainty of calendar age of the LS and CB samples. The uncertainty of chronology of the CB sediments around the AL/YD boundary was discussed in the former chapter. This had been connected with large discrepancy between the CB/GISP2 and LG/GRIP chronologies around 12.8 ka BP (Figure 3). Around 14 ka BP, all chronologies converge, making the CB time scale quite confident in that period. For all the reasons above we maintain the original date of the LP sequence.

The general slope of $^{14}C$-calibration curve documented by our data seems a bit higher than that reflected with the Suigetsu set, but it agrees very well with that shown by the Cariaco points. Moreover, our data reveal three periods of rather constant $^{14}C$ age at 12,500, 12,100–12,200, and

11,700 BP, separated by rapid declines of $^{14}C$ age around 14.2 and 13.9 ka BP. This has not been shown by previous reconstructions, as they covered the relevant time span too sparsely.

## CONCLUSION

Except for a few outliers, the $^{14}C$ dates of terrestrial macofossils from Lakes Gościąż and Perespilno constitute a self-consistent set of $^{14}C$ calibration data, which covers the time span 12,900–10,300 cal BP and 14,450–13,700 cal BP, respectively. These data agree very well with the German pine calibration curve, and other calibration data in the Holocene section.

In the Late Glacial, the scatter of calibration data from different archives is distinct. In the period 13,000–11,500 cal BP our data agree with those from Lake Suigetsu, and indicate a constant or even increasing $^{14}C$ age between 12.9 and 12.7 ka BP, a rapid decline of $^{14}C$ age after the beginning of Younger Dryas, and a long plateau 10,400 BP around 12 ka BP. Correlation with corals seems to support the values of the reservoir correction used originally by Bard et al. (1998) and Edwards et al. (1993), in contradiction to those introduced in the INTCAL98 calibration (Stuiver et al. 1998). Around the Allerød/Younger Dryas boundary our data disagree with $^{14}C$ dates from Cariaco basin, which beyond any doubt reflects large discrepancy between calendar chronologies of GRIP/Gościąż/Perespilno and GISP2/Cariaco archives at that period. We argue the Gościąż chronology to be correct, though the deviation of the Cariaco time scale is not easy to imagine. Unlike the corals from Vanuatu, our data do not reveal large fluctuations of $^{14}C$ age between 12.4 and 11.7 ka BP, which could reflect variations of apparent age of Vanuatu corals. There is no fundamental argument to choose any set of $^{14}C$ calibration data for that period.

The older sequence from Lake Perespilno confirms the general slope of the $^{14}C$-calibration curve between 14.5 and 13.7 ka BP, documented by the data from Suigetsu and Cariaco, and indicates a rapid decline of $^{14}C$ age around 14.2 and 13.9 ka BP.

## ACKNOWLEDGMENTS

The authors wish to thank R Alley for sharing the data on the GISP2 accumulation rate, K Hughen for the $^{14}C$ calibration data and the grey-scale record of the Cariaco sediments, S Johnsen and C Hammer for the data on the GRIP time scale, and M Spurk for the data on the German pine tree-ring thickness. The work of TG has been sponsored by the Polish Committee for Scientific Research, through the grant 6 P04E 046 16, and AMS $^{14}C$ dating by the French Centre National de la Recherche Scientifique et Commissariat de l'Energie Atomique. TG wishes to thank K Więckowski (retired), A Walanus, A Rakowski, J Pawlyta (Silesian University Techn., Gliwice), and K Bałaga (M Curie-Skłodowska University, Lublin, Poland), for their kind help in raising the sediment cores. The terrestrial macrofossils have been separated with the help of D Moszyńska-Moskwa, Z Tomczyńska, M Zurzycka (Szafer Inst. Bot., Kraków) and J Czernik (Silesian University Techn., Gliwice). Some macrofossils have been identified by D Demske (currently at Freie University Berlin).

## REFERENCES

Alley RB, Meese DA, Shuman CA, Gow AJ, Taylor KC, Grootes PM, White JWC, Ram M, Waddington ED, Mayewski PA, Zielinski GA. 1993. Abrupt increase in Greenland snow accumulation at the end of the Younger Dryas event. *Nature* 362:527–9.

Alley RB, Shuman CA, Meese DA, Gow AJ, Taylor KC, Cuffey KM, Fitzpatrick JJ, Grootes PM, Zielinski GA, Ram M, Spinelli G, Elder B. 1997. Visual-stratigraphic dating of the GISP2 ice core: basis, reproducibility, and application. *Journal of Geophysical Research* C102:26,367–81.

Arnold M, Bard E, Maurice P, Valladas H, Duplessy JC. 1989. C-14 dating with the Gif-sur-Yvette Tandetron accelerator: status report and study of isotopic fractionations in the sputter ion source. *Radiocarbon* 31(2):191–9.

Bard E, Arnold M, Mangerud J, Paterne M, Labeyrie L, Duprat J, Melieres MA, Sonstegaard E, Duplessy JC. 1994. The North Atlantic atmosphere-sea surface $^{14}C$ gradient during the Younger Dryas climatic event. *Earth and Planetary Science Letters* 126:275–87.

Bard E, Arnold M, Hamelin B, Tisnerat-Laborde N, Cabioch G. 1998. Radiocarbon calibration by means of mass spectrometric $^{230}Th/^{234}U$ and $^{14}C$ ages of corals: an updated database including samples from Barbados, Mururoa and Tahiti. *Radiocarbon* 40(3):1085–92.

Birks HH, Gulliksen S, Haflidason H, Mangerud J, Possnert G. 1996. New radiocarbon dates for the Vedde Ash and Saksunarvatn Ash from Western Norway. *Quaternary Research* 45:119–27.

Brauer A, Endres CH, Günter C, Litt T, Stebich M, Negendank JFW. 1999. High resolution sediment and vegetation responses to Younger Dryas climate change in varved lake sediments from Meerfelder Maar, Germany. *Quaternary Science Reviews* 18:321–9.

Broecker WS. 1997. Thermohaline circulation, the Achilles Heel of our climate system: will man-made $CO_2$ upset the current balance? *Science* 278:1582–8.

Burr GS, Warren Beck J, Taylor FW, Recy J, Edwards RL, Cabioch G, Correge T, Donahue D, O'Malley JM. 1998. A high-resolution radiocarbon calibration between 11,700 and 12,400 calendar years BP derived from $^{230}Th$ ages of corals from Espiritu Santo Island, Vanuatu. *Radiocarbon* 40(3):1093–1106.

Edwards RL, Warren Beck J, Burr GS, Donahue DJ, Chappell JMA, Bloom AL, Druffel ERM, Taylor FW. 1993. A large drop in atmospheric $^{14}C/^{12}C$ and reduced melting in the Younger Dryas, documented with $^{230}Th$ ages of corals. *Science* 260:962–8.

Finkel RC, Nishiizumi K. 1997. Beryllium 10 concentrations in the Greenland Ice Sheet Project 2 ice core from 3-40 ka. *Journal of Geophysical Research* 102: 26,699–706.

Goslar T, Kuc T, Ralska-Jasiewiczowa M, Różański, K, Arnold M, Bard E, van Geel B, Pazdur MF, Szeroczyńska K, Wicik B, Więckowski K, Walanus A. 1993. High-resolution lacustrine record of the Late Glacial/ Holocene transition in Central Europe. *Quaternary Science Reviews* 12:287–94.

Goslar T, Arnold M, Bard E, Kuc T, Pazdur MF, Ralska-Jasiewiczowa M, Tisnerat N, Różański K, Walanus A, Wicik B, Więckowski K. 1995. High concentration of atmospheric $^{14}C$ during the Younger Dryas cold episode. *Nature* 377:414–7.

Goslar T. 1998a. Late-glacial sediments of Lake Gościąż chronological background. In: Ralska-Jasiewiczowa M, Goslar T, Madeyska T, Starkel L, editors. *Lake Gościąż, central Poland. A monographic study, part 1*: 119–24. Kraków: Szafer Institute of Botany.

Goslar T. 1998b. Floating varve chronology of Lake Gościąż. In: Ralska-Jasiewiczowa M, Goslar T, Madeyska T, Starkel L, editors. *Lake Gościąż, central Poland. A monographic study. Part 1*: 97–9. Kraków: Szafer Institute of Botany.

Goslar T, Bałaga K, Arnold M, Tisnerat N, Starnawska E, Kuźniarski M, Chróst L, Walanus A, Więckowski K. 1999a. Climate-related variations in the composition of the Late Glacial and early Holocene sediments of Lake Perespilno (eastern Poland). *Quaternary Science Reviews* 18:899–911.

Goslar T, Wohlfarth B, Björck S, Possnert G, Björck J. 1999b. Variations of atmospheric $^{14}C$ concentrations over the Alleröd-Younger Dryas transition. *Climate Dynamics* 15:29–42.

Goslar T, Arnold M, Tisnerat-Laborde N, Czernik J, Więckowski K. 2000. Variations of Younger Dryas atmospheric radiocarbon explicable without ocean circulation changes. *Nature* 403:877–80.

Goslar T, Mądry W. 1998. Using the Bayesian method to study the precision of dating by the "wiggle-matching" procedure. *Radiocarbon* 40(1):551–60.

Grönvold K, Oskarsson N, Johnsen SJ, Clausen HH, Hammer CU, Bond G, Bard E. 1995. Ash layers from Iceland in the Greenland GRIP ice core correlated with oceanic and land sediments. *Earth and Planetary Science Letters* 135:149–55.

Hughen KA, Overpeck JT, Peterson LC, Trumbore S. 1996. Rapid climate changes in the tropical Atlantic region during the last deglaciation. *Nature* 380:51–4.

Hughen KA, Overpeck JT, Lehman SJ, Kashgarian M, Southon J, Peterson LC, Alley R, Sigman D. 1998. Deglacial changes in ocean circulation from an extended radiocarbon calibration. *Nature* 391:65–8.

Johnsen SJ, Clausen HB, Dansgaard W, Fuhrer K, Gundestrup N, Hammer CU, Iversen P, Jouzel J, Stauffer B, Steffensen JP. 1992. Irregular glacial interstadials recorded in a new Greenland ice core. *Nature* 359:311–3.

Kitagawa H, van der Plicht J. 1998. Atmospheric radiocarbon calibration to 45,000 yr B.P.: Late Glacial fluctuations and cosmogenic isotope production. *Science* 279:1187–90.

Kromer B, Becker B. 1993. German oak and pine $^{14}C$ calibration, 7200-9439 BC. *Radiocarbon* 35(1):125–35.

Kromer B, Spurk M. 1998. Revision and tentative extension of the tree-ring based $^{14}C$ calibration, 9200-11,855 cal BP. *Radiocarbon* 40(3):1117–26.

Ralska-Jasiewiczowa M, Demske D, van Geel B. 1998. Late-glacial vegetation history recorded in the Lake Gościąż sediments. In: Ralska-Jasiewiczowa M, Goslar T, Madeyska T, Starkel L, editors. *Lake Gościąż, central Poland. A monographic study, part 1.* Kraków: Szafer Institute of Botany. p 128–43.

Spurk M, Friedrich M, Hofmann J, Remmele S, Frenzel B, Leuschner HH, Kromer B. 1998. Revisions and extension of the Hohenheim oak and pine chronologies: new evidence about the timing of the Younger Dryas/ Preboreal transition. *Radiocarbon* 40(3):1107–16.

Stuiver M, Reimer PJ, Bard E, Warren Beck J, Burr GS, Hughen KA, Kromer B, McCormac G, van der Plicht J, Spurk M. 1998. INTCAL98 Radiocarbon age calibration, 24,000-0 cal BP. *Radiocarbon* 40(3):1041–83.

RADIOCARBON, Vol 42, Nr 3, 2000, p 349–353 

# RADIOCARBON DATING OF VARVE CHRONOLOGIES: SOPPENSEE AND HOLZMAAR LAKES AFTER TEN YEARS

Irka Hajdas • Georges Bonani

Institut für Teilchenphysik, ETH Hönggerberg, 8093 Zurich, Switzerland. Email: hajdas@particle.phys.ethz.ch.

Bernd Zolitschka

Geomorphologie und Polarforschung (GEOPOL), Institut für Geographie, Universitaet Bremen, Celsiusstr. FVG-M, D-28359 Bremen, Germany

**ABSTRACT.** During the last decade, several radiocarbon-dated varve chronologies have been produced. The main goal at first was the extension of the $^{14}C$ calibration curve beyond 10,000 BP. This paper aims to discuss varve chronologies of Soppensee and Holzmaar Lakes. Although both chronologies encountered problems, high-resolution $^{14}C$ dating and relative varve time have been obtained for events during the Late Glacial.

## INTRODUCTION

Twenty years ago, Bernd Becker and Bernd Kromer were working on a link between German oak and pine in order to extend the tree-ring calibration curve (Becker and Kromer 1986). Around that time, a series of samples consisting of terrestrial macrofossils, which were preserved in sediments, were dated by accelerator mass spectrometry (AMS) (Andrée et al. 1986; Zbinden 1987; Zbinden et al. 1989). This showed that variations in the atmospheric $^{14}C$ content of the past could be reconstructed by dating terrestrial macrofossils. Laminated lake sediments were considered to be most suitable for precise dating. Sediments recovered from Soppensee, a small lake in Switzerland, appeared to contain varves (annual laminations) and sufficient amounts of terrestrial macrofossils (Lotter 1989). Laminations were present in the Late Glacial (LG) part of the record and the first 3000 years of the Holocene. Varve chronologies were constructed, and terrestrial macrofossils were dated and combined to a $^{14}C$–varve chronology. Because the laminations in the LG part of the record were not continuous, corrections had to be applied to the varve chronology (Hajdas et al. 1993).

The varve chronology of Lake Holzmaar (Germany) has been developed earlier and independently of the Soppensee chronology (Zolitschka 1990). $^{14}C$ dating of the Holzmaar record seemed to be a sufficient cross-check for the Soppensee chronology. In both records, a layer of ash from a volcanic eruption of the Laacher See (LST) was present. This allowed the correlation of these records. After correcting the late Holocene sediments of the Holzmaar varve chronology, both records showed a close correlation (Hajdas 1993). During the last ten years, new records have been established, refining the dating of the LG period (Goslar et al. 1995; Hughen et al. 1998a, 1998b). Here we present an assessment of an error in the varve chronologies for both the Soppensee and Holzmaar records. $^{14}C$ chronologies remain valid and allow reconstruction of atmospheric $^{14}C$ variations during the LG.

### Soppensee

The $^{14}C$ time scale for sediments of Soppensee is based on AMS dating of terrestrial macrofossils. High resolution $^{14}C$ dating was performed on sediments between 7000 and 10,000 BP. Because the sediment in Soppensee is not laminated from the top, a floating $^{14}C$-varve chronology was constructed. Fifty $^{14}C$ dates were paired with relative varve ages and were matched to the calibration curve in order to establish the absolute time scale. The chronology beyond 10,000 BP was based on 31 $^{14}C$ dates and a corrected varve chronology (Hajdas et al. 1993). Figure 1 shows the Soppensee $^{14}C$ varve chronology, plotted with the most recent tree-ring chronology (Kromer and Spurk 1998). The agreement between the Holocene part of the varve chronology and the tree rings shows that the combination of varve chronologies and $^{14}C$ dating of terrestrial macrofossils can be used for precise time control. The $^{14}C$ plateaux at 8250, 8750, 9600, and 10,000 BP are clearly reproduced in the Soppensee chronology. Earlier in 1993, there was an indication in the varve chronology for a plateau at 8900 BP (Hajdas 1993). Also, the younger flank of the 10 ka plateau in the Soppensee chronology suggested a need for a correction of the tree-ring chronology at the time (Hajdas 1993). Problems in the Soppensee record arise at the Younger Dryas (YD) biozone and the presence of unlaminated segments in this part of the record. Correction for their presence was based on an estimation of the sedimentation rate. This resulted in a number of 550 varves, that had to be added to the YD biozone. The duration of the YD in the Soppensee was very close to the duration found in the GRIP ice core (1150 yr; Johnsen et al. 1992) and the Gościąż varve chronology (1140 yr; Goslar et al. 1995). Therefore, at that time, it appeared that our correction for unlaminated sediments was adequate. Figure 1 shows the chronology, with boundaries of the YD biozone as defined by palynology. The Younger Dryas/Preboreal (YD/PB) boundary in Soppensee is about 600 years younger than the same boundary dated in other European records (Goslar et al. 1995; Björck et al. 1996). As a result, a part of the European Preboreal (PB) was included into our YD chronology and obscured underestimation of the correction discussed above. As shown in Figure 1, additional 500–600 years should be included in the Soppensee chronology of the YD biozone. This correction in the Soppensee chronology now results in an age of 12,850 cal BP for an age for the LST layer. A similar age of 12,880 cal BP for the LST is determined by recent dating of the Meerfelder Maar (MFM) varve chronology and deduced from the dating of the YD boundaries in ice cores of Greenland (Brauer et al. 1999; Brauer et al. this issue; von Grafenstein et al. 1999).

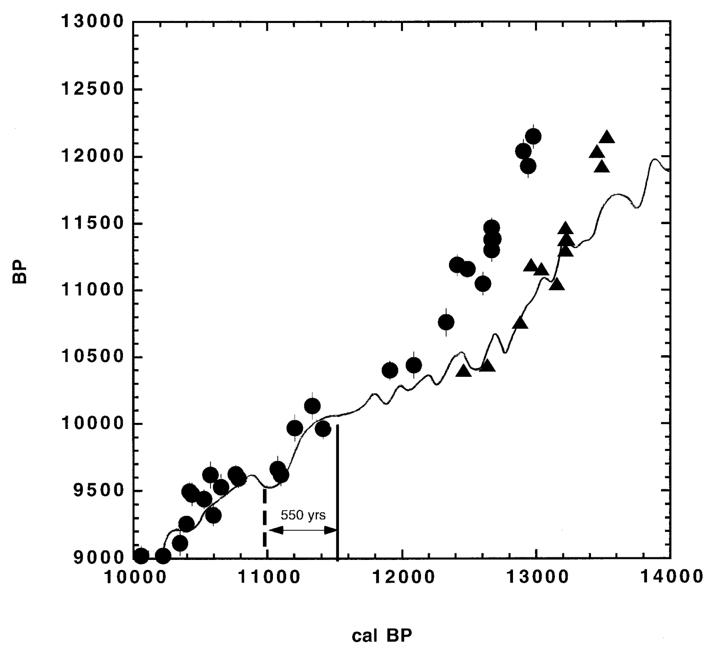


Figure 1 Soppensee $^{14}C$-varve chronology (filled circles) plotted with INTCAL98 (all the points with one sigma uncertainty) (Stuiver et al. 1998). The solid line marks the end of the YD according to the European records at 11,550 cal BP (see text). The line through the data points shows the end of the YD biozone as defined in Soppensee at 10,986 cal BP. Triangles show the Soppensee chronology with additional 550 yr added to all the points beyond 12,000 cal BP.

### Holzmaar

Terrestrial macrofossils were washed from the sediment and $^{14}C$ dated using AMS. Next, the $^{14}C$ ages were paired with the corresponding varve time as published by Zolitschka (1990). The sediment in the Holzmaar cores is laminated from the top, but comparison of the $^{14}C$–varve chronology with the calibration curve yielded an error in the varve chronology of the late Holocene. The shift between 2000 and 3838 cal BP has been corrected for 878 varve years; the rest of the Holocene remained in very good agreement with the tree-ring chronology (Hajdas et al. 1995). Although the Holzmaar chronology was concordant with the Soppensee chronology, there was a difference in duration of the YD. The YD in Holzmaar was defined by a change in sediment: 550 yr (11,940–11,490 cal BP), i.e. about 600 yr shorter than the YD in the GRIP ice core and the Lake Gościąż sediments (Johnsen et al. 1992; Goslar et al. 1995). Additional samples were dated to identify the 10 ka and 9.5 ka plateaux (Table 1) in the Holzmaar chronology. Recently, the varve chronology of Holzmaar has been corrected for varves missing in the YD biozone, i.e. beyond the YD/PB transition, which was dated to be 11,490 cal BP (Hajdas et al. 1995). Also, new pollen analysis showed that varves were missing inside the YD biozone (Leroy et al. 2000), suggesting the need for a correction of 320 varves beyond 12,025 cal BP.

Table 1 AMS $^{14}C$ dates obtained on macrofossils selected from Holzmaar sediment core in order to reconstruct 10,000 BP plateau

| Lab nr (ETH-) | Sample (HZM-) | Core depth | $^{14}C$ age (BP) | $\delta^{13}C$ (PDB ‰) | Material dated |
|---|---|---|---|---|---|
| 13503 | 40 | 871.3 | 9550 ± 80 | −23.1 ± 1.2 | Bark |
| 13504 | 41 | 876 | 9665 ± 100 | −24.7 ± 1.2 | Bark, seeds, catkin scale, needle fragments |
| 13505 | 42 | 878.8 | 9565 ± 110 | −21.4 ± 1.3 | Seeds, bark |
| 13506 | 43 | 886 | 9830 ± 100 | −20.6 ± 1.3 | Needle, bark, seeds |
| 13507 | 44 | 890.5 | 9805 ± 190 | −19.0 ± 1.5 | Bark |
| 13508 | 45 | 895 | 9905 ± 80 | −28.7 ± 1.2 | Bark |
| 13509 | 46 | 897.5 | 10,060 ± 80 | −27.8 ± 1.3 | Macrofossils: bark, seeds, catkin scale |
| 13510 | 47 | 899.9 | 10,110 ± 110 | −24 ± 1.2 | Macrofossils: bark, seeds, needle |
| 13511 | 48 | 903.7 | 11,040 ± 140 | −17.1 ± 1.2 | Macrofossils |
| 13512 | 49 | 920.2 | 10,090 ± 85 | −26.0 ± 1.2 | Macrofossils: needles, Betula seeds, catkin scale, piece of wood or bark |
| 13513 | 50 | 929.7 | 10.080 ± 110 | −24.1 ± 1.2 | Macrofossils: twig fr., needle fr., leaf fr. |
| 13514 | 51 | 942 | 10,350 ± 90 | −26.2 ± 1.3 | Macrofossils: twig, small pieces of needles, well-preserved bark |

In Figure 2, $^{14}C$ dates are plotted together with the newly corrected varve ages (Zolitschka, forthcoming). When compared with the INTCAL98 recommended calibration curve (Stuiver et al. 1998), this correction still appears to be an underestimation, but a better agreement has been obtained with all other chronologies of the LG. The best illustration of the agreement with the GRIP ice core chronology is the age of the LST layer. Brauer et al. (1999) demonstrated that the varve chronology of lake MFM dates the LST to 12,880 cal BP. The eruption of the Lacheer See preceded the YD cooling by some 200 years (Hajdas et al. 1995). Therefore, the age of the LST should be between 12,800 and 13,000 cal BP, based on the timing of the Alleröd/Younger Dryas (AL/YD) transition as found in both the GRIP and GISP2 ice cores. The calibrated age of the LST ranges between 13,000 and 13,200 cal BP (the $^{14}C$ date is 11230 ± 40 BP). The difference of about 200 years between European records (MFM, Gościąż) and calibrated age of the LST corresponds to the difference in length of the YD in GRIP and GISP2, 1150 and 1300 years, respectively. The INTCAL98 calibration data, which are based on U/Th dated corals and Carioco basin varve chro-

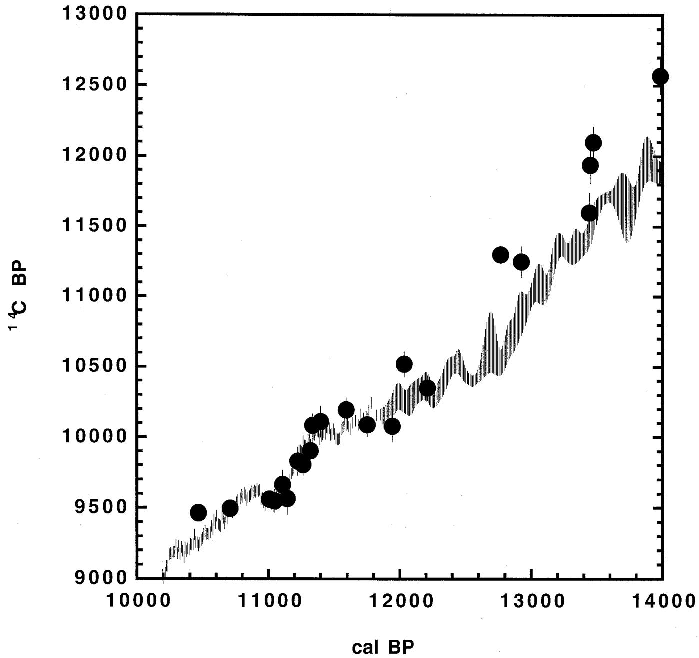


Figure 2 Holzmaar $^{14}C$ chronology plotted against the corrected varve chronology (Zolitschka, forthcoming) and the INTCAL98 calibration curve (Stuiver et al. 1998). Additional $^{14}C$ dates were obtained to reconstruct the $^{14}C$ plateau at 10,000 BP (Table 1).

nology (Stuiver et al. 1998), are closer to the GISP2 chronology. However, the agreement between European records and the GRIP chronology is striking (Brauer et al. 1999; von Grafenstein et al. 1999; Goslar et al. 2000). Nevertheless, the difference in the YD duration as well as dating of the YD boundaries in both ice cores should be minimized.

## CONCLUSION

The chronologies of both Soppensee and Holzmaar represent the first attempts to extend the calibration curve by using varve chronologies. Both lake records contributed to a chronology of the last deglaciation and to the reconstruction of the atmospheric $^{14}C$ content, despite problems as discussed in this paper. This was only possible because of the high-resolution $^{14}C$ dating of these records. Characteristic features of the $^{14}C$ calibration curve (such as plateaux) can also be seen in unlaminated sediments and can be used for correlation between records and dating of events (Hajdas et al. 1998). Therefore it seems that $^{14}C$ dating is a necessary assessment for all varve chronologies. Further extension of the $^{14}C$ calibration curve will require $^{14}C$ dating of a perfectly laminated record. Although perfect laminations exist, only an agreement between many sites can result in a final calibration curve.

## REFERENCES

Andrée M, Oeschger H, Siegenthaler U, Ammann B, Tobolski K. 1986. $^{14}C$ dating of macrofossils in lake sediments. *Radiocarbon* 28(2A):411–6.

Becker B, Kromer B. 1986. Extension of the Holocene dendrochronology by the Preboreal pine series, 8800 to 10,100 BP *Radiocarbon* 28(2B):961–7.

Björck S, Kromer B, Johnsen S, Bennike O, Hammarlund D, Lemdahl G, Possnert G, Rasmussen TL, Wohlfarth B, Hammer CU, Spurk M. 1996. Synchronized terrestrial-atmospheric deglacial records around the North Atlantic. *Science* 274:1155–60.

Brauer A, Endres C, Gunter C, Litt T, Stebich M, Negendank J. 1999. High resolution sediment and vegetation responses to Younger Dryas climate change in varved lake sediments from Meerfelder Maar, Germany. *Quaternary Science Reviews* 18:321–9.

Brauer A, Endres C, Zolitschka B, Negendank JFW. 2000. AMS radiocarbon and varve chronology from the annually laminated sediment record of lake Meerfelder Maar, Germany. *Radiocarbon*. This issue.

Goslar T, Arnold M, Bard E, Kuc T, Pazdur M, Ralska-Jasiewiczowa M, Rozanski K, Tisnerat N, Walanus A, Wicik B, Wieckowski K. 1995. High concentration of atmospheric $^{14}C$ during the Younger Dryas. *Nature* 377:414–7.

Goslar T, Arnold M, Tisnerat LN, Czernik J, Wieckowski K. 2000. Variations of Younger Dryas atmospheric radiocarbon explicable without ocean circulation changes. *Nature* 403:877–80.

Hajdas I. 1993. Extension of the radiocarbon calibration curve by AMS dating of laminated sediments of lake Soppensee and lake Holzmaar. *Diss. ETH* Nr.10157, ETH Zurich.

Hajdas I, Bonani G, Boden P, Peteet DM, Mann DH. 1998. Cold reversal on Kodiak Island, Alaska, correlated with the European Younger Dryas by using variations of atmospheric C-14 content. *Geology* 26: 1047–50.

Hajdas I, Ivy SD, Beer J, Bonani G, Imboden D, Lotter AF, Sturm M, Suter M. 1993. AMS radiocarbon dating and varve chronology of lake Soppensee: 6000 to 12,000 $^{14}C$ years BP. *Climate Dynamics* 9:107–16.

Hajdas I, Ivy SD, Bonani G, Lotter AF, Zolitschka B, Schlüchter C. 1995. Radiocarbon age of the Laacher See Tephra: 11,230 ± 40 BP. *Radiocarbon* 37(2):149–54.

Hajdas I, Zolitschka B, Ivy SD, Beer J, Bonani G, Leroy SAG, Ramrath M, Negendank JFW, Suter M. 1995. AMS radiocarbon dating of annually laminated sediments from lake Holzmaar, Germany. *Quaternary Science Reviews* 14:137–43.

Hughen KA, Overpeck JT, Lehman SJ, Kashgarian M, Southon JR. 1998a. A new $^{14}C$ calibration data set for the last deglaciation based on marine varves. *Radiocarbon* 40(3):1483–94.

Hughen KA, Overpeck JT, Lehman SJ, Kashgarin M, Southon J, Peterson LC, Alley R, Sigman DM. 1998b. Deglacial changes in ocean circulation from an extended radiocarbon calibration. *Nature* 391:65–8.

Johnsen SJ, Clausen HB, Dansgaard W, Iversen P, Jouzel J, Stauffer B, Steffensen JP. 1992. Irregular glacial interstadials recorded in a new Greenland ice core. *Nature* 359:311–3.

Kromer B, Spurk M. 1998. Revision and tentative extension of the tree-ring based $^{14}C$ calibration, 9200–11,855 cal BP. *Radiocarbon* 40(3):1117–25.

Leroy S, Zolitschka B, Negendank J, Seret G. 2000. Palynological analyses in the laminated sediment of Lake Holzmaar (Eifel, Germany): duration of Lateglacial and Preboreal biozones. *Boreas* 29:52–71.

Lotter AF. 1989. Evidence of annual layering in Holocene sediments of Soppensee, Switzerland. *Aquatic Sciences* 52:19–30.

Stuiver M, Reimer PJ, Bard E, Beck JW, Burr GS, Hughen KA, Kromer B, McCormac G, van der Plicht J, Spurk M. 1998. INTCAL98 radiocarbon age calibration, 24,000–0 cal BP. *Radiocarbon* 40(3):1041–83.

von Grafenstein U, Erlenkeuser H, Brauer A, Jouzel J, Johnsen SJ. 1999. A mid-European decadal isotope-climate record from 15,500 to 5000 years BP. *Science* 284:1654–7.

Zbinden H. 1987. *$^{14}C$ Messungen an Pflanzenresten aus Sediment*. Universität Bern: Physikalisches Institut.

Zbinden H, Andrée M, Oeschger H, Ammann B, Lotter A, Bonani G, Wölfli W. 1989. Atmospheric radiocarbon at the end of the Last Glacial: an estimate based on AMS radiocarbon dates on terrestrial macrofossils from lake sediment. *Radiocarbon* 31(3):795–804.

Zolitschka B. 1990. Spätquartäre Jahreszeitlich geschichtete Seesedimente ausgewählter Eifelmaare. *Documenta Naturae* 60:1–226.

Zolitschka B, Brauer A, Negendank JFW, Stockhausen H, Lang A. Annually dated late Weichselian continental paleoclimate record from the Eifel, Germany. *Geology* 28(9):783-86.

RADIOCARBON, Vol 42, Nr 3, 2000, p 355–368 

# AMS RADIOCARBON AND VARVE CHRONOLOGY FROM THE ANNUALLY LAMINATED SEDIMENT RECORD OF LAKE MEERFELDER MAAR, GERMANY

Achim Brauer • Christoph Endres • Bernd Zolitschka • Jörg FW Negendank

GeoForschungsZentrum (GFZ), Projektbereich 3.3, Sedimente und Beckenbildung, Telegrafenberg, D-14473 Potsdam, Germany. Email: brau@gfz-potsdam.de.

**ABSTRACT.** The Holocene varve chronology of annually laminated sediment sequences from Lake Meerfelder Maar agree for most of the record with dendro-calibrated accelerator mass spectronomy radiocarbon dates from the same site. Only between 9710 and 9950 cal BP does an offset of 240 yr appear between both data sets. At this position, a micro-disturbance in the varve succession has been detected by thin section analyses and was quantified in terms of missing varves. A comparison with the nearby record from Lake Holzmaar, as well providing high resolution AMS $^{14}C$ and varve chronologies, revealed that such gaps (ca. 2% in time for the entire Holocene) are exceptional for these long-varved maar lake records. Moreover, since sections of missing years appear for both profiles at different stratigraphic positions, a combination of both the Meerfelder Maar and Holzmaar records enables us to bridge erroneous zones in varve chronologies. This confirms the high potential of two long-varved records in close vicinity to each other for the elimination of dating errors and for increasing chronological precision at a time resolution that is normally regarded as within the counting errors. Late Glacial varve and $^{14}C$ data beyond the dendro-calibration from Meerfelder Maar and their tentative tele-connections to other high resolution data sets reveal unexplained age discrepancies in the calendar year time scale of about 200 years.

## INTRODUCTION

Lacustrine sediment archives are an important tool for studying the palaeoclimatic and palaeoenvironmental history on continents because of the large variety of proxy data they provide. One basic prerequisite, however, is a precise and reliable chronology often based on radiocarbon dating. Long laminated lake sediment profiles have, in addition, the possibility of independent dating: varve chronology. This provides not only a potential to contribute to the extension of the tree ring $^{14}C$ calibration curve, which presently reaches back to 11,871 cal BP (Kromer and Spurk 1998) but also increases the precision of dating certain lake sediments. This has been shown earlier for Lake Holzmaar, Germany (Hajdas et al. 1995a, this issue), Lake Soppensee, Switzerland (Hajdas et al. 1993, this issue), Lake Gościąż, Poland (Goslar et al. 1995, this issue), the stacked Swedish varve chronology (Wohlfarth et al. 1995, this issue), and more recently, Lake Suigetsu, Japan (Kitagawa and van der Plicht 1998a, 1998b, this issue). However, results of lake sediment dating sometimes appears to be contradictory, especially considering the Late Glacial and its last climate deterioration, the Younger Dryas. Refinements, re-examinations, and re-evaluations as well as the presentation of new lacustrine profiles improved the understanding of some of these discrepancies. An age of 11,500–11,600 cal BP for the Younger Dryas/Holocene transition has now generally been accepted (Gulliksen et al. 1998). The beginning of the Younger Dryas is still not covered by tree-ring calibration, but a reliable age between 12,600 and 12,700 cal BP has been reported from Lakes Gościąż (Goslar and Madry 1998) and Meerfelder Maar (Brauer et al. 1999a). Evaluating the remaining small discrepancies of Late Glacial calendar year time scales from different archives still needs to be improved by defining suitable correlation horizons and by obtaining more high resolution radiocarbon data from varved records (Brauer et al. 1999b).

In this study, we present a new accelerator mass spectronomy radiocarbon dataset from the annually laminated lake sediment profile from Lake Meerfelder Maar in the Eifel region of Germany. This site was chosen because of the presence of a long continuous varve succession from about 1500 to 14,200 cal BP and because Meerfelder Maar is located in close vicinity to Lake Holzmaar. Both records contain two tephra layers. Their correlation provides a means of independent control and allows the detection of possible errors in either of the chronological datasets.

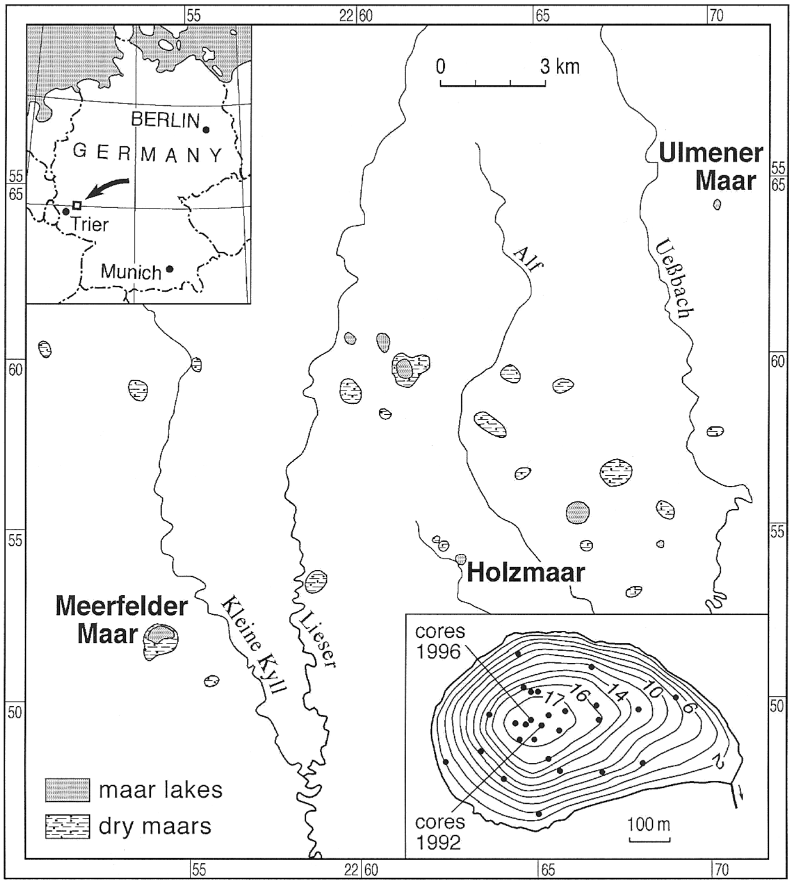


Figure 1 Location of Lake Meerfelder Maar (MFM) within the Westeifel Volcanic Field and bathymetric map of the lake including all drilling locations. The series of five parallel cores from 1996 used for the present study is marked only with one circle and indicated by an arrow.

## MATERIAL AND METHODS

### Site and Sediments

Lake Meerfelder Maar (MFM) is a small maar lake of volcanic origin in the Westeifel, western Germany (Figure 1). It belongs to the Quaternary Westeifel Volcanic Field, which consists of 250 eruption centers, at least 50 of them being maars (Büchel and Krawczyk 1986). Presently, eight of the maar craters are filled with water, including Lakes MFM and Holzmaar (HZM), with MFM located about 10 km west of HZM (Figure 1). MFM, situated at 336 m above sea level (asl), has a surface area of 0.248 km$^2$ and a maximum depth of 18 m. The lake basin only covers one third of the entire crater while the other part is covered by delta sediments deposited by a stream (Meerbach) entering from the south. There are no calcareous rocks present within the catchment, so MFM is a softwater lake. The lake is currently eutrophic, but tended to be hypertrophic several times in this century because of intensive human activity in the catchment area. Age determinations of the MFM volcanic eruption are rather rough, but a minimum age of 35,000 cal BP can be regarded as certain

(Zolitschka et al. 1995). Numerous sediment cores have been obtained from MFM, with the longest one (45 m) still not reaching the crater bottom (Irion and Negendank 1984; Negendank 1989; Negendank et al. 1990). In 1996, five new overlapping sediment cores were recovered from the center of the lake (Figure 1) and combined to a composite profile of 11.20 m in length (Figure 2). The sediment profile displays four main lithological units (Figure 2).

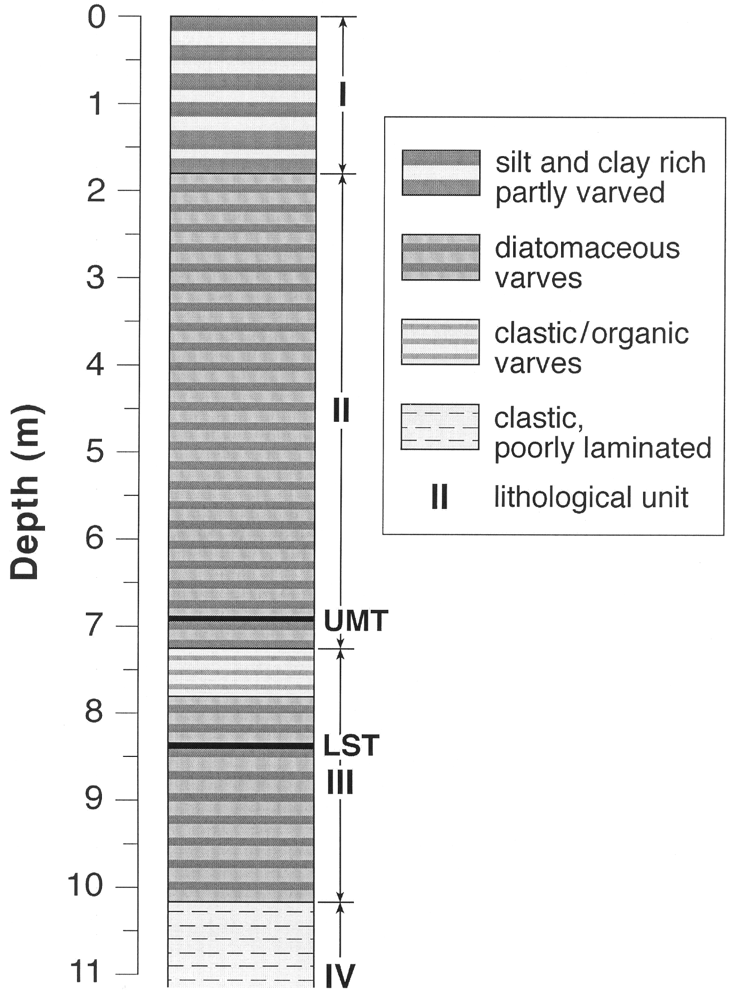


Figure 2 Lake Meerfelder Maar sediment record with four main lithological units and two tephra layers: UMT=Ulmener Maar Tephra; LST=Laacher See Tephra.

The basal part (11.20–10.40 m; lithozone IV) is a reddish-brown minerogenic mud which shows only a few, indistinct cm-thick laminations. The contents in organic matter and diatom frustules are very low. Dry density values of 0.9–1.4 g cm$^{-3}$ reflect the dominance of minerogenic detritus and are the highest of the whole profile. This sediment unit has been deposited under periglacial conditions during the end of the last glaciation and the sharp shift to the following sediment unit marks the transition to the Late Glacial.

During the Late Glacial (10.40–7.25 m; lithozone III), fine laminations have been continuously formed but their lithological composition is very heterogeneous. Olive-colored, organic-rich sediments are frequently intercalated by sections of reddish-brown minerogenic deposits. In contrast to the basal sediment unit, these minerogenic sediments are annually laminated. One of these sections, dominated by minerogenic sediments, is formed during the second half of the Younger Dryas (YD) and its transition to predominantly organic sedimentation at 7.25 m depth marks the onset of the Holocene.

Most of the Holocene sediments (7.25–1.80 m; lithozone II) are composed of a finely laminated organic diatomaceous gyttja. The contents in organic carbon range between 7 and 27%. Frustules of planktonic diatoms are abundant and form spring and summer sublayers of the varves, while frustules of littoral diatoms are found in autumn sublayers. Authigenic iron-rich minerals (vivianite, siderite, pyrite) are common throughout the profile and in some periods even form the main minerogenic component.

The uppermost part of the profile (0–1.80 m; lithozone I) is characterized by higher amounts of minerogenic detritus often deposited in turbidites and detrital layers. This change in deposition was caused by human disturbances in the catchment leading to an increase in soil erosion. Varves occasionally occur but they have not been continuously preserved in the studied cores.

Two tephra layers are recognized within the Late Glacial and the early Holocene part of the profile. The Laacher See Tephra (LST), an important time marker found in many Allerød sediment sequences all over Europe (van den Bogaard and Schmincke 1985), is a 7-cm-thick, dark, coarse sand layer in 8.40 m depth. The second volcanic explosion is recorded during the Preboreal and assigned to the eruption of the Ulmener Maar volcano which is located about 20 km NE of MFM (Zolitschka et al. 1995). This Ulmener Maar Tephra (UMT) occurs in 6.91 m depth and is a 0.3-mm thick layer detectable only after microscopic inspection.

**Methods**

A composite profile of the five sediment cores examined was defined by macroscopic comparison and correlation (Figure 2). This first step allowed us to eliminate disturbed sections in any of the cores. Thereafter, a continuous series of large-scale thin sections was prepared from the composite profile. An overlap of at least 2 cm between each thin section provided a detailed correlation at a single-varve scale confirming the macroscopic correlation. Thus, the whole record was examined microscopically under parallel and polarized light. Magnifications used were 25× (overview), 100× (varve counting), and 400–1000× (detail studies). In addition to varve counting, this method enables sediment composition changes as well as possible micro-disturbances to be recognized.

The sediment remaining after sub-sampling for thin sections was used to prepare $^{14}C$ samples. To avoid obtaining ages that are too old by dating bulk sediment samples which might include reworked material (Olsson 1986, 1991), only terrestrial plant macrofossils have been AMS $^{14}C$-dated (Zbinden et al. 1989). Following the method described in Hajdas (1993), 2-cm-thick sediment slices have been cut out of all reliably correlated cores (mostly 3–5) in order to get as much sediment as possible per sample. Every $^{14}C$ sample has been precisely assigned in the corresponding thin section in order to microscopically detect sedimentological evidence for possible reworked material, such as micro-turbidites.

The fresh sediment was dissolved in 10% KOH at room temperature for 12–24 hr and then sieved and washed. If necessary, this procedure was repeated, until all organic and fine sediment material was removed. The residue was then examined under a binocular microscope. All identifiable land plant remains were picked out with a fine tweezers. The plant material was washed again carefully. The samples were then stored in distilled water at 4 °C until further pretreatment and target preparation for AMS measurements. Most of the measurements presented here were performed at the Leibniz Labor, Kiel. Four samples from older cores, which had been previously prepared in the same way and measured at the AMS laboratory in Zürich, have been precisely correlated to the reference profile. Pretreatment and target preparation methods of the Kiel and Zürich laboratories are described in Nadeau et al. (1998) (Kiel) and Bonani et al. (1987) (Zürich). Due to the scarcity of plant remains in MFM sediments, the sample weights were in the range of 0.3–2.0 mg carbon.

## RESULTS

### Varve Counting

Counting of the varves resulted in a floating varve chronology from 1500 to 14,200 cal BP between 1.75 and 9.60 m sediment depth. Above 1.75 m and below 9.60 m the sediment is not continuously varved and, therefore, no precise varve chronology was established. Instead, the thickness of occasionally occurring varves was used for high resolution sedimentation rate determination in order to provide the best possible age estimates for these parts of the record.

Counting from 1.75 down to 6.91 m sediment depth (Ulmener Maar Tephra, 34 cm above the Late Glacial/Holocene boundary) was carried out in 1-cm steps providing numbers of varves for each cm (method 1). The counting error was determined by multiple counting (same investigator) and was found to be 1–2% in about 80% of the profile, and not exceeding 4% for the rest. From 5.56 m down to 9.60 m (base of continuous varve series), varve thickness has also been measured (method 2) in addition to simple counting. This method is regarded as more sensitive to detect counting uncertainties especially in sections of low varve thickness in combination with poor varve quality because each varve boundary has to be defined more precisely. In profile sections with good varve quality, the deviation between both methods is also 1–2% even when counting results have been achieved by different investigators. However, in the only section of poor varve quality and very thin varves (0.2–0.3 mm) between 6.44 and 6.60 m, the discrepancy reached almost 20%. In this case the counts provided by method 2 have been regarded as more reliable.

### Radiocarbon Ages

Between 1.38 and 9.97 m sediment depth, 51 samples contained sufficient determinable plant material to perform AMS $^{14}C$ measurements (Table 1). They range from 1010–15,370 BP, and their 1$\sigma$ errors range between 30 and 210 yr, with one outlier reaching 350 yr (sample # KIA2525). The relative errors are negatively correlated to the sample sizes (Figure 3). The $\delta^{13}C$ values range between –32.3 and –20.0‰ relative to PDB. Eight samples show deviations from the overall depth–$^{14}C$ age function towards older ages (Figure 4). Microscopic examination of sediment sections corresponding to these samples show the presence of reworked material, too small to be recognized macroscopically, which was either deposited in the autumn/winter sublayer of a varve or as small turbidite. These dates have been excluded from chronological considerations because they do not represent the age of deposition of the respective sediment section. Three dates, which are obviously too young, are from very small samples (#KIA927, #KIA2533, #ETH15144) and thus might be contaminated by modern carbon. After excluding all doubtful data, 40 $^{14}C$ dates remain which lie within the varved part of the profile.

Table 1 Results of $^{14}C$ dating and varve counting of MFM sediments[a]

| Lab nr | Sediment depth (cm) | Varves per sample | $\delta^{13}C$ | ± 1 σ | $^{14}C$ age BP | ± 1 σ | Varve age cal BP |
|---|---|---|---|---|---|---|---|
| KIA2907 | 138.5 | — | –27.04 | 0.08 | 1010 | 30 | — |
| KIA2906 | 178.5 | 10 | –28.29 | 0.08 | 1270 | 30 | 1615 |
| KIA 947 | 207.0 | 8 | –27.86 | 0.12 | 1970 | 40 | 2050 |
| KIA2905 | 228.5 | 14 | –27.57 | 0.11 | 2110 | 30 | 2205 |
| KIA2904 | 238.5 | 11 | –28.97 | 0.18 | 2160 | 30 | 2270 |
| KIA2903 | 268.5 | 18 | –28.11 | 0.10 | 2770 | 50 | 2640 |
| KIA2901 | 288.0 | 35 | –27.44 | 0.12 | 2720 | 40 | 2950 |
| KIA2900 | 308.0 | 33 | –29.32 | 0.12 | 3220 | 60 | 3310 |
| KIA 946 | 358.0 | 39 | –30.67 | 0.11 | 3900 | 50 | 4280 |
| KIA 945 | 388.0 | 29 | –27.75 | 0.15 | 4340 | 60 | 4830 |
| KIA 944 | 408.0 | 59 | –28.76 | 0.23 | 4600 | 60 | 5360 |
| ETH15136 | 424.0 | 27 | –24.30 | 1.20 | 5470[b] | 65 | 5700 |
| ETH15137 | 430.0 | 25 | –22.60 | 1.20 | 5190 | 95 | 5750 |
| KIA 941 | 492.0 | 37 | –29.28 | 0.13 | 5820 | 100 | 6630 |
| KIA 940 | 502.0 | 25 | –25.01 | 0.11 | 5960 | 70 | 6790 |
| ETH15139 | 505.0 | 30 | –26.20 | 1.10 | 6145 | 85 | 6830 |
| KIA 939 | 512.0 | 27 | –31.15 | 0.34 | 6030 | 110 | 6930 |
| KIA 938 | 541.0 | 45 | –23.44 | 0.19 | 6550 | 80 | 7440 |
| KIA 937 | 550.5 | 49 | –26.55 | 0.27 | 6870 | 80 | 7630 |
| KIA 936 | 570.5 | 54 | –31.09 | 0.23 | 7170 | 140 | 8085 |
| KIA 935 | 580.5 | 34 | –25.70 | 0.13 | 7810 | 80 | 8345 |
| KIA 934 | 600.5 | 57 | –25.53 | 0.14 | 8270[b] | 80 | 8770 |
| KIA 932 | 610.5 | 40 | –30.34 | 0.23 | 8080 | 130 | 9020 |
| KIA 933 | 610.5 | 40 | –30.01 | 0.12 | 8040 | 130 | 9020 |
| KIA 931 | 620.5 | 35 | –27.77 | 0.13 | 8020 | 190 | 9180 |
| KIA 930 | 630.5 | 40 | –25.34 | 0.19 | 8880[b] | 90 | 9390 |
| KIA 929 | 681.0 | 31 | –25.73 | 0.16 | 9770 | 120 | 10,830 |
| KIA2538 | 689.0 | 33 | –26.97 | 0.62 | 9610 | 40 | 10,970 |
| KIA 928 | 701.0 | 36 | –26.00 | 0.07 | 9660 | 90 | 11,160 |
| KIA2896 | 707.0 | 37 | –26.93 | 0.20 | 10,310 | 60 | 11,260 |
| KIA2537 | 711.0 | 51 | –29.30 | 0.56 | 10,000 | 120 | 11,340 |
| KIA2536 | 719.0 | 34 | –25.39 | 0.62 | 10,300 | 90 | 11,490 |
| KIA 927 | 721.0 | 35 | –29.30 | 0.27 | 9510 | 220 | 11,530 |
| ETH15144 | 771.0 | 20 | –27.00 | 1.20 | 9685 | 105 | 12,150 |
| KIA2535 | 789.5 | 19 | –20.00 | 0.56 | 13,870[b] | 90 | 12,320 |
| KIA2895 | 823.5 | 18 | –28.62 | 0.17 | 11,910[b] | 130 | 12,650 |
| KIA2534 | 825.5 | 20 | –23.06 | 1.50 | 13,770[b] | 80 | 12,670 |
| KIA2894 | 829.5 | 67 | –24.89 | 0.13 | 11,130 | 90 | 12,750 |
| KIA2533 | 831.5 | 61 | –25.68 | 1.57 | 10,740 | 120 | 12,820 |
| KIA2532 | 918.5 | 8 | –27.69 | 1.68 | 12,050 | 80 | 13,840 |
| KIA2531 | 920.5 | 8 | –27.31 | 0.57 | 12,100 | 80 | 13,850 |
| KIA2530 | 922.5 | 6 | –27.91 | 0.59 | 11,950 | 80 | 13,860 |
| KIA2529 | 924.5 | 15 | –28.43 | 0.69 | 11,880 | 80 | 13,870 |
| KIA2892 | 932.5 | 19 | –24.92 | 0.32 | 12,660 | 70 | 13,930 |
| KIA2528 | 934.5 | 17 | –26.79 | 0.57 | 11,980 | 100 | 13,950 |
| KIA2527 | 942.5 | 10 | –27.15 | 0.99 | 12,060 | 100 | 14,000 |
| KIA2526 | 944.5 | 13 | –32.31 | 1.13 | 13,240[b] | 100 | 14,010 |
| KIA2525 | 948.5 | 13 | –30.04 | 1.15 | 15,370[b] | 210 | 14,045 |
| KIA2891 | 950.5 | 14 | –26.37 | 0.30 | 12,320 | 90 | 14,060 |
| KIA2524 | 952.5 | 14 | –28.12 | 0.57 | 12,340 | 90 | 14,070 |
| KIA2890 | 996.5 | 10 | –29.52 | 0.25 | 11,930 | 160 | 14,315 |

[a]Lab numbers beginning with "KIA" were measured at Leibniz-Laboratorium, Kiel, and lab numbers beginning with "ETH" were measured at AMS Laboratory of ETH Zurich. $^{14}C$ ages are expressed as conventional ages (Stuiver and Polach 1977). In the shaded area, a correction of +240 yr was applied to the varve chronology. For further details, see text.

[b]Dates rejected due to reworked organic material

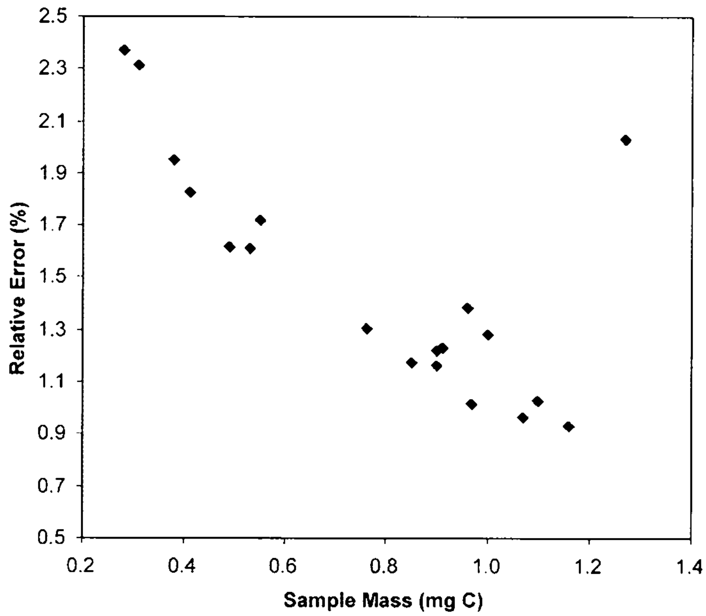


Figure 3 Relative errors of AMS $^{14}C$ measurements as a function of sample weights

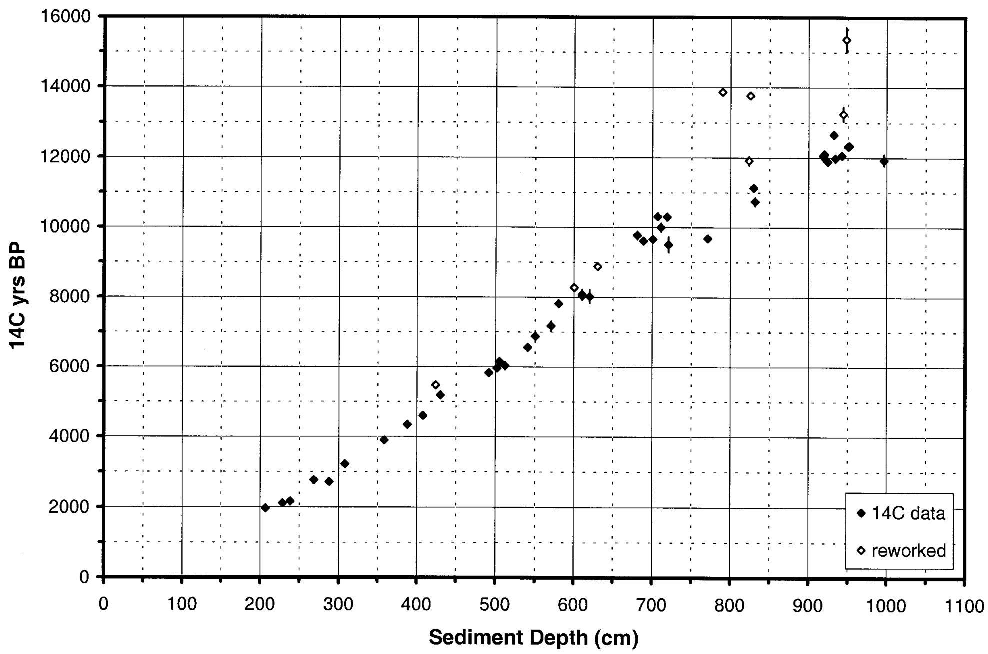


Figure 4 Sediment depth versus $^{14}C$ ages of MFM as given in Table 1. Unless indicated, $1\sigma$ errors of the $^{14}C$ measurements are smaller than data symbols.

Unfortunately, it was not possible to find terrestrial macrofossils directly at the base or top of the LST. The closest sample to the LST is #KIA2533 (77 varves above) with a $^{14}C$ age of 10,740 ± 120 BP. However, because of its very small sample size, it appears to be too young. The neighboring sample is #KIA2894 (138 varves above). Its $^{14}C$ age is 11,130 ± 90 BP which is in agreement with high precision $^{14}C$ dates of trees buried by the Laacher See ash near the eruption center (mean age 11,063 ± 12 BP; Friedrich et al. 1999). $^{14}C$ ages closest to UMT are 9660 ± 90 BP (KIA928, 151 varves below) and 9610 ± 40 BP (KIA2538, 39 varves above).

#### Radiocarbon Versus Varve Ages

Two methods have been applied to relate the floating MFM chronology to a calendar year time scale. First, all $^{14}C$ data from the period before the Ulmener Maar Tephra (UMT) were matched to the tree-ring calibration curve by the $\chi^2$ method. This results in an age of 10,760 cal BP for the (UMT), which is younger than previous varve ages of 11,000 ±110 cal BP from HZM (Zolitschka 1998). Unfortunately, the UMT falls into the 9.5 ka $^{14}C$ plateau, so that tree ring calibration of $^{14}C$ dates from the UMT results in a 1 $\sigma$ interval larger than the discrepancy to be explained. The second possibility of linking the MFM chronology to a calendar year time scale is to use the UMT age of 11,000 cal BP as a tephrochronological marker. Then, however, $^{14}C$ ages above 6.44 m sediment depth become apparently 240 yr too young. There are three possible explanations for this phenomenon:

1. The Holocene $^{14}C$ samples might have been contaminated with modern $^{14}C$ resulting in ages that are too young. This, however, is unlikely because all samples were prepared following standard methods that are designed to minimize the possibility of contamination and have been applied successfully in many other studies in the past. Furthermore, the fairly constant nature of the shift, if explained by modern carbon, would imply a constant relative contribution of contamination to the absolute sample masses, which by themselves vary between 0.4 and 1.5 mg C. Thus, the observed discrepancy cannot be explained by sample contamination.
2. The accepted age of 11,000 cal BP for the UMT is too old, which is unlikely because varve dating of UMT in HZM is well established by multiple counting (Zolitschka 1998). In addition, in the MFM varve chronology, the UMT eruption occurred 590 varves (in HZM 600 varves) after the end of the YD. This climatic signal is well expressed in both lakes (Zolitschka 1998; Brauer et al. 1999) and thus can be used for additional correlation. Since the accepted age for the end of the YD is between 11,500 and 11,600 cal BP (Gulliksen et al. 1998), an age of 11,000 calendar yr for the UMT is assumed to be reliable.
3. Missing years in the MFM varve chronology might be the reason for the observed discrepancy. If the $^{14}C$ data are considered as correct and matched to the tree-ring curve, both curves agree back to about 9710 cal BP where the offset occurs (Table 1). This is exactly at the section of poorly developed varves (644–660 cm) that have caused a maximum deviation between repeated counts by different methods. Varves within this section are difficult to distinguish from each other, because they lack a significant influx of minerogenic sediment during autumn and/or winter. After the spring/summer, diatom blooms follows a thin layer of amorphous and particulate organic matter including authigenic minerals like vivianite and siderite. At the upper end of these varve facies a 1.5-cm-thick micro-disturbance appears in the profile. After this disturbance, an abrupt change in varve facies occurs: increased minerogenic influx leads to the formation of distinct winter layers containing silt and clay. Probably, both sedimentological features, the micro-disturbance followed by an abrupt facies-change indicate the presence of a small hiatus in the record which might have caused a loss of the missing 240 varves. Using the mean sedimentation rate for the minerogenic-poor varve facies, the missing sediment section is assumed to be about 4–5 cm.

In conclusion, the offset between MFM varve and $^{14}C$ chronologies is neither the result of erroneous $^{14}C$ ages nor the result of previously incorrect dating of the UMT marker layer. The favored alternative explanation for the observed discrepancy is a 4–5 cm micro-hiatus recognized by microscopic investigation at 644 cm sediment depth. Because of this reason the MFM varve chronology has been corrected for the missing 240 yr at 9710 cal BP (Table 1). Only the combination of varve chronology and independent high resolution AMS $^{14}C$ dating with their matching to the tree-ring data allows to identify and quantify such a small hiatus.

## LOCAL CORRELATION

The presence of another varved record from Lake Holzmaar (HZM) less than 10 km away provides a unique possibility of correlating two high-resolution $^{14}C$- and varve-dated profiles. From HZM, a varve chronology has been established from recent times back to 14,000 cal BP (Zolitschka 1991; 1998) which has been further extended into the Last Glacial Maximum to 22,500 cal BP by counting clastic periglacial varves (Brauer et al. 1994). Hajdas et al. (1995a) presented an AMS $^{14}C$ data set on terrestrial plant macrofossils from HZM sediments covering the last 14,000 cal yr. Based on these $^{14}C$ dates and their calibration according to Stuiver and Reimer (1993), Hajdas et al. (1995a) suggested a correction of the HZM varve chronology by +878 yr within the period between 4500 and 3600 cal BP. More recently, this correction was reduced to about +350 varves by identifying more varves in this section of poor varve preservation in additional cores (Zolitschka 1998). The corresponding period in MFM is well varved and confirms that new correction.

The period between 9710 and 9950 cal BP, corresponding to the section where in MFM the 240-yr hiatus occurs, can be placed without any dating difficulties in the HZM varve sequence. These findings allow us to conclude that such minor disturbances within the varve records of MFM and HZM are caused by local sedimentological processes, probably triggered by different basin morphology and hydrology. Both disturbances are macroscopically not visible and in the range of less than 400 yr. Corrections made in both of the varve chronologies are furthermore confirmed by varve counting in the other record. Including these corrections of the varve data, there is a good agreement between both records and the tree-ring calibration for the entire Holocene (Figure 5).

For the Late Glacial correlation of both records the two tephra layers from Laacher See (LST) and Ulmener Maar (UMT) are used. Varve counts between both tephra layers in the HZM record are 320 less than those in MFM, such that a hiatus of this length within the Younger Dryas has been proposed (Zolitschka 1998; Brauer et al. 1999). As expected, $^{14}C$ dates from samples in stratigraphically close position to the tephra layers in both records are in good agreement. Based on their own data and literature data of different sites, Hajdas et al. (1995b) gave a mean $^{14}C$ age of 11,230 ± 40 BP for the LST, which is slightly older than the mean age of 11,063 ± 12 BP recently given by Friedrich et al. (1999). In MFM, a sample 138 varves above LST is dated at 11,130 ± 90 BP. Two AMS ages of plant samples associated with UMT at HZM are reported by Hajdas et al. (1995a) as 9515 ± 75 BP and 9650 ± 85 BP. These dates are in agreement with the two ages for the UMT measured from MFM (9660 ± 90 BP and 9610 ± 40 BP).

The combination of both varve and high resolution $^{14}C$ dating allows us to locate and quantify even short sections (about 2% of the varved sequences) of unidentified varves in the profiles of MFM and HZM. Since these sections do not occur at the same stratigraphical positions in both records, the combination of both profiles provides a reliable calendar year time scale from the Eifel region (Figure 6). This is further confirmed by independent $^{40}Ar/^{39}Ar$ dating of Sanidine crystals from LST yielding 12,900 ± 400 yr BP (van den Bogaard 1995), which is in agreement with the date of 12,880 ± 120 yr BP from MFM (Brauer et al. 1999).

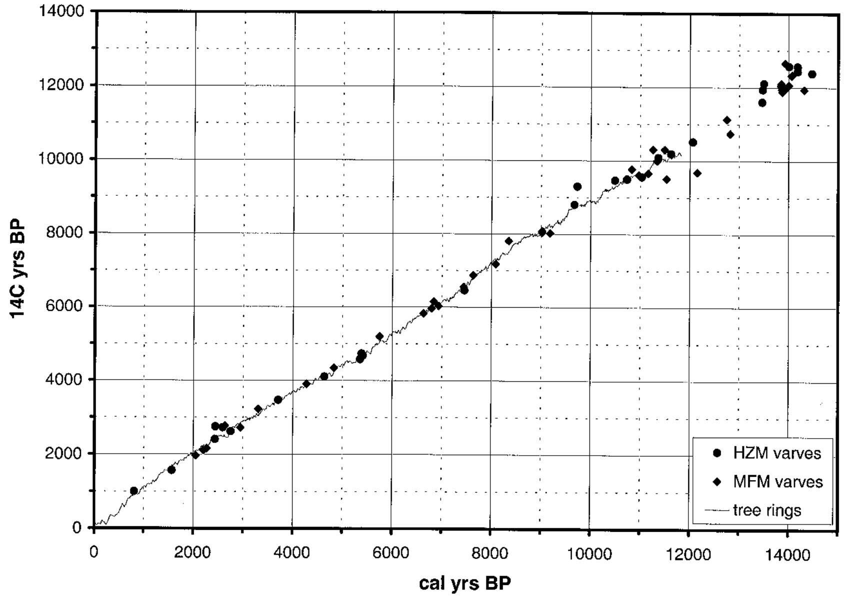


Figure 5 Varve versus $^{14}C$ ages from MFM and HZM. The tree-ring calibration curve serves as a reference. Varve time scales from MFM and HZM are corrected as discussed in the text.

**Global Correlation**

A comparison with $^{14}C$ chronologies from other sediment archives focuses on the Late Glacial since there is still a need for further terrestrial $^{14}C$ calibration due to the problems caused by $^{14}C$ plateaus. Although the present $^{14}C$ data set from MFM is not dense enough yet for an independent calibration, a link to other records provides information about the range of present uncertainties. In general, MFM and HZM data sets are within the spread found for other lacustrine varved records (Figure 7) as well as for marine data from corals and the Cariaco Basin varves (Figure 8).

The remaining small discrepancies between the different records become visible when using isochronous marker horizons for correlation such as, for example, the LST, especially for the period beyond the tree ring calibration. Accepting the LST $^{14}C$ age of 11,063 ± 12 BP from Friedrich et al. (1999), which is within the 1$\sigma$ confidence interval of the date from the MFM record, and calibrating this age with Cariaco varves (INTCAL98: Stuiver et al. 1998) results in an age for the LST ranging from 13,010–13,200 cal BP. This is 130–320 yr older than the MFM varve age. Another global marker horizon is the first abrupt and short cold spell after the Late Glacial warming, even if we consider that such climatic events do not necessarily have to be synchronous. This cold event is palynologically defined as the Oldest Dryas in MFM (Litt and Stebich 1999), but in many other records is also called Older Dryas (e.g. Björck et al. 1996), or GI-1d according to the INTIMATE stratigraphy based on the GRIP ice core (Björck et al. 1998). Four $^{14}C$ dates from this event, which has been clearly identified in MFM and correlated to the Greenland ice cores (Brauer et al. 1999), range in between 11,880 ± 80 and 12,100 ± 80 BP (KIA2529–KIA2532, Table 1). The corresponding calendar year age as determined by varve counting is from 13,800 to 13,900 cal yr BP and thus about 200 years younger than in the GISP2 (Alley et al. 1993) and Cariaco Basin records, which exactly match each other (Hughen et al. 1998). On the other hand, $^{14}C$ dates for this climatic event from the Cariaco Basin record (Hughen et al. 1998; Stuiver et al. 1998) range between 11,898 ± 68 and 12,084 ± 83 BP and are in perfect agree-

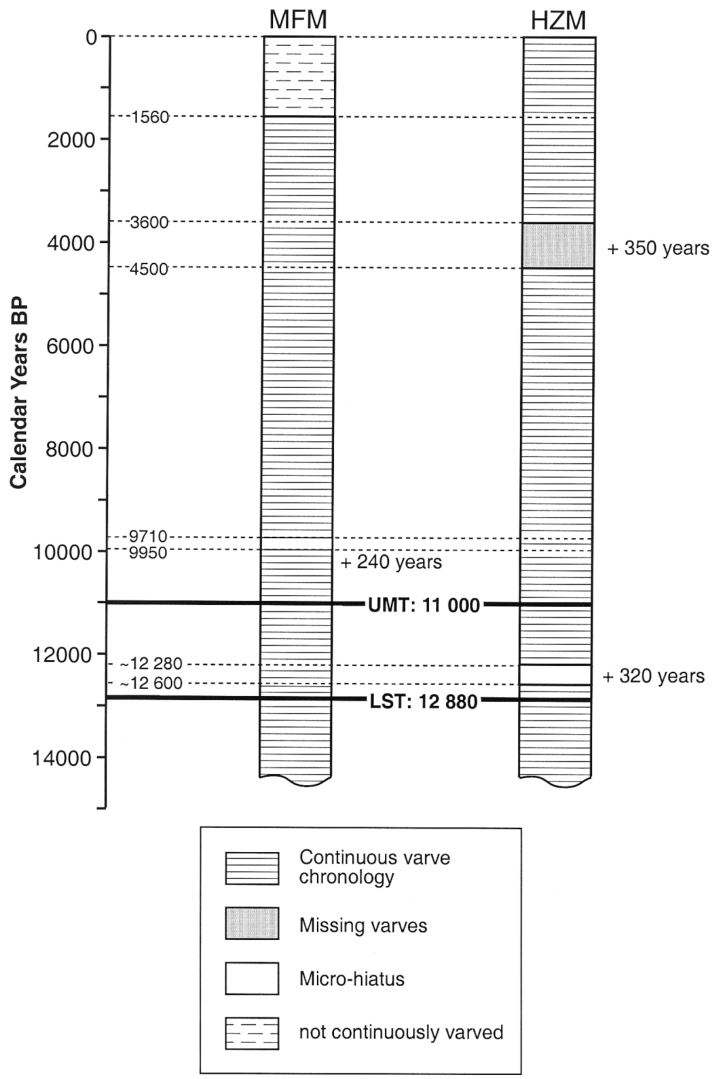


Figure 6 Schematic profiles of MFM and HZM sediment profiles indicating sections of missing varves. The number of missing varves is determined by varve counting in the opposing profile and/or dendro-calibrated $^{14}$C data.

ment with MFM data. Thus, the discrepancy of about 200 yr between the MFM and Cariaco Basin record appears only in the calendar year and not in the $^{14}$C time scale.

There are two possible explanations for this discrepancy: 1) $\Delta^{14}$C variations during the early Late Glacial resulting in a $^{14}$C plateau between around 13,800 and 14,100 cal BP (Stuiver et al. 1998). In consequence, the short climatic deterioration would have been a non-synchronous event which is rather unlikely taking into consideration the great similarity of Late Glacial proxy-climatic records, or 2) the observed difference in calendar time scale is an effect of discrepancies between the Cariaco and MFM varve chronologies. This interpretation is supported by the above described age discrep-

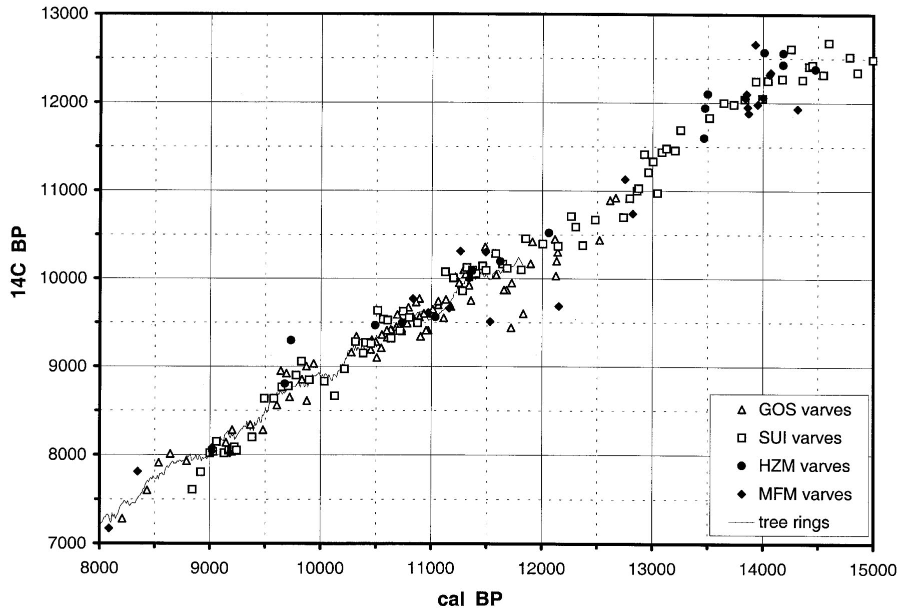


Figure 7 Comparison of MFM and HZM $^{14}C$ calibration data with other lake sediment archives. GOS = Lake Gościąż, Poland (Goslar et al. 1995); SUI = Lake Suigetsu, Japan (Kitagawa and van der Plicht 1998a, 1998b).

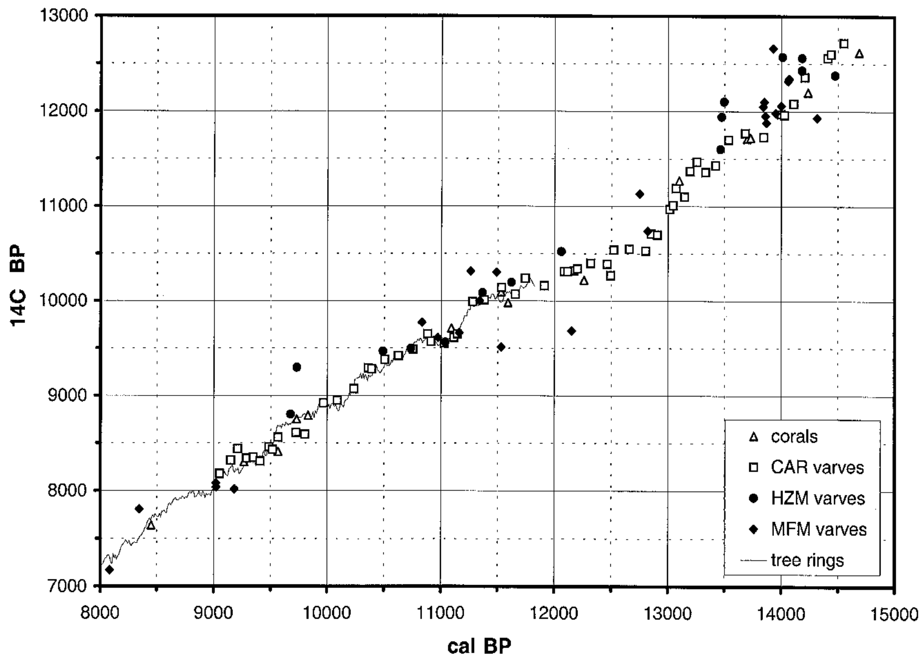


Figure 8 Comparison of MFM and HZM $^{14}C$ calibration data with marine archives. CAR = Cariaco Basin, Venezuela (Hughen et al. 1998); corals = U-Th-dated coral material (Bard et al. 1998).

ancy of the LST calendar year age when comparing the MFM varve time scale and the precise $^{14}C$ date from Friedrich et al. (1999) after calibration with the Cariaco Basin data. At both points of comparison, the LST and the Oldest Dryas/GI-1d Event, the MFM data is in better agreement with the Lake Suigetsu record (Kitagawa and van der Plicht 1998a, 1998b). In the Suigetsu record, 1) a $^{14}C$ age of 11,030 ± 55 BP, which is close to the LST date of 11,063 ± 65 BP (Friedrich et al., forthcoming), yields a calendar year age of 12,874 BP (MFM varve age: 12,880 cal yr BP) and, 2) $^{14}C$ dates between 11,830 ± 65 and 12,040 ± 55 BP correspond to varve ages between 13,514 and 13,834 cal BP (MFM varve age: 13,800–13,900 cal BP). Since the Cariaco Basin data are confirmed by the GISP2 time scale and since at the moment there are too few $^{14}C$ data from the Late Glacial available from MFM, this dating problem cannot be solved at this stage. In conclusion, age discrepancies in the range of about 200 yr between Late Glacial calendar-year time scales remain unexplained and require further high-resolution calibration data sets, as well as a better definition of global marker horizons for improving tele-connections of various archives.

## ACKNOWLEDGMENTS

We would like to thank Thomas Litt for his help with determining plant macrofossils. Andreas Hendrich provided support in the preparation of figures. This study has been supported by the Deutsche Forschungsgemeinschaft (DFG) within the SPP “Wandel der Geo-Biosphäre während der letzten 15000 Jahre” (Grant NE 154/29-3). This study is a contribution to the European Lake Drilling Programme (ELDP).

## REFERENCES

Alley RB, Meese DA, Shuman CA, Gow AJ, Taylor KC, Grootes PM, White JWC, Ram M, Waddington ED, Mayewski PA, Zielinski GA. 1993. Abrupt increase in Greenland snow accumulation at the end of the Younger Dryas event. *Nature* 362:527–9.

Bard E, Arnold M, Hamelin B, Tisnerat-Laborde N, Cabioch G. 1998. Radiocarbon calibration by means of mass spectrometric $^{230}Th/^{234}U$ and $^{14}C$ ages of corals: an updated database including samples from Barbados, Mururoa and Tahiti. *Radiocarbon* 40(3):1085–92.

Bonani G, Beer J, Hofmann H, Synal HA, Suter M, Wölfli W, Pfleiderer C, Junghans C, Münnich KO. 1987. Fractionation, precision and accuracy in $^{14}C$ and $^{13}C$ measurements. *Nuclear Instruments and Methods in Physics* B29:87–90.

Björck S, Kromer B, Johnsen S, Bennike O, Hammerlund D, Lemdahl G, Possnert G, Rasmussen TL, Wohlfarth B, Hammer CU, Spurk M. 1996. Synchronised terrestrial-atmospheric deglacial records around the North Atlantic. *Science* 274:1155–1160.

Björck S, Walker MJC, Cwynar LC, Johnsen S, Knudsen KL, Lowe JJ, Wohlfarth B, INTIMATE Members. 1998. An event stratigraphy for the Last Termination in the North Atlantic region based on the Greenland ice-core record: a proposal by the INTIMATE group. *Journal of Quaternary Science* 13(4):283–92.

Brauer A, Hajdas I, Negendank JFW, Vos H, Rein B and Zolitschka B. 1994. Warvenchronologie. Eine Methode zur absoluten Datierung und Rekonstruktion kurzer und mittlerer solarer Periodizitäten. *Geowissenschaften* 12:325–32.

Brauer A, Endres C, Günter C, Litt T, Stebich M, Negendank JFW. 1999a. High resolution sediment and vegetation responses to Younger Dryas climate change in varved lake sediments from Meerfelder Maar, Germany. *Quaternary Science Reviews* 18:321–329.

Brauer A, Endres C, Negendank JFW. 1999b. Late Glacial calendar year chronology based on annually laminated lake sediments from Lake Meerfelder Maar, Germany. *Quaternary International* 61:17–25.

Büchel G, Krawczyk E. 1986. Zur Genese der Dauner Maare im Vulkanfeld Westeifel. *Mainzer Geowissenschaftliche Mitteilungen* 15:219–38.

Friedrich M, Kromer B, Spurk M, Hofmann J, Kaiser KF. 1999. Paleo-environment and radiocarbon calibration as derived from Late Glacial/Early Holocene tree-ring chronologies. *Quaternary International* 61:27–39.

Goslar T, Arnold M, Bard E, Kuc T, Pazdur M.F, Ralska-Jasiewiczowa M, Rozanski K, Tisnerat N, Walanus A, Wicik B, Wieckowski K. 1995. High concentration of atmosphere-rich $^{14}C$ during the Younger Dryas cold episode. *Nature* 377:414–17.

Goslar T, Madry W. 1998. Using the Bayesian method to study the precision of dating by the “wiggle matching” procedure. *Radiocarbon* 40(1):551–60.

Goslar T, Arnold M, Tisnerat-Laborde N, Hatte C, Paterne M, Ralska-Jasiewiczowa M. 2000. Radiocarbon calibration by means of varves versus $^{14}C$ ages of terrestrial macrofossils from Lake Gościąż and Lake Perespilno, Poland. *Radiocarbon.* This issue.

Gulliksen S, Birks HH, Possnert G, Mangerud J. 1998. A calendar age estimate of the Younger Dryas-Holocene boundary at Kråkenes, western Norway. *The Holocene* 8(3):249–59.

Hajdas I. 1993. Extension of the radiocarbon calibration curve by AMS dating of laminated sediments of lake Soppensee and lake Holzmaar. PhD. Thesis, ETH Zürich. 147 p.

Hajdas I, Ivy SD, Beer J, Bonani G, Imboden D, Lotter AF, Sturm M, Suter M. 1993. AMS radiocarbon dating and varve chronology of lake Soppensee: 6000–12000 $^{14}$C years BP. *Climate Dynamics* 9:107–16.

Hajdas I, Zolitschka B, Ivy-Ochs SD, Beer J, Bonani G, Leroy SAG, Negendank JFW, Ramrath M, Suter M. 1995a. AMS radiocarbon dating of annually laminated sediments from lake Holzmaar, Germany. *Quaternary Science Reviews* 14:37–143.

Hajdas I, Ivy-Ochs SD, Bonani G, Lotter AF, Zolitschka B, Schlüchter C. 1995b. Radiocarbon age of the Laacher See Tephra: 11,230 ± 40 BP. *Radiocarbon* 37(2):149–54.

Hajdas I, Bonani G, Zolitschka B. 2000. Radiocarbon dating of varve chronologies: Soppensee and Holzmaar after ten years. *Radiocarbon.* This issue.

Hughen KA, Overpeck JT, Lehman SJ, Kashgarian M, Southon J, Peterson LC, Alley R, Sigman DM. 1998. Deglacial changes in ocean circulation from an extended radiocarbon calibration. *Nature* 391:65–8.

Irion G, Negendank JFW, editors. 1984. Das Meerfelder Maar. *Courier Forschungsinstitut Senckenberg* 65. Frankfurt A.M. 101 p.

Johnsen SJ, Dahl-Jensen D, Dansgaard W, Gundestrup N. 1995. Greenland palaeotemperatures derived from GRIP bore hole temperature and ice core isotope profiles. *Tellus* 47B:624–629.

Kitagawa H, van der Plicht J. 1998a. A 40,000-year varve chronology from Lake Suigetsu, Japan: extension of the $^{14}$C calibration curve. *Radiocarbon* 40(1):505–15.

Kitagawa H, van der Plicht J. 1998b. Atmospheric radiocarbon calibration to 45,000 yr BP: Late Glacial fluctuations and cosmogenic isotope production. *Science,* 279:1187–90.

Kitagawa H, van der Plicht J. 2000. Atmospheric radiocarbon calibration beyond 11,900 cal BP from Lake Suigetsu laminated sediments. *Radiocarbon*. This issue.

Kromer B, Spurk M. 1998. Revision and tentative extension of the tree-ring based $^{14}$C calibration 9200 to 11,870 cal BP. *Radiocarbon* 40(3):1117–25.

Litt T, Stebich M. 1999. Bio- and chronostratigraphy of the Late Glacial in the Eifel region, Germany. *Quaternary International* 61:5–16.

Nadeau MJ, Schleicher M, Gottdang A, Mouse DJW, Grootes PM. 1996. Performances and characteristics of the Leibniz-Labor AMS facility mass spectrometer. *Radiocarbon* 38(1):94.

Negendank JFW. 1989. Pleistozäne und holozäne Maarsedimente der Eifel. *Zeitschrift der Deutschen Geologischen Gesellschaft* 140:13–24.

Negendank JFW, Brauer A, Zolitschka B. 1990. Die Eifelmaare als erdgeschichtliche Fallen und Quellen zur Rekonstruktion des Paläoenvironments. *Mainzer geowissenschaftliche Mitteilungen* 19:235–65.

Olsson IU. 1986. Radiometric dating. In: Berglund BE, editor. *Handbook of Holocene palaeoecology and palaeohydrology.* Chichester: John Wiley & Sons. p 273–312.

Olsson IU. 1991. Accuracy and precision in sediment chronology. *Hydrobiology* 214:25–34.

Stuiver M, Reimer PJ. 1993. Extended $^{14}$C data base and revised CALIB 3.0 $^{14}$C age calibration program. *Radiocarbon* 35(1):215–30.

Stuiver M, Reimer PJ, Bard E, Beck JW, Burr GS, Hughen KA, Kromer B, McCormac G, van der Plicht J, Spurk M. 1998. INTCAL98 radiocarbon age calibration, 24,000–0 cal BP. *Radiocarbon* 40(3):1041–84.

van den Bogaard P, Schmincke HU. 1985. Laacher See Tephra: a widespread isochronous late Quaternary tephra layer in central and northern Europe. *Geological Society of America Bulletin* 96:1554–71.

van den Bogaard P. 1995. $^{40}$Ar/$^{39}$Ar ages of sanidine phenocrysts from Laacher See Tephra (12,900 yr BP): chronostratigraphic and petrological significance. *Earth and Planetary Science Letters* 133:163–74.

Wohlfarth B, Björck S, Possnert G. 1995. The Swedish time scale: a potential calibration tool for the radiocarbon time scale during the Late Weichselian. *Radiocarbon* 37(2):347–59.

Wohlfarth B, Possnert G. 2000. AMS radiocarbon measurements from the Swedish varved corals. *Radiocarbon.* This issue.

Zbinden H, Andrée M, Oeschger H, Ammann B, Lotter A, Bonani G, Wölfli W. 1989. Atmospheric radiocarbon at the end of the last Glacial: an estimate based on AMS radiocarbon dates on terrestrial macrofossils from lake sediment. *Radiocarbon* 31(3):795–804.

Zolitschka B. 1991. Absolute dating of late Quaternary lacustrine sediments by high resolution varve chronology. *Hydrobiology* 214:59–61.

Zolitschka B. 1998. Paläoklimatische Bedeutung laminierter Sedimente. *Relief, Boden, Paläoklima* 13. Berlin, Stuttgart: Gebrüder Bornträger Verlag. 176 p.

Zolitschka B, Negendank JFW, Lottermoser BG. 1995. Sedimentological proove and dating of the early Holocene volcanic eruption of Ulmener Maar (Vulkaneifel, Germany). *Geologische Rundschau* 84:213–19.

RADIOCARBON, Vol 42, Nr 3, 2000, p 370–381 

# ATMOSPHERIC RADIOCARBON CALIBRATION BEYOND 11,900 CAL BP FROM LAKE SUIGETSU LAMINATED SEDIMENTS

Hiroyuki Kitagawa

Institute for Hydrospheric-Atmospheric Sciences, Nagoya University, Furo-cho, Chikusa-ku, Nagoya, 464-8601, Japan. Email: Kitagawa@ihas.nagoya-u.ac.jp.

Johannes van der Plicht

Centre for Isotope Research, Groningen University, Nijenborgh 4, 9747 AG Groningen, the Netherlands. Email: plicht@phys.rug.nl.

**ABSTRACT.** This paper presents an updated atmospheric radiocarbon calibration from annually laminated (varved) sediments from Lake Suigetsu (LS), central Japan. As presented earlier, the LS varved sediments can be used to extend the radiocarbon time scale beyond the tree ring calibration range that reaches 11,900 cal BP. We have increased the density of $^{14}C$ measurements for terrestrial macrofossils from the same core analyzed previously. The combined data set now consists of 333 measurements, and is compared with other calibration data.

## INTRODUCTION

The latest radiocarbon calibration curve (INTCAL98; Stuiver et al. 1998) was produced by combining several data sets of dendrochronologically dated tree rings for the Holocene, and uranium-thorium (U-Th) dated corals and marine sediments for the Glacial. Using the calibration data set and appropriate computer programs, the conversion of radiocarbon- to calibrated ages is now possible for 24,000–0 cal BP (Before Present, 0 cal BP = AD 1950). To generate the atmospheric $^{14}C$ calibration curve before 11,900 cal BP, however, only a limited number of marine data with an assumed past marine reservoir age has been used.

Atmospheric $^{14}C$ calibration data with higher resolution for the period before 11,900 cal BP can be obtained from laminated sediments. The terrestrial macrofossils (e.g. leaves, branches, and insects) can be dated "absolutely" by counting varve numbers. They can overcome the uncertain assumptions for past marine reservoir ages, and can produce an atmospheric calibration curve with much higher resolution.

We have measured $^{14}C$ dates for terrestrial macrofossils from a long sequence of varved sediments from Lake Suigetsu (Kitagawa and van der Plicht 1998a, 1998b). Recently, we increased the density of $^{14}C$ measurements for terrestrial macrofossils from the same core analyzed previously. Combining the previous and new data sets, we have investigated the fine structure of the atmospheric $^{14}C$ calibration curve before 11,900 cal BP. The $^{14}C$ calibration data from the LS varved sediments are presented here and compared with other calibration records.

## METHODS

### Radiocarbon Dating

$^{14}C$ dating has been performed on terrestrial macrofossils (leaves, branches and insects) from the upper 35-m section of a single 75-m-long core (lab code SG) collected in 1993. All macrofossils used in this study were single pieces retaining its original form, in order to exclude the possibility of reworked material from the surroundings of the lake. To minimize potential contamination, we applied a strong acid-alkali-acid treatment to all the samples.

$^{14}C/^{12}C$ and $^{13}C/^{12}C$ ratios were measured at the Groningen AMS facility (van der Plicht et al. 1995; Wijma and van der Plicht 1997) during 1994–1998. The background was determined by measuring fossil macrofossils collected from deep layers of the same core, with ages in the range 90–100 ka estimated by the tephra chronology of the LS core (Takemura et al. 1994). The average blank correction for the larger samples (>0.7 mg of carbon) is 0.30 ± 0.03 (1$\sigma$) percent modern carbon. For smaller samples, we applied a mass-dependent correction based on the results from the $^{14}$C-free macrofossils. Duplicate measurements were averaged. The agreement between the previous and new data is excellent. The numbers are listed in Table 1 (see Appendix).

### Varve Chronology

The 29,100-yr-long varve chronology in the section 10.42–30.45 m has been constructed using image analysis of around 1500 high resolution digital pictures (Kitagawa and van der Plicht 1998a, 1998b). This was done using the SG core and two short piston cores. The Sakate ash layer (varve nr 9895, corresponding age 18,725 cal BP) was recognized in the deepest part of the short piston cores and 18.67-m deep in the SG cores. The tentative varve chronology produced from the SG core was reassessed based on the observation of the younger sediments above the Sakate ash layer. However, the LS varve chronology of the deeper section below the Sakate ash layer was produced by the varve counting of a single SG core. Beyond 18.8 ka cal BP, the accuracy in the LS varve chronology would become worse, and these ages quoted in this paper should be considered as minimum ages.

### Absolute Age Determination and Its Uncertainty

The absolute age of the LS floating varve chronology has been determined by wiggle-matching 22 $^{14}$C dates from the younger part of the LS sediment to the revised German oak $^{14}$C calibration curve (Spurk et al. 1998; Kromer and Spurk 1998). The previous matching (Kitagawa and van der Plicht 1988a, 1998b) is not revised, even with new data set.

The mean deviation of $^{14}$C between our LS data and the revised oak data is 60 ± 130 $^{14}$C yr (1$\sigma$ level). Omitting four outliers (using a 2$\sigma$ criterion) yields 55 ± 100 $^{14}$C yr. Likewise, we compared the LS $^{14}$C calibration data with the combined German oak and German pine data (Spurk et al. 1998; Kromer and Spurk 1998). The mean deviation is then 40 ± 170 $^{14}$C yr (n=54), and –5 ± 100 $^{14}$C yr when nine outliers are omitted. The apparent deviations might be caused by reworked macrofossils in the LS sediments and/or a blank correction problem. But except for a few outliers, the LS calibration data agree very well with the tree-ring curve.

The uncertainty in the absolute age estimation of the LS varve chronology mainly comes from two sources: 1) the varve chronology itself, and 2) the determination of the absolute age by wiggle matching the younger part of the sediment to the tree-ring curve. Since the detectability of the varve depends on the quality of the lamination, it is not straightforward to estimate the uncertainty in the LS varve chronology. Based on duplicate counting of selected sections (about 10% of the 29,100-yr-long varve chronology), we estimate the uncertainty to be less than 1.5%. In order to construct a more precise LS varve chronology, microscopic observation of thin sections will be performed in the near future. Another uncertainty in the LS varve chronology is caused by possibly incomplete sampling. The SG core was sampled for every 90-cm-long section from one drilling hole. The comparison with short piston cores suggests that the sampling does not cause critical loss of varves: typically 0–2 cm to a maximum of 3 cm for every sampling of about 90 cm, corresponding to about 20–30 and 50 yr for the Holocene and the Late Glacial, respectively. However, the sampling loss causes an accumulation error in the LS varve chronology older than about 19,920 cal BP, corresponding to a depth of 19.39 m in the SG core.

## RESULTS AND COMPARISON WITH OTHER RECORDS

### Deglaciation Period

The updated atmospheric $^{14}C$ calibration dataset from the LS varved sediments is compared with INTCAL98 (Figure 1). Back to 12.5 ka cal BP, the LS data agree in general with INTCAL98, which is constructed from dendrochronologically dated tree rings, U-Th dated corals (Bard et al. 1998; Burr et al. 1998; Edwards et al. 1993) and marine sediments from the Cariaco basin (Hughen et al. 1998; Stuiver et al. 1998). Our LS calibration dataset also agrees well with new data from varved sediments of Lake Gościąż in Poland (Goslar et al. 2000a, 2000b), where a $^{14}C$ plateau is observed at 10,400 BP (between 11.8 and 12.2 ka cal BP) and a rapid increase in $^{14}C$ age to 12.5 ka cal BP.

Before 12.5 ka cal BP, there seems to be a systematic age offset by about 200 $^{14}C$ yr (Stuiver et al. 1998). It is possible that this is caused by an underestimation of about 200 varves at 12–13 ka cal BP. However, a similar age offset has been observed in Lake Gościąż (Goslar et al. 2000a). We note that at present we have no indication or evidence for missing varves in this time interval.

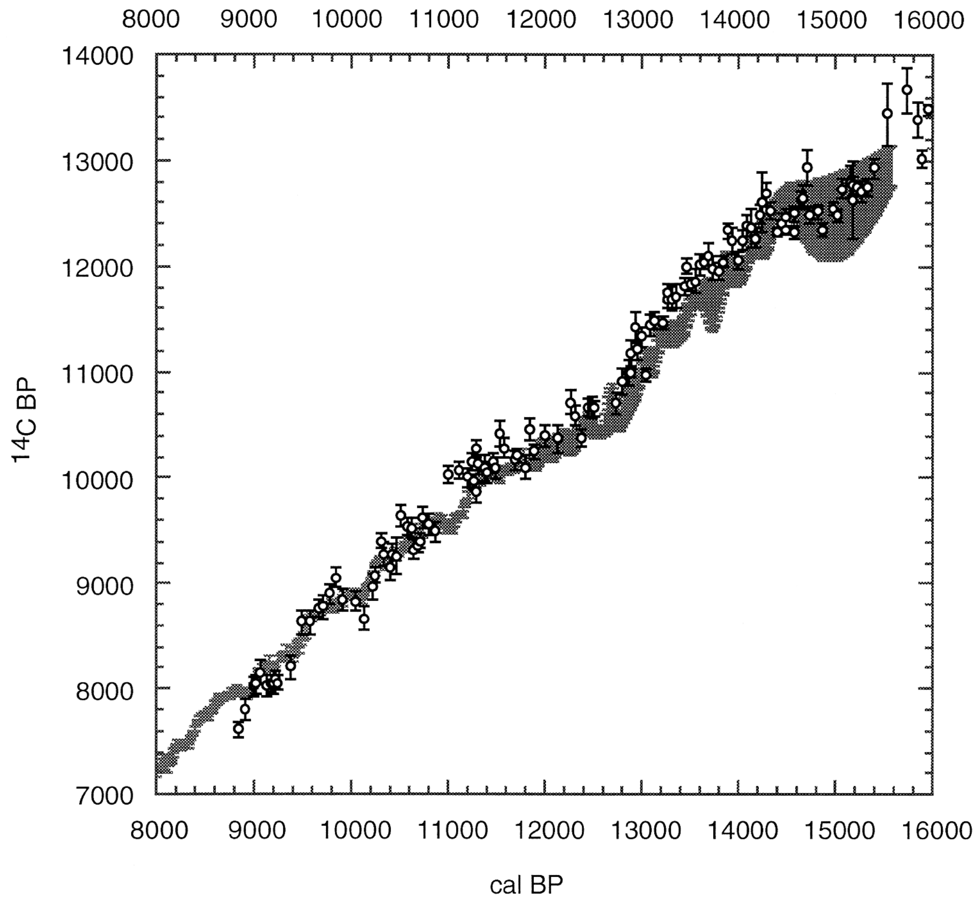


Figure 1 Comparison of atmospheric $^{14}C$ calibration from the varved sediments of Lake Suigetsu (LS) between 8000 and 16,000 cal BP (open circles with ±1σ error bar) with INTCAL98 calibration curve (shadowed by ±1σ; Stuiver et al. 1998).

Another possible explanation is the uncertainty of the marine reservoir correction (R) applied in INTCAL98. In the marine-derived section of INTCAL98, the following assumptions were made: 1) R remains constant for each individual site, and 2) for the period before 10 ka cal BP, R in the whole tropical surface ocean had a constant value of 500 $^{14}C$ yr (and 400 $^{14}C$ yr for samples younger than 10 ka cal BP). If the R values used in INTCAL98 are corrected to the original site-specific reservoir corrections of the corals (300 $^{14}C$ yr for Tahiti and Mururoa and 400 $^{14}C$ yr for Barbados; Bard et al. 1998), the systematic age offset decreases to the error range of the LS varve chronology.

Although there are still uncertainties in the absolute age axis of our $^{14}C$ calibration as well as in the $^{14}C$ age axis of INTCAL98 before 12 ka cal BP, our data show periods of a rather constant $^{14}C$ age (plateaux) at 11.6, 12.1, and 12.5 ka BP. This is consistent with the data from Lake Gościąż (Goslar et al. 2000a).

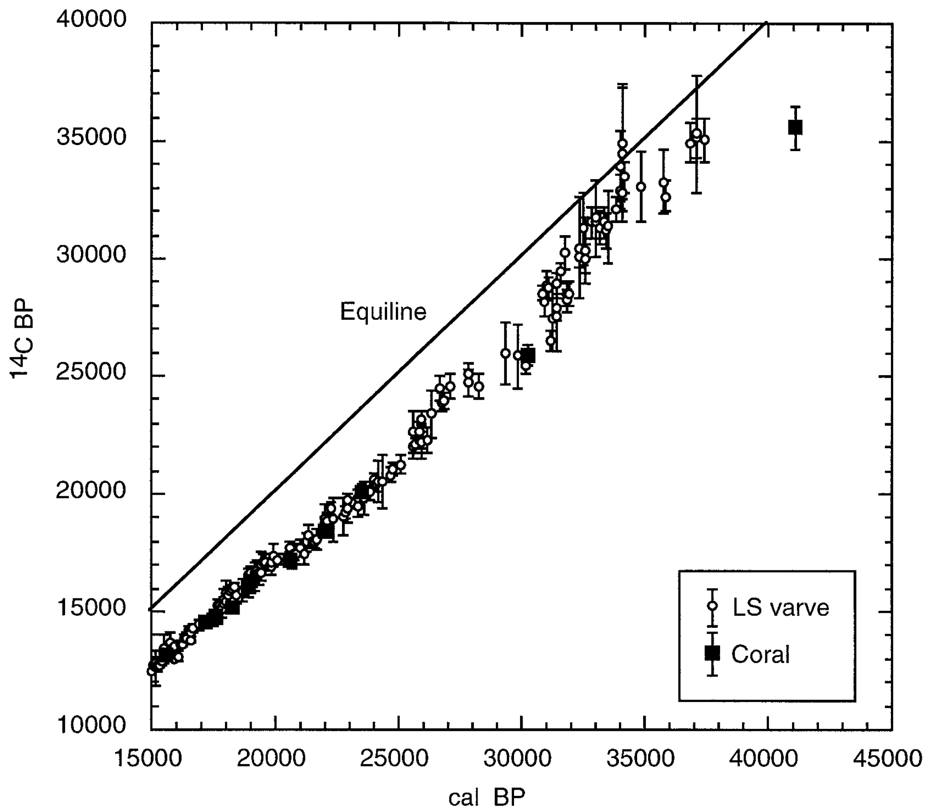


Figure 2 Radiocarbon calibration data from the varved sediments of Lake Suigetsu and U-Th dated corals (Bard et al. 1998) between 15,000 and 41,000 cal BP. Note that the error bars are ±2σ.

#### Full Glacial Period

The older part of the LS $^{14}C$ calibration dataset is compared with calibration data obtained from corals (Figure 2). Between 15,000 and around 24,000 cal BP, the long-term trend of the LS calibration agrees in general with the extended atmospheric calibration curve (INTCAL98) obtained from the U-Th dated corals (Bard et al. 1998), confirming the long-term increasing difference between $^{14}C$ and calendar ages. This trend agrees with the available calibration data obtained by cross-calibration of stable isotope ratios ($^{18}$O from planktonic foraminifera) in North Atlantic cores with the Greenland GISP2 ice core (Voelker et al. 1998), U-Th age based calibration of South African stalagmites (Vogel and Kronfeld 1997) and Lake Lisan sediments in the northern Jordan Valley (Schramm et al. 2000; Stein et al. 2000).

Before 24 ka cal BP, Bard et al.(1988) report two additional calibration datapoints at 30 and 41 ka cal BP, suggesting that the age difference between $^{14}$C and calibrated timescales increase to 3000–4000 and 4000–6000 $^{14}$C yr, respectively. This large difference is confirmed by $^{14}$C calibration data, obtained from U-Th dated sediments of Lake Lisan (Schramn et al. 2000). However, our data for Lake Suigetsu show a very different trend, suggesting a decrease of the $^{14}$C/calendar age difference between 30 and 35 ka cal BP. The precise calendar age determination for the LS varved sediment becomes more difficult with increased age because we reconstructed the LS varve chronology from one single core. Furthermore, possible contamination becomes more critical for older and smaller samples. The older part of the LS $^{14}$C calibration curve remains still tentative, and additional work is needed to confirm the $^{14}$C calibration in this age range.

### Fine Structure of the Glacial Calibration

The time resolution of the LS calibration dataset for the Glacial period permits the investigation of fine structure in the atmospheric $^{14}$C calibration curve. This curve can be strongly influenced by changes in $^{14}$C production as well as by rearrangements in equilibrium between major C reservoirs (atmosphere, ocean and biosphere). For example, our data documents three periods of rather constant $^{14}$C age at 12.5, 17.2, and possibly 25 ka BP, recognized at 14.3–15.0, 20.0–22, and 28–30 ka cal BP, respectively. Stuiver et al. (1998) suggest possible $^{14}$C age plateaux during the Glacial, related to paleo-oceanic changes. Further discussions of the possible century- and millennium-scale fluctuations recognized in our Lake Suigetsu calibration data will be reported elsewhere.

## CONCLUSION

The long sequence of varved sediments from Lake Suigetsu (Japan) permits an unique opportunity to establish a high-resolution atmospheric $^{14}$C calibration curve back to 45,000 years or more. In general, varve-counting dating is only possible if the record is truly continuous; i.e. there is no hiatus or the hiatus is exactly known in time. Indeed the varve chronologies from Sweden (Wohlfarth 1996), Holzmaar in Germany (Hajdas et al. 1995), and Soppensee in Switzerland (Hajdas et al. 1993) have been shifted by several hundred years toward an older age. For Lake Suigetsu, independent checks of varve-$^{14}$C calibration still need to confirm our $^{14}$C calibration curve, in particular beyond 24,000 cal BP. Nevertheless, some fine structure during the glacial has been partly revealed.

## ACKNOWLEDGMENTS

All the $^{14}$C AMS measurements were performed during 1995–1998 at Groningen AMS Facility (the Netherlands). We thank Stef Wijma for precise AMS $^{14}$C measurements.

## REFERENCES

Bard E, Arnold M, Hamelin B, Tisneart-Laborde, Cabioch G. 1998. Radiocarbon calibration by means of mass spectrometric $^{230}$Th/$^{234}$U and $^{14}$C ages of coral: An updated database including samples from Barbados, Mururoa and Tahiti. *Radiocarbon* 40(3):1085–92.

Burr GS, Beck JW, Taylor FW, Récy J, Edwards RL, Cabioch G, Corrège T, Donahue DJ, O'Malley JM. 1998. A high-resolution radiocarbon calibration between 11,700 and 12,400 cal BP derived from $^{230}$Th ages of corals from Espiritu Santo Island, Vanuatu. *Radiocarbon* 40(3):1085–92.

Edwards RL, Beck JW, Burr GS, Donahue DL, Chappell JMA, Bloom AL, Druffel ERM, Taylor FW. 1993. A large drop in atmospheric $^{4}$C/$^{12}$C and reduced melting in the Younger Dryas, documented with $^{230}$Th ages of corals. *Science* 260:962–7.

Goslar T, Arnold M, Tisnerat-Laborde N, Czernik J, Wieckowski K. 2000a. Variation of Younger Dryas atmospheric radiocarbon explicable without ocean circulation changes. *Nature* 403:877–80.

Goslar T, Arnold M, Tisnerat-Laborde, Hatte C, Paterne M, Ralska-Jasiewiczowa M. 2000b. Radiocarbon calibration by means of varves versus $^{14}$C ages of terrestrial macrofossils from Lake Gościąż and Lake Perespilno, Poland. *Radiocarbon*. This issue.

Hajdas I, Ivy SD, Beer J, Bonani G, Imboden D, Lotter AF, Sturm M, Suter M. 1993. AMS radiocarbon dating and varve chronology of Lake Soppensee: 6000 to 12000 $^{14}$C years BP. *Climatic Dynamics* 9:107–16.

Hajdas I, Zolischka B, Ivy-Ochs SD, Beer J, Bonani, Leroy SAG, Negendank JW, Ramrath M, Suter M. 1995. AMS radiocarbon dating of annually laminated sediments from Lake Holzmaar, Germany. *Quaternary Science Reviews* 14:137–43.

Hughen KA, Overpeck JT, Lehman SJ, Kashgrian M, Southon J, Peterson LC, Alley R, Sigman DM. 1998. Deglacial changes in ocean circulation from an extended radiocarbon calibration. *Nature* 391:65–8.

Kitagawa H, van der Plicht J. 1998a. Atmospheric radiocarbon calibration to 45,000 yr BP: Late Glacial fluctuations and cosmogenic isotope production. *Science* 279:1178–90.

Kitagawa H, van der Plicht J. 1998b. A 40,000-year varve chronology from Lake Suigetsu, Japan: extension of the radiocarbon calibration curve. *Radiocarbon* 40(1):505–15.

Kromer B, Spurk M. 1998. Revision and tentative extension of the tree-ring based $^{14}$C calibration, 9200–11,855 cal BP. *Radiocarbon* 40(3):1117–25.

Schramm A, Stein M, Goldstein SL. 2000. Calibration of the $^{14}$C time scale to >40 ka by $^{234}$U-$^{230}$Th dating of Lake Lisan sediments (last glacial Dead Sea). *Earth and Planetary Science Letters* 149:121–9.

Stein M, et al. 2000. Radiocarbon calibration beyond the dendrochronology range. *Radiocarbon*. This issue.

Stuiver M, Reimer PJ, Bard E, Beck JW, Burr GS, Hughen KA, Kromer B, McCormac G, van der Plicht J, Spurk M. 1998. INTCAL98 radiocarbon age calibration, 24,000-0 cal BP. *Radiocarbon* 40(3):1041–83.

Spurk M, Friedrich M, Hofmann J, Remmele S, Frenzel B, Leuschner HH, Kromer B. 1998. Revisions and extensions of the Hohenheim oak and pine chronologies: new evidence about the timing of the Younger Dryas/ Preboreal transition. *Radiocarbon* 40(3):1107–16.

Takemura K, Kitagawa H, Hayashida A, Yasuda Y. 1994. Sediment facies and chronology of core samples from lake Mikata, Lake Suigetsu and Kurota Lowland, central Japan: sedimentary environment in Mikata Lowland since the last interglacial time. *Journal of Geography* 103(3):233–42.

van der Plicht J, Aerts A, Wijma S, Zondervan A. 1995. First results from the Groningen AMS facility. *Radiocarbon* 37(2):657–61.

Vogel JC, Kronfeld J. 1997. Calibration of radiocarbon dates for the late Pleistocene using U/Th dates on stalagmites. *Radiocarbon* 39(1):27–32.

Voelker AHL, Sarnthein M, Grootes PM, Erlenkeuser H, Laj C, Mazaud A, Nadeau M-J, Schleicher M. 1998. Correlation of marine $^{14}$C ages from the Nordic sea with GISP2 isotope record implications for radiocarbon calibration beyond 25 ka BP. *Radiocarbon* 40(1): 517–34.

Wijma S, van der Plicht S. 1997. The Groningen AMS tandetron. *Nuclear Instruments and Method in Physics Research* B123: 218–20.

Wohlfarth B. 1996. The chronology of the last termination: a review of radiocarbon dated, high-resolution terrestrial stratigraphy. *Quaternary Science Reviews* 15:267–84.

## APPENDIX

Table 1 Varve and $^{14}C$ chronologies of varved sediments from Lake Suigetsu. In the first column, I shows already reported data (Kitagawa and van der Plicht 1998a, 1998b); II and III show the new data measured in March, 1998 and August, 1998, respectively. Duplicate measurements are averaged.

| | | Depth (cm) | | Varve age (cal BP) | | $^{14}C$ age | Lab code |
|---|---|---|---|---|---|---|---|
| ID | Sample | Upper | Lower | Upper | Lower | (BP ±1σ) | GrA- |
| I | SG13D01 | 1042.0 | 1045.3 | 8828 | 8862 | 7610 ± 70 | 6234 |
| I | SG13D04 | 1051.8 | 1055.0 | 8907 | 8931 | 7810 ± 100 | 2849 |
| I | SG13D07 | 1061.5 | 1064.8 | 8984 | 9013 | 8020 ± 90 | 6233 |
| I | SG13D08 | 1064.8 | 1068.0 | 9013 | 9050 | 8040 ± 90 | 6232 |
| I | SG13D09 | 1069.1 | 1073.4 | 9050 | 9078 | 8150 ± 110 | 2839 |
| I | SG13C03 | 1077.8 | 1081.0 | 9118 | 9138 | 8020 ± 100 | 2914 |
| I | SG13C05 | 1084.3 | 1087.5 | 9158 | 9183 | 8050 ± 80 | 6235 |
| I | SG13C06 | 1087.5 | 1090.8 | 9183 | 9207 | 8040 ± 100 | 6236 |
| I | SG13C07 | 1090.8 | 1094.0 | 9207 | 9224 | 8090 ± 90 | 2840 |
| I | SG13C09 | 1095.6 | 1098.3 | 9243 | 9263 | 8050 ± 70 | 2947; 2948 |
| I | SG13B05 | 1113.5 | 1118.4 | 9373 | 9402 | 8200 ± 110 | 2901 |
| I | SG13A04 | 1126.5 | 1129.8 | 9481 | 9501 | 8640 ± 110 | 2842 |
| I | SG14D03 | 1139.5 | 1142.7 | 9575 | 9600 | 8640 ± 110 | 2843 |
| I | SG14D06 | 1149.2 | 1152.5 | 9646 | 9671 | 8770 ± 80 | 3087 |
| I | SG14C01 | 1156.8 | 1160.1 | 9705 | 9727 | 8780 ± 110 | 2835 |
| I | SG14C04 | 1166.6 | 1169.8 | 9769 | 9800 | 8900 ± 90 | 3085 |
| I | SG14C06 | 1173.0 | 1176.3 | 9825 | 9848 | 9060 ± 90 | 3080 |
| I | SG14B02 | 1182.2 | 1185.5 | 9892 | 9918 | 8850 ± 110 | 2844 |
| I | SG14B07 | 1198.5 | 1201.7 | 10,030 | 10,055 | 8830 ± 100 | 3082 |
| I | SG14A04 | 1211.5 | 1214.7 | 10,127 | 10,146 | 8670 ± 110 | 2890 |
| I | SG15D01 | 1225.0 | 1228.4 | 10,213 | 10,239 | 8970 ± 120 | 3079 |
| II | SG15D02 | 1228.4 | 1231.8 | 10,239 | 10,261 | 9070 ± 70 | 8184 |
| III | SGD-012 | 1237.4 | 1238.6 | 10,307 | 10,316 | 9400 ± 70 | 10,243 |
| I | SG15D05 | 1238.5 | 1241.9 | 10,316 | 10,350 | 9280 ± 120 | 2971 |
| I | SG15D07 | 1245.3 | 1248.7 | 10,377 | 10,403 | 9150 ± 120 | 2845 |
| I | SG15C01 | 1248.7 | 1252.1 | 10,403 | 10,425 | 9270 ± 120 | 2921 |
| I | SG15C03 | 1255.5 | 1258.9 | 10,450 | 10,470 | 9260 ± 180 | 4585 |
| I | SG15C06 | 1265.6 | 1269.0 | 10,510 | 10,532 | 9640 ± 100 | 2915 |
| I | SG15C08 | 1272.4 | 1275.8 | 10,556 | 10,580 | 9540 ± 80 | 3081 |
| I | SG15B02 | 1279.2 | 1282.6 | 10,603 | 10,626 | 9530 ± 90 | 2847 |
| I | SG15B03 | 1282.6 | 1286.0 | 10,626 | 10,655 | 9320 ± 90 | 2944 |
| II | SG15B05 | 1289.3 | 1292.7 | 10,680 | 10,706 | 9360 ± 60 | 8183 |
| I | SG15B06 | 1292.7 | 1296.1 | 10,706 | 10,732 | 9410 ± 80 | 2913 |
| I | SG15B07 | 1296.1 | 1299.5 | 10,732 | 10,758 | 9630 ± 100 | 2912 |
| I | SG15A01 | 1303.5 | 1306.8 | 10,785 | 10,809 | 9560 ± 110 | 3083 |
| I | SG15A04 | 1313.6 | 1317.0 | 10,857 | 10,880 | 9500 ± 90 | 2907 |
| III | SGD-089 | 1326.2 | 1327.4 | 10,995 | 11,009 | 10,030 ± 80 | 10,260 |
| I | SG16D06 | 1334.8 | 1338.6 | 11,102 | 11,144 | 10,080 ± 90 | 3086 |
| I | SG16C01 | 1342.5 | 1345.9 | 11,180 | 11,215 | 10,010 ± 100 | 2904 |
| III | SGD-109 | 1348.9 | 1350.0 | 11,243 | 11,253 | 10,150 ± 80 | 10,240 |
| II | SG16C03 | 1349.2 | 1352.5 | 11,246 | 11,278 | 9960 ± 80 | 8182 |
| I | SG16C04 | 1352.5 | 1355.8 | 11,278 | 11,303 | 9860 ± 100 | 2905 |
| I | SG16C04 | 1352.5 | 1355.8 | 11,278 | 11,303 | 9860 ± 100 | 2905 |
| III | SGD-114 | 1354.5 | 1355.7 | 11,293 | 11,301 | 10,280 ± 90 | 10,233 |

Table 1 Varve and $^{14}C$ chronologies of varved sediments from Lake Suigetsu. In the first column, I shows already reported data (Kitagawa and van der Plicht 1998a, 1998b); II and III show the new data measured in March, 1998 and August, 1998, respectively. Duplicate measurements are averaged. *(Continued)*

| | | Depth (cm) | | Varve age (cal BP) | | $^{14}C$ age | Lab code |
|---|---|---|---|---|---|---|---|
| ID | Sample | Upper | Lower | Upper | Lower | (BP $\pm 1\sigma$) | GrA- |
| I | SG16C05 | 1355.8 | 1359.7 | 11,303 | 11,336 | 10,130 ± 100 | 2911 |
| I | SG16B01 | 1362.5 | 1365.8 | 11,358 | 11,384 | 10,100 ± 130 | 2961 |
| I | SG16B02 | 1365.8 | 1369.2 | 11,384 | 11,414 | 10,060 ± 100 | 2838 |
| I | SG16B04 | 1372.5 | 1375.8 | 11,447 | 11,474 | 10,150 ± 100 | 2917 |
| I | SG16B05 | 1375.8 | 1379.1 | 11,474 | 11,506 | 10,100 ± 100 | 2916 |
| III | SGD-138 | 1382.8 | 1383.3 | 11,539 | 11,545 | 10,410 ± 120 | 10,234 |
| I | SG16A02 | 1385.3 | 1388.6 | 11,562 | 11,596 | 10,290 ± 90 | 3078 |
| I | SG16A05 | 1395.2 | 1398.6 | 11,664 | 11,699 | 10,170 ± 100 | 2902 |
| I | SG16A06 | 1398.6 | 1401.9 | 11,699 | 11,733 | 10,120 ± 100 | 2909 |
| II | SG16A06 | 1398.6 | 1401.9 | 11,699 | 11,733 | 10,270 ± 70 | 8181 |
| I | SG17D01 | 1408.0 | 1411.1 | 11,789 | 11,827 | 10,100 ± 110 | 2969 |
| I | SG17D02 | 1411.1 | 1414.1 | 11,827 | 11,870 | 10,460 ± 100 | 2836 |
| II | SG17D03 | 1414.1 | 1417.2 | 11,870 | 11,905 | 10,250 ± 80 | 1736 |
| I | SG17D06 | 1423.3 | 1426.3 | 11,986 | 1,2023 | 10,400 ± 110 | 2970 |
| I | SG17D10 | 1435.5 | 1438.0 | 12,129 | 12,157 | 10,370 ± 130 | 2981 |
| I | SG17C03 | 1444.1 | 1447.2 | 12,240 | 12,282 | 10,710 ± 110 | 2837 |
| I | SG17C04 | 1447.2 | 1450.2 | 12,282 | 12,322 | 10,590 ± 100 | 2913 |
| I | SG17B01 | 1453.3 | 1456.3 | 12,352 | 12,383 | 10,380 ± 90 | 2906 |
| II | SG17B03 | 1459.4 | 1462.4 | 12,421 | 12,461 | 10,670 ± 80 | 8179 |
| I | SG17B04 | 1462.4 | 1465.5 | 12,461 | 12,500 | 10,670 ± 100 | 2848 |
| II | SG17B05 | 1465.5 | 1468.5 | 12,500 | 12,537 | 10,660 ± 70 | 8178 |
| I | SG17A02 | 1482.2 | 1485.3 | 12,718 | 12,754 | 10,700 ± 100 | 2908 |
| I | SG17A04 | 1488.3 | 1491.4 | 12,782 | 12,805 | 10,920 ± 130 | 2920 |
| I | SG17A07 | 1496.5 | 1498.0 | 12,851 | 12,864 | 11,000 ± 130 | 3077 |
| I,II | SG18E01 | 1498.0 | 1501.0 | 12,864 | 12,910 | 10,990 ± 40 | 4532; 8177 |
| III | SGD-248 | 1499.6 | 1500.6 | 12,887 | 12,905 | 11,180 ± 130 | 10,268 |
| I | SG18E02 | 1501.0 | 1504.0 | 12,910 | 12,947 | 11,420 ± 150 | 5634 |
| I | SG18E03 | 1504.0 | 1507.0 | 12,947 | 12,987 | 11,210 ± 90 | 5635 |
| I | SG18E04 | 1507.0 | 1509.9 | 12,987 | 13,028 | 11,340 ± 90 | 5637 |
| I | SG18E05 | 1509.9 | 1512.9 | 13,028 | 13,067 | 10,980 ± 60 | 4533 |
| I | SG18E06 | 1512.9 | 1515.9 | 13,067 | 13,112 | 11,440 ± 110 | 5638 |
| I | SG18E07 | 1515.9 | 1518.9 | 13,112 | 13,151 | 11,480 ± 90 | 5639 |
| I | SG18D01 | 1521.4 | 1524.4 | 13,188 | 13,236 | 11,460 ± 60 | 4534 |
| I | SG18D02 | 1524.4 | 1527.3 | 13,236 | 13,284 | 11,690 ± 90 | 5640 |
| III | SGD-274 | 1525.8 | 1526.9 | 13,255 | 13,276 | 11,760 ± 80 | 10,232 |
| II | SG18D03 | 1527.3 | 1530.3 | 13,284 | 13,338 | 11,700 ± 120 | 8190 |
| II | SG18D04 | 1530.3 | 1533.3 | 13,338 | 13,394 | 11,720 ± 110 | 8139 |
| III | SGD-284 | 1536.0 | 1537.0 | 13,435 | 13,454 | 11,810 ± 80 | 10,238 |
| II | SG18D06 | 1536.3 | 1539.3 | 13,441 | 13,492 | 12,000 ± 80 | 1719 |
| I | SG18C01 | 1539.3 | 1542.3 | 13,492 | 13,537 | 11,830 ± 70 | 5641 |
| II | SG18C02 | 1542.3 | 1544.2 | 13,537 | 13,573 | 11,860 ± 110 | 8176 |
| II | SG18C03 | 1544.2 | 1547.2 | 13,573 | 13,621 | 12,010 ± 100 | 8151 |
| I,II | SG18C04 | 1547.2 | 1550.2 | 13,621 | 13,672 | 12,030 ± 60 | 4535 |
| II | SG18C05 | 1550.2 | 1553.2 | 13,672 | 13,717 | 12,100 ± 130 | 8194 |
| I | SG18B01 | 1553.2 | 1556.7 | 13,717 | 13,767 | 11,980 ± 110 | 5653 |
| II | SG18B02 | 1556.7 | 1559.7 | 13,767 | 13,814 | 11,960 ± 80 | 8175 |

Table 1 Varve and $^{14}C$ chronologies of varved sediments from Lake Suigetsu. In the first column, I shows already reported data (Kitagawa and van der Plicht 1998a, 1998b); II and III show the new data measured in March, 1998 and August, 1998, respectively. Duplicate measurements are averaged. *(Continued)*

| ID | Sample | Depth (cm) | | Varve age (cal BP) | | $^{14}C$ age | Lab code |
|---|---|---|---|---|---|---|---|
| | | Upper | Lower | Upper | Lower | (BP ±1σ) | GrA- |
| I | SG18B03 | 1559.7 | 1562.6 | 13,814 | 13,865 | 12,040 ± 60 | 4536 |
| II | SG18B04 | 1562.6 | 1565.6 | 13,865 | 13,914 | 12,330 ± 70 | 8147 |
| I | SG18B05 | 1565.6 | 1568.6 | 13,914 | 13,967 | 12,250 ± 130 | 6206 |
| I | SG18B06 | 1568.6 | 1572.1 | 13,967 | 14,023 | 12,050 ± 90 | 4537 |
| I | SG18A01 | 1572.1 | 1575.1 | 14,023 | 14,067 | 12,250 ± 100 | 5642 |
| II | SG18A02 | 1575.1 | 1578.1 | 14,067 | 14,116 | 12,380 ± 100 | 8189 |
| II | SG18A03 | 1578.1 | 1581.0 | 14,116 | 14,159 | 12,360 ± 190 | 8191 |
| I | SG18A04 | 1581.0 | 1584.0 | 14,159 | 14,198 | 12,270 ± 100 | 6202 |
| II | SG18A05 | 1584.0 | 1587.0 | 14,198 | 14,238 | 12,490 ± 90 | 8148 |
| I | SG18A06 | 1587.0 | 1589.0 | 14,238 | 14,267 | 12,610 ± 300 | 5654 |
| II | SG19D01 | 1589.0 | 1592.1 | 14,267 | 14,316 | 12,680 ± 120 | 8150 |
| II | SG19D02 | 1592.1 | 1595.3 | 14,316 | 14,366 | 12,520 ± 80 | 8143 |
| I,II | SG19D03 | 1595.3 | 1598.4 | 14,366 | 14,421 | 12,320 ± 50 | 4539; 8185 |
| I | SG19D04 | 1598.4 | 1601.6 | 14,421 | 14,467 | 12,410 ± 100 | 6204 |
| III | SGD-350 | 1602.4 | 1603.4 | 14,480 | 14,497 | 12,460 ± 90 | 10,231 |
| I,II | SG19D05 | 1601.6 | 1604.7 | 14,467 | 14,514 | 12,350 ± 50 | 5643; 8188 |
| I | SG19D08 | 1601.6 | 1604.7 | 14,467 | 14,514 | 12,500 ± 70 | 5644; 8160 |
| I,II | SG19D07 | 1607.8 | 1611.0 | 14,558 | 14,607 | 12,320 ± 60 | 4540 |
| III | SGD-360 | 1612.7 | 1613.8 | 14,633 | 14,648 | 12,630 ± 90 | 10,239 |
| II | SG19C01 | 1614.1 | 1617.2 | 14,651 | 14,702 | 12,660 ± 110 | 8156 |
| III | SGD-364 | 1616.8 | 1617.9 | 14,695 | 14,713 | 12,940 ± 160 | 10,235 |
| II | SG19C02 | 1617.2 | 1620.4 | 14,702 | 14,748 | 12,480 ± 90 | 8159 |
| I | SG19C04 | 1623.5 | 1626.7 | 14,787 | 14,838 | 12,520 ± 70 | 5645 |
| I | SG19C05 | 1626.7 | 1629.8 | 14,838 | 14,879 | 12,350 ± 60 | 4541 |
| II | SG19C08 | 1636.1 | 1638.2 | 14,961 | 14,992 | 12,550 ± 60 | 8173 |
| I | SG19B01 | 1638.2 | 1641.3 | 14,992 | 15,044 | 12,490 ± 60 | 4542 |
| II | SG19B02 | 1641.3 | 1644.4 | 15,044 | 15,093 | 12,740 ± 100 | 8135 |
| III | SGD-394 | 1647.8 | 1648.8 | 15,151 | 15,169 | 12,800 ± 150 | 10,242 |
| I | SG19B04 | 1647.6 | 1650.7 | 15,148 | 15,202 | 12,630 ± 370 | 5646 |
| III | SGD-395 | 1648.8 | 1649.8 | 15,169 | 15,187 | 12,770 ± 90 | 10,237 |
| I | SG19B05 | 1650.7 | 1653.9 | 15,202 | 15,251 | 12,750 ± 80 | 4543 |
| I | SG19B06 | 1653.9 | 1657.0 | 15,251 | 15,306 | 12,710 ± 110 | 6205 |
| II | SG19B07 | 1657.0 | 1660.1 | 1,5306 | 15,370 | 12,750 ± 80 | 8140 |
| II | SG19A01 | 1660.1 | 1663.3 | 15,370 | 15,427 | 12,930 ± 90 | 8136 |
| I | SG19A03 | 1667.4 | 1670.6 | 15,501 | 15,555 | 13,440 ± 300 | 5648 |
| I | SG20D01 | 1680.0 | 1683.3 | 15,713 | 15,764 | 13,670 ± 220 | 4550 |
| I | SG20D03 | 1686.5 | 1689.8 | 15,815 | 15,867 | 13,390 ± 170 | 5649 |
| I | SG20D04 | 1689.8 | 1693.0 | 15,867 | 15,926 | 13,020 ± 80 | 4551 |
| I,II | SG20D05 | 1693.0 | 1696.3 | 15,926 | 15,982 | 13,480 ± 60 | 5650; 8130 |
| I | SG20C03 | 1693.0 | 1696.3 | 15,926 | 15,982 | 13,630 ± 50 | 4552; 8128 |
| II | SG20C01 | 1702.8 | 1706.0 | 16,096 | 16,137 | 13,110 ± 110 | 5636 |
| I,II | SG20C02 | 1706.0 | 1709.3 | 16,137 | 16,183 | 13,610 ± 70 | 8134 |
| I | SG20C05 | 1715.8 | 1719.0 | 16,298 | 16,351 | 13,890 ± 80 | 5651 |
| I | SG20C06 | 1719.0 | 1722.3 | 16,351 | 16,408 | 13,860 ± 130 | 4553 |
| I,II | SG20B01 | 1726.0 | 1729.3 | 16,474 | 16,528 | 14,220 ± 80 | 6203; 8142 |
| I | SG20B02 | 1729.3 | 1732.5 | 16,528 | 16,577 | 13,820 ± 70 | 4554 |

Table 1 Varve and $^{14}$C chronologies of varved sediments from Lake Suigetsu. In the first column, I shows already reported data (Kitagawa and van der Plicht 1998a, 1998b); II and III show the new data measured in March, 1998 and August, 1998, respectively. Duplicate measurements are averaged. *(Continued)*

| | | Depth (cm) | | Varve age (cal BP) | | $^{14}$C age | Lab code |
|---|---|---|---|---|---|---|---|
| ID | Sample | Upper | Lower | Upper | Lower | (BP ±1σ) | GrA- |
| II | SG20B03 | 1732.5 | 1735.8 | 16,577 | 16,633 | 14,160 ± 120 | 8133 |
| I | SG20B04 | 1735.8 | 1739.0 | 16,633 | 16,688 | 14,300 ± 90 | 5652 |
| I | SG20A03 | 1755.3 | 1758.5 | 16,928 | 16,982 | 14,440 ± 100 | 4555 |
| II | SG20A05 | 1761.8 | 1765.0 | 17,028 | 17,072 | 14,580 ± 90 | 8132 |
| I | SG21D04 | 1779.8 | 1782.7 | 17,318 | 17,366 | 14,700 ± 60 | 4556 |
| II | SG21D06 | 1785.7 | 1788.6 | 17,417 | 17,463 | 14,740 ± 80 | 8193 |
| I | SG21D07 | 1788.6 | 1791.5 | 17,463 | 17,503 | 14,600 ± 90 | 4557 |
| II | SG21D08 | 1791.5 | 1793.5 | 17,503 | 17,536 | 14,630 ± 110 | 8113 |
| I | SG21C02 | 1796.4 | 1799.3 | 17,582 | 17,631 | 14,630 ± 60 | 4558 |
| I | SG21C03 | 1799.3 | 1802.3 | 17,631 | 17,683 | 14,860 ± 200 | 4559 |
| II | SG21C04 | 1802.3 | 1805.2 | 17,683 | 17,727 | 15,240 ± 150 | 8116 |
| II | SG21C05 | 1805.2 | 1808.1 | 17,727 | 17,773 | 15,280 ± 80 | 8111 |
| II | SG21C06 | 1808.1 | 1811.0 | 17,773 | 17,820 | 15,200 ± 90 | 8120 |
| I | SG21C07 | 1811.0 | 1814.0 | 17,820 | 17,863 | 15,130 ± 190 | 4556 |
| II | SG21B01 | 1814.0 | 1816.9 | 17,863 | 17,911 | 15,390 ± 120 | 8119 |
| II | SG21B02 | 1816.9 | 1819.8 | 17,911 | 17,955 | 15,540 ± 210 | 8112 |
| I | SG21B03 | 1819.8 | 1822.8 | 17,955 | 18,006 | 15,760 ± 270 | 4561 |
| I | SG21B04 | 1822.8 | 1825.7 | 18,006 | 18,059 | 15,480 ± 140 | 5658 |
| I | SG21B05 | 1825.7 | 1828.6 | 18,059 | 18,109 | 15,730 ± 150 | 5668 |
| II | SG21B06 | 1828.6 | 1831.6 | 18,109 | 18,159 | 15,860 ± 80 | 8114 |
| II | SG21A02 | 1837.4 | 1840.3 | 18,265 | 18,311 | 15,990 ± 80 | 8186 |
| II | SG21A03 | 1840.3 | 1843.3 | 18,311 | 18,367 | 16,040 ± 80 | 8192 |
| I | SG21A05 | 1846.2 | 1850.1 | 18,419 | 18,485 | 15,700 ± 180 | 4562 |
| I | SG22D03 | 1862.1 | 1866.1 | 18,688 | 18,729 | 15,920 ± 230 | 4564 |
| I | SG22D06 | 1872.7 | 1875.2 | 18,823 | 18,851 | 15,990 ± 180 | 4565 |
| II | SG22C02 | 1877.3 | 1880.3 | 18,880 | 18,929 | 16,350 ± 90 | 8124 |
| II | SG22C03 | 1880.3 | 1883.3 | 18,929 | 18,979 | 16,570 ± 130 | 8118 |
| II | SG22C04 | 1883.3 | 1886.4 | 18,979 | 19,036 | 16,700 ± 130 | 8123 |
| I | SG22C06 | 1889.4 | 1894.5 | 19,083 | 19,179 | 16,280 ± 200 | 4566 |
| II | SG22C07 | 1894.5 | 1896.5 | 19,179 | 19,212 | 16,680 ± 210 | 8122 |
| I | SG22B02 | 1899.5 | 1902.6 | 19,266 | 19,320 | 16,750 ± 220 | 5669 |
| II | SG22B03 | 1902.6 | 1905.6 | 19,320 | 19,374 | 16,640 ± 260 | 8115 |
| I | SG22B04 | 1905.6 | 1908.6 | 19,374 | 19,422 | 16,700 ± 180 | 5668 |
| I | SG22B05 | 1908.6 | 1912.7 | 19,422 | 19,498 | 17,070 ± 240 | 4567 |
| II | SG22B06 | 1912.7 | 1915.7 | 19,498 | 19,554 | 17,110 ± 170 | 8127 |
| I | SG22A01 | 1917.7 | 1920.8 | 19,589 | 19,646 | 17,140 ± 170 | 4586 |
| II | SG22A03 | 1924.8 | 1926.9 | 19,725 | 19,766 | 16,950 ± 80 | 8155 |
| I | SG22A04 | 1926.9 | 1929.9 | 19,766 | 19,825 | 16,950 ± 190 | 4569 |
| I,I | SG22A05 | 1929.9 | 1932.9 | 19,825 | 19,883 | 17,140 ± 90 | 4570; 8187 |
| I | SG22A06 | 1932.9 | 1936.0 | 19,883 | 19,939 | 17,380 ± 240 | 5660 |
| III | SG23D02 | 1943.2 | 1946.3 | 20,084 | 20,142 | 17,220 ± 120 | 10,245 |
| I | SG23-4 | 1968.9 | 1969.8 | 20,588 | 20,606 | 17,750 ± 140 | 6193 |
| III | SG23C04 | 1971.5 | 1974.6 | 20,636 | 20,684 | 17,200 ± 180 | 10,246 |
| III | SG23C05 | 1974.6 | 1977.7 | 20,684 | 20,744 | 17,470 ± 130 | 10,247 |
| III | SG23C07 | 1980.9 | 1984.0 | 20,794 | 20,850 | 17,450 ± 210 | 10,269 |

Table 1 Varve and $^{14}C$ chronologies of varved sediments from Lake Suigetsu. In the first column, I shows already reported data (Kitagawa and van der Plicht 1998a, 1998b); II and III show the new data measured in March, 1998 and August, 1998, respectively. Duplicate measurements are averaged. *(Continued)*

| | | Depth (cm) | | Varve age (cal BP) | | $^{14}C$ age | Lab code |
|---|---|---|---|---|---|---|---|
| ID | Sample | Upper | Lower | Upper | Lower | (BP ±1σ) | GrA- |
| III | SG23B04 | 1993.4 | 1996.6 | 21,015 | 21,070 | 17,750 ± 160 | 10,249 |
| III | SG23B06 | 1999.7 | 2002.9 | 21,123 | 21,173 | 17,430 ± 200 | 10,248 |
| III | SG23A01 | 2006.0 | 2009.2 | 21,219 | 21,274 | 17,960 ± 200 | 10,270 |
| III | SG23A03 | 2012.3 | 2015.4 | 21,332 | 21,379 | 18,240 ± 230 | 10,250 |
| III | SG23A07 | 2024.9 | 2028.0 | 21,518 | 21,566 | 17,960 ± 130 | 10,252 |
| III | SG24E01 | 2028.0 | 2031.0 | 21,566 | 21,622 | 17,970 ± 130 | 10,253 |
| III | SG24E02 | 2031.0 | 2034.0 | 21,622 | 21,675 | 18,090 ± 230 | 10,254 |
| I | SG24-5 | 2050.5 | 2051.6 | 21,961 | 21,979 | 18,810 ± 110 | 6192 |
| III | SG24D03 | 2051.1 | 2054.1 | 21,972 | 22,027 | 18,770 ± 130 | 10,255 |
| I | SG24-4 | 2053.8 | 2054.8 | 22,021 | 22,037 | 18,980 ± 290 | 6191 |
| III | SG24D04 | 2054.1 | 2057.2 | 22,027 | 22,080 | 18,780 ± 200 | 10,383 |
| III | SG24D05 | 2057.2 | 2060.2 | 22,080 | 22,136 | 18,830 ± 150 | 10,256 |
| I | SG24-3 | 2064.9 | 2065.9 | 22,211 | 22,224 | 19,370 ± 140 | 6190 |
| III | SG24C02 | 2068.7 | 2071.7 | 22,273 | 22,325 | 18,930 ± 450 | 10,258 |
| III | SG24B05 | 2094.9 | 2097.9 | 22,696 | 22,742 | 19,030 ± 390 | 10,262 |
| III | SG24B08 | 2103.9 | 2105.9 | 22,840 | 22,877 | 19,190 ± 130 | 10,263 |
| I | SG24-1 | 2106.4 | 2107.4 | 22,884 | 22,901 | 19,430 ± 310 | 6189 |
| III | SG24A01 | 2105.9 | 2108.9 | 22,877 | 22,924 | 19,760 ± 140 | 10,261 |
| III | SG25E05 | 2131.1 | 2134.1 | 23,280 | 23,331 | 19,810 ± 200 | 10,264 |
| III | SG25E06 | 2134.1 | 2137.1 | 23,331 | 23,386 | 19,460 ± 200 | 10,265 |
| III | SG25D01 | 2140.2 | 2143.2 | 23,441 | 23,494 | 20,040 ± 210 | 10,266 |
| I | SG25-2 | 2149.0 | 2150.1 | 23,600 | 23,618 | 19,830 ± 370 | 6188 |
| III | SG25C02 | 2163.3 | 2166.3 | 23,833 | 23,885 | 20,110 ± 200 | 19,401 |
| I | SG25-1 | 2175.0 | 2176.0 | 24,030 | 24,046 | 20,630 ± 130 | 6187 |
| III | SG25C06 | 2175.3 | 2178.4 | 24,036 | 24,090 | 20,430 ± 150 | 10,361 |
| III | SG25C08 | 2181.4 | 2183.4 | 24,144 | 24,182 | 20,500 ± 450 | 10,362 |
| III | SG25B03 | 2189.4 | 2192.4 | 24,301 | 24,347 | 20,540 ± 560 | 10,367 |
| III | SG26D01 | 2210.0 | 2213.0 | 24,630 | 24,692 | 20,830 ± 150 | 10,360 |
| III | SG26D03 | 2216.1 | 2219.1 | 24,750 | 24,813 | 21,060 ± 150 | 10,368 |
| III | SG26C01 | 2234.3 | 2237.4 | 25,104 | 25,151 | 21,270 ± 200 | 10,404 |
| III | SG26B03 | 2263.7 | 2266.7 | 25,581 | 25,627 | 22,060 ± 260 | 10,369 |
| I | SG26-3 | 2264.8 | 2266.9 | 25,600 | 25,629 | 22,600 ± 440 | 6186 |
| III | SG26B05 | 2269.8 | 2272.8 | 25,679 | 25,733 | 22,080 ± 160 | 10,370 |
| I | SG26-2 | 2277.9 | 2278.9 | 25,803 | 25,818 | 22,630 ± 220 | 6185 |
| III | SG26A01 | 2278.9 | 2281.9 | 25,819 | 25,859 | 22,280 ± 160 | 10,371 |
| III | SG26A02 | 2281.9 | 2285.0 | 25,859 | 25,906 | 22,280 ± 170 | 10,372 |
| I | SG26-1 | 2285.6 | 2286.6 | 25,915 | 25,932 | 23,170 ± 150 | 6184 |
| III | SG26A03 | 2285.0 | 2288.0 | 25,906 | 25,954 | 22,230 ± 390 | 10,373 |
| III | SG26A07 | 2297.2 | 2301.0 | 26,100 | 26,162 | 22,300 ± 260 | 10,375 |
| I | SG27-7 | 2311.3 | 2312.3 | 26,336 | 26,351 | 23,400 ± 500 | 6183 |
| I | SG27-5 | 2333.9 | 2334.9 | 26,696 | 26,714 | 24,500 ± 270 | 6182 |
| I | SG27-4 | 2336.2 | 2337.3 | 26,742 | 26,757 | 23,890 ± 210 | 6181 |
| I | SG27-3 | 2339.5 | 2340.6 | 26,790 | 26,819 | 23,970 ± 170 | 6180 |
| I | SG27-2 | 2355.5 | 2356.5 | 27,047 | 27,061 | 24,600 ± 270 | 6179 |
| I | SG28-4 | 2406.2 | 2407.2 | 27,803 | 27,821 | 24,700 ± 270 | 6178 |
| I | SG28-3 | 2408.7 | 2409.7 | 27,847 | 27,862 | 25,130 ± 190 | 6177 |

Table 1 Varve and $^{14}C$ chronologies of varved sediments from Lake Suigetsu. In the first column, I shows already reported data (Kitagawa and van der Plicht 1998a, 1998b); II and III show the new data measured in March, 1998 and August, 1998, respectively. Duplicate measurements are averaged. *(Continued)*

| ID | Sample | Depth (cm) Upper | Depth (cm) Lower | Varve age (cal BP) Upper | Varve age (cal BP) Lower | $^{14}C$ age (BP ±1σ) | Lab code GrA- |
|---|---|---|---|---|---|---|---|
| I | SG28-2 | 2433.0 | 2434.0 | 28,275 | 28,290 | 24,550 ± 270 | 6176 |
| I | SG29-3 | 2508.6 | 2509.6 | 29,353 | 29,374 | 25,980 ± 670 | 6173 |
| I | SG29-2 | 2537.7 | 2538.7 | 29,860 | 29,876 | 25,840 ± 670 | 6172 |
| I | SG29-1 | 2560.5 | 2561.6 | 30,166 | 30,177 | 25,450 ± 190 | 6171 |
| III | SG30D06 | 2600.9 | 2604.5 | 30,780 | 30,852 | 28,530 ± 150 | 10,381 |
| III | SG30C01 | 2604.5 | 2607.6 | 30,852 | 30,905 | 28,140 ± 290 | 10,378 |
| III | SG30C03 | 2610.7 | 2613.8 | 30,964 | 31,016 | 28,860 ± 290 | 10,380 |
| III | SG30C04 | 2613.8 | 2616.8 | 31,016 | 31,081 | 28,770 ± 230 | 10,376 |
| I | SG30-5 | 2622.9 | 2623.9 | 31,192 | 31,209 | 26,460 ± 220 | 6168 |
| III | SG30C07 | 2623.0 | 2626.1 | 31,194 | 31,250 | 27,420 ± 670 | 10,395 |
| III | SG30C10 | 2632.3 | 2635.3 | 31,355 | 31,411 | 27,520 ± 720 | 10,388 |
| III | SG30B01 | 2635.3 | 2637.4 | 31,411 | 31,444 | 28,960 ± 230 | 10,389 |
| I | SG30-4 | 2635.9 | 2636.9 | 31,421 | 31,438 | 27,880 ± 240 | 6169 |
| III | SG30B05 | 2646.6 | 2649.2 | 31,578 | 31,617 | 29,450 ± 190 | 10,391 |
| III | SG30A04 | 2658.5 | 2661.6 | 31,759 | 31,809 | 30,270 ± 330 | 10,390 |
| I | SG30R-1 | 2661.0 | 2662.1 | 31,801 | 31,816 | 28,500 ± 250 | 6174 |
| I | SG30-3 | 2662.9 | 2664.0 | 31,829 | 31,845 | 28,220 ± 250 | 6170 |
| I | SG30-1 | 2671.2 | 2672.3 | 31,939 | 31,955 | 28,500 ± 260 | 6167 |
| III | SG31-7 | 2697.8 | 2698.9 | 32,320 | 32,337 | 30,080 ± 200 | 5618 |
| I | SG31D08 | 2698.8 | 2695.5 | 32,336 | 32,389 | 30,470 ± 060 | 10,415 |
| III | SG31C02 | 2709.2 | 2712.5 | 32,505 | 32,559 | 31,310 ± 770 | 10,416 |
| I | SG31-6 | 2716.0 | 2717.1 | 32,606 | 32,620 | 30,010 ± 310 | 5617 |
| III | SG31C04 | 2715.8 | 2719.1 | 32,603 | 32,652 | 30,360 ± 700 | 10,417 |
| I | SG31-5 | 2732.0 | 2733.1 | 32,834 | 32,850 | 31,550 ± 340 | 5616 |
| I | SG31-4 | 2739.5 | 2740.6 | 32,969 | 32,989 | 31,550 ± 340 | 5615 |
| III | SG31B05 | 2741.0 | 2744.3 | 32,995 | 33,047 | 31,750 ± 810 | 10,419 |
| I | SG31-1 | 2751.3 | 2752.4 | 33,162 | 33,176 | 31,350 ± 360 | 5613 |
| I | SG31-3 | 2760.9 | 2762.0 | 33,317 | 33,336 | 31,550 ± 330 | 5614 |
| I | SG31-7 | 2764.1 | 2765.2 | 33,371 | 33,388 | 31,190 ± 360 | 5625 |
| III | SG32F03 | 2770.0 | 2773.2 | 33,470 | 33,526 | 31,380 ± 760 | 10,422 |
| I | SG32-6 | 2791.7 | 2792.7 | 33,853 | 33,871 | 32,140 ± 260 | 5624 |
| III | SG32D02 | 2797.8 | 2801.0 | 33,943 | 33,996 | 33,980 ± 740 | 10,426 |
| I | SG32-5 | 2800.1 | 2801.2 | 33,980 | 33,998 | 32,880 ± 370 | 5623 |
| III | SG32C01 | 2804.2 | 2807.4 | 34,053 | 34,100 | 34,940 ± 180 | 10,429 |
| I | SG32-4 | 2806.5 | 2807.5 | 34,086 | 34,101 | 32,830 ± 380 | 5622 |
| III | SG32C02 | 2807.4 | 2810.7 | 34,100 | 34,144 | 34,500 ± 470 | 10,430 |
| I | SG32-2 | 2812.8 | 2813.9 | 34,177 | 34,194 | 33,480 ± 350 | 5620 |
| I | SG32-1 | 2855.1 | 2856.2 | 34,841 | 34,858 | 33,070 ± 730 | 5619 |
| I | SG33-4 | 2913.3 | 2914.4 | 35,733 | 35,749 | 33,270 ± 680 | 5626 |
| I | SG33-3 | 2920.1 | 2921.2 | 35,848 | 35,865 | 32,640 ± 330 | 5627 |
| I | SG34-2 | 2976.0 | 2977.2 | 36,798 | 36,813 | 34,950 ± 420 | 5631 |
| I | SG34-4 | 2993.7 | 2994.9 | 37,088 | 37,107 | 35,140 ± 420 | 5632 |
| III | SG34B06 | 2994.3 | 2997.8 | 37,096 | 37,155 | 35,320 ± 250 | 10,434 |
| I | SG34-3 | 3012.6 | 3013.7 | 37,392 | 37,417 | 35,070 ± 460 | 5633 |

RADIOCARBON, Vol 42, Nr 3, 2000, p 383–401 

# LAST ICE AGE MILLENNIAL SCALE CLIMATE CHANGES RECORDED IN HUON PENINSULA CORALS

Yusuke Yokoyama[1,2] • Tezer M Esat[1,3] • Kurt Lambeck[1] • L Keith Fifield[4]

**ABSTRACT.** Uranium series and radiocarbon ages were measured in corals from the uplifted coral terraces of Huon Peninsula (HP), Papua New Guinea, to provide a calibration for the $^{14}C$ time scale beyond 30 ka (kilo annum). Improved analytical procedures, and quantitative criteria for sample selection, helped discriminate diagenetically altered samples. The base-line of the calibration curve follows the trend of increasing divergence from calendar ages, as established by previous studies. Superimposed on this trend, four well-defined peaks of excess atmospheric radiocarbon were found ranging in magnitude from 100% to 700%, relative to current levels. They are related to episodes of sea-level rise and reef growth at HP. These peaks appear to be synchronous with Heinrich Events and concentrations of ice-rafted debris found in North Atlantic deep-sea cores. Relative timing of sea-level rise and atmospheric $^{14}C$ excess imply the following sequence of events: An initial sea-level high is followed by a large increase in atmospheric $^{14}C$ as the sea-level subsides. Over about 1800 years, the atmospheric radiocarbon drops to below present ambient levels. This cycle bears a close resemblance to ice-calving episodes of Dansgaard-Oeschger and Bond cycles and the slow-down or complete interruption of the North Atlantic thermohaline circulation. The increases in the atmospheric $^{14}C$ levels are attributed to the cessation of the North Atlantic circulation.

## INTRODUCTION

Calibration of the radiocarbon time scale over the last ~11 ka has been secured using tree-ring chronology (Becker and Kromer 1993). Data beyond this period, however, are not extensive (Bard 1998). $^{14}C$ dating and calendar ages ($^{230}Th/^{234}U$ dating) of corals can be determined directly (Bard et al. 1998), an advantage that is particularly relevant for time periods beyond ~25 ka. Coral samples from drill-cores offshore from Barbados (Bard et al. 1990a, 1990b, 1993, 1998) and from Huon Peninsula (Edwards et al. 1993) have been dated with accelerator mass spectrometry (AMS $^{14}C$; Nelson et al. 1977) and thermal ionization mass spectrometry (TIMS, Th/U; Edwards et al. 1987). Where there is an overlap in calendar ages determined from tree-rings and U/Th dating, the two methods are in good agreement (Bard et al. 1998; Kromer and Spurk 1998).

We have extended the previous coral-based $^{14}C$ calibration from 30 ka to beyond 50 ka using mass spectrometric $^{14}C$ and Th/U dating techniques on corals collected from Reefs II and III at Huon Peninsula, Papua New Guinea (Figure 1). In this paper, we report the new results and discuss possible causes of large excursions of atmospheric $^{14}C$ recorded in these corals. Some Th/U ages were previously available for a subset of the same corals (Chappell et al. 1996).

## MATERIALS AND METHODS

Most of the corals used in this study were collected from Bobongara (Bobo) and Kanzarua (Kanz) sections that have some of the highest uplift rates at HP (Figure 1). A number of Th/U dates and descriptions of sample locations have been provided by Chappell et al. (1996). General TIMS U-series dating methods were described by Edwards et al. (1987), and procedures used in the present work were previously documented by Stirling et al. (1995) and Esat, (1995). For $^{14}C$ dating, $CO_2$ extracted from corals was converted to graphite, in the presence of $H_2$, using Fe powder as a catalyst

[1]Research School of Earth Sciences, The Australian National University, Canberra, ACT 0200, Australia
[2]Present address: Space Sciences Laboratory, University of California at Berkeley and Lawrence Livermore National Laboratory, P.O. Box 808, L-202, Livermore, CA94550 USA. Email: yusuke@ssl.berkeley.edu.
[3]Department of Geology, The Australian National University, Canberra, ACT 0200, Australia
[4]Department of Nuclear Physics, Research School of Physical Sciences and Engineering, The Australian National University, Canberra, ACT 0200, Australia

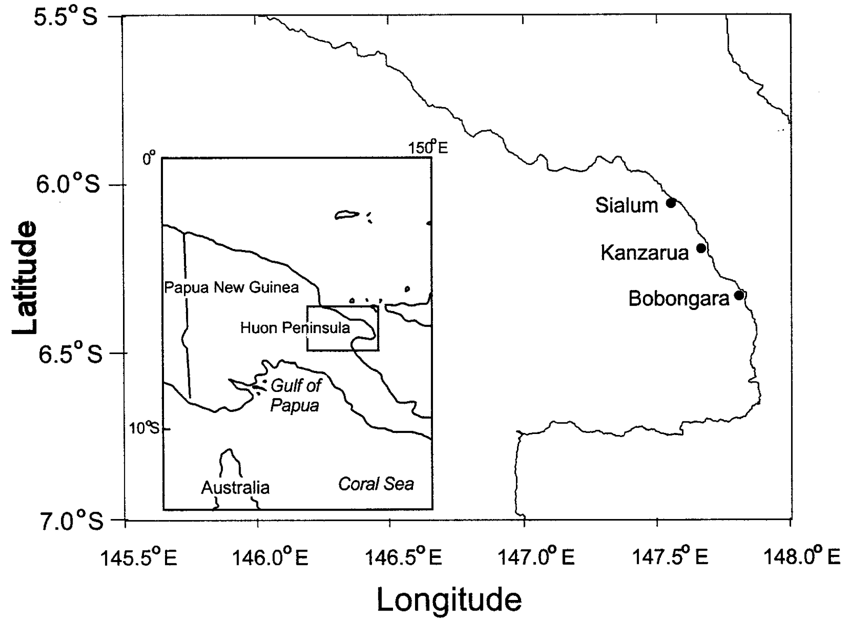


Figure 1 Location of Kanzarua and Bobongara reef sections at Huon Peninsula, Papua New Guinea.

(Vogel et al. 1984), and is described below in detail. Particulars of AMS dating at the Australian National University can be found in Fifield et al. (1993).

The graphitization method employed in the present study reliably produces high graphite yields (>85-95%). Water is formed as the byproduct of the reaction:

$$2H_2 + CO_2 \underset{625\ °C}{\overset{(Fe)}{\Rightarrow}} C + 2H_2O \tag{1}$$

The addition of dry-ice cold traps attached to the reaction vessel, efficiently trapped water vapor away from the sample and even higher graphite yields (~100%) could be achieved.

To obtain approximately 1–1.5 mg of graphite, ~1.2–1.8 mg of pre-reduced 325 mesh iron powder was typically used resulting in C:Fe ratio of 1 to 1.2. A weighed vycor-glass thimble cup (6 mm diameter and ~1 cm long) containing the iron powder was placed in a larger diameter vycor-glass tube (9 mm diameter and ~15 cm long) and labelled. All vycor glassware was precleaned ultrasonically with distilled water and baked overnight at 900 °C. The reaction tube and connecting pieces were cleaned in 1:1 $HNO_3$ and rinsed with distilled water, then stored in an oven at ~60 °C until needed. Phosphoric acid (85%) was concentrated on a hotplate with an equal amount of $H_2O_2$ (30%) to oxidize and remove organic impurities.

To reduce the possibility of contamination during the $CO_2$-graphite conversion we strived to exclude all sources of organic contamination. For this purpose, an all-metal high-vacuum system was constructed with strict control protocol on its use, including the type and age of samples allowed to be processed. The conversion line was made using 0.25-inch stainless steel tubing with Swage-Lock®

joints and stainless-steel bellow valves. All of the component parts were cleaned to remove organic residues and baked under vacuum for extended periods. The line is evacuated using a turbo-molecular pump with a liquid nitrogen trap to prevent oil contamination from the pump. A vacuum of better than $10^{-4}$ Torr can be maintained during sample processing.

The vacuum was monitored using two thermocouple gauges. Quantitative $CO_2$ and $H_2$ pressures were measured by two pressure transducers, Baratron®, which have accuracies of ±0.05% and ±0.5%. The more precise Baratron®, was used for low-pressure measurements to monitor the yield of gases evolved from the sample, within a calibrated volume, and the other Baratron®, which has a higher pressure capacity, was used to monitor $H_2$ pressure during the reduction of Fe powder. The combined volume of the Baratron®, sample-gas storage vessel, and connecting spaces was calibrated using $CO_2$ produced from precisely weighed amounts of ANU sucrose.

Coral samples were inspected under an optical microscope. For each sample, two thin sections were prepared along the coral longitudinal and latitudinal growth axes. In general, secondary alteration was present at the interstices but not within wall structures.

Calcite content of each sample was determined from X-ray powder diffraction (XRD) spectra. The measurements utilised Cu-K$\alpha$ radiation (40 kV, 30 mA) and a scintillation counter. The scan rate was 2°2″ per minute. Approximately 300 mg of powdered coral was used for each test. The detection limit for calcite was about 2% (Klug and Alexander 1974).

### Precleaning of Samples

Corals were inspected under a magnifier and physically cleaned using a dental drill to remove interstitial structures other than walls. The samples were cleaned with distilled water in an ultrasonic bath. They were then dried in an oven (~40–60 °C) and weighed. The minimum required amount of $CaCO_3$ to yield 1 mg of carbon is approximately 8.5 mg. However, we used larger sample sizes (200–300 mg), and step-wise selective dissolution.

### $CO_2$ Production and Purification

In the present study, samples in the age range 30–60 ka were collected from Reef II and Reef III, including sub-reefs, at Huon Peninsula (Chappell et al. 1996). In addition to textural investigations and XRD measurements, all samples were partially dissolved in several steps, but in a much more severe fashion compared to that previously attempted by Burr et al. (1993). Partial dissolution was first attempted by Bard et al. (1990c); however, its effectiveness was systematically demonstrated later by Burr et al. (1993) using corals older than 70 ka from Barbados and Huon Peninsula. They performed XRD measurements, bulk sample $^{14}C$ dating, and $^{14}C$ dating following step-wise dissolution. They concluded that the first 50% of acid etching effectively removed secondary, younger age carbon (Burr et al. 1993). In the present study, the first 50% of the coral was etched and discarded, and the rest of the sample was dissolved in three or more aliquots. Each aliquot was AMS dated so that at least three AMS $^{14}C$ ages were produced for every sample (Table 1).

Generally, contamination comes from extraneous material containing younger or modern carbon, which shifts "true" $^{14}C$ ages to younger values. This could occur not only during the laboratory process, but also in the natural environment through diagenesis and recrystallization. Step-wise selective dissolution could thus help to identify contaminated samples.

The present reaction vessel was designed to facilitate selective dissolution. It consisted of three compartments, the main chamber held the sample, and two accessory branches contained phosphoric acid.

Table 1 Radiocarbon results

| Lab code[a] (ANUA-) | Sample | Dissolved percent | pMC | $^{14}$C age[b] (BP) | Error[c] (year) | Error[c] (year) | Calcite[d] % |
|---|---|---|---|---|---|---|---|
| 3607 | LIG coral | 0–17 | 0.74 ± 0.13 | 39,460 | +1500 | −1270 | |
| 3608 | (Favid) | 26–30 | 0.25 ± 0.05 | 48,230 | +1880 | −1520 | |
| 3609 | | 34–49 | 0.21 ± 0.03 | 49,450 | +1310 | −1120 | |
| 3610 | | 50–53 | 0.28 ± 0.05 | 47,250 | +1520 | −1280 | |
| 3611 | | 65–70 | 0.21 ± 0.04 | 49,490 | +1660 | −1380 | |
| 3612 | | 71–100 | 0.26 ± 0.04 | 47,970 | +1200 | −1040 | |
| OZD-535 | | 0–100 | 0.52 ± 0.18 | 42,300 | +3410 | −2390 | 2.0 |
| 10017 | Tridacna A | 0–17.2 | 1.03 ± 0.08 | 36,760 | +640 | −600 | |
| 10018 | | 17.2–30.5 | 0.61 ± 0.07 | 41,020 | +980 | −870 | |
| 10019 | | 45.6–73.2 | 0.38 ± 0.05 | 44,830 | +1150 | −1010 | |
| 10020 | | 73.2–100 | 0.27 ± 0.04 | 47,420 | +1270 | −1090 | 0 |
| 9928 | Tridacna B | 50.1–67.2 | 0.31 ± 0.05 | 46,350 | +1340 | −1150 | |
| 9929 | | 67.2–80.5 | 0.34 ± 0.06 | 45,710 | +1590 | −1330 | |
| 9930 | | 80.5–100 | 0.29 ± 0.05 | 46,880 | +1500 | −1260 | 0 |
| 6105 | Kanz 4 | 63.8–76.1 | 1.50 ± 0.13 | 33,730 | +550 | −520 | |
| 6104 | (Favid) | 76.1–88.2 | 1.51 ± 0.12 | 33,660 | +440 | −410 | |
| 6103 | | 88.2–100 | 1.55 ± 0.13 | 33,480 | +540 | −500 | |
| OZD-532 | | 0–100 | 2.98 ± 0.21 | 28,200 | +590 | −550 | 0 |
| 4206 | Kanz 9 | 50.8–65.0 | 0.44 ± 0.09 | 43,630 | +1910 | −1540 | |
| 4207 | (Favid) | 65.0–79.0 | 0.41 ± 0.05 | 44,160 | +950 | −850 | |
| 4208 | | 79.0–100 | 0.49 ± 0.12 | 42,670 | +2320 | −1800 | |
| OZD-533 | | 0–100 | 1.05 ± 0.20 | 36,600 | +1700 | −1400 | 1.0 |
| 7525 | Kanz 11 | 62.3–72.9 | 1.07 ± 0.06 | 36,490 | +490 | −460 | |
| 7526 | (*Porites*) | 72.9–86.3 | 1.26 ± 0.06 | 35,150 | +420 | −400 | |
| 7527 | | 86.3–100 | 1.36 ± 0.07 | 34,520 | +450 | −420 | 3.3,1.5 |
| 7528 | Kanz 13 | 47.1–63.0 | 0.84 ± 0.05 | 38,390 | +510 | −480 | |
| 7529 | (*Porites*) | 63.0–80.3 | 0.77 ± 0.05 | 38,730 | +560 | −520 | |
| 7530 | | 80.3–100 | 0.77 ± 0.04 | 39,050 | +450 | −430 | 0.9 |
| 8202 | Kanz 15 | 60.3–73.9 | 0.98 ± 0.09 | 37,120 | +790 | −720 | |
| 8203 | (*Porites*) | 73.9–85.9 | 0.79 ± 0.11 | 38,890 | +1220 | −1060 | |
| 8204 | | 85.9–100 | 1.07 ± 0.14 | 36,460 | +1140 | −1000 | 0 |
| 6915 | Kanz U8 | 48.0–64.5 | 1.49 ± 0.11 | 33,800 | +620 | −570 | |
| 6916 | (*Porites*) | 64.5–81.8 | 1.47 ± 0.11 | 33,930 | +620 | −580 | |
| 6917 | | 81.8–100 | 1.63 ± 0.12 | 33,090 | +600 | −550 | 1.9 |
| 4230 | Kanz U9 | 46.8–58.6 | 1.63 ± 0.17 | 33,080 | +860 | −780 | |
| 4231 | (Favid) | 58.6–72.1 | 1.24 ± 0.14 | 35,280 | +910 | −840 | |
| 4303 | | 72.1–100 | 1.28 ± 0.10 | 35,010 | +750 | −630 | 4.5, 1.8 |
| 4316 | Kanz U10 | 38.6–52.4 | 2.33 ± 0.21 | 30,190 | +680 | −750 | |
| 4312 | (*Porites*) | 52.4–83.2 | 1.65 ± 0.19 | 32,980 | +980 | −870 | |
| 4307 | | 83.2–100 | 1.39 ± 0.11 | 34,350 | +660 | −610 | 2.2 |
| 6908 | Kanz U11 | 46.3–60.0 | 2.30 ± 0.16 | 30,290 | +600 | −560 | |
| 6909 | (Favid) | 60.0–73.7 | 2.38 ± 0.17 | 30,040 | +590 | −550 | |
| 6910 | | 73.7–100 | 2.51 ± 0.17 | 29,600 | +580 | −540 | 0 |
| OZD-536 | | 0–100 | 4.33 ± 0.22 | 25,200 | +420 | −400 | |

Table 1 Radiocarbon results *(Continued)*

| Lab code[a] (ANUA-) | Sample | Dissolved percent | pMC | $^{14}$C age[b] (BP) | Error[c] (years) | Error[c] (years) | Calcite[d] % |
|---|---|---|---|---|---|---|---|
| 4317 | Kanz U12 | 49.6–61.2 | 2.10 ± 0.19 | 31,050 | +760 | −690 | |
| 4308 | (Favid) | 92.0–100 | 1.84 ± 0.14 | 32,100 | +650 | −600 | 0.5 |
| OZD-537 | | 0–100 | 2.73 ± 0.23 | 28,900 | +710 | −650 | |
| 6829 | Kanz U13 | 50.5–61.4 | 1.84 ± 0.12 | 32,100 | +530 | −500 | |
| 4313 | (Favid) | 61.4–71.9 | 1.07 ± 0.11 | 36,440 | +880 | −790 | |
| 4309 | | 71.9–100 | 1.78 ± 0.17 | 32,350 | +800 | −730 | 0.9 |
| OZD-542 | | 0–100 | 1.91 ± 0.17 | 31,800 | +750 | −680 | |
| 6107 | Kanz U14 | 69.3–79.9 | 1.05 ± 0.10 | 36,630 | +800 | −730 | |
| 6108 | (*Porites*) | 79.9–89.1 | 0.83 ± 0.07 | 38,500 | +700 | −640 | |
| 6109 | | 89.1–100 | 1.04 ± 0.08 | 36,600 | +680 | −630 | 2.5 |
| OZD-540 | | 0–100 | 1.53 ± 0.21 | 33,600 | +1200 | −1030 | |
| 6825 | Kanz U15 | 70.0–80.5 | 0.97 ± 0.07 | 37,210 | +590 | −550 | |
| 6824 | (Favid) | 80.5–89.5 | 0.94 ± 0.07 | 37,490 | +600 | −560 | |
| 6823 | | 89.5–100 | 1.22 ± 0.07 | 35,410 | +500 | −470 | 0.1 |
| 6828 | Kanz U16 | 59.0–73.1 | 1.91 ± 0.10 | 31,810 | +450 | −420 | |
| 6827 | (*Porites*) | 73.1–86.7 | 2.04 ± 0.11 | 31,290 | +430 | −410 | |
| 6826 | | 86.7–100 | 1.76 ± 0.11 | 32,450 | +510 | −480 | 3.2 |
| 6818 | Kanz A | 47.9–58.2 | 2.96 ± 0.14 | 28,280 | +380 | −360 | |
| 6817 | (Favid) | 58.2–69.0 | 2.81 ± 0.16 | 28,690 | +480 | −450 | |
| 6816 | | 69.0–100 | 2.90 ± 0.16 | 28,440 | +470 | −440 | 1.0 |
| 4209 | Bobo U10 | 56.2–67.7 | 2.47 ± 0.16 | 28,730 | +550 | −510 | |
| 4210 | (Favid) | 67.7–97.4 | 1.62 ± 0.12 | 33,120 | +640 | −590 | 0 |
| 4212 | Bobo U11 | 51.9–61.7 | 3.46 ± 0.22 | 27,020 | +530 | −500 | |
| 4213 | (Favid) | 61.7–71.5 | 4.34 ± 0.34 | 25,210 | +660 | −610 | |
| 4214 | | 71.5–100 | 4.66 ± 0.36 | 24,630 | +640 | −590 | 7.5, 2.9 |
| 4315 | Bobo U17 | 44.5–53.1 | 3.05 ± 0.26 | 28030 | +710 | −650 | |
| 4216 | (Favid) | 53.1–63.9 | 4.64 ± 0.35 | 24,670 | +640 | −590 | |
| 4217 | | 63.9–100 | 3.65 ± 0.24 | 26,590 | +550 | −520 | 5.1, 2.4 |
| OZD-538 | | 0–100 | 5.24 ± 0.30 | 23,700 | +470 | −450 | |
| 9507 | Bobo U18 | 0–31.0 | 6.09 ± 0.25 | 22,480 | +340 | −320 | |
| 4218 | (Favid) | 45.9–60.0 | 1.57 ± 0.16 | 33,340 | +880 | −800 | |
| 4219 | | 60.0–83.5 | 1.54 ± 0.21 | 33,530 | +1160 | −1010 | |
| 4220 | | 83.5–100 | 1.89 ± 0.14 | 31,880 | +600 | −560 | 0 |
| OZD-544 | | 0–100 | 1.84 ± 0.20 | 22,100 | +930 | −830 | |
| 4221 | Bobo U20 | 49.8–63.3 | 2.27 ± 0.22 | 30,410 | +810 | −740 | |
| 4222 | (Favid) | 63.3–78.1 | 2.13 ± 0.19 | 30,920 | +750 | −680 | |
| 4223 | | 78.1–100 | 2.06 ± 0.17 | 31,190 | +690 | −630 | 0 |
| 4225 | Bobo U21 | 56.8–73.1 | 3.65 ± 0.30 | 26,590 | +680 | −630 | |
| 4226 | (Favid) | 73.1–100 | 3.91 ± 0.30 | 26,050 | +640 | −590 | 1.0 |
| OZD-543 | | 0–100 | 7.08 ± 0.32 | 21,250 | +370 | −340 | |
| 4227 | Bobo U24 | 49.5–61.3 | 3.30 ± 0.27 | 27,400 | +680 | −630 | |
| 4228 | (Favid) | 61.3–72.9 | 2.92 ± 0.25 | 28,390 | +710 | −650 | |
| 4229 | | 72.9–100 | 3.44 ± 0.25 | 27,070 | +600 | −560 | 1.0 |
| 9504 | Bobo U28 | 0–30.0 | 18.2 ± 0.62 | 13,700 | +280 | −270 | |

Table 1 Radiocarbon results *(Continued)*

| Lab code[a] (ANUA-) | Sample | Dissolved percent | pMC | $^{14}$C age[b] (BP) | Error[c] (years) | Error[c] (years) | Calcite[d] % |
|---|---|---|---|---|---|---|---|
| 6912 | (Favid) | 60.3–71.8 | 4.71 ± 0.31 | 24,550 | +540 | –510 | |
| 6913 | | 71.8–86.7 | 4.53 ± 0.30 | 24,870 | +550 | –510 | |
| 6914 | | 86.7–100 | 5.34 ± 0.35 | 23,540 | +550 | –520 | 2.0 |
| OZD-539 | | 0–100 | 7.91 ± 0.62 | 20,400 | +330 | –320 | |
| 9502 | Bobo U30 | 0–29.0 | 7.85 ± 0.43 | 20,440 | +450 | –430 | |
| 6115 | (Favid) | 64.8–76.0 | 4.09 ± 0.26 | 25,680 | +530 | –500 | |
| 6114 | | 76.0–87.3 | 4.10 ± 0.27 | 25,660 | +540 | –510 | |
| 6113 | | 87.3–100 | 3.70 ± 0.24 | 26,500 | +550 | –510 | 1.0 |
| OZD-541 | | 0–100 | 7.75 ± 0.27 | 20,550 | +280 | –280 | |
| 8205 | SEN(N)8 | 62.3–72.0 | 0.48 ± 0.09 | 42,970 | +1680 | –1390 | |
| 8206 | (Porites) | 72.0–86.9 | 0.60 ± 0.08 | 41,130 | +1160 | –1010 | |
| 8203 | | 86.9–100 | 0.59 ± 0.10 | 41,220 | +1500 | –1260 | 1.6 |
| 6822 | GBR-A | 62.5–74.4 | 17.06 ± 0.75 | 14,200 | +360 | –340 | |
| 6820 | (Galaxea | 74.4–86.7 | 16.93 ± 0.72 | 14,270 | +350 | –340 | |
| 6819 | clavus) | 86.7–100 | 16.67 ± 0.64 | 14,390 | +320 | –300 | 0 |

[a]All samples were measured at ANU except the OZD-series which were measured at ANSTO (Australian Nuclear Science and Technology Organisation).
[b]Age obtained using Libby's half life (5568 yr).
[c]Errors are quoted as two sigma.
[d]XRD analyses for bulk samples. Where two entries are given, the second corresponds to wall fraction following mechanical cleaning to remove septa.

The vessel was connected by a Cajon Ultra-Torr® fitting to the main vacuum line. After 1.5 hr of pumping and out-gassing of the acid, a vacuum of $10^{-4}$ Torr could be achieved. The vessel was then tilted to drip acid onto the sample to start the reaction. The $CO_2$ produced was dried by passing through two spiral traps immersed in a dry ice-ethanol mixture (–78.8 °C), and cryogenically collected at liquid nitrogen temperature. The $CO_2$ pressure was measured at intervals to determine the amount of sample dissolved. The dried $CO_2$ was then transferred via one of several outlets to the graphitisation apparatus described previously. The iron powder had previously been reduced in situ with ~400 Torr $H_2$ at 400 °C for several hours. The setup includes a cold finger to trap water vapor, and a pressure transducer to monitor the progress of the conversion reaction. The apparatus has a double valve system for isolating and removing the samples from the vacuum system. ANU sucrose was used as a standard. The sucrose was weighed and placed in a vycor tube (6 mm diameter and ~20 cm long) with CuO and Ag wire. The tube was evacuated and sealed with a torch and placed in an oven at 900 °C for 8–10 hr to combust and convert the sucrose to $CO_2$. The rest of the procedure was the same as that used for samples.

After evacuating the sample tube (<$10^{-4}$ Torr) at liquid nitrogen temperature, it was filled with approximately 2.2 times molar fraction of excess $H_2$ relative to $CO_2$. The valves were closed and graphitization reaction started by inserting the end of the tube into a high temperature oven at 625 °C at a separate location. Up to four sample tubes could be heated at the same time. Water vapor produced by the reaction was removed by a cold finger in a dry-ice-ethanol bath attached to the graphitization apparatus. The change in pressure due to $H_2$ consumption was monitored with pressure transducer. Pressure readings indicated that most of the reaction had occurred during he first 0.5–1 hr, and was essentially complete within 3 hr. However, to ensure full conversion, the process was continued for at least 6 hr.

Graphite yields were calculated by both weighing the residue, and from the measured pressure difference, and ranged from 85% to 100%. Conversion efficiency was typically greater than 95%. At such high efficiencies, graphitization related carbon isotope fractionation is expected to be minimal (e.g. McNichol et al. 1992; Kitagawa et al. 1993; Brown and Southon 1997).

Background $^{14}C$ levels were monitored regularly using the international old calcite standard, IAEA-C1 (Rozanski et al. 1992). The background values ranged from 0.04 pMC (percent modern carbon) to 0.30 pMC, and were typically 0.25 pMC, equivalent to an age of 48,000 yr. Therefore, samples as old as 40,000 yr could be reliably measured using the present system and procedures.

## RESULTS AND DISCUSSION

### Integrity of Samples

The basic requirement in $^{14}C$ and U/Th dating is the assumption of closed system behavior for the isotopes used in the measurement. In general, two sources of contamination can be expected in $^{14}C$ dating. One from contamination in the laboratory, including during the graphitization process, and the other is from inherent diagenesis in corals.

The former can be assessed by using "old" carbonate, which ideally contains no $^{14}C$. In our laboratory, we have used Carrara marble (IAEA C-1) that yielded a range of ages from 47,000 to 50,000 BP for the total analytical blank, including AMS analysis. Therefore, any dates younger than this age are reliable, assuming sample integrity. Numerous studies have attempted to characterize the cause and circumstances of diagenetic processes in corals (e.g. Bathurst 1968; Lighty 1985; Moore 1989; Strasser et al. 1997) however, the nature of the mechanism is still unclear (Bar-Matthews et al. 1993). To evaluate its effects in corals several criteria have previously been employed such as microscopic textural analysis, XRD measurements, stable isotope measurements, total uranium contents, the amount of $^{232}Th$ in the coral, trace element analysis, and measurement of the initial $^{234}U/^{238}U$ ratio $\delta^{234}U(T)$.

#### *Textural Investigation and XRD Analysis*

Evaluating the possibility of open system behavior for $^{14}C$ is much more difficult than for Th and U isotopes. However, to some extent, it is possible to check for secondary material, as pristine coral consists only of aragonite. XRD can be used to check for secondary calcite. We have investigated textures with a petrographic microscope and XRD analyses. In most of the samples, secondary fillings were observed in the voids of the coral. These were mechanically removed using a dental drill prior to leaching. Thus, even in cases where minor secondary replacement was observed, and detected in XRD analyses of whole samples, they were removed. All the samples had typically less than 2% calcite, which is within the uncertainty of detection limits (Table 1).

#### *Stable Isotope Analysis*

For each sample, stable isotopes of oxygen and carbon were measured. If marine carbonates preserve their original composition, both isotopes values should be around zero. Stein et al. (1993) conducted an extensive study of Huon LIG corals. Oxygen isotopes are likely to have been affected if exotic isotopes were introduced into the coral skeleton through percolation of meteoric water. However, oxygen and carbon isotopes appear not to have responded to small-scale diagenetic alteration in corals. The present corals are significantly younger than LIG corals used by Stein et al. (1993), and as such they are less likely to have detectable variations in oxygen or carbon isotopes correlated with small scale diagenesis. The test results showed that carbon and oxygen isotope values were within acceptable ranges as found by Stein et al. (1993).

### *Uranium Concentration*

Uranium concentration of corals in this study range between ~2 and 3.5 ppm. These values are consistent with previously reported results for younger age corals (Hamelin et al. 1991), Holocene corals (Edwards et al. 1988; Zhu et al. 1993), and the LIG corals (Edwards et al. 1986; Hamelin et al. 1991; Edwards et al. 1987; Stirling et al. 1995, 1998). Species dependence of uranium content in corals has been reported previously (Zhu et al. 1993; Stirling 1995). Stirling (1995) reported that uranium content of *Acropora* was higher than other species such as *Porites* or *Favidae*, but Zhu et al. (1993), pointed out that *Acropora* and *Montipora* corals have inherently higher $^{238}$U values in Holocene corals. Therefore, the variations in Uranium content might be species dependent, but generally range from 2 to 4 ppm. All corals used in the present study are well within this range.

### *$^{232}$Th Concentration in the Corals*

$^{232}$Th in modern corals is typically less than 0.5 ppb (Edwards et al. 1986; Chen et al. 1991). In the freshwater or marine environment, voids can be filled with externally introduced detritus material. Therefore, if $^{232}$Th abundance departs significantly from the 0.5 ppb limit, it may indicate the presence of secondary contamination. Previous researchers have attempted to correct for excess levels of $^{232}$Th, although the correction is not generally considered to be reliable (e.g. Chen, et al. 1991). The effect is to shift the measured Th-U age toward younger ages.

In the present study, for most corals, $^{232}$Th is well below the 0.5 ppb limit. One coral has ≈1.1 ppb. This coral was collected at a depth of −175 m in the Great Barrier Reef (Veeh and Veevers 1970). It had not been exposed to aerial or subaerial environment. Therefore, the excess $^{232}$Th must have been added in the marine environment. There are no discernable systematic correlations between $^{232}$Th and U/Th age, $\delta^{234}$U(T), or $\Delta^{14}$C.

### *$\delta^{234}$U(T)*

Behavior of trace chemical elements with degree of diagenesis was studied in Caribbean corals by Bar-Matthews et al. (1993). These authors investigated both textural structures with an optical microscope and a scanning electron microscope, and then conducted chemical analyses. They concluded that textural analysis is necessary, yet it is not a quantitative or reliable test in evaluating the degree of diagenesis. Most of the alteration was observed in the voids of corals as secondary filling and calcium carbonate deposition. However, cementation in these corals was not always by calcite, but in many cases through secondary aragonite (Bar-Matthews et al. 1993). Therefore, they were presumably altered in the marine environment, quite likely at the intertidal or supertidal zone as indicated by other studies (e.g. Bar-Mathews et al. 1993; Lighty 1985).

Many studies have detailed the shift in $\delta^{234}$U(T) through diagenesis (Edwards 1988; Ku et al. 1990; Banner et al. 1991; Bard et al. 1991; Chen et al. 1991; Stein et al. 1993; Gallup et al. 1994; Stirling et al. 1995, 1998). The magnitude of $\delta^{234}$U(T) tends to be elevated as the degree of diagenesis increases. Gallup et al. (1994) demonstrated this trend for corals from Barbados and the Bahamas. Also, Stirling (1998) observed a similar increase in $\delta^{234}$U(T) with age for corals from Western Australia. We have used a similar acceptance criterion: $\delta^{234}$U(T) = 149 ± 10‰ as used in previous studies (e.g. Stirling et al. 1998).

**Radiocarbon and Th-U Dating of Corals from Huon Peninsula**

Veracity of the results from $^{14}C$ and Th-U dating of corals ultimately depend on the quality of the samples. This is a vexing issue that cannot be resolved with complete certainty, but relies on a battery of tests, each of which provide, at best, circumstantial evidence for or against. We have employed a quantitative test of $^{14}C$ dates that relies on progressive dissolution of coral samples. We have determined empirically that the first 50% of a leached coral sample is more likely to have been contaminated by extraneous, younger age carbon, than the last 50% (Burr et al. 1993). We have adopted a procedure whereby the first 50% of a sample was selectively dissolved and discarded. The remainder was dissolved in at least three steps and each aliquot was $^{14}C$-AMS dated. This procedure was applied to each dated sample. The data for all of the samples can be found in Figure 2 and Table 1. In every case, within twice the statistical uncertainty, the last three aliquots have identical $^{14}C$ ages. Samples included in the discussion below pass all of these tests within limits of assigned errors. A major concern with $^{14}C$ dates for samples older than 30 ka is the possibility of contamination with younger age or modern carbon. There is no absolute *a priori* test to determine the issue. In particular, for the 52 ka samples reported below, the $^{14}C$ ages range from 35 to 45 ka BP and may need to be viewed with some caution. However, we consider that the selective dissolution test is the best quantitative indicator that can be devised at present.

We tested the effectiveness of this procedure by using corals as old as 120,000 yr that grew during the Last Interglacial (LIG). Burr et al. (1992), conducted step-wise dissolution of a reef IV coral, from Huon Peninsula, which was previously dated (72.8 ± 2.2 ka; Chappell et al. 1996). The first 40% of this coral was contaminated by younger carbon; the next 60% gave an age close to the analytical background. We have used a LIG coral from Western Australia (WA-1) that was previously Th-U dated (Stirling et al. 1995) and has an age of 124.7 ± 0.9 ka with an initial $\delta^{234}U(T)$ ratio of 152 ± 2. WA-1 appears to be pristine under the optical microscope, and no calcite was detected by XRD analysis. The first 0–17% aliquot from WA-1 shows a considerably younger $^{14}C$ age compared to the analytical background (~48,000 BP). However, the next 5 aliquots, indicate an almost uniform age of around 49,000 BP. Two other LI corals from Western Australia were treated similarly and radiocarbon dated. For the first coral, the (0% to 54%) aliquot gave an age of 35,270 ± 1490 BP. The remainder of the sample (54% to 100%) was dated at 47,690 ± 1500 BP. The second coral was dissolved in three steps (15% to 28%, 28% to 36%, and 55% to 100%) and yielded the corresponding ages of 40,960 BP, 42,560 BP, and 50,770 BP, respectively.

Giant clams, *Tridacna gigas* do not incorporate U in their aragonite skeleton and cannot be dated by U-series methods. *Tridacna* were previously collected from Huon terraces IIIa and IIIb from locations of known age. The harder skeleton of *Tridacna* may be expected to be resistant to alteration compared to fossil corals and therefore provide more reliable $^{14}C$ ages. However, the estimated age of available *Tridacna* samples in the collection was over 50,000 yr. We $^{14}C$ dated two samples. A *Tridacna* from reef IIIa shows a nearly constant age profile at ~47,000 BP which is close to the analytical background of the present system. Another *Tridacna* was treated in a similar fashion. The first 17% indicated younger carbon contamination. However the last ~50% yielded consistent results of ~47,000 BP. Both *Tridacna* consist of 100 % aragonite as determined by XRD analysis. It appears that the harder skeleton of *Tridacna* is also susceptible to alteration in the outer layers.

Most of the samples used in the present study have also been measured at another laboratory. Samples were sent to ANSTO (Australian Nuclear Science and Technology Organization) for $^{14}C$ dating (Hotchkis et al. 1996). Measurements of $^{14}C$ at ANSTO were on whole coral samples, without selective dissolution. This is shown as the (0–100%) fully dissolved fraction in Figure 2. As can be seen,

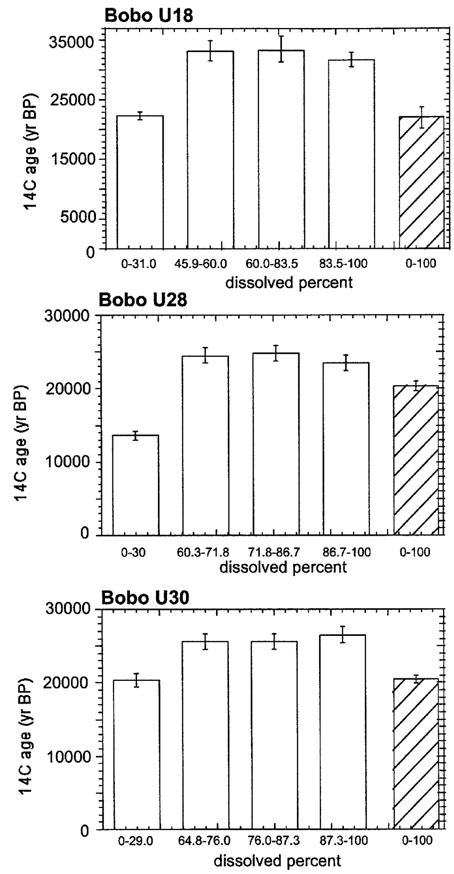


Figure 2a All the samples used in the present study were subjected to step-wise dissolution as shown in these examples. The fraction of dissolved coral was determined from pressure and temperature measurements of evolved $CO_2$ in a calibrated volume. The hatched columns (0–100%) show the results of bulk analysis for a different piece of the same coral.

all of the dates measured at ANSTO are significantly younger than those for partially dissolved samples. This, and the discussion in previous sections, clearly indicate the importance of step-wise dissolution.

In summary, the above experiments illustrate the following points: First, the necessity of strict criteria based on textural analysis, XRD and step-wise dissolution. Second, that approximately the first 20% of dissolved samples are likely to be contaminated by younger carbon. And third, that after 50% dissolution, most of the contamination is eliminated.

Overall, tests using step-wise dissolution appear to be the only way to ascertain the veracity of $^{14}C$ ages of corals. Our results are consistent with the experiments of Burr et al. (1993) that after 50% etching, $^{14}C$ age approaches analytical background levels. The criteria we have applied to each sample requires $^{14}C$ dating of at least three aliquots, after the first 50% of the sample is selectively dissolved and discarded. The results were considered acceptable if the three dates agreed within analytical uncertainties. Although, this appears to be the best quantitative method available so far, it does not guarantee that samples are fully free of diagenesis at a level not to affect age determinations.

The new data comprise of 25 new TIMS Th-U dates and over 200 AMS available dates (Table 2). The $^{14}C$ ages and Th-U calendar ages are shown in Figure 3 together with data from other studies. Sample age was calculated from the weighted mean of three available ages measured following 50%

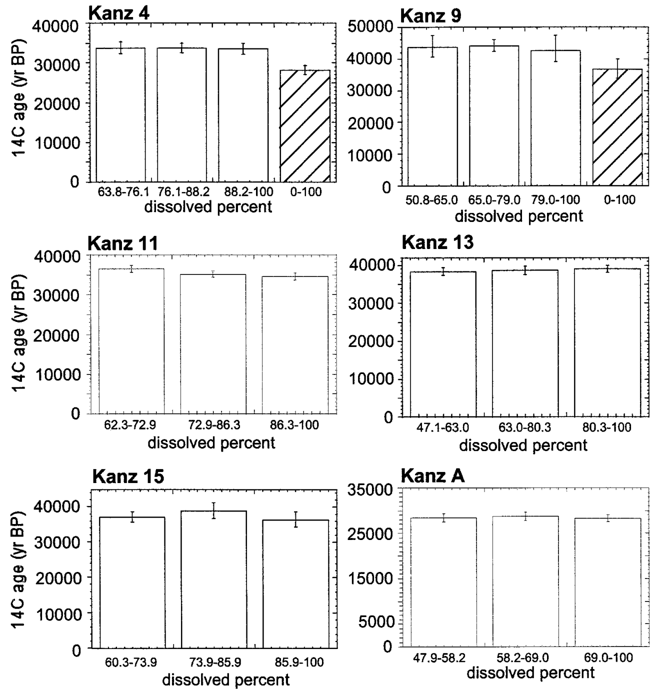


Figure 2b Same as Figure 2a but for different corals

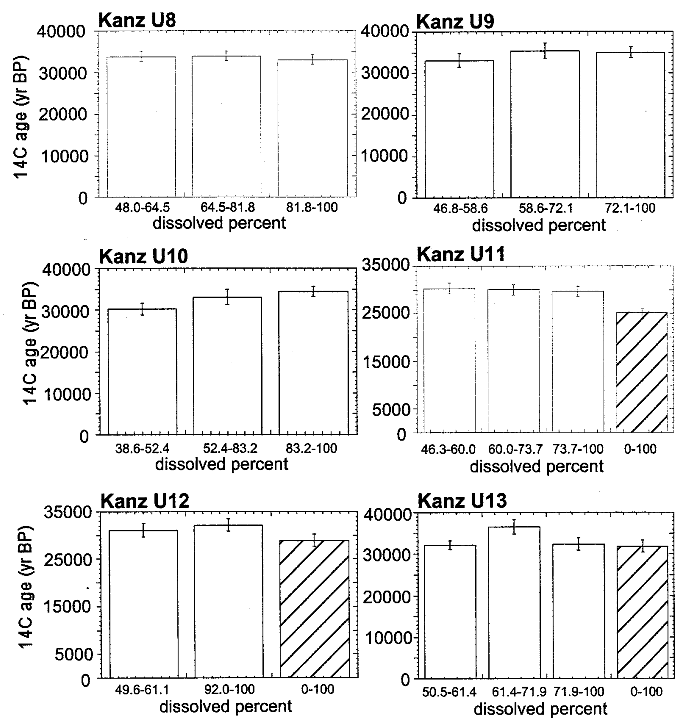


Figure 2c Same as Figure 2a but for different corals

Table 2 U/Th and $^{14}C$ results

| Sample[a] | U/Th age (ka cal BP) | $^{14}C$ age (ka BP)[b] | $\Delta^{14}C$ (‰)[c] | Reef[d] | Sea-levels and height (m)[e] |
|---|---|---|---|---|---|
| *Kanzarua* | | | | | |
| Kanz 4 | 51.5 ± 1.6 | 33.6 ± 0.4 | 6678 | IIIa | −58 (86) |
| Kanz 4$^{\alpha}$ | 51.2 ± 0.8 | | | | |
| Kanz 9 | 53.4 ± 0.3 | 43.9 ± 0.8 | 1759 | IIIa | −72 (78) |
| Kanz 9$^{T}$ | 54.6 ± 0.7 | | | | |
| Kanz 11$^{p}$ | 51.3 ± 0.3 | 35.4 ± 0.3 | 5063 | IIIa | −65 (78) |
| Kanz 13$^{p}$ | 38.3 ± 0.5 | 38.9 ± 0.3 | −187 | IIIb | −59 (48) |
| Kanz 15$^{p}$ | 42.0 ± 0.6 | 37.5 ± 0.6 | 511 | IIIc | −79 (39) |
| Kanz U8$^{p}$ | 37.0 ± 0.6 | 33.6 ± 0.4 | 333 | IIa | −77 (27) |
| Kanz U9 | 42.3 ± 0.2 | 34.7 ± 0.5 | 1075 | IIa | -91 (28) |
| Kanz U9$^{\alpha}$ | 41.8 ± 0.6 | | | | |
| Kanz U9$^{T}$ | 42.2 ± 0.3 | | | | |
| Kanz U10$^{p}$ | 43.7 ± 0.3 | 33.2 ± 0.5 | 2162 | IIIc | −73 (49) |
| Kanz U11 | 37.9 ± 0.3 | 30.0 ± 0.3 | 1351 | IIa | −79 (27) |
| Kanz U12 | 37.5 ± 0.7 | 31.7 ± 0.5 | 794 | IIa | −79 (26) |
| Kanz U13 | 35.8 ± 0.4 | 33.8 ± 0.5 | 139 | IIa | −74 (26) |
| Kanz U14$^{T}$ | 34.8 ± 0.8 | 37.4 ± 0.4 | −360 | IIa | −72 (26) |
| Kanz U15 | 33.4 ± 0.2 | 36.7 ± 0.3 | −409 | II | −71 (23) |
| Kanz U16$^{p}$ | 30.4 ± 0.4 | 31.8 ± 0.3 | −249 | II | −56 (29) |
| Kanz A | 37.5 ± 0.2 | 28.5 ± 0.3 | 1696 | II | −80 (25) |
| *Bobongara* | | | | | |
| Bobo U10 | 37.2 ± 0.2 | 31.7 ± 0.4 | 731 | IIa | −74 (49) |
| Bobo U11 | 37.9 ± 0.3 | 26.0 ± 0.3 | 2820 | IIa | −76 (49) |
| Bobo U17 | 32.0 ± 0.2 | 26.6 ± 0.4 | 741 | IIc | −86 (20) |
| Bobo U18 | 42.4 ± 0.2 | 32.7 ± 0.5 | 1897 | IIb | −103 (37) |
| Bobo U20 | 37.6 ± 0.2 | 30.9 ± 0.4 | 1023 | IIb | −84 (40) |
| Bobo U21 | 29.7 ± 0.2 | 26.3 ± 0.5 | 373 | IIc | −68 (30) |
| Bobo U21$^{\alpha}$ | 33.4 ± 0.6 | | | | |
| Bobo U24 | 32.2 ± 0.2 | 27.6 ± 0.4 | 583 | IIc | −76 (30) |
| Bobo U24$^{\alpha}$ | 33.0 ± 0.5 | | | | |
| Bobo U28 | 32.3 ± 0.5 | 24.4 ± 0.3 | 1388 | IIc | −85 (22) |
| Bobo U30 | 31.5 ± 0.2 | 26.0 ± 0.3 | 791 | IIc | −77 (27) |
| *Others* | | | | | |
| SEN(N)8$^{p}$ | 52.4 ± 1.3 | 41.7 ± 0.8 | 2172 | IIIc | nA |
| GBR-A | 17.0 ± 0.1 | 14.3 ± 0.2 | 315 | | |
| GBR-A$^{\alpha}$ | 17.0 ± 1.0 | | | | (−175) |

[a]Except where indicated, all samples are from the *Faviidae* family; the superscript p denotes *Porites* corals. Analyses on *Faviidae* corals are for the wall fractions only. The superscript $\alpha$ and T indicate previously reported values using $\alpha$-counting and TIMS measurements, respectively (Chappell et al. 1996).

[b]Using Libby's half-life (5568 yr). The $^{14}C$-age is the weighted mean of ages from aliquots corresponding to the final 50% of coral mass selectively dissolved in at least three steps (Table 1).

[c]The $\Delta^{14}C$ value is the per mil difference between the initial $^{14}C/^{12}C$ of a sample (normalized for isotopic fractionation) and the $^{14}C/^{12}C$ of a standard; the standard has a value similar to the initial $^{14}C/^{12}C$ ration of 19th century wood. The $\Delta^{14}C$ is defined and discussed in (Stuiver and Polach 1977) and equals $(Fe^{\lambda T}-1)\times 1000$ per mil, where $F$ is the fraction modern (Donahue et al. 1990), $\lambda$ is the decay constant that corresponds to the 5730 year half-life, and $T$ is the age in cal BP. In the present study, $\Delta^{14}C$ is calculated using the measured initial $^{14}C/^{12}C$ ratio and the $^{230}Th$ age. Quoted errors include errors in the measured $^{14}C/^{12}C$ ratio and $^{230}Th$ age.

[d]Reef numbering is described in (Ota et al. 1992; Chappell et al. 1996).

[e]Sea-levels obtained using both the height of corals as shown in brackets and uplift rates for both Kanzarua (2.8 m/ka) and Bobongara (3.3m/ka) reported by (Chappell et al. 1996).

dissolution. The weighted average is within twice the experimental error of individual measurements. Results from one coral from the Great Barrier Reef, originally dated by Veeh and Veevers (1970) with conventional $^{14}C$ and Th-U (13,600–13,860 ± 0.220 ka BP and 17,000 ± 1000 ka, respectively), are in good agreement with present results (14,390 ± 0.150 ka BP and 16,981 ± 0.112 ka). This sample is well within the field of other data of similar age (Figure 3). All of the other corals are from the uplifted Huon Peninsula coral terraces of Papua New Guinea collected during the 1992 international expedition (Ota et al. 1994). Four samples were previously Th-U dated using TIMS and five others by α-spectrometry (Chappell et al. 1996); they are included with the new results. The previous data have larger analytical uncertainties (Omura et al. 1995; Chappell et al. 1996), however, they are in good agreement with the new TIMS data.

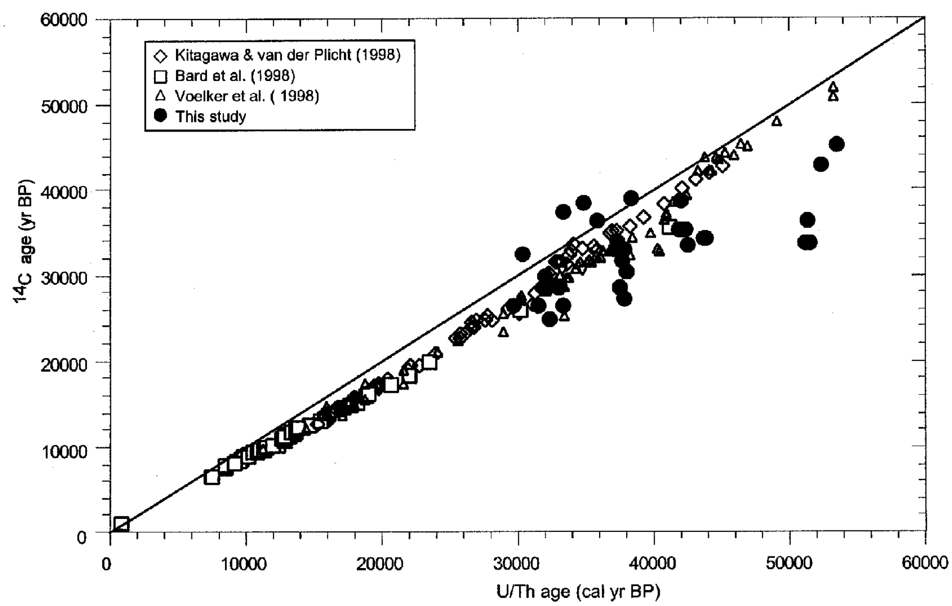


Figure 3 The present coral $^{14}C$ and U-series ages, and previously published data. The baseline of younger $^{14}C$ ages appear to be consistent in all the data sets. The present data show four distinct peaks of $^{14}C$ excess. In between these peaks some $^{14}C$ ages appear to be older than the corresponding calendar ages.

The measured Th-U ages of corals, from the uplifted Huon Peninsula Reefs II and III (Chappell 1974; Chappell et al. 1996), range between 29 ka and 55 ka. Several trends are apparent in the data; first, there is a noticeable increase in the divergence of the $^{14}C$ ages from calendar dates, from 30 ka to 50 ka, that follows the same trend as the bulk of the previous data; second, there are significant, 1000‰ to 7000‰ (equivalent to age shifts of 7 ka up to 17 ka) $\Delta^{14}C$ excursions at periods that correspond to particular reef-building episodes and sea-level rises at Huon Peninsula; and third, some $^{14}C$ ages in between the "peaks" are older than corresponding calendar ages.

That the Th-U ages cluster at particular times is no surprise as we are specifically dating corals from discrete reef sections; we do not have a continuous record of coral growth over this time period. However, the magnitude of the $^{14}C$ age excursions from calendar ages is unprecedented. The present data are shown on an expanded scale in Figure 4. It is clear that data with $^{14}C$ ages older than calendar ages are distributed in-between the peaks. Two previous coral data points are within the range of present ages; one is a 30,200 yr old coral from Barbados, and the other a 42,000 yr old coral from Huon (Bard et al. 1993, 1998; Figure 3). Both of these overlap with the baseline defined by the present measurements (Figure 3). At tectonically uplifting sites, coral terraces grow when sea-level rise overtakes uplift. The uplift rate along the Huon coast is variable but typically in the order of 3 m per 1000 yr and the sea-level history has been derived previously (Chappell et al. 1996). The coincidence between sea-level rises and large excursions in $^{14}C$ is, at first sight, puzzling. However, we believe that these events can be directly linked to rapid global climate changes, in particular, in the North Atlantic, and are also connected with Heinrich Events and periodic re-organizations of the North Atlantic thermohaline circulation.

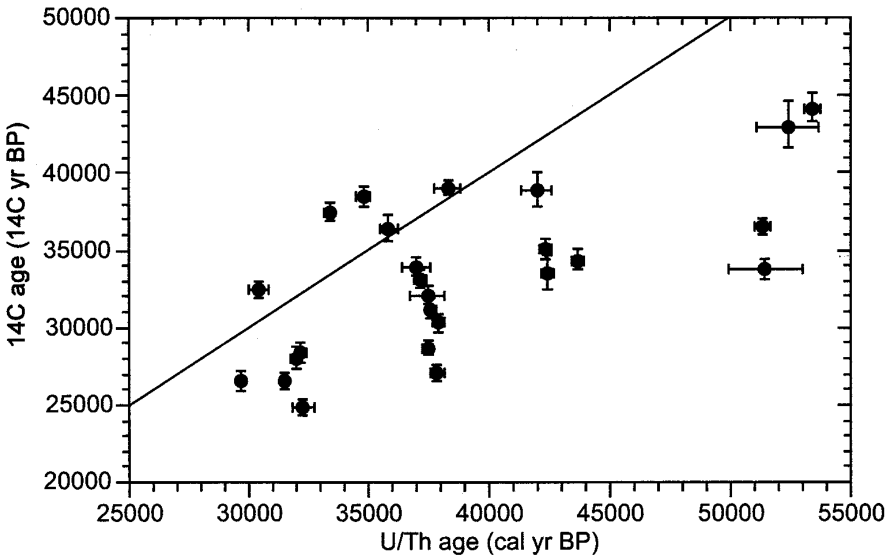


Figure 4 $^{14}C$ and Th-U ages plotted in an expanded scale diagram. Errors are 2σ mean. Four peaks of excess $^{14}C$ are clearly evident. There is no trend of increasing $^{14}C$ excess with age as the ≈37 ka peak is larger than the ≈43 ka peak. This, and other, detailed arguments based on tests of closed system behavior argue against an interpretation based on contamination by younger age or modern carbon as an explanation for the observed peaks.

There are large variations in the reported calendar ages of various Heinrich Events (Andrew 1998). This arises, in part, from mishandling of $^{14}C$ to calendar age conversions. Some $^{14}C$ ages are not even calibrated, but reported as absolute ages. Secondly, as the present data shows, the variability in $^{14}C$ ages may be due to rapid variations in atmospheric $^{14}C$. We consider that data obtained by Bond et al. (1993) on the abundance of *Neogloboquadrina pachydermas* from the North Atlantic core V23-81 to represent one of the best examples of the timing and signature of Heinrich Events. The $^{14}C$ scale of this data set was converted to calendar ages using the prescription given by Bard et al. (1998). The results are shown in Figure 5 from a paper by Lund and Mix (1998). Inspection of Figure 5 shows that the $^{14}C$ peaks in the calibration curve match almost exactly with the timing of minima in the foraminiferal abundance and Heinrich Events. The 32 ka (calendar age) $^{14}C$ peak matches with H3. The 37.5 ka $^{14}C$ peak matches with the sharp cold stadial at 37.5 ka which is not marked as a Heinrich Event, but appears to belong to the same class. The 42.3 ka $^{14}C$ peak matches with H4 at ≈42 ka, and the

52 ka $^{14}C$ peak matches with H5 at 52 ka. This correspondence is remarkable and is highly unlikely to be coincidental.

The important point is that the Huon Peninsula terraces, which represent episodes of sea-level rise, appear to have been built as a direct consequence of large-scale discharges of icebergs into the North Atlantic and the associated sea-level rise. The present data assert that, concurrent with each episode, there was a huge rise in atmospheric $^{14}C$. The $^{14}C$ excess, $\Delta^{14}C$, is shown in Figure 5. The theoretical maximum $^{14}C$ excess in the atmosphere, if all the sinks are cut off, is 5870% (Siegenthaler et al. 1980) and 200% excess levels can be reached within a few hundred years. It appears that the present data provide direct evidence for the slow-down or shut-down of the North Atlantic thermohaline circulation as expounded by Broecker (1997, 1998). Furthermore, it solves a puzzle, again put forward by Broecker (1998):

> Currently, ≈80% of the $^{14}C$ atoms required to replace those undergoing decay in the deep sea enter via the Atlantic's conveyor circulation. Hence, if this route were to be shut down during the course of the 1200-calendar-year duration of the Younger Dryas, an enormous offset in the $^{14}C$ timescale might be expected.

A few $^{14}C$ ages, older than calendar ages, appear between the large $^{14}C$ excursions. Presumably, they correspond to the resumption of the thermohaline circulation and transport of $^{14}C$ to the deep ocean, initially at a rate greater than present. There is theoretical support for such age reversals in the calculations by Stocker and Wright (1998), when surface reservoir ages increase rapidly at the time of the commencement of the circulation. Interruption of the thermohaline circulation may be expected to redirect the northward movement of warm equatorial waters in the Atlantic to the Southern Ocean. Coupled with 5–10 m sea-level rise from North Atlantic icebergs, the Antarctic ice sheet may also be destabilized. The possibility that fresh water injection into Antarctic waters may interrupt the Antarctic deep-water formation has not been assessed in detail. However, Clark et al. (1996) consider a contribution to the melt-water-pulse-1A from the Antarctic ice sheet is most likely.

The 37 ka peak in the present data and the nominal 37 ka peaks in $^{10}Be$ and $^{36}Cl$ polar and deep-sea records, at first sight, appear to be generic. However, there is considerable uncertainty in the calendar age of the $^{10}Be/^{36}Cl$ peak. Various studies place this peak anywhere from 37 ka to 42 ka (Aldahan and Possnert 1998). It corresponds to a relatively long period when the geomagnetic field was low. Similarly the $^{10}Be$ peak is broad (≈3000 yr). Whether the 37 ka peak in the present data is the same as the $^{10}Be$ and $^{36}Cl$ peaks remains an open question.

Large $\Delta^{14}C$ peaks have been observed by Kitagawa and van der Plicht (1998) at 32–33 ka ($\Delta^{14}C$ up to 850‰), by Voelker et al. (1998) at 33 ka ($\Delta^{14}C$ ≈700‰) and 39 ka ($\Delta^{14}C$ ≈1200‰), and by Bard (1998) at 41 ka ($\Delta^{14}C$ ≈700‰). Given the uncertainties in exact timing of these events, they could be related to the $^{14}C$-excesses found in the present work. The magnitude of present $\Delta^{14}C$ range from 1000‰ to 2000‰ to 7000‰. These values are within a factor of two to three of the previously determined highs. The difference between calendar and $^{14}C$ ages of the 51.5 ka peak is 17.8 ka. Due to the old calendar age of this and similar samples, they could have been highly susceptible to small amounts of contamination assuming the "true" $^{14}C$ ages were closer to 50 ka. However, a recent study by Schramm et al. (2000) of Lake Lisan sediments has identified a similar peak, U-Th dated at 51.2 ka with an age difference of greater then 9 ka, which tends to support the present findings.

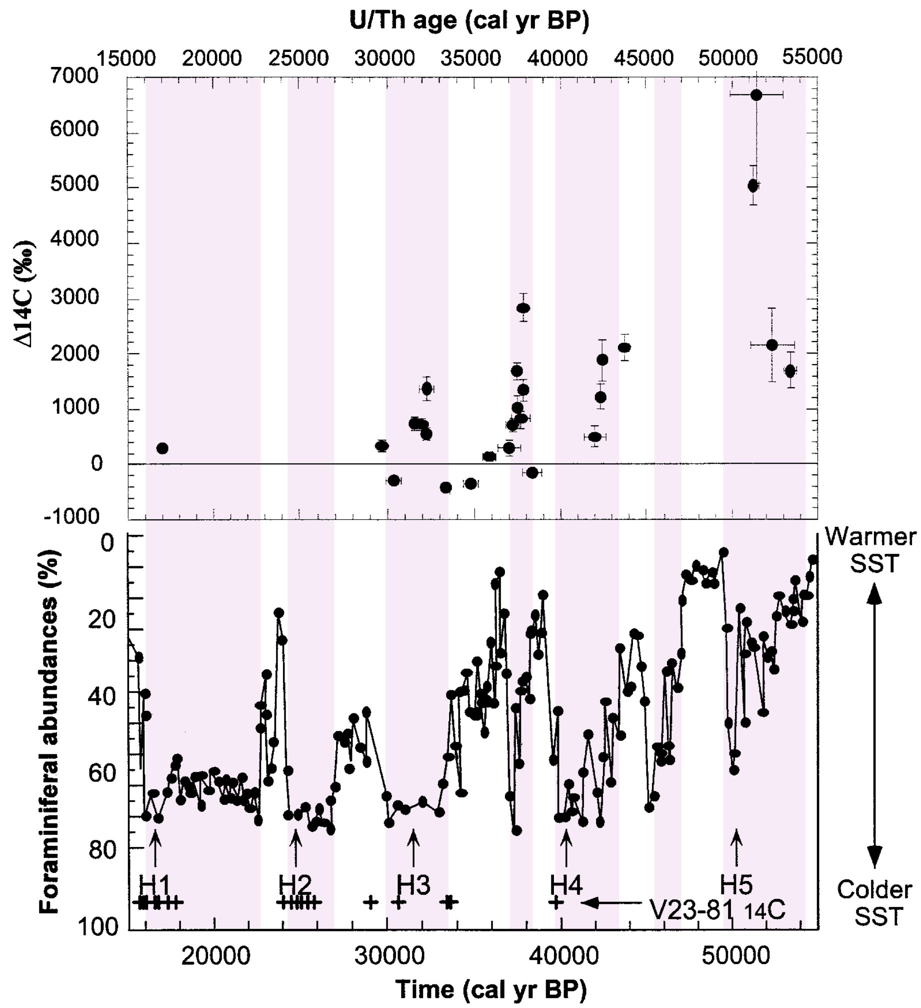


Figure 5 The upper panel shows the results from the present study. The lower panel is from the North Atlantic deep-sea core V23-81 showing systematic fluctuations in the abundance of *N. pachyderma* (s) correlated with the timing of Heinrich Events and cold stadials (Lund and Mix 1998). The time scale was derived from $^{14}C$ data using the calibration recommended by Bard et al. (1993). Between H3 and H4, a brief duration sharp peak corresponds to an excess $^{14}C$ peak found in the present data at 37.5 ka. This peak is not labeled as an Heinrich Event but appears to belong to the same class. Heinrich Events H3, H4, and H5 correlate with peaks of $^{14}C$. Such a correlation is unlikely to be coincidental and implies a genetic relationship between Heinrich Events, pulses of excess atmospheric $^{14}C$, sea-level rise and episodes of reef construction at Huon Peninsula. We surmise that the connecting factor between these events is the interruption of the North Atlantic Thermohaline circulation following periodic partial disruptions of the Laurentide ice-sheet.

## CONCLUSION

More than 250 AMS $^{14}C$ dates and 25 high-precision TIMS U-series ages have been determined for 30,000–50,000-yr-old corals from the uplifted terraces of Huon Peninsula in Papua New Guinea. Previously extensive efforts to define a $^{14}C$ calibration curve for the period beyond around 12,000 yr, through directly measured calendar ages, only yielded a few scattered points. A new $CO_2$ extraction and graphatization line was constructed and used for processing "old" carbonate samples only. $^{14}C$

dates of samples older than 20,000 yr may be affected by secondary younger carbon contamination. For this reason, each coral sample was subjected to partial dissolution, and the results were considered acceptable only when the $^{14}C$ ages of at least three aliquots were self consistent within errors. This is the only quantitative test of diagenetic alteration in corals for $^{14}C$ dating purposes. In addition, conventional screening methods were applied, including textural investigation of thin sections under a petrographic microscope, XRD, and stable isotope analyses. For these reasons, results obtained in the present study are considered as reliable as can be ascertained with presently available methods. However, in some circumstances, it is still possible that contaminated samples could pass through the above tests. For example, the high $^{14}C$ excesses found in ≈50 ka (calendar age) corals, although supported by recent dating of Lake Lisan sediments (Schramm et al. 2000), may need further work for confirmation. In addition to tests for $^{14}C$ contamination, the samples were tested for open system behavior for U and Th isotopes, such as total U and $^{232}Th$ concentrations, and $\delta^{234}U(T)$ values. Most samples were within acceptable limits of these tests.

The results of the $^{14}C$ time-scale calibration experiments can be summarized as follows: First, the trend for increasing divergence between $^{14}C$ ages and calendar ages appears to continue beyond 30 ka and up to 50 ka; the limit of present measurements. At the younger end, data from the present study overlap with previous data. Second, four discrete age peaks of enhanced $^{14}C$ concentration were observed. The clustering in age is expected as the samples come from distinct, individual reef sections. However, the prominent peaks of $\Delta^{14}C$, including some negative values, in between the peaks, were unexpected. It is possible that the peaks are due to secondary, younger age, or modern carbon contamination. While this is acknowledged, and some of the older ≈50 ka samples may have been affected, it is unlikely to be the dominant cause given the battery of tests the samples were required to pass. The negative values of $\Delta^{14}C$, that systematically cluster in between the peaks, could not be produced by such contamination.

The four $^{14}C$ peaks appear correlated with the timing of North Atlantic Heinrich Events and ice-rafted debris deposits in deep sea cores. The accepted explanation for these Dangaard-Oeschger and Bond cycles involve reorganizations in the global ocean circulation system. The North Atlantic deep-water formation during glacial periods appears to be sensitive to fresh meltwater input into the North Atlantic by periodic instabilities in the ice sheets that launched armadas of icebergs into Hudson Bay and resulted in sea-level rises. Slow-down or closure of the circulation is expected to significantly raise atmospheric $^{14}C$ levels. The present data show an initial high sea-level followed by steep rise in atmospheric $^{14}C$ levels as the sea-level falls. The high concentration lasts for less than ≈1000 yr and drops below original ambient levels over several thousand years. The negative values of $\Delta^{14}C$ indicate the vigorous restart of the NADW circulation or enhanced ventilation at other oceans. Deep water formation around the Antarctic continent is believed to be equal to that in the North Atlantic. Cessation of the North Atlantic circulation is likely to redirect warm equatorial waters to the Southern Ocean and coupled with a high sea-level pulse is likely to destabilize the Antarctic ice sheet as well. $^{14}C$ and Th-U results obtained in the present work constitute a direct confirmation of severe and abrupt climate oscillations observed in Greenland ice cores and deep sea sediments. They provide direct evidence for the start-stop behavior of the North Atlantic conveyor belt circulation during the last glacial as put forward mainly by Wallace S Broecker (1998), and the increasingly evident global influence of these events beyond the boundaries of North Atlantic.

**ACKNOWLEDGMENTS**

We thank GS Burr, PU Clark, and J Jouzel for their helpful comments, and J van der Plicht for editorial assistance. Some of the coral samples were AMS dated at ANSTO supported by AINSE grant (97/060R).

## REFERENCES


Aldahan A, Possnert G. 1998. A high resolution $^{10}Be$ profile from deep sea sediment covering the last 70 ka: indication for globally synchronized environmental events. *Quaternary Geochronology* 17:1023–32.

Andrews JT. 1998. Abrupt changes (Heinrich Events) in late Quaternary North Atlantic marine environments: a history and review of data and concepts. *Journal of Quaternary Sciences* 13(1):3–16.

Banner JL, Wasserburg GJ, Chen JH, Humphery JD. 1991. Uranium-series evidence on diagenesis and Hydrology in Pleistocene carbonates of Barbados, West Indies. *Earth and Planetary Science Letters* 107:129–37.

Bar-Matthews M, Wasserburg GJ, Chen JH. 1993. Diagenesis of fossil coral skeletons: correlation between trace elements, textures and $^{234}U/^{238}U$. *Geochimica et Cosmochimica Acta* 57:257–76.

Bard E, Hamelin B, Fairbanks RG. 1990a. U-Th ages obtained by mass spectrometry in corals from Barbados: sea level during the past 130,000 years. *Nature* 346: 456–8.

Bard E, Hamelin B, Fairbanks RG, Zindler A. 1990b. Calibration of the $^{14}C$ timescale over the past 30,000 years using mass spectrometric U-Th ages from Barbados corals. *Nature* 345:405–10.

Bard E, Fairbanks, RG, Zindler A, Mathieu G, Arnold M. 1990c. U/Th and $^{14}C$ ages of corals from Barbados and their use for calibrating the $^{14}C$ time scale beyond 9000 years B.P. *Nuclear Instruments and Methods in Physics Research* B52:461–68.

Bard E, Fairbanks RG, Hamelin B, Zindler A, Hoang CT. 1991. Uranium-234 anomalies in corals older than 150,000 years. *Geochimica et Cosmochimica Acta* 55:2385–90.

Bard E, Arnold M, Fairbanks RG, Hamelin B. 1993. $^{230}Th$-$^{234}U$ and $^{14}C$ ages obtained by mass spectrometry on corals. *Radiocarbon* 35(1):191–9.

Bard E. 1998. Geochemical and geophysical implications of the radiocarbon calibration. *Geochimical et Cosmochimica Acta* 62:2025–38.

Bard E, Arnold M, Hamelin B, Tisnerat-Laborde N, Cabioch, G. 1998. Radiocarbon calibration by means of mass spectrometric $^{230}Th/^{234}U$ and $^{14}C$ ages of corals. An updated data base including samples from Barbados, Mururoa and Tahiti. *Radiocarbon* 40(3):1085–92.

Bathurst RGC. 1968. Precipitation of ooids and other aragonitic fabrics in warm seas. In: Müller G, Friedman G, editors. *Recent development in carbonate sedimentology in Central Europe*, Springer-Kerlag. 1–10.

Becker B, Kromer B. 1993. The continental tree-ring record-absolute chronology, $^{14}C$ calibration and climatic change at 11 ka. *Palaeogeography Palaeoclimatology Palaeoecology* 103:67–71.

Broecker WS. 1997. Thermohaline circulation, the Achilles Heel of our climate system: will man-made $CO_2$ upset the current balance? *Science* 278:1582–8.

Broecker WS. 1998. Paleocean circulation during the last deglaciation: a bipolar seesaw? *Paleoceanography* 13(2):119–21.

Brown TA, Southon JR. 1997. Corrections for contamination background in AMS $^{14}C$ measurements. *Nuclear Instruments and Methods in Physics Research* B123:208–13.

Burr GSE, Edwards RL, Donahue DJ, Druffel ERM, Taylor FW. 1992. Mass Spectrometric $^{14}C$ and U-Th measurements in coral. *Radiocarbon* 34(3):611–18.

Chappell J. 1974. Geology of coral terraces, Huon peninsula, New Guinea: a study for Quaternary tectonic movements and sea-level changes. *Geological Society of America Bulletin* 85:553–70.

Chappell J, Omura A, Esat T, McCulloch M, Pandolfi J, Ota Y, Pillans B. 1996. Reconciliation of late Quaternary sea levels derived from coral terraces at Huon Peninsula with deep sea oxygene isotope records. *Earth and Planetary Science Letters* 141:227–36.

Chen JH, Curran HA, White B, Wasserburg GJ. 1991. Precise chronology of the last interglacial period: $^{234}U$-$^{230}Th$ data from fossil coral reefs in the Bahamas. *Geological Society of America Bulletin* 103:82–97.

Clark PU, Alley RB, Keigwin LD, Licciardi JM, Johnsen SJ, Wang H. 1996. Origin of the first global meltwater pulse following the last glacial maximum. *Paleoceanography* 11(2):563–77.

Donahue DJ, Linick TW, Jull AJT. 1990. Isotope-ratio and background corrections for accelerator mass spectrometry radiocarbon measurements. *Radiocarbon* 32(2):135–142.

Edwards RL, Chen JH, Wasserburg GJ. 1986. $^{238}U$-$^{234}U$-$^{230}Th$-$^{232}Th$ systematics and precise measurement of time over the past 500,000 years. *Earth and Planetary Science Letters* 81:175–192.

Edwards RL, Chen JH, Ku T-L, Wasserburg GJ. 1987. Precise timing of the Last Interglacial Maximum from mass spectrometric determination of Thorium-230 in corals. *Science* 236:1547–53.

Edwards RL, Taylor FW, Wasserburg GJ. 1988. Dating earthquakes with high-precision thorium-230 ages of very young corals. *Earth and Planetary Science Letters* 90:371–81.

Edwards RL, Beck JW, Burr GS, Donahue DJ, Chappell JMA, Bloom AL, Druffel ERM, Taylor FW. 1993. A large drop in atmospheric $^{14}C/^{12}C$ and reduced melting in the Younger Dryas, documented with $^{230}Th$ ages of corals. *Science* 260:962–8.

Esat T. 1995. Charge collection thermal ion mass spectrometry of thorium. *International Journal of Mass Spectrometry and Ion Processes* 148:159–70.

Fifield K, Allan GL, Ophel TR, Head J. 1992. Accelerator mass spectrometry of $^{14}C$ at The Australian National University. *Radiocarbon* 34(3):452–7.

Gallup CD, Edwards RL, Johnson RG. 1994. The timing of high sea levels over the past 200,000 years. *Science* 263:796–800.

Hamelin B, Bard E, Zindler A, Fairbanks RG. 1991. $^{234}U/^{238}U$ mass spectrometry of corals: how accurate is the U-Th age of the last interglacial period? *Earth and Planetary Science Letters* 106:169–80.

Hotchkis MAC, Fink D, Hua Q, Jacobsen GE, Lawson EM, Smith AM, Tuniz, C. 1996. High-precision radiocarbon measurements at the ANTARES AMS centre. *Nuclear Instruments and Methods in Physics Research* B113:457–60.

Kitagawa H, Masuzawa T, Nakamura T, Matsumoto E. 1993. A batch preparation method for graphite targets with low background for AMS $^{14}C$ measurements. *Radiocarbon* 35(2):295–300.

Kitagawa H, van der Plicht J. 1998. Atmospheric radiocarbon calibration to 45,000 yr B.P.: late glacial fluctuations and cosmogenic isotope production. *Science* 279:1187–90.

Klug HP, Alexander LR. 1974. *X-ray diffraction procedures for polycrystalline and amorphous materials*. John Wiley & Sons. 966 p.

Kromer B, Spurk M. 1998. Revision and tentative extension of the tree-ring $^{14}C$ calibration 9200 to 11,900 cal BP. *Radiocarbon* 40(3):1117–25.

Ku T-L, Ivanovich M, Luo S. 1990. U-series dating of last interglacial high sea stands: Barbados revisited. *Quaternary Research* 33:129–47.

Lighty RG. 1985. Preservation of internal reef porosity and diagenetic sealing of submerged early Holoncene Barrier Reef, Southeastern Florida shelf. In: Schneidermann N, Harris PM. editors. *Carbonate Cements*. Society of Economic Palaeontologists and Mineralogists Special Publication 36:123–51.

Lund DC, Mix AC. 1998. Millennial-scale deep water oscillations: reflections of the North Atlantic in the deep Pacific from 10 to 60 ka. *Paleoceanography* 13(1):10–19.

McNichol AP, Gagnon AR, Jones GA, Osbone EA. 1992. Illumination of a black box: analysis of gas composition during graphite target preparation. *Radiocarbon* 34(3):321–9.

Moore CH. 1989. *Carbonate diagenesis and porosity; development in sedimentology.* Amsterdam: Elsevier.

Nelson DE, Korteling RG, Stott WR. 1977. Carbon-14: direct-detection at natural concentrations. *Science* 198:507–8.

Omura A, Ise A, Sasaki K, Takashi S, Hasebe Y. 1995. Resolution and reliability of the $\alpha$-spectrometric $^{230}Th/^{234}U$ Method for age determination. *Quaternary Research (Japan)* 34:195–207.

Ota Y. 1994. *Study on coral reef terraces of the Huon Peninsula, Papua New Guinea.* Yokohama, Yokohama National University Press. 171p.

Rozanski K, Stichler W, Gonfiantini R, Scott EM, Beukens RP, Kromer B, van der Plicht J. 1992. The IAEA $^{14}C$ intercomparison exercise 1990. *Radiocarbon* 34(3):506–19.

Schramm A, Stein M, Goldstein SL. 2000. Calibration of the $^{14}C$ time scale to >40 ka by $^{234}U$-$^{230}Th$ dating of Lake Lisan sediments (last glacial Dead Sea). *Earth and Planetary Science Letters* 175:27–40.

Siegenthaler U, Heimann M, Oeschger H. 1980. $^{14}C$ variations caused by changes in the global carbon cycle. *Radiocarbon* 22(2):177–91.

Stein M, Wasserburg, GJ, Aharon P, Chen JH, Zhu ZR, Bloom A, Chappell J. 1993. TIMS U-series dating and stable isotopes of the last interglacial event in Papua New Guinea. *Geochimica et Cosmochimica Acta* 57: 2541–54.

Stirling CH, Esat TM, McCulloch MT, Lambeck K. 1995. High-precision U-series dating of corals from Western Australia and implications for the timing and duration of the Last Interglacial. *Earth and Planetary Science Letters* 135:115–30.

Stirling CH. 1996. *Hig-precision U-series dating of corals from Western Australia: implications for Last Interglacial sea-levels.* The Australian National University.

Stirling CH, Esat TM, Lambeck K, McCulloch MT. 1998. Timing and duration of the Last Interglacial: evidence for a restricted interval of widespread coral growth. *Earth and Planetary Science Letters* 160: 745–62.

Stocker TF, Write DG. 1998. The effect of a succession of ocean ventilation changes on $^{14}C$. *Radiocarbon* 40(1):359–66.

Strasser A, Strohmenger C. 1997. Early diagenesis in Pleistocene coral reefs, southern Sinai, Egypt: response to tectonics, sea-level and climate. *Sedimentology* 44:537–58.

Stuiver M, Polach HA. 1977. Reporting of $^{14}C$ data. *Radiocarbon* 19(3):355–63.

Veeh HH, Veevers JJ. 1970. Sea-level at −175m off the Great Barrier Reef 13,600 to 17,000 years ago. *Nature* 226:536–7.

Voelker AHL, Sarnthein M, Grootes PM, Erlenkeuser H, Laj C, Mazaud A, Nadeau M-J, Schleicher M. 1998. Correlation of marine $^{14}C$ ages from th Nordic seas with the GISP2 isotope record: implications for radiocarbon calibration beyond 25 ka. *Radiocarbon* 40(1): 517–34.

Vogel JS, Southon JR, Nelso DE, Brown TA. 1984. Performance of catalytically condensed carbon for use in accelerator mass spectrometry. *Nuclear Instruments and Methods in Physics Research* B5:289–93.

Zhu ZR, Wyrwoll K-H, Collins LB, Chen JH, Wasserburg GJ, Eisenhauer A. 1993. High-precision U-series dating of Last Interglacial events by mass spectrometry: Houtman Abrolhos Islands, western Australia. *Earth and Planetary Science Letters* 118:281–93.

RADIOCARBON, Vol 42, Nr 3, 2000, p 403–414 

# COMPARISON OF U-SERIES AND RADIOCARBON DATES OF SPELEOTHEMS

Tomasz Goslar[1] • Helena Hercman[2] • Anna Pazdur[1]

**ABSTRACT.** The paper presents a comparison of U-series and radiocarbon dates of speleothems collected in several caves in central and southern Europe and southeast Africa. Despite a large spread of dates, mainly due to contamination with younger carbon, the group of corresponding $^{14}$C and $^{230}$Th/U ages of speleothem samples seems to be coherent with the previous suggestion of large deviation between the $^{14}$C and the absolute time scale between 35 and 45 ka BP. This agrees with the result of frequency analysis of published $^{14}$C and $^{230}$Th/U ages of speleothem.

## INTRODUCTION

Calibration of the radiocarbon time scale has been a subject of research for more than 40 years. Recently, the $^{14}$C calibration has been extended far beyond the beginning of Holocene, due to the data from corals (Bard et al. 1998), and from annually laminated oceanic and lacustrine sediments (Hughen et al. 1998; Goslar et al. 1995; Kitagawa and van der Plicht 1998). These data indicate deviation between the $^{14}$C and the absolute time scale increasing from 1000 to >3000 years between 11 and 24 ka BP.

The $^{14}$C calibration is important not only to geochronologists, but it is also related to reconstruction of past geomagnetic fields (e.g. Mazaud et al. 1991; Laj et al. 1996; Bard 1998), solar activity (e.g. Stuiver and Braziunas 1993; Bard 1998), and water circulation in the ocean (e.g. Goslar et al. 1995, 1999; Hughen et al. 1998; Bard 1998). The latter factor appeared best reflected in the Younger Dryas period, and with much lower confidence at the beginning of Bølling interstadial slightly after 15,000 cal BP (Stuiver et al. 1998). For the earlier time, large variations of atmospheric $^{14}$C concentration are expected because of the changes of the geomagnetic field (Laj et al. 1996; Tric et al. 1992), connected even with disappearance of deviation between $^{14}$C and absolute time scales before 40 ka BP (Mazaud et al. 1991). For the period before 23 ka BP, however, only two $^{14}$C dates of corals are available (Bard et al. 1998). They are supplemented by some dates from laminated sediments of Lake Suigetsu, Japan, but the relevant part of the Suigetsu varve chronology is based on only a single core, and therefore, needs to be confirmed (Kitagawa and van der Plicht 1998).

Another material enabling comparison of $^{14}$C and calendar time scales is speleothem. Using $^{14}$C and $^{230}$Th/U ages of stalagmite from the Cango Cave in South Africa, Vogel (1983) found large deviations between both time scales in the late Pleistocene, well before the coral dates became available. In recent years, the set of the Cango dates has been enlarged and completed with dates from Lynd's Cave, Tasmania (Vogel and Kronfeld 1997). A similar study was published by Holmgren et al. (1994), who dated stalagmites from the Lobatse II Cave, Botswana. Our goal was to enlarge significantly the set of speleothem dates, by $^{14}$C and $^{230}$Th/U dating of stalagmites from many sites in Europe and Africa.

## MATERIAL AND METHODS

In our research, we used speleothem samples collected in several caves (Table 1, Figure 1) in central and southern Europe, and in southeast Africa. For dating, we selected the largest stalagmites accessible. From each specimen, a slice about 1 cm thick was cut out along the stalagmite axis, and for dating we used sections with large and clear carbonate crystals, transparent on the slices. These 0.3–3 cm

[1]Radiocarbon Laboratory, Institute of Physics, Silesian University of Technology, ul. Krzywoustego 2, 44-100 Gliwice, Poland. Email: goslar@zeus.polsl.gliwice.pl.
[2]Institute of Geological Sciences, Polish Academy of Sciences, ul. Twarda 51/55, 00-818 Warsaw, Poland

Table 1 $^{14}C$ and $^{230}Th/U$ dates for speleothems obtained in the present work. Column 4 gives the $^{14}C$ age, corrected for the reservoir effect. Columns 6–8 list the activity ratios of the U and Th isotopes, and column 9 the U-series ages adjusted for initial Th.

| Sample | Distance from base (mm) | $^{14}C$ age (BP) | Corrected $^{14}C$ age (BP) | U (ppm) | $\frac{^{234}U}{^{238}U}$ | $\frac{^{230}Th}{^{232}Th}$ | $\frac{^{230}Th}{^{234}U}$ | $^{230}Th/U$ age (cal BP) | Corrected $^{230}Th/U$ age (cal BP) |
|---|---|---|---|---|---|---|---|---|---|
| *Sudety Mountains (Poland)* | | | | | | | | | |
| Niedźwiedzia 1A | 0–18 | 10,540 ± 80 | 8840 ± 1000 | 0.144 ± 0.004 | 1.20 ± 0.03 | 18.5 | 0.112 ± 0.003 | 12,810 ± 370 | 11,830 ± 700 |
| Niedźwiedzia 1B | 18–60 | 10,410 ± 70 | 8710 ± 1000 | | | | | | |
| Niedźwiedzia 1C | 86–122 | 9090 ± 80 | 7390 ± 1000 | 0.064 ± 0.002 | 1.53 ± 0.07 | 6.5 | 0.103 ± 0.002 | 11,750 ± 280 | 9160 ± 1500 |
| Niedźwiedzia 1D | 182–217 | 5380 ± 80 | 3680 ± 1000 | 0.060 ± 0.002 | 1.89 ± 0.09 | 4.6 | 0.103 ± 0.002 | 11,660 ± 240 | 7970 ± 1500 |
| Niedźwiedzia 5/2 | | 4480 ± 60 | 2780 ± 1000 | 0.016 ± 0.002 | 4.75 ± 0.52 | 7 | 0.171 ± 0.035 | 19,930 ± 4450 | 16,000 ± 5500 |
| *Moravian Karst (Czech Republic)* | | | | | | | | | |
| Holstynska 2/1 | | | | 0.34 ± 0.01 | 1.89 ± 0.03 | 52 | 0.130 ± 0.007 | 15,000 ± 800 | |
| Holstynska 2/2 | | 13,350 ± 170 | 11,650 ± 1050 | 0.604 ± 0.010 | 1.68 ± 0.03 | 205 | 0.114 ± 0.005 | 13,100 ± 600 | |
| Holstynska 2/4 | | 8810 ± 70 | 7110 ± 1000 | 0.519 ± 0.01 | 1.35 ± 0.02 | 12 | 0.093 ± 0.006 | 10,500 ± 700 | 9230 ± 1100 |
| Kadlec 1 | | 8590 ± 150 | 6890 ± 1000 | 0.144 ± 0.008 | 1.38 ± 0.10 | 1.6 | 0.11 ± 0.01 | 13,400 ± 900 | 890 ± 5500 |
| Kadlec 2 | | 8140 ± 60 | 6440 ± 1000 | 0.115 ± 0.005 | 1.42 ± 0.07 | 2 | 0.171 ± 0.004 | 20,160 ± 510 | 5280 ± 5700 |
| *Cracow-Wieluń Upland (Poland)* | | | | | | | | | |
| Dziewicza 1/5 | | 47,800 ± 1500 | 46,100 ± 1800 | 0.047 ± 0.003 | 2.41 ± 0.17 | 8.8 | 0.53 ± 0.05 | 76,100 ± 10,200 | 66,900 ± 13,400 |
| Bez Nazwy 1/1 | 30–40 | 30,400 ± 1900 | 28,700 ± 2200 | 0.070 ± 0.003 | 1.75 ± 0.10 | 4.8 | 0.36 ± 0.01 | 47,040 ± 1420 | 34,800 ± 1500 |
| Bez Nazwy 1/2 | 20–30 | 44,500 ± 2200 | 42,800 ± 2500 | 0.054 ± 0.002 | 2.09 ± 0.11 | 4.6 | 0.51 ± 0.01 | 72,920 ± 2580 | 55,100 ± 2800 |
| W Tomaszówkach 2 | | 35,200 ± 600 | 33,500 ± 1200 | 0.050 ± 0.002 | 1.99 ± 0.11 | 3 | 0.34 ± 0.03 | 44,130 ± 4270 | 24,200 ± 6200 |
| Wierna A+B+C | 70–180 | 47,200 + 4300 −2800 | 45,500 + 4400 −3000 | | | | | | |
| Wierna B+C | 100–180 | | | 0.117 ± 0.003 | 1.09 ± 0.03 | 84 | 1.01 ± 0.02 | >350,000 | |
| Wierna D+E+F | 182–282 | >46,000 | >44,000 | | | | | | |
| Wierna D+E | 180–250 | | | 0.110 ± 0.004 | 0.976 ± 0.05 | 29 | 1.04 ± 0.05 | >350,000 | |
| Wierna G | 280–300 | 40,200 + 2600 −2000 | 38,500 + 2800 −2300 | | | | | | |
| Wierna H | 300–320 | >46,300 >46,700 | >44,500 >45,000 | | | | | | |

Table 1 $^{14}C$ and $^{230}Th/U$ dates for speleothems obtained in the present work. Column 4 gives the $^{14}C$ age, corrected for the reservoir effect. Columns 6–8 list the activity ratios of the U and Th isotopes, and column 9 the U-series ages adjusted for initial Th. (*Continued*)

| Sample | Distance from base (mm) | $^{14}C$ age (BP) | Corrected $^{14}C$ age (BP) | U (ppm) | $^{234}U/^{238}U$ | $^{230}Th/^{232}Th$ | $^{230}Th/^{234}U$ | $^{230}Th/U$ age (cal BP) | Corrected $^{230}Th/U$ age (cal BP) |
|---|---|---|---|---|---|---|---|---|---|
| Wierna H+M | 300–410 | | | 0.118 ± 0.004 | 1.06 ± 0.05 | 62 | 1.04 ± 0.03 | >350,000 | |
| Wierna L+M | 350–420 | >46,900 | >45,000 | | | | | | |
| Wierna N+O+P | 420–540 | 42,400 + 3100 −2300 | 40,700 + 3300 −2500 | | | | | | |
| Wierna P | 530–540 | 34,100 + 2500 −1800 | 32,500 + 2700 −2100 | | | | | | |
| Wierna O+P | 460–540 | | | 0.126 ± 0.004 | 1.12 ± 0.04 | 34 | 0.975 ± 0.029 | 310,000 + 36,000 −29,000 | |
| *Tatra Mountains (Poland)* | | | | | | | | | |
| Czarna 8/1 | | 5140 ± 60 | 3440 ± 1000 | | | | | | |
| Czarna 8/2 | | 1750 ± 80 | 50 ± 1000 | 0.131 ± 0.005 | 2.57 ± 0.10 | 2.8 | 0.075 ± 0.001 | 8370 ± 140 | 4050 ± 1600 |
| *Low Tatra Mountains (Slovakia)* | | | | | | | | | |
| Lodowa 2/4 | | 6160 ± 60 | 4460 ± 1000 | 0.490 ± 0.011 | 2.90 ± 0.05 | >1000 | 0.042 ± 0.003 | 4700 ± 300 | |
| Slobody 7/1 | 1–11 | | | 2.74 ± 0.04 | 1.47 ± 0.02 | 382 | 0.091 ± 0.004 | 10,300 ± 450 | |
| Slobody 7A | 31–50 | 11,400 ± 180 | 9700 ± 1050 | 3.14 ± 0.07 | 1.45 ± 0.03 | 67 | 0.088 ± 0.003 | 10,000 ± 370 | |
| Slobody 7B | 105–120 | 7650 ± 140 | 5950 ± 1000 | 3.78 ± 0.07 | 1.46 ± 0.02 | 261 | 0.052 ± 0.001 | 5740 ± 160 | |
| Slobody 7/2 | 170–180 | | | 4.30 ± 0.07 | 1.32 ± 0.01 | 155 | 0.031 ± 0.002 | 3400 ± 190 | |
| Slobody 7/3 | 184–197 | | | 4.27 ± 0.07 | 1.33 ± 0.02 | >1000 | 0.029 ± 0.002 | 3200 ± 170 | |
| Slobody 7C | 205–217 | 5280 ± 130 | 3580 ± 1000 | 3.95 ± 0.07 | 1.47 ± 0.02 | 23 | 0.028 ± 0.0005 | 3050 ± 50 | |
| Slobody 7D | 282–290 | 3830 ± 110 | 2130 ± 1000 | 3.69 ± 0.05 | 1.38 ± 0.01 | 28 | 0.013 ± 0.0002 | 1420 ± 30 | |
| Slobody 7/4 | 295–303 | | | 5.62 ± 0.11 | 1.15 ± 0.02 | >1000 | 0.008 ± 0.001 | 820 ± 90 | |
| *Pieniny (Poland)* | | | | | | | | | |
| Pieniny 1/1 | 1–10 | 5050 ± 60 | 3350 ± 1000 | 0.184 ± 0.006 | 1.66 ± 0.06 | 7.7 | 0.124 ± 0.002 | 14,230 ± 290 | 11,600 ± 1200 |
| Pieniny 1/2 | 18–29 | 4700 ± 60 | 3000 ± 1000 | 0.193 ± 0.005 | 1.72 ± 0.04 | 3.8 | 0.040 ± 0.001 | 4490 ± 70 | 2730 ± 650 |
| Pieniny 1a/1 | | 4750 ± 60 | 3050 ± 1000 | 0.188 ± 0.005 | 1.63 ± 0.04 | 2.8 | 0.036 ± 0.001 | 3980 ± 80 | 1880 ± 780 |
| Pieniny 1a/2 | | 4170 ± 60 | 2470 ± 1000 | 0.217 ± 0.006 | 1.71 ± 0.05 | 2.7 | 0.033 ± 0.001 | 3640 ± 70 | 1620 ± 740 |
| Pieniny 2.1/1 | 1–6 | 4250 ± 80 | 2550 ± 1000 | 0.152 ± 0.005 | 1.71 ± 0.06 | 3.2 | 0.095 ± 0.002 | 10,720 ± 200 | 5720 ± 1910 |

Table 1 $^{14}C$ and $^{230}Th/U$ dates for speleothems obtained in the present work. Column 4 gives the $^{14}C$ age, corrected for the reservoir effect. Columns 6–8 list the activity ratios of the U and Th isotopes, and column 9 the U-series ages adjusted for initial Th. (*Continued*)

| Sample | Distance from base (mm) | $^{14}C$ age (BP) | Corrected $^{14}C$ age (BP) | U (ppm) | $\frac{^{234}U}{^{238}U}$ | $\frac{^{230}Th}{^{232}Th}$ | $\frac{^{230}Th}{^{234}U}$ | $^{230}Th/U$ age (cal BP) | Corrected $^{230}Th/U$ age (cal BP) |
|---|---|---|---|---|---|---|---|---|---|
| Pieniny 2.1/2 | 6–13 | 4440 ± 80 | 2740 ± 1000 | | | | | | |
| Pieniny 2.1/3 | 13–20 | 4120 ± 60 | 2420 ± 1000 | 0.147 ± 0.005 | 1.84 ± 0.07 | 3.2 | 0.061 ± 0.002 | 6870 ± 180 | 3660 ± 1270 |
| *Slovak Karst (Slovakia)* | | | | | | | | | |
| Krasnohorska 1A | | 35,500 ± 1700 | 33,800 ± 2000 | 0.035 ± 0.002 | 2.17 ± 0.16 | 5.9 | 0.44 ± 0.01 | 58,880 ± 1900 | 47,200 ± 6200 |
| Krasnohorska KZSA | | 36,600 ± 5000 | 34,900 ± 5100 | 0.185 ± 0.011 | 3.80 ± 0.25 | 22 | 0.42 ± 0.03 | 52,000 ± 4500 | |
| *Ruse region (Bulgaria)* | | | | | | | | | |
| Bulgaria OCz 1 | | 37,000 ± 1400 | 35,300 ± 1700 | 0.092 ± 0.004 | 1.46 ± 0.07 | >1000 | 0.33 ± 0.02 | 42,700 ± 3600 | |
| Bulgaria OCz 2 | | 12,900 ± 150 | 11,200 ± 1000 | 0.167 ± 0.005 | 1.67 ± 0.06 | >1000 | 0.19 ± 0.02 | 22,400 ± 2600 | |
| Bulgaria Bulg 1 | | 38,300 ± 700 | 36,600 ± 1250 | 0.096 ± 0.007 | 1.08 ± 0.11 | 31 | 0.38 ± 0.03 | 52,000 ± 5000 | |
| Bulgaria Bulg 2 | | 21,650 ± 280 | 19,950 ± 1100 | | | | | | |
| Bulgaria Bulg 3 | | 15,650 ± 100 | 13,950 ± 1000 | 0.132 ± 0.005 | 1.14 ± 0.06 | 10 | 0.18 ± 0.05 | 21,450 ± 7000 | 18,500 ± 8000 |
| Bulgaria Bulg 4 | | 11,250 ± 140 | 9550 ± 1000 | 0.105 ± 0.003 | 1.17 ± 0.04 | 22 | 0.019 ± 0.06 | 2000 ± 7000 | |
| *Tanzania* | | | | | | | | | |
| Tanzania MAF1A | 0–26 | 33,700 ± 1100 | 32,000 ± 1500 | 0.509 ± 0.013 | 1.10 ± 0.03 | 24 | 0.31 ± 0.01 | 40,190 ± 850 | |
| Tanzania MAF1B | 90–104 | 36,700 +3700 −2600 | 35,000 ± 3800 | 0.231 ± 0.005 | 1.12 ± 0.03 | 18 | 0.31 ± 0.01 | 39,600 ± 720 | 37,000 ± 1000 |
| Tanzania MAF1C | 151–165 | 32,000 ± 1600 | 30,300 ± 1900 | 0.226 ± 0.008 | 1.31 ± 0.05 | 33 | 0.34 ± 0.01 | 44,400 ± 2000 | |
| Tanzania MAF1D | 244–258 | 33,800 ± 1700 | 32,100 ± 2000 | 0.26 ± 0.01 | 1.02 ± 0.05 | 28 | 0.288 ± 0.007 | 37,000 ± 1000 | |
| Tanzania MAF1E | 282–296 | 31,600 ± 1600 | 29,900 ± 1900 | | | | | | |
| Tanzania MAF1F | 334–346 | 29,800 ± 1300 | 28,100 ± 1700 | 0.183 ± 0.006 | 1.17 ± 0.05 | 8.8 | 0.36 ± 0.01 | 47,160 ± 1130 | 40,000 ± 2000 |

(most frequently 0.5–1.5 cm) wide sections were cut out along growth layers, and divided in two portions. The edges of some stalagmites had fine-grained structure, and these sections were avoided. Also, we did not use sections containing depositional discontinuities.

One portion was dated by the $^{14}C$ method in the Gliwice Radiocarbon Laboratory, using the $CO_2$-filled proportional counters. Prior to separation of $CO_2$ for dating the outer part of the sample (about 20% of sample mass) was leached out with 4% HCl. Table 1 lists the $^{14}C$ dating results.

The twin sample was dated by the $^{230}Th/U$ method at the Institute of Geological Sciences, Polish Academy of Sciences, Warsaw. Standard radiometric dating procedure of the $^{230}Th/^{234}U$ method was used (Ivanovich and Harmon 1992). Samples of 10–40 g were dissolved in about 6 mol nitric acid. Uranium and thorium fractions were separated by chromatography. $^{234}U$, $^{238}U$, $^{230}Th$, and $^{232}Th$ activities were measured by using isotope dilution with a $^{228}Th/^{232}U$ spike. All measurements were done with alpha spectrometry using OCTET PC (EG&G ORTEC). The ages were calculated by standard algorithm (Ivanovich and Harmon 1992). Reported errors are 1 sigma. For the samples with $^{230}Th/^{232}Th$ <20, correction for detrital thorium was performed using an assumed initial $^{230}Th/^{232}Th$ of $1.5 \pm 0.5$. Results of the measurements are listed in Table 1.


Figure 1 Map showing regions in Europe, where the samples listed in Table 1 have been collected. 1. Sudety Mountains (Poland), 2. Moravian Karst (Czech Republic), 3. Cracow-Wieluń Upland (Poland), 4. Tatra Mountains (Poland), 5. Low Tatra Mountains (Slovakia), 6. Pieniny (Poland), 7. Slovak Karst (Slovakia), 8. Ruse region (Bulgaria), 9. One speleothem comes from Tanzania, Africa (collected by K Holmgren).

## DISCUSSION

$^{14}C$ dates of speleothem samples are obviously affected by the "reservoir effect" because the $^{14}C$ in precipitating speleothem is diluted with the $^{14}C$-free carbon from leached carbonate rocks. Therefore, the $^{14}C$ age of speleothem is greater than that of organisms deriving carbon from the atmosphere. So-called "apparent ages" are obtained. In the range of the $^{14}C$ calibration curve, the dilution factor can be assessed when the absolute age of the speleothem is known. Recent compilation of bibliographic data (Genty and Massault 1997) suggests that the dilution factors usually range between 0.7 and 0.9 (corresponding to apparent ages between 2750 and 750 yr), with the mean value of about 0.8 (apparent age of 1700 yr). In our studies the reservoir corrections of the speleothem samples from the Slobody Cave (Figure 2) are fairly constant over the whole Holocene and range from 2300 to 2700 yr. However, for most of our samples the reservoir correction is not exactly known, and (cf. Table 1) we used a value of 1700 ± 1000 yr.

The precision of the $^{230}$Th/U ages strongly depends on the concentrations of uranium and detrital thorium. In our collection, the lowest U concentration (usually <0.1 ppm) was revealed by the samples from the Cracow-Wieluń Upland. Activity of detrital $^{230}$Th, which is not produced from the decay of $^{234}$U in the speleothem, is routinely subtracted from the measured total $^{230}$Th activity (if $^{230}$Th/$^{232}$Th activity ratio is less than 20). It is determined through the measurement of $^{232}$Th activity, and an assumed initial activity ratio of $^{232}$Th and $^{230}$Th in the detrital minerals. This ratio is, however, usually not exactly known, but ranges between 1 and 2 according to bibliographic data.

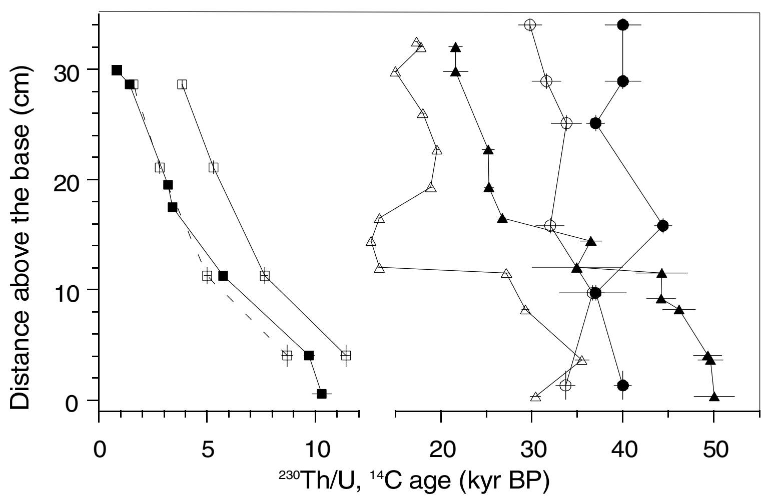


Figure 2 Profiles of $^{230}$Th/U (solid symbols) and $^{14}$C (open symbols) age of selected stalagmites. Squares = Slobody Cave; circles = MAF, Tanzania (this work); triangles = Lobatse II, Botswana (Holmgren et al. 1994). Open squares connected with dashed line represent $^{14}$C ages of samples in equilibrium with atmospheric carbon, obtained from $^{230}$Th/U ages using the $^{14}$C calibration curve.

The uncertainty of the $^{230}$Th/$^{232}$Th activity ratio affects the accuracy of the $^{230}$Th/U age, especially when the activity of $^{232}$Th is high. For a few samples, the error in $^{230}$Th/U age reached as much as several thousand years (Table 1).

In Figure 3 we compare the $^{14}$C and $^{230}$Th/U ages of our samples, together with the earlier published datings of speleothem and lignite (Goede and Vogel 1991; Holmgren et al. 1994; Vogel and Kronfeld 1997; Geyh and Schlüchter 1998), and with the coral $^{14}$C calibration data (Bard et al. 1998). The spread of our data points (Figure 3) is large. Comparison with the calibration dates suggests that many $^{14}$C ages are too low, or $^{230}$Th/U ages too high. The former case appears more probable, as young (or modern) carbonate might be deposited in the original structure of porous speleothem or in fractures. Such contamination distinctly affects $^{14}$C ages of old samples, while its influence on the

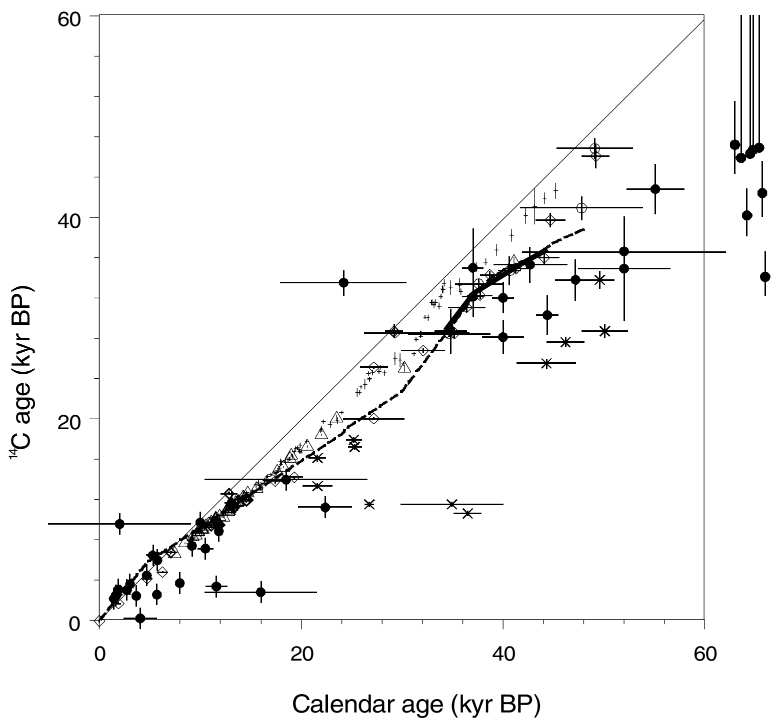


Figure 3 Comparison of $^{14}C$ and $^{230}Th/U$ ages of speleothem samples used in this work (●) with other relevant dates. The circles beyond the right edge of the plot represent samples from the Wierna stalagmite, dated with $^{230}Th/U$ to >300 ka BP. Δ = corals from Barbados, Tahiti and Mururoa Atoll (Bard et al. 1998); ◊ = stalagmites from Cango Cave, South Africa and Lynd's Cave, Tasmania (Vogel and Kronfeld 1998); × = stalagmite from Lobatse II Cave (Holmgren et al. 1994); O = lignite from Kärnten and Gossau, Switzerland (Geyh and Schlüchter 1998); † = annually laminated sediments of Lake Suigetsu, Japan (Kitagawa and van der Plicht 1998). $^{14}C$ ages of our samples have been corrected for the apparent age 1700 ± 1000 yr. Dashed line shows relationship between $^{14}C$ and absolute time scales, obtained by analysis of frequency distributions of not-paired $^{14}C$ and $^{230}Th/U$ ages of speleothem samples (discussed in the text).

$^{230}Th/U$ ages is much smaller. For example, 5% contamination of 40 ka old speleothem would change the $^{230}Th/U$ age by less than 2000, and the $^{14}C$ age by almost 15,000 years. Such an effect was observed for the stalagmite from the Lobatse II Cave (Holmgren et al. 1994) through the non-monotonous profile of $^{14}C$ age between 10 and 20 cm (Figure 2). Contamination with younger carbon is also evident in the speleothem from the Wierna Cave. This speleothem, dated with a $^{230}Th/U$ age to >300 ka BP, gave four finite $^{14}C$ ages, one of them even less than 40,000 BP (Figure 3). With this explanation in mind, one could expect the "true" relationship between $^{14}C$ and calendar time scales represented by the upper edge of the range covered by our dates. Such an edge can be traced between 35 and 45 ka BP, and indeed, it well agrees with the other dates.

On the other hand, profiles of $^{14}C$ and $^{230}Th/U$ ages in the stalagmite from Tanzania (MAF, Figure 2) suggest some problems with the $^{230}Th/U$ dates rather than $^{14}C$ dates. This could be due to open-system conditions, which affected $^{234}U/^{238}U$ as well as $^{230}Th/^{234}U$ activity ratios (cf. Figure 4). It is worth noting, that the two MAF dates, outlying from the monotonous $^{230}Th/U$ profile (Figure 2), are just those producing the large spread of dates between 35 and 50 ka BP (Figure 3).

The large spread of our dates precludes detailed conclusions concerning $^{14}C$ calibration. Nevertheless, a lack of dates with $^{14}C$ ages older than the $^{230}Th/U$ one between 35 and 45 ka BP is coherent with the suggestion from earlier $^{230}Th/U$ and $^{14}C$ dates (Vogel and Kronfeld 1997; Geyh and Schlüchter 1998; Bard et al. 1998) that the deviation between both time scales was large in that period. The cluster of $^{230}Th/U$-$^{14}C$ dates (Figure 3) clearly disagrees with the comparison of $^{14}C$ and varve ages from Lake Suigetsu (Kitagawa and van der Plicht 1998), perhaps an effect of non-continuous varve chronology in the oldest part of the Suigetsu sediments.

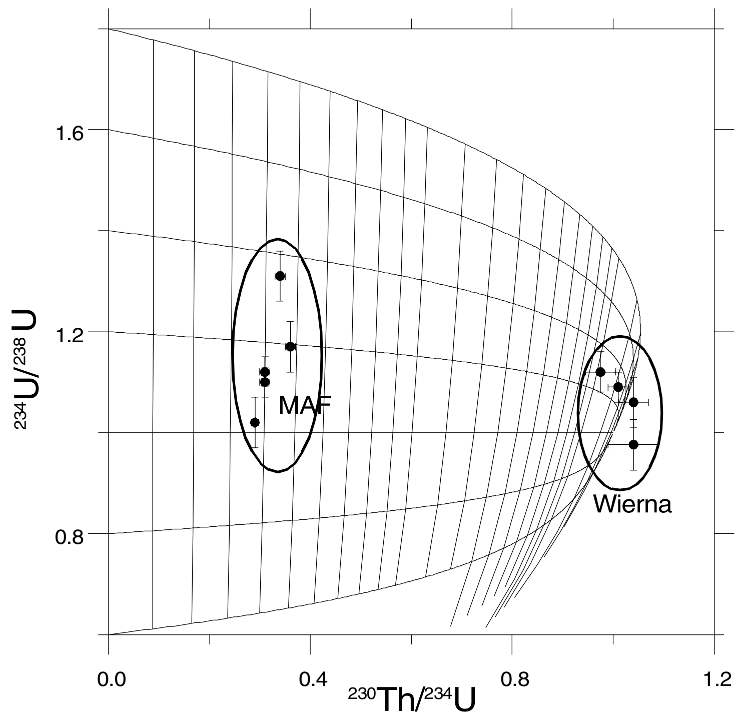


Figure 4 Plot of $^{234}U/^{238}U$ vs. $^{230}Th/^{234}U$ activity ratios for the samples from Wierna Cave and MAF, Tanzania

**Comparison of Frequency Distribution of $^{14}C$ and $^{230}Th/U$ Ages of Speleothems**

Though few speleothem samples have been dated by both the $^{14}C$ and $^{230}Th/U$ methods, there are many speleothem samples dated by only one of these methods. Looking through our bibliography, we found 133 "single" $^{14}C$ dates and 252 $^{230}Th/U$ dates of speleothem samples (younger than 60 ka) from Europe (Table 2). These dates are not uniformly distributed in time, reflecting some periods more favoring speleothem growth than the other ones.

The maxima of distributions of $^{14}C$ and $^{230}Th/U$ ages (Figure 5a) are not synchronous, most distinctly for period before 30 ka BP, an effect presumably reflecting deviation between both time scales. We tried thus to find such dependence between $^{14}C$ and calendar time scales (the so-called "transfer function", Figure 5b) which explains most of the time lags between both distributions. This function transfers the horizontal scale of distribution of $^{14}C$ dates (Figure 5c). The clue is to find such a function, which gives a minimum sum of squares of differences between the $^{230}Th/U$ and transferred $^{14}C$ distribution curves.

Table 2 Sources of dates used in comparison of frequency distribution of $^{14}C$ and $^{230}Th/U$ ages of speleothem

| Location | Nr of dates | References |
|---|---|---|
| *Radiocarbon method* | | |
| Croatia, Slovenia, Bosnia | 73 | Srdoč et al. (1973, 1975, 1977, 1979, 1981, 1982, 1984, 1989, 1992) |
| Germany | 10 | Geyh and Hennig (1986) |
| Tatra Mountains, Poland | 13 | Duliński M. (1988); Hercman (1991) |
| Slovakia | 5 | Hercman et al. (1994) |
| Cracow-Wieluń Upland, Poland | 32 | Pazdur et al. (1994) |
| Total | 133 | |
| *Uranium-Thorium method* | | |
| Crakow-Wieluń Upland, Poland | 10 | Głazek (1986); H Hercman, unpublished |
| Tatra Mountains, Poland; | 31 | Duliński M. (1988); Hercman et al. (1998); H Hercman, unpublished |
| Sudety Mountains, Holy Cross Mountains, Poland | 18 | Hercman et al. (1995); H Hercman, unpublished |
| Great Britain | 116 | Hennig et al. (1983); Atkinson et al. (1986); Rowe et al. (1989); Gascoyne et al. (1983); Ford et al. (1983); Sutcliffe et al. (1985) |
| Moravian Karst, Czech Republic | 11 | Hercman et al. (1997); H Hercman, unpublished |
| France | 18 | Bakalowicz et al. (1984); Maire and Quinif (1987) |
| Germany | 33 | Hennig et al. (1983 |
| Low Tatra Mountains, Slovakia | 15 | Duliński M. (1988); Hercman et al. (1997); H Hercman, unpublished |
| Total | 252 | |

The optimal transfer function has been found with the computer algorithm VARFIT (Goslar 1993). This algorithm searches the optimum in the large class of allowed transfer functions, using the dynamic programming method (Bellman and Dreyfus 1962). In our case, the class of allowed transfer functions was limited by two conditions. First, we allowed that for any age the $^{14}C$ time scale could be stretched or stressed by no more than 50%. This limitation obviously reflects the fact that the concentration of $^{14}C$ in the atmosphere never changed too abruptly. Second, we fixed the age of 34,000 BP transferred at 38 ka BP, to synchronize distinct maximum in both distributions. Without such a fixation, the VARFIT synchronized 34,000 BP with another maximum of the $^{230}Th/U$ distribution, at 44 ka BP, the result being completely unlikely, in view of other calibration data.

The obtained transfer function agrees well (Figure 3) with the coral data in the period 0–20 ka BP, and between 35 and 45 ka BP it fits very well with the line traced by the pairs of $^{14}C$ and $^{230}Th/U$ ages of speleothems. Some offset between 20 and 35 ka BP is insignificant as only few $^{14}C$ and $^{230}Th/U$-dated speleothem samples from this period are available. This result seems to confirm that large deviation between $^{14}C$ and calendar time scales did not disappear before 35,000 BP. However, as the uncertainty of the transfer function is not known, the transfer function approach yields only tentative conclusions.

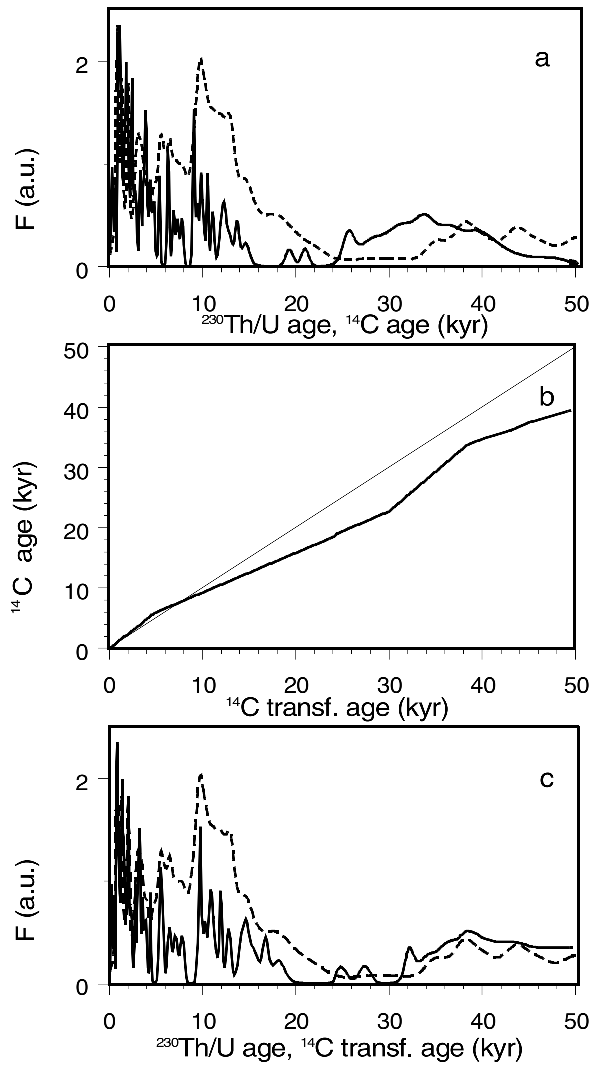


Figure 5 **a**: Comparison of frequency distributions of $^{14}C$ (solid line) and $^{230}Th/U$ (dashed line) ages of speleothem, selected from literature. **b**: relationship between $^{14}C$ and $^{230}Th/U$ time scales (transfer function) which best explains the time lags between distributions from section **a**. **c**: as in section **a**, with the time scale of $^{14}C$ distribution modified according to the transfer function shown in section **b**.

## CONCLUSION

$^{14}C$ dates of speleothem are commonly treated with caution because of the reservoir effect, producing an apparent age that is usually not accurately known. However, in light of our data and some previous research (Holmgren et al. 1994), the reservoir effect may be of minor importance when compared to contamination with younger carbon. The latter effect can alter $^{14}C$ ages of old (>30 ka) samples by several thousand years. Despite the large spread, our pairs of $^{14}C$ and $^{230}Th/U$ ages of speleothem samples seem coherent with the previously published data on corals, speleothem and lignite, which suggested a large deviation between $^{14}C$ and absolute time scales between 35 and 45 ka BP. The around 4000-year deviation seems also supported through the analysis of frequency distributions of $^{14}C$ and $^{230}Th/U$ ages of speleothem. In this analysis, a much larger set of ages, obtained with one of these methods only, was used.

## ACKNOWLEDGMENTS

This study was sponsored by the State Committee for Scientific Research through grant nr 283/PO4/96/11 to Helena Hercman. The authors wish to thank K Holmgren, Stockholm University, Sweden, for sharing the speleothem from Tanzania.

## REFERENCES

Atkinson TC, Lawson TJ, Smart PL, Harmon RS, Hess JW. 1986. New data on speleothem deposition and palaeoclimate in Britain over the last forty thousand years. *Journal of Quaternary Science* 1:67–72.

Bakalowicz M, Sorriaux P, Ford DC. 1984. Quaternary glacial events in the Pyrenees from U-series dating of speleothems in the Niaux-Lombrives-Sabart caves, Ariege, France. *Norsk Geografisk Tidsskrift* 38:193–7.

Bard E. 1998. Geochemical and geophysical implications of the radiocarbon calibration. *Geochimica et Cosmochimica Acta* 62:2025–38.

Bard E, Arnold M, Hamelin B, Tisnerat-Laborde N, Cabioch G. 1998. Radiocarbon calibration by means of mass spectrometric $^{230}Th/^{234}U$ and $^{14}C$ ages of corals: an updated database including samples from Barbados, Mururoa and Tahiti. *Radiocarbon* 40(3):1085–92.

Bellman RE, Dreyfus SE. 1962. *Applied dynamic programming*. Princeton University Press, Princeton, New Jersey.

Duliński M. 1988. Skład izotopowy tlenu i wodoru w naciekach jaskiniowych datowanych metodą $^{230}Th/^{234}U$ jako obraz zmian paleoklimatycznych na obszarach kontynentalnych (in Polish). Thesis, MIFiTJ AGH, Kraków.

Ford DC, Gascoyne M, Beck JS. 1983. Speleothem dates and Pleistocene Chronology in the Peak District of Derbyshire. *Transactions of the British Cave Research Association* 10(2):103–15.

Gascoyne M, Schwarcz HP, Ford DC. 1983. Uranium-Series ages of Speleothem from Northwest England: Correlation with Quaternary Climate. *Philosophical Transactions of the Royal Society, London* B 301:143–64.

Genty D, Massault M. 1997. Bomb $^{14}C$ recorded in laminated speleothems: calculation of dead carbon proportion. *Radiocarbon* 39(1): 33–48.

Geyh MA, Hennig GJ. 1986. Multiple Dating of a Long Flowstone Profile. *Radiocarbon* 28(2A):503–9.

Geyh MA, Schlüchter C. 1998. Calibration of the $^{14}C$ time scale beyond 22,000 BP. *Radiocarbon* 40(1): 475–82.

Głazek J. 1986. Wyniki datowań nacieków jaskiniowych z terenu Polski metodą$^{230}Th/^{234}U$. *Zeszyty Naukowe Politechniki Śląskiej, Geochronometria* 2:55–65.

Goede A, Vogel JC. 1991. Trace element variations and dating of a Late Pleistocene Tasmanian Speleothem. *Palaeogeography, Palaeoclimatology, Palaeoecology* 88:121–31.

Goslar T. 1993. Seasonal component changes found in the youngest part of the Lake Gościąż laminated sediment. *Polish Botanical Studies, Guidebook Series* 8: 189–202 (in Polish with English summary).

Goslar T, Arnold M, Bard E, Kuc T, Pazdur MF, Ralska-Jasiewiczowa M, Różański K, Tisnerat N, Walanus A, Wicik B, Więckowski, K. 1995. High concentration of atmospheric $^{14}C$ during the Younger Dryas cold episode. *Nature* 377:414–7.

Goslar T, Wohlfarth B, Björck S, Possnert G, Björck J. 1999. Variations of atmospheric $^{14}C$ concentrations over the Alleröd-Younger Dryas transition. *Climate Dynamics* 15:29–42.

Hennig GJ, Grün R, Brunnacker K. 1983. Speleothems, travertines and paleoclimates. *Quaternary Research* 20:1–29.

Hercman H. 1991. Rekonstrukcja elementów środowiska geologicznego Tatr Zachodnich na podstawie datowania izotopowego nacieków jaskiniowych. *Zeszyty Naukowe Politechniki Śląskiej, Geochronometria* 8:1–139.

Hercman H, Pazdur A, Pazdur MF, Mitter P. 1994. Datowanie izotopowe nacieków z wybranych jaskiń Słowackiego Krasu. *Zeszyty Naukowe Politechniki Śląskiej, Geochronometria* 10:81–96.

Hercman H, Lauritzen SE, Głazek J. 1995. Uranium-Series Dating of Speleothems from Niedzwiedzia and Radochowska Caves, Sudetes (Poland). *Theoretical and Applied Karstology* 8:37–48.

Hercman H, Bella P, Głazek J, Gradziński M, Lauritzen SE, Lovlie R. 1997. Uranium-Series dating of Speleothems from Demanova Ice Cave: a Step to Age Estimation of the Demanova Cave System (the Nizke Tatry Mts., Slovakia). *Annales Societalis Geologorum Poloniae* 67:439–50.

Hercman H, Lauritzen SE, Głazek J, Vit J. 1997. Uranium-Series dating of Speleothems from Amaterska and Holstejnska Caves, Moravian Karst, Czech Republic. *Proceedings of the 12th International Congress of Speleology* 1:45–7.

Hercman H, Nowicki T, Lauritzen SE. 1998. Rozwój systemu jaskiniowego Szczeliny Chochołowskiej (Tatry Zachodnie) w świetle datowań nacieków metodą uranowo-torową. *Studia Geologica Polonica* 113:85–103.

Holmgren K, Lauritzen SE, Possnert G. 1994. $^{230}Th/^{234}U$ dating of a Late Pleistocene stalagmite in Lobatse II Cave, Botswana. *Quaternary Science Reviews* 13: 111–9.

Hughen KA, Overpeck JT, Lehman SJ, Kashgarian M, Southon J, Peterson LC, Alley R, Sigman DM. 1998. Deglacial changes in ocean circulation from an extended radiocarbon calibration. *Nature* 391:65–8.

Ivanovich M, Harmon RS. 1992. Uranium Series Disequilibrium: Application to Environmental Problems. Oxford: 571.

Kitagawa H, van der Plicht J. 1998. Atmospheric radiocarbon calibration to 45,000 yr B.P.: late glacial fluctuations and cosmogenic isotope production. *Science* 279:1187–90.

Laj C, Mazaud A, Duplessy JC. 1996. Geomagnetic intensity and 14C abundance in the atmosphere and ocean during the past 50 kyr. *Geophysical Research Letters* 23:2045–8.

Maire R, Quinif Y. 1987. Chronostratigraphie et evolution sedimentaire en milieu Alpin dans la Galerie Aranzadi (Gouffre de la Pierre Saint Martin, Pyrenees, France). *Annales Societe Geolique de Belgique*, 110.

Mazaud A, Laj C, Bard E, Arnold M, Tric E. 1991. Geomagnetic field control of $^{14}$C production over the last 80 ky: implications for the radiocarbon time-scale. *Geophysical Research Letters* 18:1885–8.

Pazdur A, Hercman H, Górny A, Olszewski M. 1994. Wstępne wyniki badań nad chronologią powstawania nacieków w jaskiniach Wyżyny Krakowsko-Wieluńskiej. *Zeszyty Naukowe Politechniki Śląskiej, Geochronometria* 10:61–79.

Rowe PJ, Atkinson TC, Jenkinson RDS. 1989. Uranium-Series Dating of Cave Deposits at Creswell Crags Gorge, England. *Cave Science* 16:3–17.

Srdoč D, Slipcevic A, Paninic J, Obelić B, Breyer B. 1973. Rudjer Boskovic Institute radiocarbon measurements II. *Radiocarbon* 15(2):435–41.

Srdoč D, Slipcevic A, Planinic J. 1975. Rudjer Boskovic Institute radiocarbon measurements III. *Radiocarbon* 17(1):149-–55.

Srdoč D, Slipcevic A, Obelić B, Horvatinčić N. 1977. Rudjer Boskovic Institute radiocarbon measurements IV. *Radiocarbon* 19(3):465–75.

Srdoč D, Slipcevic A, Obelić B, Horvatinčić N. 1979. Rudjer Boskovic Institute radiocarbon measurements V. *Radiocarbon* 21(1):131–7.

Srdoč D, Slipcevic A, Obelić B, Horvatinčić N. 1981. Rudjer Boskovic Institute radiocarbon measurements VI. *Radiocarbon* 23(3):410–21.

Srdoč D, Horvatinčić N, Obelić B. 1982. Rudjer Boskovic Institute radiocarbon measurements VII. *Radiocarbon* 24(3):352–71.

Srdoč D, Obelić B, Horvatinčić N, Krajcar I. 1984. Rudjer Boskovic Institute radiocarbon measurements VIII. *Radiocarbon* 26(3):449–60.

Srdoč D, Obelić B, Horvatinčić N, Bronič IK. 1989. Rudjer Boskovic Institute radiocarbon measurements XI. *Radiocarbon* 31(1):85–98.

Srdoč D, Horvatinčić N, Bronić IK, Obelić B. 1992. Rudjer Boskovic Institute radiocarbon measurements XII. *Radiocarbon* 34(1):155–75.

Stuiver M, Braziunas T. 1993. Sun, ocean, climate and atmospheric $^{14}CO_2$: an evaluation of causal and spectral relationships. *The Holocene* 3:289–305.

Stuiver M, Reimer PJ, Bard E, Warren Beck J, Burr GS, Hughen KA, Kromer B, McCormac G, van der Plicht J, Spurk M. 1998. INTCAL98 Radiocarbon age calibration, 24,000-0 cal BP. *Radiocarbon* 40(3):1041–83.

Sutcliffe AJ, Harmon RS, Ivanovich M, Rae A, Hess JW. 1985. Wolverine in Northern England at About 83,000 yr B.P.: Faunal Evidence for Climatic Change during Isotope Stage 5. *Quaternary Research* 24:73–86.

Tric E, Valet JP, Tucholka P, Paterne M, Labeyrie L, Guichard F, Tauxe L, Fontugne M. 1992. Paleointensity of the Geomagnetic field during the last 80,000 years. *Journal of Geophysical Research* B97:9337–51.

Vogel J. 1983. $^{14}$C variations during the Upper Pleistocene. *Radiocarbon* 25(2):213–8.

Vogel JC, Kronfeld J. 1997. Calibration of radiocarbon dates for the Late Pleistocene using U-Th dates on stalagmites. *Radiocarbon* 39(1):27–32.

RADIOCARBON, Vol 42, Nr 3, 2000, p 415–422 

# RADIOCARBON CALIBRATION BEYOND THE DENDROCHRONOLOGY RANGE

Mordechai Stein[1] • Steven L Goldstein[2] • Alexandra Schramm[3]

**ABSTRACT.** The radiocarbon timescale has been calibrated by dendrochronology back to 11.8 ka cal BP, and extended to 14.8 ka cal BP using laminated marine sediments from the Cariaco Basin. Extension to nearly 23.5 ka cal BP is based on comparison between $^{14}C$ and U-Th ages of corals. Recently, attempts to further extend the calibration curve to >40 kyr are based on laminated sediments from Lake Suigetsu, Japan, foraminifera in North Atlantic sediments, South African cave deposits, tufa from Spain, and stalagmites from the Bahamas. Here we compare these records with a new comparison curve obtained by $^{234}U$-$^{230}Th$ ages of aragonite deposited at Lake Lisan (the last Glacial Dead Sea). This comparison reveals broad agreement for the time interval of 20–32 ka cal BP, but the data diverge over other intervals. All records agree that $\Delta^{14}C$ values range between ~250–450‰ at 20–32 ka cal BP. For ages >32 ka cal BP, the Lake Suigetsu data indicate low $\Delta^{14}C$ values of less than 200‰ and small shifts. The other records broadly agree that $\Delta^{14}C$ values range between ~250 and 600‰ at 32–39 ka cal BP. At ~42 ka cal BP, the North Atlantic calibration shows low $\Delta^{14}C$ values, while the corals, Lisan aragonites, and the Spanish tufa indicate a large deviations of 700–900‰. This age is slightly younger than recent estimates of the timing of the Laschamp Geomagnetic Event, and are consistent with increased $^{14}C$ production during this event.

## INTRODUCTION

Radiocarbon is the most important chronometer used for the late Pleistocene and Holocene, with applications to a range of disciplines including earth sciences, archaeology, and anthropology. However, ages in $^{14}C$ years are not equal to calendar years because the $^{14}C$ activity in the atmosphere has varied with time, and great efforts are underway to generate a calibration to calendar ages (Stuiver and van der Plicht 1998, and references therein). A precise calibration of the $^{14}C$ time scale has been established based on dendrochronology to 11.8 ka cal BP (Becker and Kromer 1991; Björck et al. 1996; Kromer and Spurk 1998). The calibration has been extended to 14.5 ka cal BP by counting of laminated marine sediments (Hughen et al. 1998), and by U-series dating of corals (Bard et al. 1998; Burr et al. 1998).

Beyond 14.5 ka cal BP, calibration can be extended semi-continuously to 23.5 ka cal BP by U-series dating of corals (Stuiver and van der Plicht 1998). Bard et al. (1990, 1998) showed that $^{14}C$ ages are ~3 ka younger than calendar ages at ~23.5 ka cal BP. Over the time interval of 24–60 ka cal BP, which includes most of the last Glacial period, there have been major changes in the Earth's climate, and secular variations and short-term excursions in the Earth's magnetic field intensity, all of which can affect the atmospheric $^{14}C$ activity (cf. Mazaud et al. 1991; Tric et al. 1992; Edwards et al. 1993 Laj et al. 1996). Bard et al. (1990, 1998) report two additional coral calibration points, at ~30 and ~41 ka cal BP. At these times the age differences are even higher, with $^{14}C$ ages younger than calendar ages, and age differences are ~3–4 and ~4–6 ka, respectively.

Some recent studies have tried to fill the gaps. Kitagawa and van der Plicht (1998a, 1998b) report a $^{14}C$ age calibration to 45 ka cal BP based on laminated sediments from Lake Suigetsu, Japan. Voelker et al. (1998) report a calibration to 53 ka cal BP using a chronology based on cross-calibration of planktonic foraminiferal stable isotope ratios in North Atlantic cores with the Greenland GISP2 ice core record. Vogel and Kronfeld (1997) report some U-Th ages obtained by α-counting of South African stalagmites. Richards et al. (1999) compared $^{14}C$ with $^{234}U$-$^{230}Th$ and $^{235}U$-$^{231}Pa$ ages mea-

[1]Corresponding author. Institute of Earth Sciences, The Hebrew University, Givat Ram, Jerusalem, 91904, Israel. Email: motis@vms.huji.ac.il.
[2]Lamont-Doherty Earth Observatory and Department of Earth and Environmental Sciences, Columbia University, Palisades NY 10964, USA
[3]Max-Planck-Institut für Chemie, Postfach 3060, D-55020 Mainz, Germany

sured by thermal ionization mass spectrometry (TIMS) on stalagmites from the Bahamas. Bischoff et al. (1994) reported a calibration point at ~40 ka cal BP from U-Th dating by TIMS of a tufa in Spain.

Construction of a precise calendar age calibration becomes more difficult with increasing age. Problems include higher absolute errors on determinations of the calendar ages with increasing age, and the large influence of small amounts of sample contamination with fossil or recent carbon on the $^{14}C$ ages. For example, the possibility of unrecognized gaps or other complications in varve counting (Kitagawa and van der Plicht 1998b), or ambiguities in stable isotope cross-correlations between core records (Guyodo and Valet 1996), make dating by a method using radioactive decay desirable. On the other hand, open system behavior, uncertainty of corrections for initial $^{230}Th$ in samples, can affect the accuracy of the $^{234}U$-$^{230}Th$ radioactive time clock. Ultimately, comparisons of different records and methods are necessary for a credible calibration from 23.5 ka cal BP to the analytical limits of $^{14}C$ determinations.

Recently, we used a calendar chronology based on $^{234}U$-$^{230}Th$ dating by TIMS of aragonitic sediments deposited from Lake Lisan, the last glacial precursor of the Dead Sea, to extend the $^{14}C$ time scale calibration to >40 kyr (Schramm et al. 2000). In this paper we summarize the results of the Lisan study and compare the Lisan calibration curve to the other schemes described in the literature.

## METHODS

### U-Series Dating by Mass Spectrometry

U-series dating by mass spectrometry has become an important means to obtain precise ages of late Quaternary corals (cf. Edwards et al. 1987; Stein et al. 1993), continental sediments such as vein calcite (Winograd et al. 1992), and cave deposits (Kaufman et al. 1998). Obtaining precise U-series ages on continental carbonate sediments has been problematic, because they typically contain significant amounts of non-authogenic U and Th, which must be considered in age evaluations (Bischoff and Fitzpatrick 1991; Kaufman 1993; Ku and Liang 1984; Luo and Ku 1991). This situation contrasts with corals, for example, which typically have negligible amounts of initial Th, and thus ages are determined simply by assuming that all the $^{230}Th$ in a sample is derived from the $^{238}U$ and $^{234}U$ (cf. Edwards et al. 1987; Chen et al. 1991; Stein et al. 1993).

There were major efforts made during the late 1980s, through drilling of coral reefs, to obtain samples that cover the time interval beyond the dendrochronology range. These include off-shore drilling at Barbados (Fairbanks 1989), and on-shore drilling in the Huon Peninsula, Papua New Guinea (Chappell and Polack 1990). Bard and colleagues dated the Barbados cores by $^{14}C$ and the TIMS U-series method, extending the calibration curve back to ~22 ka (Bard et al 1990). Their results were later augmented by samples from Tahiti, and Mururoa (Bard et al. 1998). The Huon core was used for $^{14}C$/U-series age comparison in a continuous interval between 11,000 and 7000 yr (Edwards et al. 1993). This core yielded similar results to the Barbados record, except for the interval of the Younger Dryas Event. The Huon core indicates an abrupt offset between the $^{14}C$ and U-series ages during the later part and after the Younger Dryas Event, suggesting a large drop in the atmospheric $^{14}C/^{12}C$. The integrity of the measured ages for corals is evaluated on the basis of the initial $^{238}U/^{238}U$ activity, which should be the same as seawater (1.144 ± 0.007; Chen et al. 1986). The major unknown in using corals for $^{14}C$ calibration is changes in the marine carbon reservoir. The present day correction is ~400 yr, and this figure is assumed for fossil corals as well (Bard et al. 1990, 1998; Edwards et al. 1993; Hughen et al. 1998).

## RESULTS

### $^{234}U$-$^{230}Th$ and $^{14}C$ ages of Lisan Sediments

Laminated lake sediments are another candidate for calibrating the $^{14}C$ timescale by $^{234}U$-$^{230}Th$ dating. Schramm et al. (2000a, 2000b) reported TIMS $^{234}U$-$^{230}Th$ and $^{14}C$ ages within a 40-m-thick measured and described section of the Lisan Formation. The ages range from ~70–17 ka, thus spanning a large portion of the last Glacial period. The U-series analyses were made on aragonite from laminated sediments, which can be dated both by U-series and $^{14}C$ techniques. The Lisan Formation is exposed along the Jordan–Dead Sea Valley. The aragonites precipitated from the surface water and are preserved in their primary state. They have high U concentrations (≈3 ppm) and are often free of detritus (based on XRD and chemical analyses) and thus appear to be excellent candidates for $^{234}U$-$^{230}Th$ dating. The $^{234}U$-$^{230}Th$ ages that were obtained for the Lisan aragonite are based on analysis of two or more samples taken from individual laminae within a few centimeters of each other. The $^{234}U$-$^{230}Th$ ages were determined for groups of samples from the same stratigraphic level by isochrons, and were also calculated for each individual sample. The "single sample" ages are based on corrections for small detrital contributions of the U and Th and for initial aqueous $^{230}Th$. The presence of an aqueous Th component was deduced from covariations of Th concentrations with Nb, Zr, and Fe (that is, insoluble trace elements indicating detritus in the samples). These covariations indicated that when the "detrital" element concentrations equaled zero, indicating pure aragonite, there was a residual Th concentration of 0.07–0.1 ppm. The correction used for initial Th is based on a modern aragonite collected from the Dead Sea containing negligible detritus but with 0.06 ppm Th and an apparent $^{234}U$-$^{230}Th$ age of ~2500 yr. Both the isochron and the single sample ages show excellent internal consistency and agreement with the stratigraphic order of the section. The aragonite ages range from 67 ka cal BP at 2 m above the base of the section, to ~19 ka cal BP at ~2 m beneath the top of the measured and described section at Perazim Valley near the southeastern end of the Dead Sea. Detailed discussion of the geochronological methods are given elsewhere (Schramm et al. 2000a, 2000b).

The validity of $^{14}C$ ages of aragonites depends on the correct assessment of the degree of equilibrium between the precipitating $CaCO_3$ and atmospheric $CO_2$. Waters flowing over carbonate terrains like the Judean Mountains west of the Jordan-Arava Valley, or percolating through carbonate aquifers, may contain substantial amounts of fossil carbon. If this carbon becomes incorporated into the aragonite, the $^{14}C$ ages will be too old. Lake Lisan had a density-layered structure, which was stabilized by freshwater addition to the lake. Stein et al. (1997) showed that the aragonite precipitated from the upper fresh water-rich layer, which was in contact with the atmosphere. They interpreted thick sequences of laminated aragonite and detritus throughout the section as signifying significant intervals with a stable stratification. For a first order approximation of the $^{14}C$ composition of Lake Lisan surface layer, Schramm et al. (2000) used the Dead Sea and incoming freshwater as an analog.

A surface sample taken in December 1977 had a $^{14}C$ activity of 108%, slightly lower than the atmospheric value of 122 ± 2% measured above Rehovot (Carmi et al. 1985), and implying a reservoir age of about 1000 yr. Reported "ages" of runoff water from the Judean Hills, draining mainly Mesozoic carbonate terrain west of the Dead Sea, and normalized to the atmospheric value of 122 ± 2% measured above Rehovot, range as high as 2900 BP, but are more generally between 600–1800 BP (Talma et al. 1997). A Dead Sea sample was taken in December 1977 when the lake had a stratified configuration, as well as water entering the Jordan River from Lake Kinneret (the Sea of Galilee). Both show elevated $^{14}C$ levels of about 107%, corresponding to $^{14}C$ ages of 1000 yr.

Based on these data, Schramm et al. (2000a) used a reservoir correction of 1000 yr for the aragonite $^{14}C$. The validity of this correction is supported by the agreement between the Lisan aragonite $^{14}C$-

calendar age calibration with the coral calibration (Bard et al. 1998) back to 23.5 ka cal BP (Figure 1). Data on organic remains over the range of 34–38 ka cal BP are consistent with this correction, although these samples have larger errors.

## DISCUSSION

### Comparisons with Other Data Sets

Two recent efforts to calibrate $^{14}C$ ages at high resolution have been published by Kitagawa and van der Plicht (1998) and Voelker et al. (1998). Both use non-radiometric methods to generate a chronology.

Kitagawa and van der Plicht (1998) obtained a high-resolution $^{14}C$ age record of macrofossils (leaves, twigs, and insect wings) from Lake Suigetsu, Japan, using laminated sediments from a 75-m continuous core. The laminae reflect deposition of dark clay and seasonal diatom blooms. The calendar timescale is based on laminae counting. Until 11.8 ka cal BP they use a floating chronology matched to the dendrochronology curve, and until ~38 ka calendar ages are determined through varve counting. For older ages, where the laminations are unclear, they assume a constant sedimentation rate. They must assume no hiatus occurs within the sedimentary sequence. Under these conditions, they estimate an accumulated error of ~2000 years at 40 ka cal BP.

Voelker et al. (1998) generated a high-resolution set of $^{14}C$ ages on planktonic foraminifera in two North Atlantic cores. The determination of the calendar ages is not based on direct age determinations of the cores, but is based on the assumption that down core planktonic foraminiferal stable isotope variations can be matched to the $\delta^{18}O$ temperature record of the GISP2 ice core in Greenland, and that changes occurred simultaneously. The $^{14}C$ ages of the various correlated climatic events were subsequently linked to the GISP 2 chronology, which is based on ice layer counting.

For all these records with ages older than Holocene, where $^{14}C$ ages can no longer be calibrated with absolute dating by dendrochronology, errors in the calibrated time scale become more significant and larger calendar age uncertainties have to be tolerated. We compared the Lake Lisan data with the other datasets by plotting the $\Delta^{14}C$ values of the dated samples against their "calendar age" (Figure 1). A higher $\Delta^{14}C$ value means a higher atmospheric $^{14}C/^{12}C$ ratio. When evaluating different records, it is important to consider 1) how the absolute values of the age offsets compare, and 2) independent of the absolute values, how well the patterns match to each other. If the $^{14}C$ reservoir correction of a data set is incorrect, but the calendar age is correct, its pattern should be parallel to the others, offset to different $\Delta^{14}C$ values. If the calendar age is systematically incorrect, but the $^{14}C$ age is either correct or systematically incorrect, the pattern will remain parallel but both calendar ages and the $\Delta^{14}C$ values will show an offset.

The Lake Lisan and the coral data show remarkable consistency over the interval that overlaps with the nearly continuous coral record to 23.5 ka cal BP. During this interval, the $\Delta^{14}C$ value is ~400‰. The coral data indicate that $\Delta^{14}C$ value increases to ~600‰ by ~30 ka cal BP, and to ~750‰ at 41 ka cal BP. Near these "checkpoints" the Lisan data are within 2$\sigma$ error of the coral data. The $\Delta^{14}C$ value of ~900‰ at ~42 ka cal BP is further supported by $^{234}U$-$^{230}Th$ ages of tufa sandwiching organic material in rock shelters at Catalunya, Spain (Bischoff et al. 1994), and speleothems from South Africa (Vogel and Kronfeld 1997), despite the higher errors in the calendar ages since the U-Th ages are determined by $\alpha$-counting. All these studies indicate high $\Delta^{14}C$ values of 700–900‰ at ~41–43 ka cal BP compared with data at ~38 ka cal BP. These high values are observed to occur directly after the Laschamp geomagnetic anomaly, based on recent determinations of its age. This a

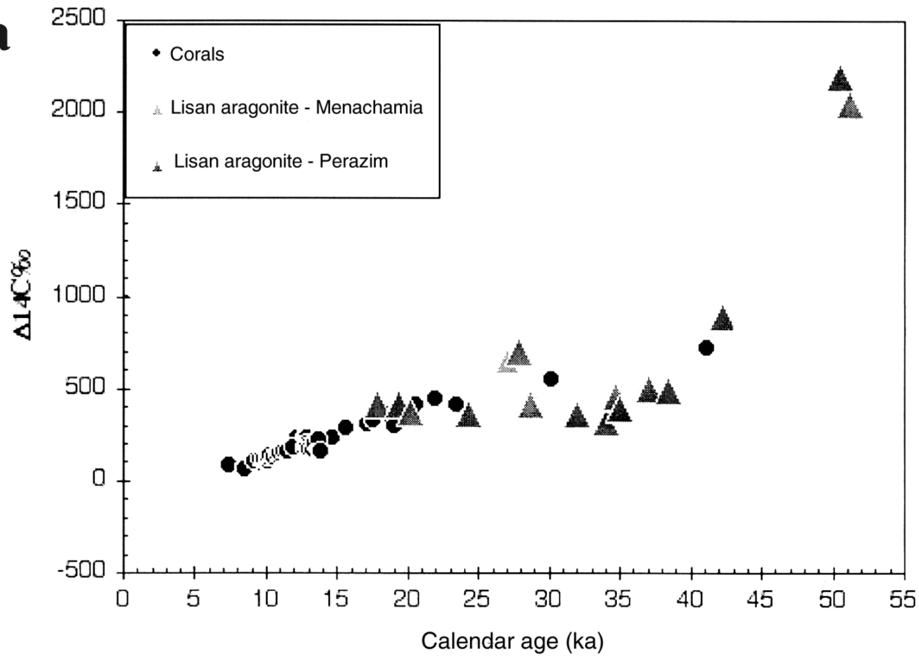


b

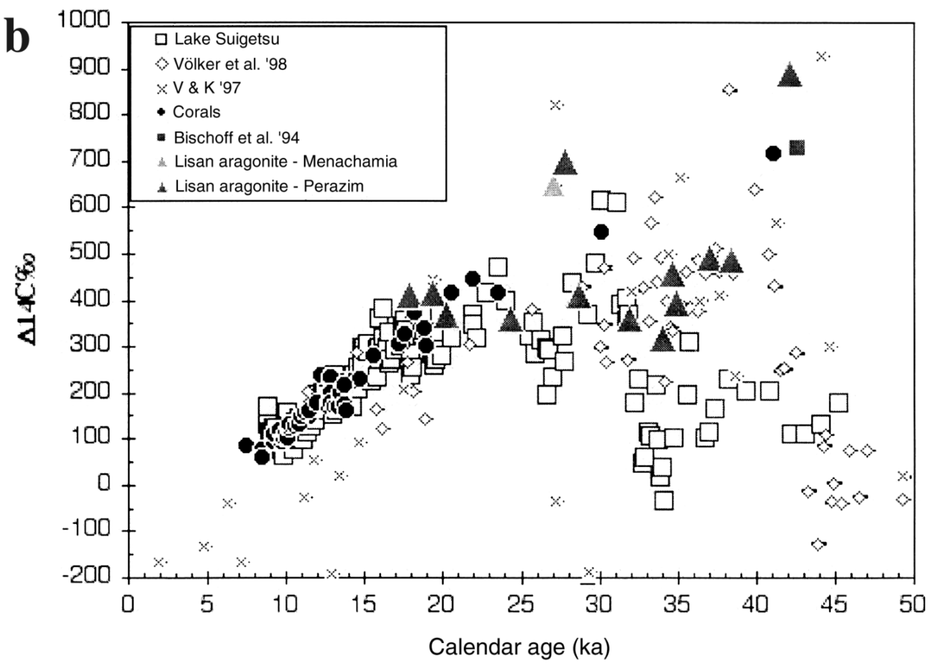


Figure 1 (a) Calendar age (ka cal BP) versus $\Delta^{14}C$ values in corals (Bard et al. 1998) and Lisan aragonite (this study); (b) Calendar age (ka cal BP) versus $\Delta^{14}C$ values for all presently available data. Data include the Lisan Formation (this study), corals (Bard et al. 1998), laminated sediments from Lake Suigetsu, Japan (Kitagawa and van der Plicht 1998a, 1998b), North Atlantic planktonic foraminifera (Voelker et al. 1998), cave deposits from South Africa (Vogel and Kronfeld 1997) and tufa from Spain (Bischoff et al. 1994).

geomagnetic excursion has been recently found within the Lisan section at stratigraphic levels corresponding to 41 ka cal BP (Marco et al. 1998; Ron et al. 2000). The Laschamp Event is associated with a geomagnetic intensity minimum, causing a higher production of cosmogenic nuclides such $^{14}C$. Therefore, the paleomagnetic data and the high $\Delta^{14}C$ observed at this age are consistent with each other.

The Lisan data indicate a sharp decrease in the $\Delta^{14}C$ value between 41 and 38 ka cal BP to ~450‰, consistent with a decrease in $^{14}C$ production following the geomagnetic excursion. During the interval 38–32 ka cal BP the Lisan $\Delta^{14}C$ values show a small decrease to ~350‰. There are indications for structure in the $^{14}C$-calendar age variations. An apparent excursion to high $\Delta^{14}C$ values of >600‰ between 28 and 29 ka cal BP is found in two samples from widely separated locations: the measured and described section in Perazim Valley in the south and Menahemya near Lake Kinneret (Schramm et al. 2000a). This might be related to the Mono Lake geomagnetic excursion, dated at 28 $^{14}C$ ka BP (Liddicoat 1992). However, this excursion has not been found globally. We are currently investigating whether the Mono Lake Event is reflected also in the Lisan sediments. Although the Lisan record effectively maps out the large-scale features of $^{14}C$ age changes throughout the interval 23.5–42 ka cal BP, the resolution of Lisan $^{14}C$ dates is still too low to make firm conclusions about short-term fluctuations in the atmospheric $^{14}C/^{12}C$ ratio.

Comparison of the different data sets yields the following relations (Figure 1):

1. Between 30 and 20 ka cal BP they generally show good agreement. An exception is at 27–28 ka cal BP. The high $\Delta^{14}C$ values of the Lisan aragonite at this age agrees with a South African cave date. However, they are not observed in the Lake Suigetsu record, which shows an apparent short-term $\Delta^{14}C$ decrease. There are few North Atlantic foraminifera data within this age interval.
2. Between 38 and 33 ka cal BP, the North Atlantic foraminifera and Lake Lisan aragonites show high $\Delta^{14}C$ values of 300–700‰. The few South African speleothem data generally agree. However, the high resolution Lake Suigetsu data are much lower, remaining within 100–200‰ from the equiline from the end of the record at ~45 ka cal BP through this age interval. The low $\Delta^{14}C$ values suggest that the Lake Suigetsu calendar ages throughout this interval are underestimated. Indeed, Kitagawa and van der Plicht (1998a) note that the Lake Suigetsu data beyond 31 ka cal BP are inconsistent with other calibrations, and that the ages above 20 ka cal BP should be considered as minimum ages due to the possibility of missing varves. The assumption of a constant sedimentation rate for ages older than 38 ka cal BP is likely to introduce additional uncertainties.
3. From 43 to 53 ka cal BP, the North Atlantic $\Delta^{14}C$ values are low, generally close to the equiline. Two Lisan aragonites show an consistent age offsets of >2000‰ at ~51–52 ka cal BP. Comparable calendar/$^{14}C$ age differences have been found in Labrador Sea cores, but have been attributed to $^{14}C$ contamination (Guyodo and Valet 1996; Stoner et al. 1995). A $^{14}C$ age of 50 ka cal BP corresponds to more than 9 half-lives, and we consider the data on >43 ka cal BP samples as yet unconfirmed. Nevertheless, it is intriguing that an anomaly in the paleomagnetic direction was identified in the Lisan sediments at 51–52 ka (termed by Marco et al. 1998 as the Lisan geomagnetic event). The only other report of an excursion at this time is from a study in the Gulf of California (Levi and Karlin 1989), which attributed it to the Laschamp Event. The possibility that an increase in $^{14}C$ production occurred at this time will require further confirmation.

## CONCLUSION

In view of the central role of $^{14}C$ ages for a late Pleistocene geochronology, more studies are necessary to establish the changing patterns in atmospheric $^{14}C/^{12}C$ ratios, and their relationship to climate, ocean circulation, magnetic field intensity, and solar flux changes. Comparison of the available data calibrating $^{14}C$ ages beyond ~20 ka cal BP shows a broad agreement between records to ~31 ka cal BP and disagreements between the available records from 30 to 50 ka cal BP. A recent paleomagnetic study of the Lisan Formation suggests that a high $^{14}C$ activity at ~41 ka cal BP is the result of increased production associated with the Laschamp paleomagnetic excursion event at 43–40 ka (Marco et al. 1998).

Despite the significant progress in the documentation of variations in the atmospheric $^{14}C$ activity, many open questions remain and call for further detailed study. Will the high age offset at ~50 ka cal BP, as observed in two Lisan samples, be confirmed by additional data? Is there any relationship to the geomagnetic excursion observed in Lisan Formation at ~51 ka cal BP Marco et al. (1998), at present only observed in Lake Lisan and possibly the Gulf of California records? What is the high-resolution structure of the changes in atmospheric $^{14}C$ activity earlier than 24 ka cal BP? Do the high $\Delta^{14}C$ values seen in two Lake Lisan aragonites at ~27 ka cal BP indicate a short-term increase in atmospheric $^{14}C/^{12}C$ ratios, and might it be associated with the Mono Lake geomagnetic event? Lake Lisan sediments, for which radiometric ages, paleomagnetic and paleoclimatic data can be combined, are excellent candidates to address these questions, and have great potential for further establishing a high resolution history of $^{14}C/^{12}C$ variations beyond 20 ka cal BP. Comparisons between this record and other excellent records will be needed in the coming few years to resolve the open issues.

## ACKNOWLEDGMENTS

This work is part of the "Lisan project", which has been funded by grants from the German-Israeli Foundation for Scientific Research and Development (GIF grant #332), the US–Israel Binational Science Foundation (BSF grant #96-227), and the Israeli Science Foundation (ISF grant #694.95).

## REFERENCES

Bard E, Hamelin B, Fairbanks RG, Zindler A. 1990. Calibration of the $^{14}C$ timescale over the past 30,000 years using mass spectrometric U-Th ages from Barbados corals. *Nature* 345:405–10.

Bard E, Arnold M, Hamelin B, Tisnerat-Laborde N, Cabioch G. 1998. Radiocarbon calibration by means of mass spectrometric $^{230}Th/^{234}U$ and $^{14}C$ ages of corals. An update data base including samples from Barbados, Mururoa and Tahiti. *Radiocarbon* 40(3):1085–92.

Becker B, Kromer B. 1991. Dendrochronology and radiocarbon calibration of the early Holocene. In: Barton N, Roberts AJ, Roe DA, editors. *The Late Glacial in north-west Europe*. p 22–4.

Bischoff JL, Fitzpatrick JA. 1991. U-series dating of impure carbonates: an isochron technique using total-sample dissolution. *Geochemica et Cosmochemica Acta* 55:543–54.

Bischoff JL et al. 1994. Dating of the Basal Aurignacian Sandwich at Abric Romani (Catalunya, Spain) by radiocarbon and uranium- series. *Journal of Archeological Science* 21:541–51.

Björck S et al. 1996. Synchronized terrestrial-atmosphere deglacial records around the North Atlantic. *Science* 274:1155–60.

Burr GS, Beck JW, Taylor FW, Récy J, Edwards RL, Cabioch G, Corrège T, Donahue DJ, O'Malley JM. 1998. A high-resolution radiocarbon calibration between 11,700 and 12,400 calendar years BP derived from $^{230}TH$ ages of corals from Espiritu Santo Island, Vanuatu. *Radiocarbon* 40(3):1093–105.

Carmi I, Stiller M, Kaufman A. 1985. The effect of atmospheric $^{14}C$ variations on the $^{14}C$ levels in the Jordan River system. *Radiocarbon* 27(2B):305–13.

Chappell J, Polach. 1991. Radiocarbon dating of corals from a 52 meter deep boring in New Guinea. *Nature* 349:147–9.

Chen JH, Edwards RL, Wasserburg GJ. 1986. $^{238}U$, $^{234}U$ and $^{232}Th$ in seawater. *Earth and Planetary Science Letters* 80:241–52.

Chen JH, Curran HA, White B, Wasserburg GJ. 1991. Precise chronology of the last interglacial period. $^{234}U$-$^{230}Th$ data from fossil coral reefs in the Bahamas. *Geological Society of America Bulletin* 103:82–97.

Edwards RL, Chen JH, Wasserburg GJ. 1987. $^{238}U$-$^{234}U$-$^{230}Th$-$^{232}Th$ systematic and the precise measurement of time in the past 500,000 years. *Earth and Planetary*

*Science Letters* 81:175–92.

Edwards RL, et al. 1993. A large drop in atmospheric $^{14}C/^{12}C$ and reduced melting in the Younger Dryas, documented with $^{230}Th$ ages of corals. *Science* 260: 962–8.

Fairbanks RG. 1989. Sea level rise during the last deglaciation as record in Barbados corals. *Nature* 342:637–42.

Guyodo Y, Valet JP. 1996. Relative variations in geomagnetic intensity from sedimentary records: the past 200,00 years. *Earth and Planetary Science Letters* 143:23–36.

Hughen KA, et al. 1998. Deglacial changes in ocean circulation from an extended radiocarbon calibration. *Nature* 391:65–8.

Kaufman A. 1993. An evaluation of several methods for determining $^{230}Th/U$ ages in impure carbonates. *Geochimica et Cosmochimica Acta* 57:2303–17.

Kaufman A, Wasserburg G J, Porcelli D, Bar-Matthews M, Ayalon A. 1998. U-Th isotope systematics from the Soreq cave, israel and climatic correlations. *Earth and Planetary Science Letters* 156:141–55.

Kitagawa H, van der Plicht J. 1998a. Atmospheric Radiocarbon Calibration to 45,000 yr B.P.: Late Glacial Fluctuations and Cosmogenic Isotope Production. *Science* 279:1187–90.

Kitagawa H, van der Plicht J. 1998b. A 40,000 year varve chronology from Lake Suigetsu, Japan: extension of the $^{14}C$ calibration curve. *Radiocarbon* 40(1):505–15.

Kromer B, Spurk M. 1998. Revision and tentative extension of the tree-ring based $^{14}C$ calibration. *Radiocarbon* 35(1):125–36.

Ku TL, Liang ZC. 1984. The dating of impure carbonates with decay-series isotopes. *Nuclear Instruments and Methods in Physics and Research* 223:563–71.

Laj C, A Mazaud, Duplessy JC. 1996. Geomagnetic intensity and $^{14}C$ abundance in the atmosphere and ocean during the past 50 kyr. *Geophysical Research Letters* 23:2045–8.

Levi S, Karlin R. 1989. A sixty thousand year paleomagnetic record from the Gulf of California sediments: secular variation, late Quaternary excursions and geomagnetic implications. *Earth and Planetary Science Letters* 92:219–33.

Liddicoat JC. 1992. Mono Lake Excursion in Mono Basin, California, and at Carson Sink and Pyramid Lake, Nevada. *Geophysical Journal International* 108:442–52.

Luo S, Ku TL. 1991. U- series isochron dating: A generalized method employing total- sample dissolution. *Geochemica et Cosmochemica Acta* 55:555–64.

Marco S, Ron H, McWilliams M, Stein M. 1998. High resolution secular variation record from Lake Lisan sediments (paleo-Dead Sea). *Earth and Planetary Science Letters* 161:145–60.

Mazaud AC, Laj E, Bard M, Arnold, Tric E. 1991. Geomagnetic field control of $^{14}C$ production over the last 80 kyr: implications for the radiocarbon time-scale. *Geophysical Research Letters* 18:1885–8.

Richards DA, Beck JW, Donahue DJ, Smart PL, Edwards RL. 1999. Thorium-230 and Carbon -14 dating of speleothems from the Bahamas: implications for the calibration of the radiocarbon timescale. *Proceedings of the 9th Goldschmidt Conference, Boston*. p 245.

Ron H, Stein M, Goldstein SL, Marco S. The duration of geomagnetic excursions documented in Lake Lisan sediments (Paleo-Dead Sea). *Earth and Planetary Science Letters*. Submitted.

Schramm A, Stein M, Goldstein SL. 2000a. Calibration of the $^{14}C$ time scale to >40 ka by $^{234}U$-$^{230}Th$ dating of Lake Lisan sediments (last Glacial Dead Sea). *Earth and Planetary Science Letters* 175:27–40.

Schramm A, Stein M, Goldstein SL. 2000b. $^{234}U$-$^{230}Th$ dating of Lake Lisan (Paleo-Dead Sea) aragonite by TIMS. *Geochimica et Cosmochimica Acta*. Submitted.

Stein M, Wasserburg GJ, Aharon P, Chen JH, Zhu ZR, Bloom A, Chappell J. 1993. TIMS U-series dating and stable isotopes of the last interglacial event in Papua new Guinea. *Geochimica et Cosmochimica Acta* 53: 2541–54.

Stein M, Starinsky A, Goldstein SL, Katz A, Machlus M, Schramm A. 1997. Strontium isotopic, chemical, and sedimentological evidence for the evolution of Lake Lisan and the Dead Sea. *Geochimica et Cosmochimica Acta* 61:3975–92.

Stiller M, Chung YC. 1984. Radium in the Dead Sea: A possible tracer for the duration of meromixis. *Limnology and Oceanography* 29:574–86.

Stoner JS, Channell JET, Hillaire-Marcel C. 1995. Late Pleistocene relative geomagnetis paleointensity from the deep Labrador Sea: regional and global correlations. *Earth and Planetary Science Letters* 134:237–52.

Stuiver M, van der Plicht J. 1998. INTCAL98. *Radiocarbon* 40(3):1041–164.

Talma AS, Vogel JC, Stiller M. 1997. The radiocarbon content of the Dead Sea. The Dead Sea: The lake and its setting. In: Niemi TM, Ben-Avraham Z, Gat JR. editors. *Oxford monographs on geology and geophysics* 34. Oxford: Oxford University Press. p 171–83.

Tric EJP, Valet P, Tucholka M, Paterne L, Labeyrie F, Guichard L, Tauxe, Fontugne M. 1992. Paleointensity of the geomagnetic field during the last 80,000 years. *Journal of Geophysical Research* 97(B6):9337–51.Voelker AHL et al. 1998. Correlation of marine $^{14}C$ ages from the Nordic seas with the GISP2 isotope record: implications for radiocarbon calibration beyond 25 ka BP. *Radiocarbon* 40(1):517–34.

Vogel JC, Kronfeld J. 1997. Calibration of radiocarbon dates for the late Pleistocene using U/Th dates on stalagmites. *Radiocarbon* 39:27–32.

Winograd IJ, Coplen TB, Landwehr JM, Riggs AC, Ludwig KR, Szabo BJ, Kolesar PT, Revesz KM. 1992. Continuous 500,000-year climate record from vein calcites in Devils Hole, Nevada. *Science* 258:255–60.

RADIOCARBON, Vol 42, Nr 3, 2000, p 423–435 

# SUBFOSSIL TREE DEPOSITS IN THE MIDDLE DURANCE (SOUTHERN ALPS, FRANCE): ENVIRONMENTAL CHANGES FROM ALLERØD TO ATLANTIC

C Miramont[1] • O Sivan[1] • T Rosique[2] • JL Edouard[1] • M Jorda[3]

**ABSTRACT.** The purpose of this paper is to analyze the numerous holocene subfossil trees (*Pinus silvestris*) buried in alluvial deposits in the Southern French Alps. These trees lived between the Allerød and Subboreal periods, according to $^{14}C$ dates. Our dendochronological studies explain the trees' sudden death as due to morphological crisis brought on by climatic oscillations. Tree-ring series could be used to identify the variability of early Holocene atmospheric $^{14}C$ levels.

## INTRODUCTION

In the Middle Durance region (Southern Alps, France; Figure 1A), numerous groups of subfossil trees (*pinus silvestris*) are buried in alluvial and colluvial deposits. The trees, which are remarkably well preserved, have been radiocarbon dated between the Allerød and the Subboreal periods (Archambault 1967, 1968, 1969; Delibrias et al. 1984; Gautier 1992; Rosique 1994, 1996; Miramont 1998; Sivan 1999). These trees, which have not been extensively studied to date, have the potential to reveal much about the paleoenvironments—paleoclimate, geomorphology, paleoecology—of the first part of the Postglacial period. The goals of this article are: 1) to inventory the deposits of subfossil trees known to exist in the southern French Alps, and 2) to present the first results of the dendrogeomorphologic study of the trees in the Saignon and Charanc basins.

The middle Durance basin is an area with mountains ranging in altitude from 500 to 2000 m. It is influenced by both Mediterranean and mountain climates. The region is dominated by an outcrop of calcareous marl, notably from the superior Jurrasic ("terres noires"). As these structures exist on steep slopes highly susceptible to erosion, they are particularly sensitive to paleoenvironmental changes. Therefore, climatic changes since the Late Glacial period are well recorded in alluvial fillings.

Figure 1B and Table 1 show all of the known Holocene subfossil tree sites in the Southern Alps, as well as their $^{14}C$ dates. The subfossil trees are found in distinct geographical areas. The Buëch basin has been studied the most and has the most known tree sites. The tributaries of the Sasse, Bléone, and Ubaye Rivers also reveal important sites. The Charanc, Saignon, Drouzet, and Messires Oddou basins are particularly rich in subfossil tree deposits. In others, only isolated trunks have been discovered. In total, about 30 sites are known, but most of the area has not been investigated, and the region's frequent flash floods and susceptibility to erosion mean that new sites could easily be exposed, or old ones easily reburied or destroyed.

*Pinus Silvestris* stumps are buried at various depths in alluvial and colluvial fillings from the first part of the postglacial period (Jorda 1980, 1993). The stumps have recently been exposed by the renewed activity of the rivers. Many of the stumps still have pieces of bark. Most of the trees are upright and rooted in lower alluvial layers, which also contain vegetal debris and often charred wood. Other trees are horizontal or broken. The trunks measure up to 60 cm in diameter and 1–3 m in height. Some of them are up to 300 years old. These subfossil trees can be distinguished from recent stumps in three ways: their unusual placement in relation to present waterways, their hardness, and their particular odor.

[1]IMEP – UMR 6116 CNRS, case 451, Faculté des Sciences et Techniques de St Jérôme, Avenue Escadrille Niemen, 13397 Marseille Cedex 20, France. Email: mirajor@aol.com; jean-louis.Edouard@LBHP.u-3mrs.fr.
[2]CEREG – EP 2037 CNRS/ULP/ENGEES, Faculté de Géographie, Université Louis Pasteur, 3 rue de l'Argonne, 67083 Strasbourg Cedex, France. Email: rosique@geographie.u-strasbg.fr.
[3]Institut de Géographie, Université de Provence, Avenue R. Schuman, 13621 Aix en Provence, France

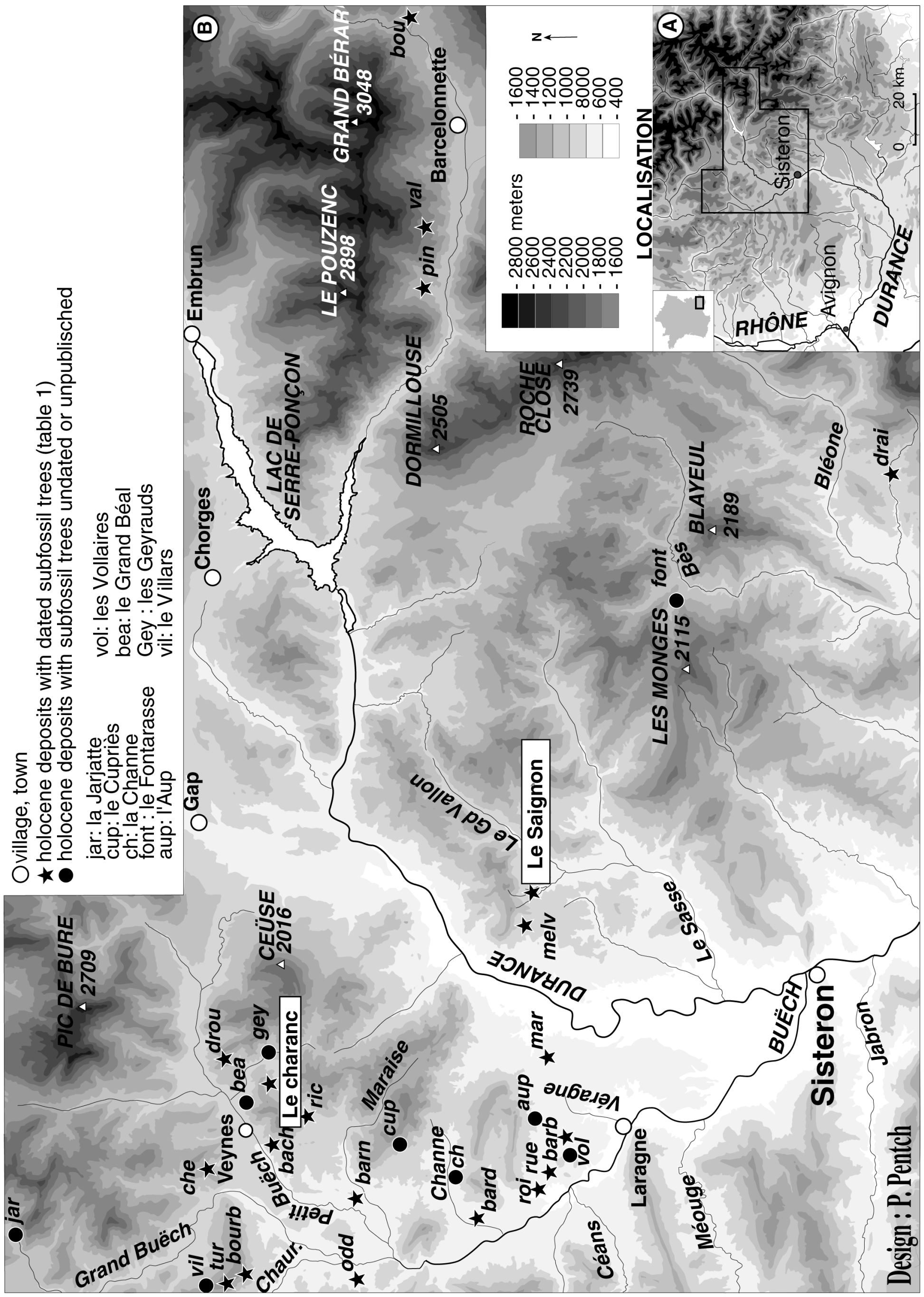

Figure 1 The middle Durance region (Southern France) showing the location of the subfossil tree deposits

Table 1 Sites, dates, and references of subfossil trees

| Basin | Tributary | Reference (Fig. 1B)° | Site | Description | $^{14}C$ dates (BP) | Lab nr | Tree nr (Fig. 2) | References |
|---|---|---|---|---|---|---|---|---|
| Buëch | La Chauranne | tur | Turonne | 10 trees | 7960 ± 185 | ? | 33 | Archambault (in Gautier 1992) |
| | | bourd | Bourboutane | Fewer than 10 trees | 7150 ± 260 | Ly-1901 | 43 | Archambault (in Gautier 1992) |
| | Grand Buëch | odd | Messires Oddou | More than 40 trees | 8620 ± 380 | Ly-558 | 15 | Archambault (in Gautier 1992) |
| | | che | Chênet | More than 10 trees | 7170 ± 160 | LGQ-714 (fragment) | 45 | Rosique (1996) |
| | Petit Buëch | cha | Charanc | More than 70 trees | 5240 ± 190 | LGQ-1076 | 49 | Rosique (1996) |
| | | | | | 6920 ± 190 | LGQ-1075 | 46 | Rosique (1996) |
| | | | | | 7250 ± 140 | LGQ-997 | 44 | Rosique (1996) |
| | | | | | 7300 ± 210 | LGQ-1074 | 42 | Rosique (1996) |
| | | | | | 7685 ± 70 | A-10223 | 39 | Sivan (1999) |
| | | | | | 8145 ± 45 | A-10224 | 31 | Sivan (1999) |
| | | | | | 8290 ± 70 | A-10222 | 29 | Sivan (1999) |
| | | | | | 8755 ± 75 | A-10225 | 16 | Sivan (1999) |
| | | drou | Drouzet aval | More than 10 trees | 11,975 ± 115 | A-10311 | 1 | Sivan (1999) |
| | | bach | Bachassette | About 10–20 trees | 12,030 ± 190 | LGQ-713 (fragment) | 2 | Rosique (1996) |
| | | | | | 10,890 ± 210 | LGQ-711 | 6 | Rosique (1996) |
| | | | | | 10,690 ± 230 | LGQ-712 (fragment) | 9 | Rosique (1996) |
| | La Maraise | barn | Barnèche | Fewer than 10 trees | 10,040 ± 260 | Ly-1902 | 10 | Archambault (in Gautier 1992) |
| | | ric | Richardet | ? | 3850 ± 65 | Ly-5013 | 50 | Gautier (1992) |
| | La Channe | bard | Bardalonne | Fewer than 10 trees | 8500 ± 200 | Gif-865 | 19 | Gidon et al. (1991) |
| | Buëch aval | rue | Ravin de Rue (Cuculianne) | 10 trees | 11,250 ± 250 | Ly-277 | 4 | Montjuvent (in Gautier 1992) |
| | | | | | 11,500 ± 250 | Gif-5314 | 3 | Delibrias et al. (1984) |
| | | | | | 10,600 ± 220 | Gif-5313 | 8 | Delibrias et al. (1984) |

Table 1 Sites, dates and references of subfossil trees *(Continued)*

| Basin | Tributary | Reference (Fig. 1B)° | Site | Description | $^{14}C$ dates (BP) | Lab nr | Tree nr (Fig. 2) | References |
|---|---|---|---|---|---|---|---|---|
| Buëch | Buëch aval | roi | Torrent des Rois | | 8260 ±190 | Gif-2217 | 27 | Gidon et al. (1991) |
| | La Véragne | barb | Les Barbiers | Fewer than 10 trees | 9250 ±190 | Ly-555 | 11 | Gidon et al. (1991) |
| | | mar | Le Mardaric | | 10,750 ± 250 | Gif-2216 | 7 | Gidon et al. (1991) |
| | | | | | 8500 ± 190 | Gif-2215 | 23 | Gidon et al. (1991) |
| Durance | Melve | melv | Sources Ponchon | | 8970 ± 210 | Gif-1139 | 14 | Gidon et al. (1991) |
| Sasse | Grand Vallon | saig | Saignon | More than 100 trees | 7320 ± 140 | Gif-3877 | 41 | Delibrias et al.(1984) |
| | | | | | 7520 ± 80 | A-8898 | 40 | Miramont (1998) |
| | | | | | 7800 ± 70 | A-9721 | 37 | Miramont (1998) |
| | | | | | 7805 ± 70 | A-8897 | 38 | Miramont (1998) |
| | | | | | 8230 ± 150 | Gif-3879 | 28 | Delibrias et al.(1984) |
| | | | | | 8275 + 65/–60 | A-9145 | 30 | Miramont (1998) |
| | | | | | 8335 ± 80 | A-8895 | 25 | Miramont (1998) |
| | | | | | 8460 ± 60 | A-8896 | 24 | Miramont (1998) |
| | | | | | 8650 + 60/–55 | A-9444 | 20 | Miramont (1998) |
| | | | | | 8650 ± 75 | A-9723 | 19 | Miramont (1998) |
| | | | | | 8725 ± 80 | A-9722 | 17 | Miramont (1998) |
| | | | | | 8765 ± 65 | A-8894 | 18 | Miramont (1998) |
| | | | | | 9090 ± 65 | AA-9445 | 12 | Miramont (1998) |
| | | | | | 9135 + 90/–85 | A-9144 | 13 | Miramont (1998) |
| | | | | | 11,180 ± 90 | A-9724 | 5 | Miramont (1998) |
| Bléone | Bouinenc | drai | Draix | Fewer than 10 trees | 8640 ± 70 | Gif-9917 | 21 | Ballais (1996) |
| | | | | | 8010 ± 80 | Gif-9918 | 32 | Ballais (1996) |
| | | | | | 7950 ± 160 | LGQ-996 | 34 | Ballais (1996) |
| | | | | | 6570 ± 190 | LGQ-995 | 47 | Ballais (1996) |
| Ubaye | La Valette | val | | More than 10 trees | 8290 ± 150 | LGQ-420 | 26 | Jorda, unpublished |
| | | | | | 7810 ± 140 | LGQ-421 | 35 | Jorda, unpublished |
| | Torrent de Bourre | bou | | Fewer than 10 trees | 7711 ± 160 | LGQ-86 | 36 | Jorda, unpublished |
| | Pinatelle | pin | | Fewer than 10 trees | 6340 ± 140 | LGQ-426 | 48 | Jorda, unpublished |

**RESULTS**

An overview of the $^{14}C$ dates of the trees is shown in Figure 2. The trees are compared with the morphogenetic evolution of the river beds in which they were found, as described by Borel et al. (1984), Jorda (1980, 1985, 1993), Jorda and Rosique (1994), Rosique (1994, 1996), and Miramont (1998). The morphogenetic activity of the region's waterways during the first part of the late glacial period was characterized by a phase of major vertical incision. From the Allerød until the Atlantic periods, the tendency was sedimentary accumulation. Large embankments were therefore formed—some up to 20 m thick—and alluvial cones were deposited at the base of the slopes, lateral to the principal direction of flow (principal Holocene filling; Jorda 1980, 1993). All of the trees (except nr 2) are buried in these embankments. There are two distinct groups of dates. The first group, consisting of 10 dates, belongs to the second part of the late glacial period; the Allerød and Younger Dryas. The second group, consisting of 39 dates, ranges from the end of the Preboreal to the beginning of the Atlantic period. This division into two groups is explained by a lower rate of sedimentation and a shift to incision during the Preboreal. This trend was obviously unfavorable for further burial of the pines. During the Boreal and the Atlantic, the rate of sedimentation was higher. After the Atlantic, the waterways once again began a period of vertical incision. This was again unfavorable for burial and conservation. Encased in the principal Holocene embankments are alluvial layers that date from the Subboreal and/or the Subatlantic, and in which only a few trees were found (nr 49 and 50 in Figure 2).

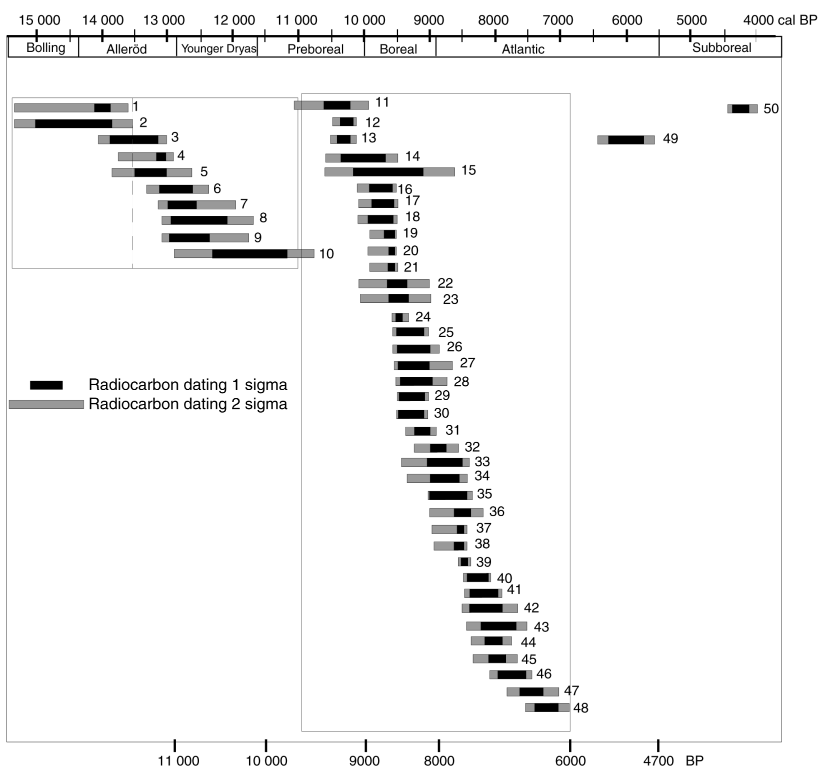


Figure 2 $^{14}C$ dates of Holocene subfossil trunks from the middle Durance basin. All the dates are calibrated with INTCAL98 (Stuiver et al. 1998). Most of the trees are buried in alluvial deposits during a time span from Allerød to Atlantic. For location and reference see Table 1 and Figure 1.

Two particularly important sites have recently been studied: Drouzet (Buëch basin; Rosique 1996; Sivan 1999) and Saignon (Sasse basin; Miramont 1998). These sites will be discussed in detail below.

### The Saignon Basin

The Saignon is a small basin of approximately 400 hectares (ha) within the larger Sasse drainage. It is dominated by calcareous marl ("terres noires"). The alluvial embankments are well developed and contain over 100 subfossil *pinus silvestris*. The trunks are found both at the bottom of the river beds and in higher strata. Geomorphological analysis of the deposits shows that they were buried by a rapid sequence of floods. This speed of burial explains the wood's remarkable conservation. The subfossil trunks are the remnants of adult forests. They were 100–300 years old.

Most of the trees were sampled for tree-ring analysis, except for some trunks because they were difficult to access, or were too badly preserved, or had fewer than 40 rings. We measured 57 different individual tree chronologies. Fifteen $^{14}$C dates were obtained (two of which are from previous studies [Delibrias et al. 1984]): they range from the Allerød to the Atlantic. These $^{14}$C dates and the geomorphological analysis of the site (stratigraphic analysis, proximity of rooted trees) permitted the identification of four distinct groups of sub-contemporaneus rooted trees (80 trees are included in these four groups, 20 trees cannot be associated with one of them). In these groups, 47 individual tree chronologies were computed. Synchronization reveals three distinct average chronologies comprising 34 of the 47 individual tree chronologies. These average chronologies, as well as typical growth curves are shown in Figure 3; the four groups are shown in Figure 4.

Group 1 includes at least two trees. $^{14}$C dating gave an age of 11,180 ± 90 BP. Two individual tree chronologies were computed but they cannot be synchronized.

Group 2 includes at least 27 trees. $^{14}$C dating gave ages of 9090 ± 65 BP and 9135 ±85 BP. Thirteen individual tree-ring chronologies were computed, nine of them were synchronized (MC 2; Figure 3).

Group 3 includes at least 34 trees. $^{14}$C dating gave the following ages: 8725 ± 80, 8765 ± 65, 8650 ± 75, 8650 ± 55, 8460 ± 60, 8335 ± 80, 8275 ± 65, and 8230 ± 65 BP. Twenty-one individual tree chronologies were computed. Fourteen tree-ring curves were synchronized (MC 3b, Figure 3). Two sub-groups (3A and 3B [Figure 4]) are distinct, wherein the trees belong to different alluvial layers.

Group 4 includes at least 17 trees. $^{14}$C dating gave the following ages: 7800 ± 70, 7805 ± 80, 7520 ± 80, and 7320 ± 140 BP. Eleven individual tree chronologies were computed. Eight tree-ring curves were synchronized (MC4; Figure 3).

Two-thirds of the individual chronologies show similar characteristics, namely a rapid reduction in growth, followed by a period with very little growth leading to the death of the trees (Figure 3). This points to rapid changes in the biotope conditions. These changes likely have a causative relation with the burial of the trees and the changing sedimentation of the period. Similar growth anomalies have been observed with subfossil trees smothered by rising water levels (Edouard 1994; Visset et al. 1994; Kaiser 1987; Munaut and Casparie 1971).

### The Drouzet Basin

The Drouzet, a tributary that joins the Petit Buëch on its left bank, runs in a valley carved from Superior Jurassic limestone (marno-calcareous). It is on the northwest side of the Ceüse-Aujour basin.

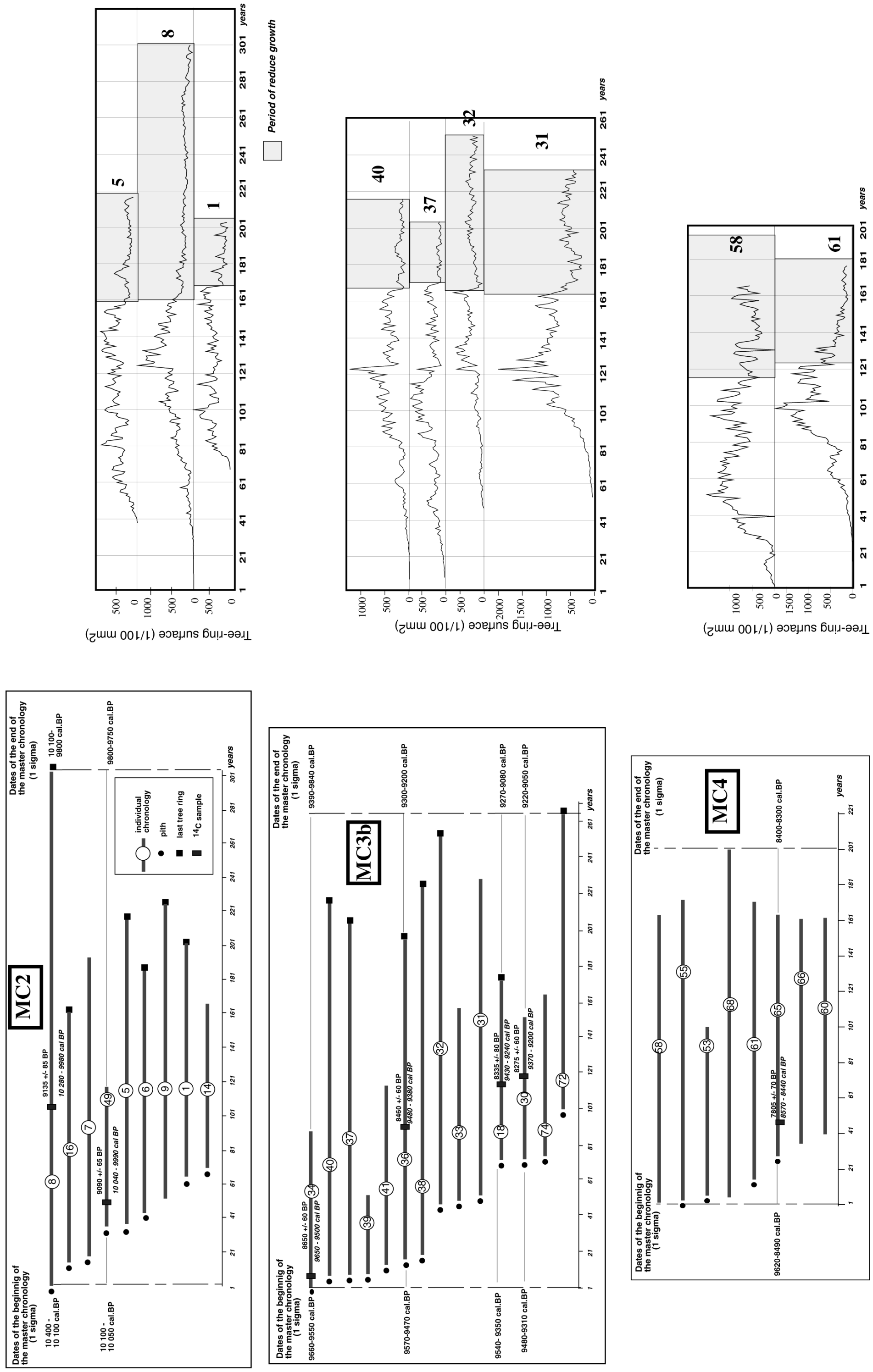


Figure 3 Left: master chronologies (MC) of Saignon subfossil trees. Right: growth curves (expressed in tree-ring surface) selected as examples from the three average chronologies

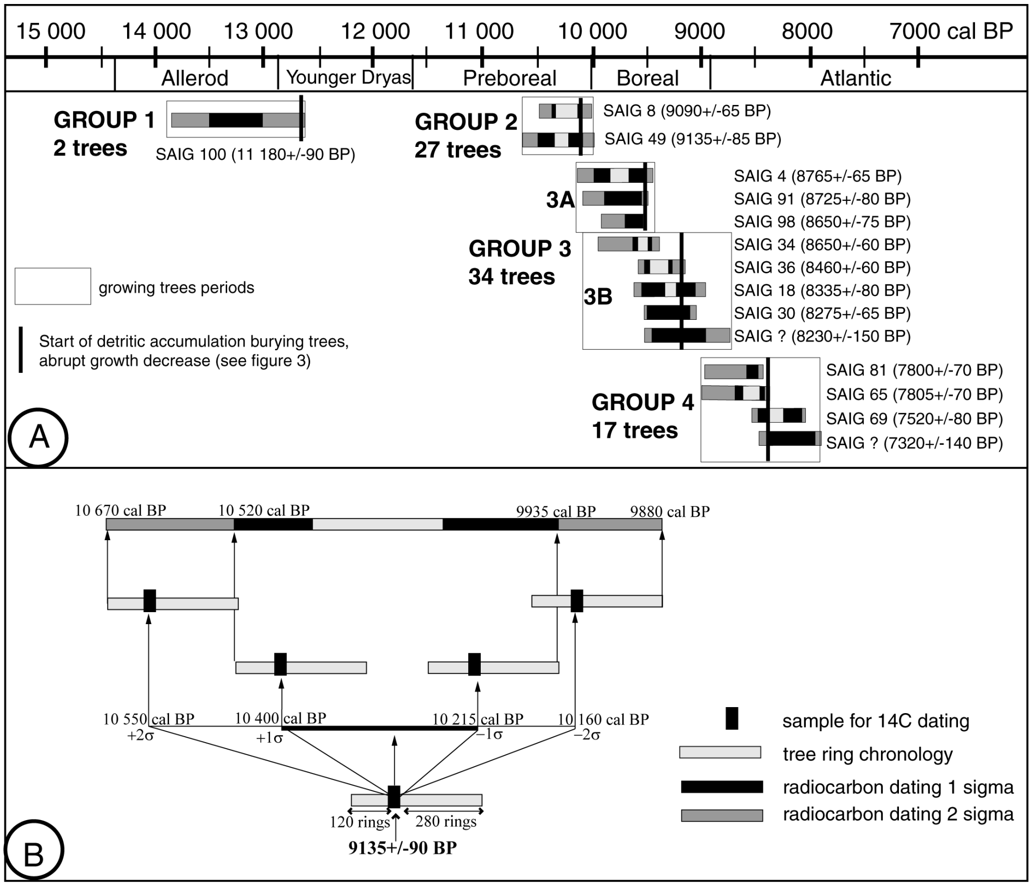


Figure 4 A: $^{14}$C dating of Saignon subfossil trunks. Groups are determined by geomorphological and stratigraphic analyses and radiocarbon dates. B: method to represent $^{14}$C dates. All the dates are calibrated with INTCAL98 (Stuiver et al. 1998).

Downstream, the river revealed a deposit of some 20 trees buried in a black clay alluvial embankment 10 m thick. One specimen has been dated from the Allerød (11,975 ± 115 BP; DROU 3; Figure 5). This is similar to two dates of specimens from tributaries to the Buëch, one from the Rue stream (Delibrias et al. 1984), and one from the Bachassette (Rosique 1996).

Upstream, the Drouzet is fed by the Charanc stream, which drains a small, steep basin of some 20 hectares. Like the Saignon, this basin is carved from Jurassic "black marls".

The deposits which constitute the "principal Holocene filling" form a glacis-terrace perched at a relative height of 20 m upstream, and 6 m downstream. More than 50 subfossil trees have been counted there. They are randomly buried in alluvial or gravelly layers. Other trunks are buried in the main embankment. Trees without roots are more frequent than in the Saignon basin. This is probably an indication for a more vigourous morphogenetic activity caused by the steepness of the basin.

The radiocarbon dates place the trees in the Boreal and Atlantic periods. They are almost contemporary to those obtained in the Saignon (Figure 5). Nine individual chronologies, with 20–300 rings, were measured (6 in the Charanc and 3 from the lower Drouzet). Some of them (like some from the

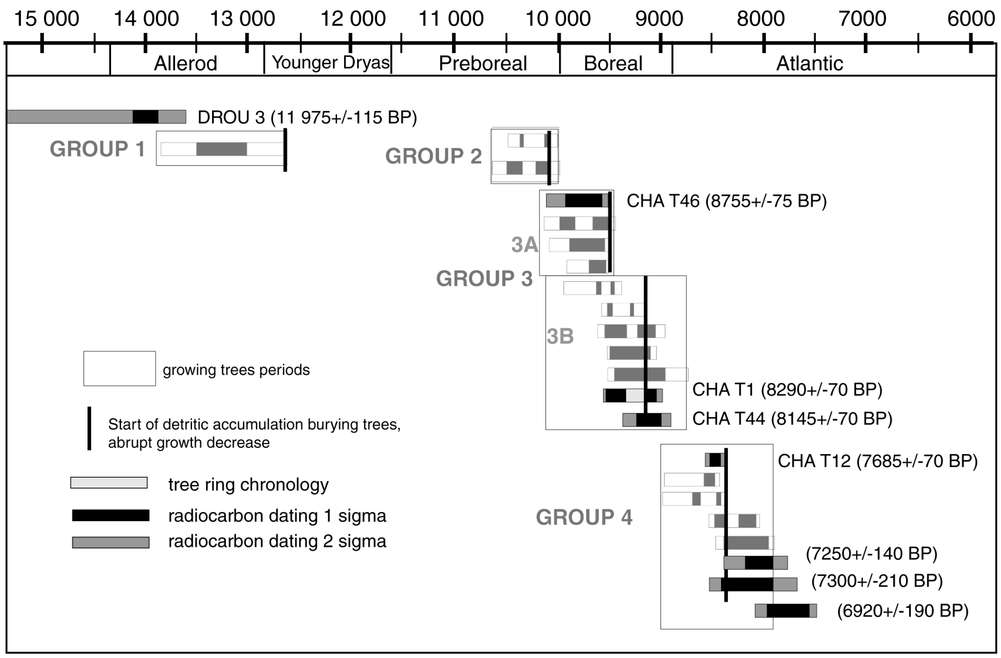


Figure 5 $^{14}$C dates of Drouzet subfossil trunks and Saignon subfossil trunks (in gray). All the dates are calibrated with INTCAL98 (Stuiver et al. 1998). The dates in the Drouzet basin are from the same time interval as those from the Saignon. This suggests that tree growing periods are simultaneous in the two basins.

Saignon basin) reflect important growth anomalies (Figure 6). The others have extremely thin growth rings (sometimes less than 0.5 mm) which suggest difficult biotope conditions. Unfortunately, it has not yet been possible to synchronize the ring chronologies from the Charanc with those from the Saignon.

## DISCUSSION

The presence, in the Middle Durance basins, of trees buried in alluvial Holocene layers demonstrates the succession of two types of dynamic morphology between the Allerød and the Atlantic periods. This is illustrated in Figure 7. One type was a period of stability or/and river bed incision which was favorable for the growth of the pine trees. This stability is due to a reduction in the detrital flow as well as more regular hydrous flow. The second type of morphogenesis was a period of floodplain accretion resulting in the accumulation of alluvial deposits. They were responsible for the burial of the pines and likely also explain the growth accidents observed in the ring chronologies.

The dates obtained from the Drouzet and Charanc basins are from the same time interval as those from the Saignon. This contemporaneity suggests a common cause, probably a climatic variation.

The nature of the deposits reveal a seasonal or annual flooding for many centuries. The geomorphological changes in the different basins are commensurate with climatic variations, notably an increase in the frequency and intensity of precipitation. These climatic crises in Haute Provence occurred at the same time as a general increase in humidity in Basse Provence (Bruneton et al. 2000). These results fit well with recent hypotheses on the paleoclimatic evolution of the first part of the Holocene (Alley et al. 1997; Magny 1995, 1997). This interpretation still has to be confirmed by further study of subfossil tree sites in the Middle Durance region.

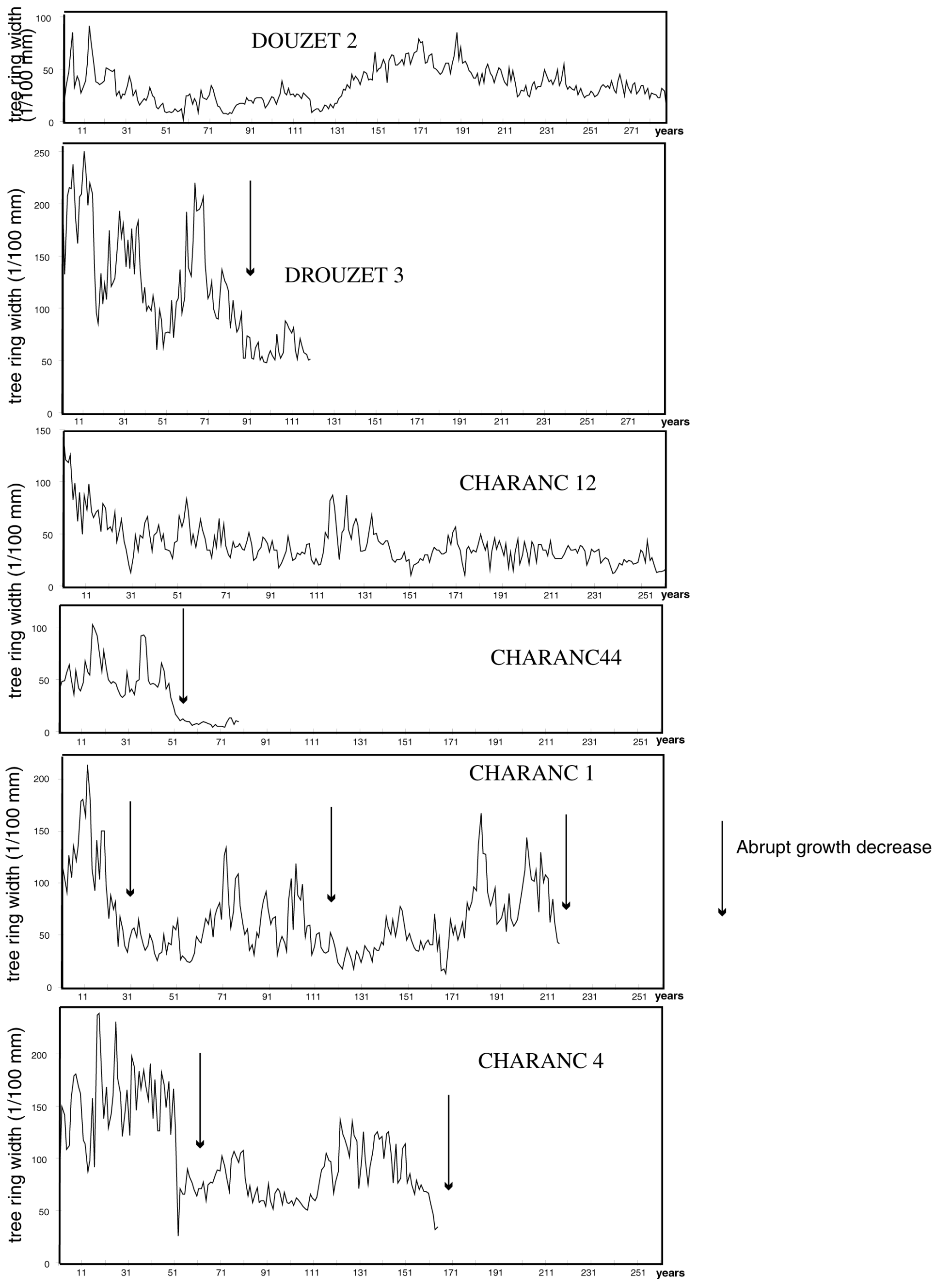


Figure 6 Examples of tree-ring curves of Drouzet basin. An abrupt decrease in growth is observed, as in the Saignon basin, due to accumulation of alluvial deposits.

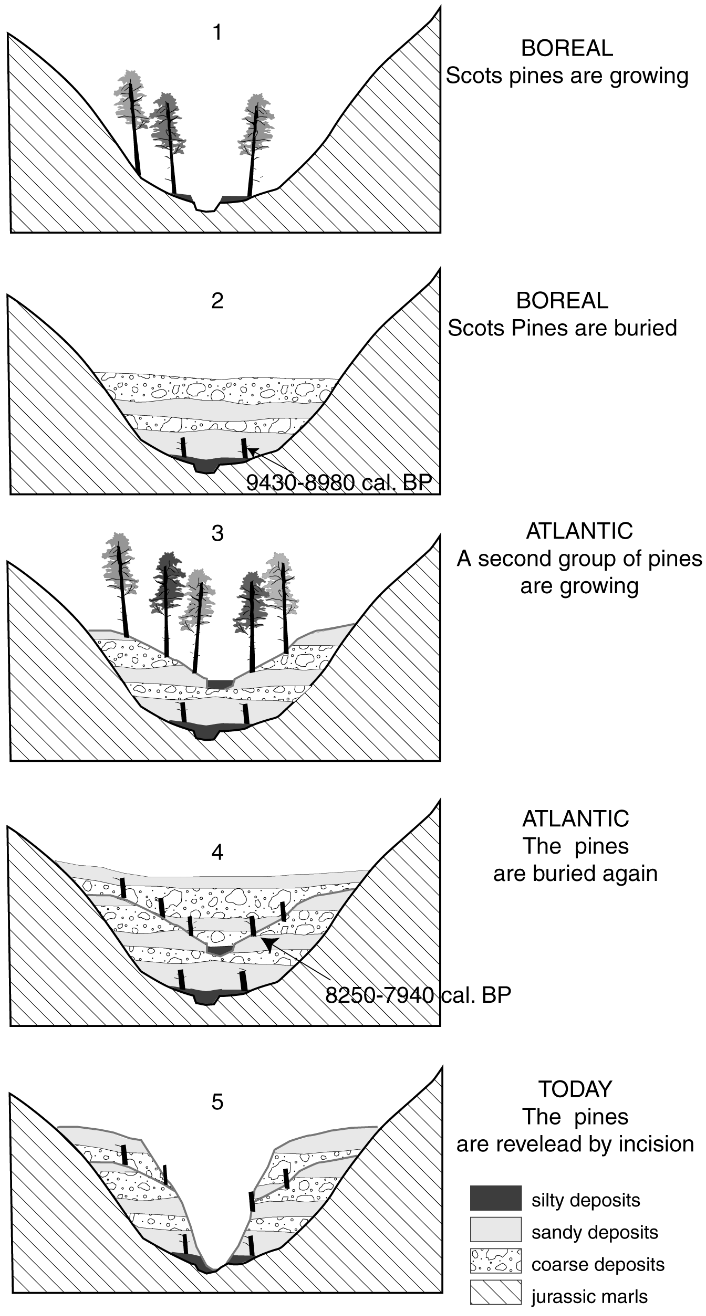


Figure 7 Schematic view, showing geomorphological changes in the Saignon valley

These tree deposits have important potential in terms of the study of paleoenvironments and especially in terms of the eventual possibility of obtaining good average chronologies for the Allerød and the Younger Dryas, for which there are only a few known subfossil trees (Becker 1993; Stuiver et al. 1998). The dendochronological analysis of these trees could permit the extension of the calibration curve of the $^{14}$C scale.

In addition, the Middle Durance floating chronologies, due to their annual resolution, can provide high resolution information about temporal changes in atmospheric $^{14}$C levels (Kromer et al. 1998), notably for the study of "the wiggles" during the end of the Late Glacial. This raises the question of the relation between the $^{14}$C variations and the climatic fluctuations experienced by the trees. The burial level of the trees permits the sedimentary and erosive events caused by climatic fluctuations to be dated, enabling the correlation with the atmospheric $^{14}$C levels as recorded in the wood.

## CONCLUSION

The Middle Durance (Southern Alps, France) basin contains many subfossil tree deposits that supply floating chronologies dated between the Allerød and the Atlantic. The dendrogeomorphological study of the sites permits us to relate the morphogenic crises of the region with episodes of inclement weather. More even than their present significance, we would like to point out the potential that these sites have. We hope, as Kromer et al. (1998), that these sections, combined with others, will ultimately help in the reconstruction of the Late Glacial and early Holocene $^{14}$C pattern.

## ACKNOWLEDGMENTS

We are grateful to J van der Plicht and J Evin for information and advice. We also express thanks to D Ronah for translation and to P Pench for design. This work was financed by the Region and the Réserve Géologique de Haute Provence.

## REFERENCES

Alley RB, Mayewski PA, Sowers T, Stuiver M, Taylor KC, Clark PU. 1997. Holocene climatic instability—a prominent widespride event 8200 yr ago. *Geology* 25:483–6.

Archambault M. 1967. Découverte des restes d'une formation forestière fossile entre deux nappes colluviales quaternaires. *Comptes Rendus de l'Académie des Sciences* 265:104–7.

Archambault M. 1968. Recensement provisoire des arbres et des formations forestières fossiles du bassin de la Moyenne Durance (Hautes Alpes). *Comptes Rendus de l'Académie des Sciences* 267:101–2104, 2284–7.

Archambault M. 1969. Faits et points de vue nouveaux sur les glacis d'érosion (exemple du bassin de la Moyenne Durance alpestre). *Bulletin de l'Association de Géographes Français* 375/376:525–37.

Ballais JL. 1996. L'âge de modelé de roubines dans les Préalpes du Sud: l'exemple de la région de Digne. *Géomorphologie: Relief, Processus et Environment* 4: 61–8.

Becker B. 1993. An 11,000-year German oak and pine dendrochronology for radiocarbon calibration. *Radiocarbon* 35(1):201–13.

Borel JL, Jorda M, Montjument G. 1984. Variations climatiques, morphogénèse et évolution de la végétation post-würmiennes dans les Alpes françaises. *Les Alpes, 25e Congrès International de Géographie*, *Paris.* p 43–53.

Bruneton H, Miramont C, Andrieu V. 2000. Dynamique de milieux méditerranéens (bassin du Saignon, Alpes du Sud, marais des Baux, Basse Provence) au cours du Mésolithique: un enregistrement morphosédimentaire des rythmes climatiques. In: *Epipaléolithique et Mésolithique: les derniers chasseurs-cueilleurs d'Europe occidentale.* Actes du Colloque international, Besançon, Octobre 1998. Paris: Les Belles Lettres. Annales de l'universile de Franche Comté, PUFC, 70-82.

Delibrias G, Gabert J, Jorda M, 1984. Données nouvelles sur la chronostratigraphie et l'évolution paléomorphologique postglaciaire des Alpes du Sud (Moyenne Durance). *Comptes Rendus de l'Académie des Sciences* 299 (II):263–6.

Edouard JL. 1994. Les lacs d'altitude dans les Alpes françaises. Contribution à la connaissance des lacs d'altitude et à l'histoire des milieux montagnards depuis la fin du Tardiglaciaire. Thèse de Doctorat de Géographie, Université Joseph Fourier, Grenoble I. 795 p.

Gautier E. 1992. Recherches sur la morphologie et la dynamique fluviales dans le bassin du Buech (Alpes du Sud). Thèse de géographie, Université de Paris-X-Nanterre. 439 p.

Gidon M, Montjuvent G, Flandrin J, Moullade M, Durozoy G, Damiani L. 1991. Notice explicative de la carte géologique de la France au 1/50000, feuille de Laragne-Montéglin (893). BRGM, Orléans. 84 p.

Jorda M. 1980. Morphogenèse et évolution des paysages dans les Alpes de Haute-Provence depuis le Tardiglaciaire. Facteurs naturels et facteurs anthropiques. *Bulletin de l'Association de Géographes Français* 472: 295–304.

Jorda M. 1985. La torrentialité holocène des Alpes françaises du sud. Facteurs anthropiques et paramètres naturels de son évolution. Symposium International: les modifications de l'environnement dans le bassin méditerranéen occidental à la fin du Pléistocène et pendant l'Holocène. Toulouse. *Cahiers Ligures de la Préhistoire*, H.S. 2:49–70.

Jorda M. 1993. Histoire des paléoenvironnements tardi- et post-glaciaires de moyenne altitude. Essai de reconstitution cinématique. *Géomorphologie et aménagement de la montagne, Hommage à P. Gabert.* Caen: CNRS. p 91–111.

Jorda M, Rosique T. 1994. Le Tardiglaciaire des Alpes françaises du Sud. Rythmes et modalités des changements bio-morphoclimatiques. *Bulletin de l'Association Française pour l'Etude du Quaternaire* 3/4:141–9.

Kaiser NFJ. 1987. Late Glacial reforestation in the Swiss Mitteland and in Wisconsin illustrated by the Daettnau and the Two Creeks buried forests. *Proceedings of the International Symposium on Ecological Aspects of Tree-Ring Analysis*. New-York, 17–21 August 1986. p 291–7.

Kromer B, Spurk M, Remmele S, Barbetti M, Toniello V. 1998. Segments of atmospheric $^{14}C$ change as derived from late glacial and early holocene floating tree-ring series. *Radiocarbon* 40(1):351–8.

Magny M. 1995. *Une histoire du climat. Des derniers mammouths au siècle de l'automobile*. Paris: Errance. 175 p.

Magny M. 1997. Eléments pour une histoire du climat entre 13000 et 6000 BP. *Bulletin de la société préhistorique française* 94(2):161–7.

Miramont C. 1998. Morphogenèse, activité érosive et détritisme alluvial holocènes dans le bassin de la Moyenne Durance. Thèse de Géographie, Université d'Aix-Marseille I. 287 p.

Munaut AV, Casparie WA. 1971. Etude dendrochronologique des *Pinus silvestris* subfossiles provenant de la tourbière d'Emmen (Drenthe, Pays-bas). *Revue Paléobotanique et Palynologie* 11:201–26.

Rosique T. 1994. Les gisements de bois fossiles conservés dans les formations détritiques tardi- et postglaciaires du bassin du Buëch (Hautes Alpes): interprétation géodynamique et paléoécologique. *Comptes Rendus de l'Académie des Sciences* 319(II):373–80.

Rosique T. 1996. Morphogenèse et évolution des paléoenvironnements alpins de la fin des temps glaciaires au début de l'Holocène: l'exemple de la Moyenne Durance (Alpes françaises du Sud). Thèse de doctorat de Géographie, Université d'Aix-Marseille I. 288 p.

Sivan O. 1999. Etude morphosédimentaire et dendrogéomorphologique des remblaiements holocènes à troncs subfossiles. Exemple de la région de Veynes (vallée du Buëch). *Mémoire de D.E.A. de Géographie*. Université d'Aix-Marseille I. 102 p.

Stuiver M, Reimer PJ, Bard E, Beck JW, Burr GS, Hughen KA, Kromer B, McCormac G, van der Plicht J, Spurk M. 1998. INTCAL98 radiocarbon age calibration, 24,000–0 cal BP. *Radiocarbon* 40(3):1041–83.

Visset L, Girardclos O, Lambert GN. 1994. La forêt de chênes sur tourbe, à l'île d'Errand, dans les marais de Brière (Massif armoricain, France). *Quaternaire* 5(2): 69–77.

RADIOCARBON, Vol 42, Nr 3, 2000, p 437–452 

# RADIOCARBON LEVELS IN THE ICELAND SEA FROM 25–53 KYR AND THEIR LINK TO THE EARTH'S MAGNETIC FIELD INTENSITY

Antje H L Voelker[1,2] • Pieter M Grootes[1] • Marie-Josee Nadeau[1] • Michael Sarnthein[3]

**ABSTRACT.** By correlating the climate records and radiocarbon ages of the planktonic foraminifera *N. pachyderma*(s) of deep-sea core PS2644 from the Iceland Sea with the annual-layer chronology of the GISP2 ice core, we obtained 80 marine $^{14}C$ calibration points for the interval 11.4–53.3 ka cal BP. Between 27 and 54 ka cal BP the continuous record of $^{14}C$/cal age differences reveals three intervals of highly increased $^{14}C$ concentrations coincident with low values of paleomagnetic field intensity, two of which are attributed to the geomagnetic Mono Lake and Laschamp excursions (33.5–34.5 ka cal BP with maximum 550‰ marine $\Delta^{14}C$, and 40.3–41.7 ka cal BP with maximum 1215‰ marine $\Delta^{14}C$, respectively). A third maximum (marine $\Delta^{14}C$: 755‰) is observed around 38 ka cal BP and attributed to the geomagnetic intensity minimum following the Laschamp excursion. During all three events the $\Delta^{14}C$ values increase rapidly with maximum values occurring at the end of the respective geomagnetic intensity minimum. During the Mono Lake Event, however, our $\Delta^{14}C$ values seem to underestimate the atmospheric level, if compared to the $^{36}Cl$ flux measured in the GRIP ice core (Wagner et al. 2000) and other records. As this excursion coincides with a meltwater event in core PS2644, the underestimation is probably caused by an increased planktonic reservoir age. The same effect also occurs from 38.5 to 40 ka cal BP when the meltwater lid of Heinrich Event 4 affected the planktonic record.

## INTRODUCTION

Radiocarbon ages have been calibrated in great detail up to 13.3 ka BP by dendro- and varve chronology with an extension based on single calibration points on corals and less precise varves up to 20 ka BP (Stuiver et al. 1998; Bard et al. 1998; Hughen et al. 1998). Beyond 20 ka BP, calibration is still problematic because dendrochronological calibration points are so far not available and single calibration points (Vogel 1983; Bischoff et al. 1994; Vogel and Kronfeld 1997; Bard et al. 1998; Geyh and Schlüchter 1998; Schramm et al. 2000) often lack the needed temporal resolution. A time scale for $^{14}C$ ages older than 14 ka BP can be provided by marine or lacustrine varves (e.g. Kitagawa and van der Plicht 1998a, 1998b) or indirectly by the annual-layer chronology of the GISP2 ice core (e.g. Voelker et al. 1998). Calibration data from marine sediment core PS2644 from the western Iceland Sea (67°52.02′N, 21°45.92′W, 777 m water depth; Figure 1) for the interval 20–55 ka cal BP reveal periods with significantly increased atmospheric $^{14}C$ concentrations, expressed as $\Delta^{14}C$, the relative deviation from the modern standard $^{14}C$ concentration in per mil, during minima in the earth's geomagnetic field intensity (Voelker et al. 1998; Voelker 1999). Increased $^{14}C$ production is corroborated by coinciding peaks in $^{10}Be$ and $^{36}Cl$ in the Greenland ice cores (Yiou et al. 1997; Baumgartner et al. 1997, 1998). We report here further data increasing the temporal resolution of the changes in marine $^{14}C$ ages during the Laschamp and Mono Lake excursions and a refinement of the correlation with the GISP2 time scale. A stacked record of the geomagnetic field intensity (NAPIS-75; Laj et al. 2000), including the magnetic data of core PS2644, permits us a direct comparison of our $\Delta^{14}C$ fluctuations with changes in the geomagnetic field intensity.

Marine sediment core PS2644 yielded a high resolution climate record showing millennial-scale oscillations (Voelker et al. 1998; Voelker 1999). By correlating the marine climate signals, especially the planktonic $\delta^{18}O$ and $\delta^{13}C$ records, with the Dansgaard-Oeschger cycles in the GISP2 $\delta^{18}O$ record we are able to calibrate the marine $^{14}C$ ages with the annual-layer GISP2 chronology (Meese et al. 1994, 1997; Bender et al. 1994). Here we assume fluctuations in the temperature on Greenland

[1]Leibniz–Labor für Altersbestimmung und Isotopenforschung, Universität Kiel, Max-Eyth Strasse 11-13, D-24118 Kiel, Germany
[2]Email: antje@sfb313.uni-kiel.de
[3]Institut für Geowissenschaften, Universität Kiel, Olshausenstrasse 40, D-24118 Kiel, Germany

are linked to changes in the hydrography at site PS2644 via the thermohaline circulation (THC) of the North Atlantic. As moisture for the precipitation on Greenland mainly originates from the North Atlantic (Johnsen et al. 1989; Charles et al. 1994; Jouzel et al. 1997), the snow's oxygen isotope ratio should monitor changes in the Sea Surface Temperature (SST) of the major North Atlantic warm water current, the Gulfstream/North Atlantic drift and its branches (e.g. Schmitz and McCartney 1993). One of these branches, the Irminger current, flows partly across the Denmark Strait into the Iceland Sea, and influences site PS2644 (Figure 1). The hydrography at this site is furthermore affected by the polar East Greenland current and its branches (Voelker et al. 1998), which also is part of the North Atlantic THC.

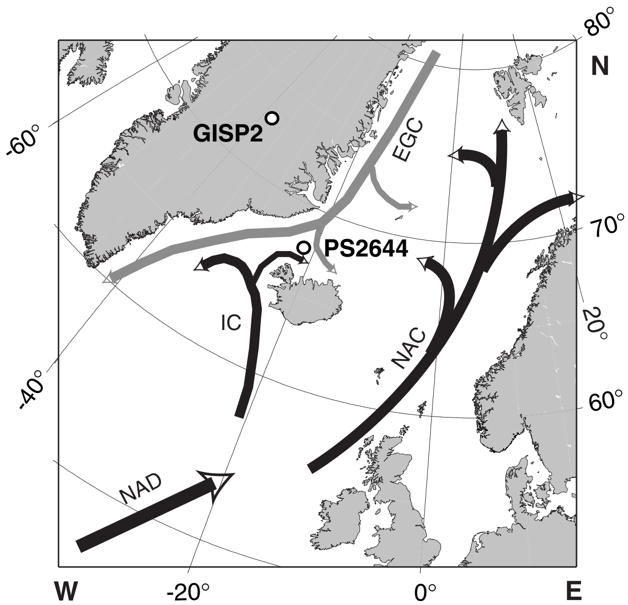


Figure 1 Map of the North Atlantic with the position of sediment core PS2644 in the western Iceland Sea and of ice core GISP2 on Greenland. Arrows mark present axis of the major surface water currents with black ones transporting warm and saline Atlantic water and gray ones fresh and cold polar water (EGC: East Greenland Current; IC: Irminger Current; NAC: Norwegian Atlantic Current; NAD: North Atlantic Drift).

## METHODS

The sediment record of core PS2644 was sampled with a resolution of 1 cm, equal to a mean time resolution of 50 yr during marine isotope stage 3 (29–58 ka cal BP) (Voelker et al. 1998). The stable isotope ratios $^{18}O/^{16}O$ and $^{13}C/^{12}C$ were measured on the planktonic foraminifera *N. pachyderma*(s) in the Leibniz Labor at Kiel University, Germany, using an automated MAT–251 mass spectrometer with carbonate system (analytical reproducibility: ±0.07‰ for $\delta^{18}O$, ±0.04‰ for $\delta^{13}C$, Sarnthein et al. 1995; Voelker et al. 1998). Paleoceanographic conditions and climate were reconstructed from a suite of sediment properties including faunal assemblages, stable isotopes, lithology and the abundance of ice rafted detritus (IRD) indicated by lithic grains >150 µm which includes the volcanic ash grains, although some were probably wind transported (Voelker 1999; data at http://www.pangaea.de). The AMS $^{14}C$ ages were measured on 10-mg samples of either the planktonic foraminifera

*N. pachyderma*(s) or the epibenthic foraminifera *Cibicides* sp. (for details see Voelker et al. 1998) at the Leibniz Labor at Kiel University. Careful cleaning and sample preparation (Schleicher et al. 1998; Nadeau et al. forthcoming) and the use of *N. pachyderma*(s) samples from marine isotope stage 5.1 of core PS2644 for background correction (Voelker et al. 1998; Voelker 1999) allowed dating of the record up to 55 ka BP. Age differences are calculated by subtracting the $^{14}C$ age not corrected for a reservoir effect from the corresponding GISP2 calendar age, alternatively, the relative deviation of the original $^{14}C$ concentration. $\Delta^{14}C$ in per mil, also based on the uncorrected $^{14}C$ ages, is referred to as "marine $\Delta^{14}C$" to clearly distinguish it from the generally used atmospheric $\Delta^{14}C$.

The $\delta^{18}O_{ice}$ of the GISP2 ice core, calibrated to VSMOW, was measured in the Quaternary Isotope Laboratory in Seattle (USA) (Grootes et al. 1993; Grootes and Stuiver 1997; Stuiver and Grootes 2000). Here we use the bidecadal data set which is based on the 20-cm resolution record (equal to an average time resolution of 12 yr during interstadials and 30 yr during stadials; Stuiver and Grootes [2000]; data available from http://depts.washington.edu/qil/datasets/gisp2_main.html).

### Correlation with the GISP2 Isotope Record

Since cores PS2644 and GISP2 both monitor changes in the thermohaline circulation of the North Atlantic, the best way to correlate them would be via a sea surface temperature record (e.g. Sachs and Lehman 1999; van Kreveld et al. 2000). Unfortunately, the diversity in the planktonic foraminifera fauna in core PS2644 in the northern North Atlantic is so small (*N. pachyderma*(s) >95%) that they can only be used as qualitative SST indicator (Voelker et al. 1998) forcing us to use the planktonic isotope record instead. This shows light $\delta^{18}O$ and $\delta^{13}C$ values together with high IRD contents (Figure 2) during cold SST's in the North Atlantic and cold temperatures above Greenland contemporary with meltwater events (Bond et al. 1993; Rasmussen et al. 1996; van Kreveld et al. 2000). The response of precipitation on Greenland to changes in the THC in the northern North Atlantic is immediate as both are connected by the atmospheric circulation. At site PS2644, an "overshooting" SST upon warming is caused by the resumed inflow of warm Atlantic water via the Irminger Current as evidenced by lower percentages of *N. pachyderma*(s) and by high abundances of (Atlantic) radiolaria and diatoms (Voelker et al. 1998; Voelker 1999; Lein 1998). Meltwater lids, on the other hand, hampered the heat transport to the north and induced a sea ice cover during at least part of the year (Sarnthein et al. 1995; Seidov et al. 1996; Cortijo et al. 1997; Voelker 1999).

The detailed tuning of the marine and the ice core followed this hierarchy: Four tephra layers (1) build a stable time frame for the correlation of the Heinrich meltwater events 1–6 (2), other meltwater events contemporary with an increased IRD content (3), and the beginning of the interstadials (4). Further tie points are based on "minor" meltwater events occurring during the interstadials (5), and finally small scale oscillations (6).

1. The tephras were identified in the sediment and the GISP2 or GRIP ice core on the base of their chemistry (Voelker 1999; Grönvold et al. 1995; Zielinski et al. 1997). While ash grains of the Saksunarvatn Ash (10,272 GISP2 cal yr) and the North Atlantic Ash Zone 2 (53,260 GISP2 cal yr) were directly detected in the GISP2 core, the ages of the Vedde Ash (12,095 GISP2 cal yr) and a Katla Ash (78,080 GISP2 cal yr), both detected only in GRIP, were obtained by matching the isotope records of both ice cores.
2. Following Bond et al. (1993) and Rasmussen et al. (1996), the Heinrich Events, the most prominent planktonic $\delta^{18}O$ minima in core PS2644 (Figure 2; Voelker et al. 1998), were related to the stadial phases preceding Dansgaard-Oeschger Events 1, 2, 4, 8, 12, and 17 in the same way as described in the next paragraph.

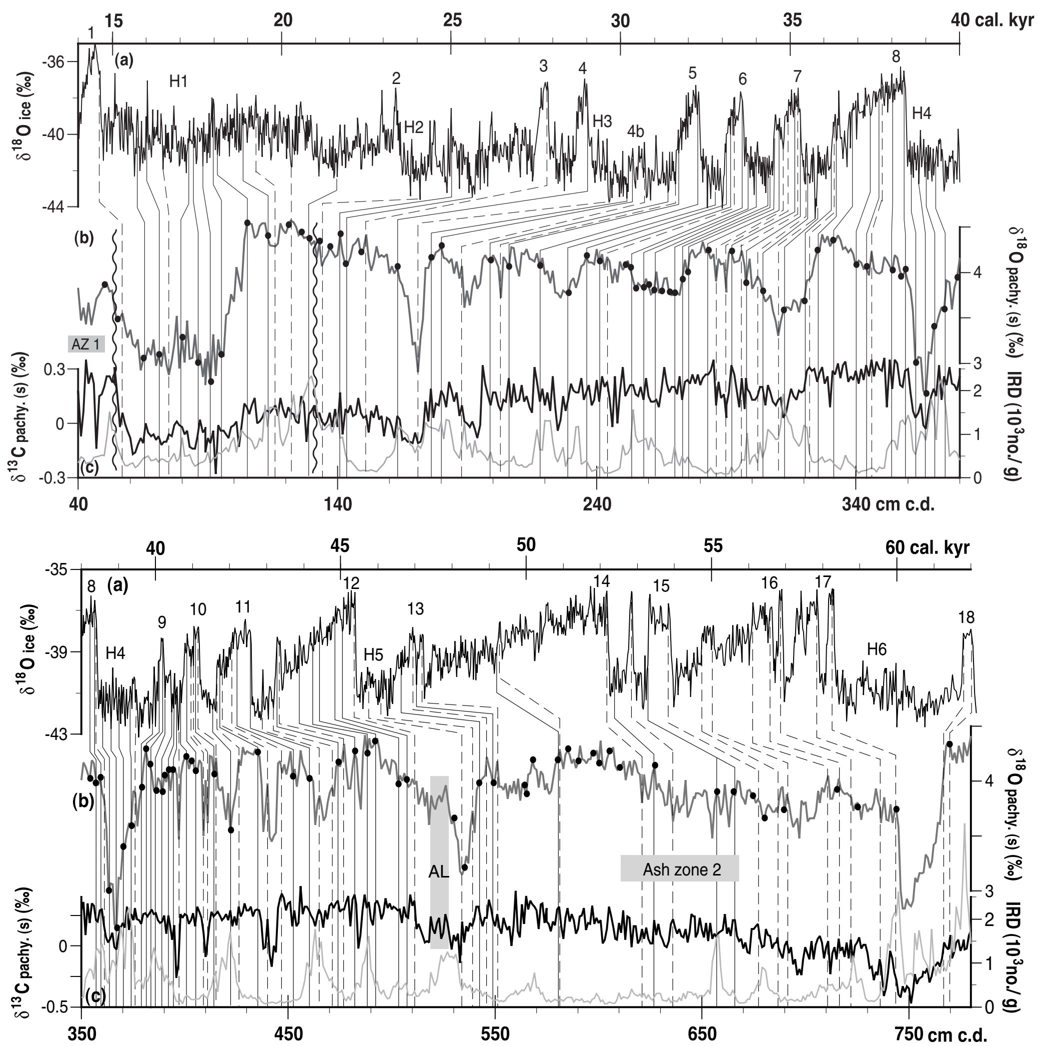


Figure 2 Correlation (vertical lines; dashed, if no calibration point) between planktonic $\delta^{18}$O (b; ‰ vs. VPDB), $\delta^{13}$C (c; black curve; ‰ vs. VPDB), and IRD (c; gray curve; nr. of lithic grains >150µm/g) records of sediment core PS2644 vs. composite depth (c.d.) and the bidecadal $\delta^{18}$O record of ice core GISP2 (a; ‰ vs. VSMOW; Stuiver and Grootes 2000). Numbers in (a) refer to Dansgaard-Oeschger Events 1–18 (Johnsen et al. 1992), H1–H6 to Heinrich Events 1–6. Black dots in (b) mark depths of $^{14}$C ages. (A): 14–40 ka BP; wavy line indicates hiatus (Voelker et al. 1998; Voelker 1999); AZ 1: North Atlantic Ash zone 1. (B): 38–62 ka BP; Ash zone 2: North Atlantic Ash zone 2; AL: ash layer.

3. Core PS2644 shows several other meltwater events which can be divided into two groups: those contemporary with an increased IRD content, and those without one (Figure 2). Following the feature of the Heinrich Events, we regard the meltwater events with IRD sedimentation north of the Denmark Strait to influence the climate basin-wide and thus tie them to the other stadial phases in the GISP2 $\delta^{18}$O record. Since it is difficult to define the first cold point of a stadial in the marine records, the preceding rapid temperature change at the interstadial/stadial transition, is used as anchor point instead. Thereby, we correlate the last heavy planktonic $\delta^{18}$O/$\delta^{13}$C value before an IRD-bearing meltwater event with the beginning of the abrupt temperature drop on

Greenland (Figure 2). Furthermore, the $\delta^{18}O$ minimum of a meltwater event is matched with the coldest (i.e. most negative) point prior to the rapid temperature rise in the GISP2 $\delta^{18}O$ record.

4. The stadial/interstadial transition is marked by a rapid temperature rise on Greenland and a rapid and contemporary increase in the planktonic $\delta^{18}O$/ $\delta^{13}C$ values in core PS2644. The heavy planktonic values indicate a well-ventilated upper ocean layer, ergo the disappearance of the meltwater lid, and are therefore related to the end of the temperature rise (Figure 2). At interstadial 12, this principle of correlation was slightly modified based on the assumption that the pronounced ash layer largely enhanced the sedimentation rate and thus influenced the climate signals (Figure 2B; Voelker 1999).
5. Like the IRD-bearing meltwater events tied to the stadials, the "no IRD" events, with a presumed lesser climatic impact, are related to temperature drops within an interstadial in the way that the heavy $\delta^{18}O/\delta^{13}C$ values prior to the meltwater event are linked to the last "warm" point preceding the drop, the planktonic $\delta^{18}O$ minimum to peak cold, and the heavy values following the meltwater event to the subsequent warming (Figure 2).
6. Finally, to calibrate almost all $^{14}C$ ages with corresponding GISP2 calendar ages we applied the rules of heavy planktonic isotope values indicating warmer, better climate conditions and light values colder temperatures also to small scale oscillations (Figure 2).

Our correlation was recently confirmed by the position of the short Mono Lake excursion in relation to the Dansgaard-Oeschger stadial/interstadial cycles within core PS2644 (stadial prior to Dansgaard-Oeschger Event 6; Figure 3). Wagner et al. (2000) observe an increased $^{36}Cl$ flux in the GRIP ice core which is attributed to the Mono Lake intensity minimum exactly at the same position. During the longer lasting Laschamp Event, our correlation also matches the peak fluxes of cosmogenic isotopes in the GRIP ice core (Yiou et al. 1997; Baumgartner et al. 1998) with the inclination swing in core PS2644 (Voelker et al. 1998).

### Limitations of the Calibration Data

The calibration data from core PS2644 are affected by three limiting factors (discussed below): uncertainty in the GISP2 calendar ages, smoothing by bioturbation, and changes in the reservoir age.

#### *GISP2 Time Scale*

The calendar ages used to calculate the $^{14}C$ deviations are based on the Meese/ Sowers time scale for the GISP2 ice core. Down to 50 ka cal BP, this time scale derives purely from annual-layer counting (Meese et al. 1994, 1997), while, beyond 50 ka cal BP, trace gas concentrations are used to correlate the Vostok chronology of Sowers et al. (1993) into the GISP2 ice core (Bender et al. 1994). The uncertainty on the time scale increases with depth and amounts to an estimated maximum ±2% up to 39,852 cal BP, maximum ±5–10% up to 44,583 cal BP and maximum ±10% up to 56,931 cal BP (Meese et al. 1997).

For the last 46 ka cal BP, i.e. the main part of our calibration curve, the validity of the GISP2 layer chronology is corroborated by the counted time scale of the nearby GRIP ice core (Hammer et al. 1997) and U/Th dates of coral terraces in Papua New Guinea (Chappell et al. 1996; Grootes and Stuiver 1997). In the older section, the GISP2 chronology might be too young as indicated by the U/Th age of the coral reef associated with Dansgaard-Oeschger interstadial 14, which is 1 ka older, and by other dates of the North Atlantic Ash Zone 2. The ignimbrite attributed to this ash zone was Ar/Ar dated with 55 ± 2 ka (Sigurdsson personal communication 1998), while the tephra is dated even older at 58.38 ka cal BP in the GRIP layer chronology (Hammer et al. 1997). However, since the different age determinations agree within the error bars, the GISP2 chronology is not wrong.

### *Bioturbation*

As in any oxygenated sediment record, bioturbation works as a low-pass filter and thus hampers a precise reconstruction of the $^{14}C$ production over time by dampening the response. In marine cores, the mixed layer depth partly depends on the flux of organic carbon ($C_{org}$) to the sea floor (Trauth et al. 1997 and references therein). Based on the low $C_{org}$-flux Trauth, Sarnthein and Arnold (1997) postulate bioturbation depths of around 2 cm for sediment cores in the northern Norwegian Sea. Using their approach and the $C_{org}$ accumulation rates of core PS2644 (average AR = 0.05 gC/ m$^2$ yr; Stein unpublished data), the average mixed layer depth would be even lower (<1 cm) in the western Iceland Sea. At an average sedimentation rate of 20 cm/ka during isotope stage 3, bioturbation would thus hardly dampen the record of $^{14}C$ production. Accordingly, from the view point of bioturbation/ mixing alone the response time in the ocean and the atmosphere would nearly be the same (50–100 yr in core PS2644 and 80 yr in the atmosphere). On the other hand, in isotope stage 2 where the sedimentation rates are much lower (Voelker 1999), a delay in the marine response of up to 250 yr might occur.

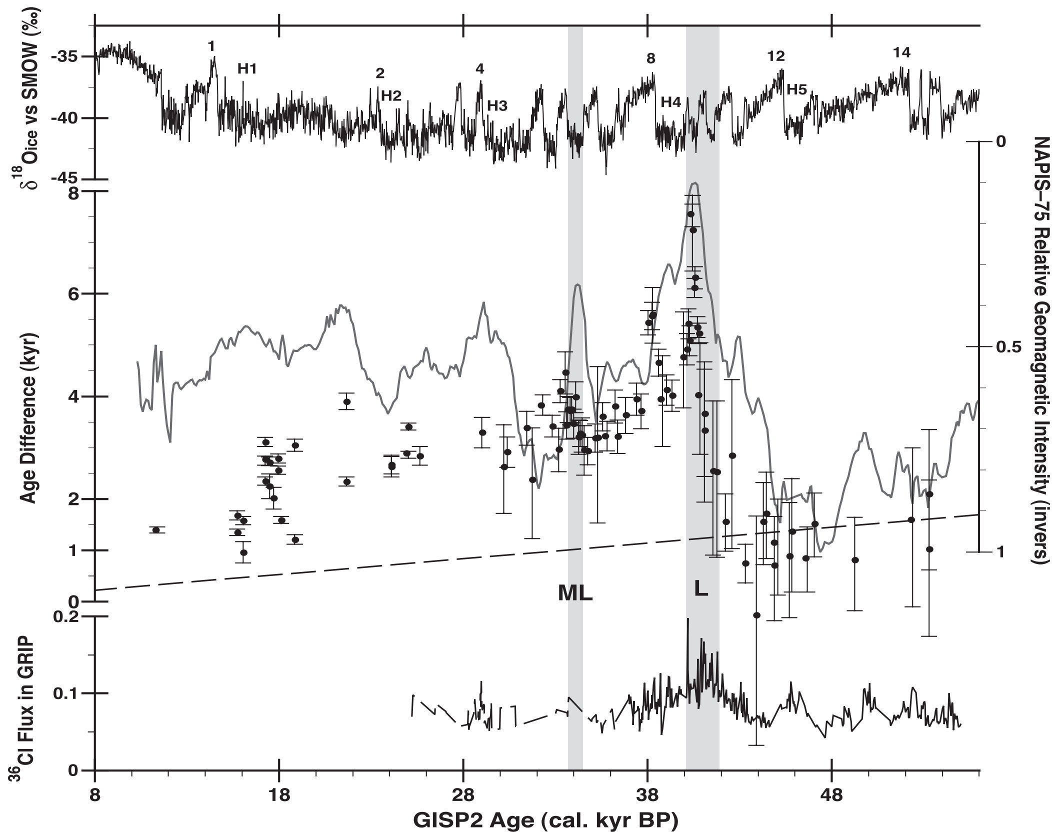


Figure 3 Age differences (± 1σ) between uncorrected $^{14}C$ (in Libby yr) and calendar ages on the GISP2 calendar age scale in comparison to the GISP2 $\delta^{18}O$ record (upper panel: major Dansgaard-Oeschger and Heinrich (H) events 1–6), the (inversed) NAPIS-75 stack of Laj et al. (2000; normalized to 1; gray), and the $^{36}Cl$ flux in GRIP (lower panel: Baumgartner et al. 1998; dashed line indicates lower resolution). The $^{36}Cl$ record, originally based on the Johnson time scale, was adjusted to the GISP2 time scale by adding 2580 years (fit of maximum flux to peak of Dansgaard-Oeschger Event 9). Dashed ascending line shows difference between conventional and physical $^{14}C$ ages. Gray bars indicate Mono Lake (ML) and Laschamp (L) excursions.

*Variation of the Reservoir Effect*

The temporal variation of the reservoir effect is hardly known for the northern North Atlantic—except for the Younger Dryas when it increased from 400 to 800–1100 yr (Bard et al. 1994; Haflidason et al. 1995). Based on atypical negative differences between benthic and planktonic $^{14}C$ ages from the same depth in core PS2644, Voelker et al. (1998) postulated fluctuating and increased reservoir ages for planktonic foraminifera in the western Iceland Sea during marine isotope stage 2. According to them, values for the planktonic reservoir age ranged between 630 and 1160 yr during Heinrich Event 1 (14.6–18.1 ka cal BP), rose up to 2240 yr during the last glacial maximum (LGM) and amounted to 950 yr around 25 ka cal BP. The large discrepancy between the benthic and planktonic reservoir age can be explained by the hydrographic conditions in the glacial Nordic Seas and the preferred living conditions of *N. pachyderma*(s). *N. pachyderma*(s) builds a second calcite crust, which contributes about 50% to the shell weight (Arikawa 1983), within or underneath the thermocline (Kohfeld et al. 1996; Simstich 1999). Therefore, its reservoir age highly depends on the ventilation of the thermocline and upper intermediate water. As indicated by the relatively low planktonic $\delta^{13}C_{DIC}$ values (0.7–1.0‰), this water was poorly ventilated during glacial times when a meltwater lid and/or sea ice covering the western Iceland and Greenland Seas hindered the exchange with the atmosphere (Sarnthein et al. 1995; Voelker 1999). Furthermore, “fossil” $CO_2$ originating either from stranded icebergs melting near site PS2644 or directly from the melting Greenland ice sheet and shelves, might have biased the $^{14}C$ concentration in the (sub)surface water, similar to the modern situation underneath the Antarctic ice shelves (Domack et al. 1989). The deep water, on the other hand, was newly convected in the Norwegian Sea as evidenced by heavy benthic $\delta^{18}O$ values (Duplessy et al. 1988; Dokken and Jansen 1999) and flowed—at least partly—across the Iceland Plateau and the Denmark Strait where it was recorded in epibenthic $\delta^{18}O$ values of up to 5.55‰, benthic $\delta^{13}C_{DIC}$ values of 1.5–1.7‰ (Voelker 1999) and younger $^{14}C$ ages. Since we assume the benthic $^{14}C$ ages during marine isotope stage 2 to originate from a young water mass, their $\Delta^{14}C$ levels, higher than those of *N. pachyderma*(s) (Table 1), should be closer to the actual atmospheric level.

According to high resolution planktonic and benthic isotope curves (Rasmussen et al. 1996; Dokken and Jansen 1999; Voelker 1999 and unpublished data) hydrographic conditions similar to the LGM also occurred during marine isotope stage 3 in the Nordic Seas and might have led to large fluctuations in the reservoir effect e.g. during Heinrich Event 4 (Sarnthein et al., forthcoming). So, because these variations in the reservoir effect cannot be quantified, our data set cannot be connected to the atmospheric values. Instead, it represents a calibration set for the local upper ocean reflecting the atmospheric changes, but modified by the local oceanography.

**Variation of the Age Differences (Marine $\Delta^{14}C$)**

The differences between the Libby $^{14}C$ ages, not corrected for the reservoir effect, and the GISP2 calendar ages vary between –260 and 7530 years, equal to –170 to +1215‰ marine $\Delta^{14}C$ (Figure 3; Table 1). During the interval 43–53.3 ka cal BP most age differences would actually be negative—like the marine $\Delta^{14}C$ values—when the 3% offset between Libby- and physical $^{14}C$-years is taken into account (Figure 3). However, starting around 46 ka cal BP (≈45 ka BP) the age differences increase steadily until 40.4 ka cal BP (≈33 ka BP) whereby the major rise from ≈2500 to >7200 yr (marine $\Delta^{14}C$: 183–1215‰) is confined to the much shorter period from 41.5 to 40.4 ka cal BP. This rapid increase coincides with the Laschamp inclination swing and drop in geomagnetic intensity in core PS2644 (Figure 4; Voelker et al. 1998; Laj et al. 2000) and with the highest $^{10}Be$ (Yiou et al. 1997) and $^{36}Cl$ fluxes in the GRIP ice core (Figure 3; Baumgartner et al. 1998). After the $\Delta^{14}C$ maximum at the end of the Laschamp excursion the age differences immediately drop to ≈5000 years

(≤704‰) during Dansgaard-Oeschger Event 9 and even lower during Heinrich Event 4 (H4; Figures 3, 4). During H4, the marine $\Delta^{14}C$ values seem to be dampened by an increased reservoir age. This is inferred because as soon as the meltwater disappeared at the beginning of Dansgaard-Oeschger interstadial 8 (38 ka cal BP/ ≈32.6 ka BP) the age differences reached a second maximum of 5600 yr (755‰). This second peak coincides with the end of the weaker magnetic intensity minimum following the Laschamp Event thereby marking the end of the high $^{14}C$ production period between 42 and 38 ka cal BP (Figures 3, 4).

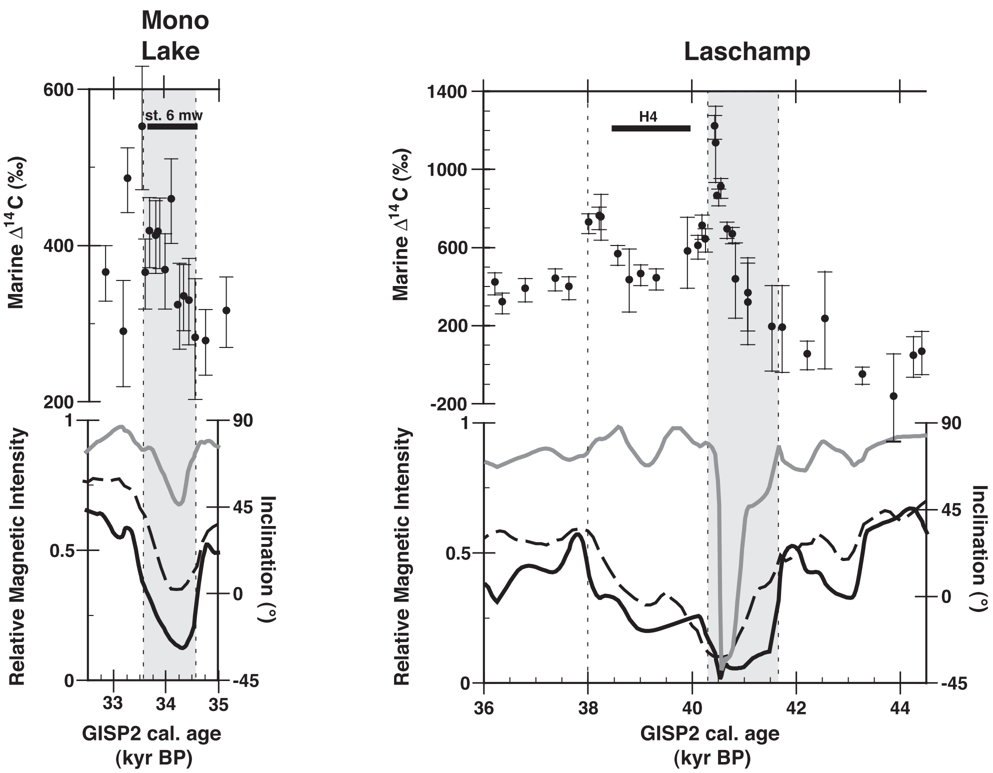


Figure 4 Close-up of marine $\Delta^{14}C$ values (± 1σ; upper panel), magnetic records of core PS2644 (lower panel; gray: inclination; black: normalized relative geomagnetic intensity based on NRM/ ARM/ $10^3$; Voelker et al. 1998), and the NAPIS–75 stack (dashed line in lower panel; Laj et al. 2000) vs. GISP2 calendar age (ka BP) for the Mono Lake and Laschamp Event. Horizontal black bar indicates interval of meltwater event during stadial 6 (st.6 mw) or Heinrich Event 4 (H4). Gray bars mark the interval of Mono Lake or Laschamp excursion, thinly dashed lines mark the beginning and end of major geomagnetic intensity minima.

After 38 ka cal BP the age differences decline to values around 3700 years (≈400‰) and even further after 35.3 ka cal BP down to around 3000 years (≈300‰) (Figure 3; Table 1). The slow but steady $\Delta^{14}C$ decrease is interrupted by a third brief maximum between 34.5 and 33.5 ka cal BP (≈29–30 ka BP), which is contemporary with the Mono Lake intensity minimum (Figure 4; Voelker et al. 1998; Laj et al. 2000). During this interval, the age anomalies rose continuously until they reached 4470 years (550‰) at the end of the intensity minimum (Figures 3, 4). As the Mono Lake excursion coincides with a meltwater event and the maximum age difference with the beginning of Dansgaard-Oeschger interstadial 6, it is comparable to the interval from 40 to 38.5 ka cal BP (≈H4).

Accordingly, most marine $\Delta^{14}C$ values should be low due to an increased reservoir effect and thereby make us underestimate the true atmospheric $\Delta^{14}C$ levels. This assumption is corroborated by the $^{36}Cl$ flux data from the GRIP ice core (Wagner et al. 2000) and by a Bahamian speleothem $^{14}C$ record (Richards et al. submitted; Beck et al. submitted), both of which show similar values for the Mono Lake and the Laschamp Event, higher than those obtained from core PS2644.

After the Mono Lake Event, the age differences decrease again to values between 3500 and 2500 yr (until 24 ka cal BP/21 ka BP). In the range between 15.7 and 21.6 ka cal BP (≈14–19 ka BP), where our age control is weaker because of subdued climatic signals in cores PS2644 and GISP2 and where the planktonic reservoir age greatly fluctuated, the data points show a large scatter (Figure 3, Table 1).

### Comparison with Other Records for Ages >20 ka cal BP

Our $\Delta^{14}C$ record, with two major increases between 30 and 55 ka cal BP, is similar to the high resolution $^{14}C$–U/Th record from Bahamian speleothems (Richards et al. submitted; Beck et al. submitted) and a marine record from the Cariaco basin (Hughen et al. 1997). For the range >20 ka cal BP a perfect match between the Bahamian record and the record from core PS2644 would be obtained by shifting the Iceland Sea data by +2000 yr (W Beck personal communication 2000). Since the U/Th dates (W Beck personal communication 2000; J Chappell personal communication 2000) as well as the GISP2 chronology appear reliable further work on the time scales is needed to resolve this age dispensary. This is especially important because the true calendar age also determines $\Delta^{14}C$. Disparity in $\Delta^{14}C$ exists during the Mono Lake Event when the Bahamian record shows $\Delta^{14}C$ values as high as during the Laschamp interval, just like the $^{36}Cl$ flux in the GRIP ice core (Wagner et al. 2000), which indicates the subdued character of the marine $\Delta^{14}C$ record. The comparison with the atmospheric record from Lake Suigetsu (Kitagawa and van der Plicht 1998a, 1998b) reveals major discrepancies with the Lake Suigetsu record often being younger, with consequently smaller $\Delta^{14}C$ deviations, and, especially, lacking the rapid increase associated with the Laschamp Event. The inconsistency is probably due to an imprecise varve chronology in Lake Suigetsu for the oldest part of the record, as stated by Kitagawa and van der Plicht (1998a).

The calibration data presented here also generally agree with single calibration points of Bard et al. (1998), Geyh and Schlüchter (1998), Schramm et al. (2000), Vogel (1983) and Vogel and Kronfeld (1997) (compilations in Voelker 1999 and Schramm et al. 2000). For the Laschamp Event, however, four calibration points from Bischoff et al. (1994), Geyh and Schlüchter (1998), and Schrammet al. (2000) place the $\Delta^{14}C$ rise up to 2000 years earlier than our data. Thereby the declination change associated with the Laschamp Event in the Lake Lisan record is dated to 42.2 U/Th years (Marco et al. 1998 with revised ages from Schramm et al. 2000). Further discrepancies with single calibration data occur between 34.5–35 ka cal BP where Geyh and Schlüchter (1998) and Vogel (1983) observe higher deviations (more in agreement with the Bahamian record).

### Geomagnetic Control of the $^{14}C$ Production 25–50 ka BP

Since $pCO_2$ records from Antarctic ice cores reveal variations of only 10–20 ppmv during isotope stages 2 and 3 (Neftel et al. 1988; Indermühle et al. 2000), changes in the global carbon cycle most likely played only a minor role in modulating the $\Delta^{14}C$ record. Major changes in North Atlantic deep water formation and the strength of the THC may have produced transient spikes in $\Delta^{14}C$ (Goslar et al. 1995; Stocker and Wright 1996, 1998; Hughen et al. 1998) Also, the offset between conventional and physical $^{14}C$ ages diminishes the maximal age differences by only 950–1160 yr (Figures 3, 4) so that the major portion of the age anomalies must be attributed to an enhanced and varying $^{14}C$ production. Increased production, further corroborated by high fluxes of the cosmogenic isotopes $^{36}$Cl and $^{10}$Be (Voelker et al. 1998), was caused by a low geomagnetic field strength which, based on absolute intensity data, was four to ten times lower during the Laschamp Event (4–14 μT; Roperch et al. 1988; Chauvin et al. 1989; Levi et al. 1990) than at "present" (49.2 ± 12.7 μT for 1943–1952 AD; Gonzalez et al. 1997) and about half as low during the Mono Lake Event (19–24 μT; Gonzalez et al. 1997; Valet et al. 1998). For the interval 27–54 ka cal BP, the similarity between our $\Delta^{14}$C record and the multi core relative intensity record of NAPIS–75 (Laj et al. 2000; Figure 3), the shape of which is confirmed by other high-resolution geomagnetic records from the North Atlantic (Stoner et al. 1995, Channell et al. 1997; Channell 1999), South Atlantic (Channell et al. 2000), and North Pacific (Roberts et al. 1997), provides strong evidence for the predominant geomagnetic modulation of the $\Delta^{14}$C record. While the $^{14}$C production peaks during the geomagnetic intensity minima resulted in apparently too young $^{14}$C ages, the production during the intensity maximum around 47 ka cal BP was probably the lowest during the last 53 ka cal BP and resulted in apparently too old $^{14}$C ages.

## CONCLUSION

The detailed correlation of sediment core PS2644 with the annual-layer chronology of the GISP2 ice core provides us with 70 marine calibration points for the interval 24 to 53.3 ka cal BP. Because at site PS2644 the reservoir age was unknown and probably varied over time, Libby $^{14}$C ages were used for a local marine calibration. The age anomalies probably represent minimum values for the atmospheric $\Delta^{14}$C changes. This is especially true for the intervals from 33.5 to 34.5 ka cal BP and from 38.5 to 40 ka cal BP when meltwater events caused an increased (planktonic) reservoir age and resulted in smaller age anomalies at site PS2644. When a high resolution atmospheric record becomes available in the future, the changes in the reservoir age of the northern North Atlantic can easily be reconstructed by subtracting the marine from the atmospheric record. The three $\Delta^{14}$C maxima concur with minima in the geomagnetic intensity which indicates the cause of the enhanced $^{14}$C production. This is further corroborated by increased flux rates of cosmogenic isotopes in ice cores from the Arctic and Antarctic (Voelker et al. 1998 and references therein; Wagner et al. 2000).

Though our data represent only marine $\Delta^{14}$C levels, they are in general agreement with most other calibration data, especially the rapid $\Delta^{14}$C increase between 44 and 40 ka cal BP and the second $\Delta^{14}$C maximum around 34 ka cal BP. For ages >32 ka cal BP, however, they highly diverge from the Lake Suigetsu record of Kitagawa and van der Plicht (1998), hinting to possible problems in the varve chronology for this time range. The high $\Delta^{14}$C variability during the interval 24–54 ka cal BP revealed by our and most other data clearly shows that a true calibration of $^{14}$C ages >20 ka BP cannot be done by interpolating between a few coral calibration points (Bard et al. 1998). The combined calibration data, however, provide a better base for calibrating $^{14}$C ages >20 ka BP. A new high resolution record based on terrestrial organic carbon dates and a sound calendar age scale are nevertheless necessary to provide true atmospheric $\Delta^{14}$C levels and to allow estimations of changes in the reservoir age in various parts of the world ocean.

## ACKNOWLEDGMENTS

These many $^{14}$C ages could not have been produced without the help of several students who helped to prepare the sediment samples or picked hundreds of foraminifera shells under the microscope for AMS samples. The technical team of the Leibniz laboratory, especially A Oriwall, is warmly thanked for the efficiency and expertise in preparing and running the AMS samples. Helmut Erlenkeuser and his team are thanked for the stable isotope measurements. AV would also like to thank Carlo Laj and Catherine Kissel from LSCE (CEA–CNRS, Gif-sur-Yvette) and Juerg Beer and Gerhard Wagner from EAWAG (Dübendorf) for the stimulating collaboration and sharing their data. This study was generously funded by the Deutsche Forschungsgemeinschaft Bonn through the Sonderforschungsbereich 313 at Kiel University.

## REFERENCES

Arikawa R. 1983. Distribution and taxonomy of globigerina pachyderma (Ehrenberg) off the Sanriku coast, northeast Honshu, Japan. *Scientific Reports Tohoku University, 2nd series (Geology)* 53(2):103–57.

Bard E, Arnold M, Mangerud J, Paterne M, Labeyrie L, Duprat J, Melieres M-A, Sonstegaard E, Duplessy J-C. 1994 The. North Atlantic atmosphere-sea surface $^{14}C$ gradient during the Younger Dryas climatic event. *Earth and Planetary Science Letters* 126:275–87.

Bard E, Arnold M, Hamelin B, Tisnerat-Laborde N, Cabioch G. 1998. Radiocarbon calibration by means of mass spectrometric $^{230}Th/^{234}U$ and $^{14}C$ ages of corals: an updated database including samples from Barbados, Mururoa and Tahiti. INTCAL98: calibration issue. *Radiocarbon* 40(3):1085–92.

Baumgartner S, Beer J, Suter M, Dittrich-Hannen B, Synal H-A, Kubik PW, Hammer C, Johnsen S. 1997. Chlorine 36 fallout in the Summit Greenland Ice Core Project ice core. *Journal of Geophysical Research* 102(C12):26,659–62.

Baumgartner S, Beer J, Masarik J, Wagner G, Meynadier L, Synal H-A. 1998. Geomagnetic modulation of the $^{36}Cl$ flux in the GRIP ice core, Greenland. *Science* 279:1330–32.

Beck WJ, Richards DA, Donahue DJ, Smart PL, Edwards RL, Hererra-Osterheld S, Burr GS, Calsoyas L, Jull AJT, Biddulph D. Extremely large variations of atmospheric $^{14}C$ concentration during marine isotope stage 3. *Science*. Submitted.

Bender M, Sowers T, Dickson M-L, Orchardo J, Grootes P, Mayewski PA, Meese DA. 1994. Climate correlations between Greenland and Antarctica during the past 100,000 years. *Nature* 372:663–66.

Bischoff JL, Kenneth L, Garcia JF, Carbonell E, Vaquero M, Stafford TW Jr, Jull AJT. 1994. Dating of the basal Aurignacian sandwich at Abric Romani (Catalunya, Spain) by radiocarbon and Uranium-Series. *Journal of Archaeological Science* 21:541–51.

Bond G, Broecker WS, Johnsen S, McManus J, Labeyrie L, Jouzel J, Bonani G. 1993. Correlations between climate records from North Atlantic sediments and Greenland ice. *Nature* 365:143–47.

Channell JET. 1999. Geomagnetic paleointensity and directional secular variation at Ocen Drilling Program (ODP) site 984 (Bjorn Drift) since 500 ka: comparisons with ODP site 983 (Gardar Drift). *Journal of Geophysical Research* 104(B10):22,937–951.

Channell JET, Hodell DA, Lehman B. 1997. Relative geomagnetic paleointensity and $\delta^{18}O$ at ODP Site 983 (Gardar Drift, North Atlantic) since 350 ka. *Earth and Planetary Science Letters* 153:103–18.

Channell JET, Stoner JS, Hodell DA, Charles CD. 2000. Geomagnetic paleointensity for the last 100 kyr from the sub-antarctic South Atlantic: a tool for inter-hemispheric correlation. *Earth and Planetary Science Letters* 175:145–60.

Chappell J, Omura A, Esat T, McCulloch M, Pandolfi J, Ota Y, Pillans B. 1996. Reconciliation of late Quaternary sea levels derived from coral terraces at Huon Peninsula with deep sea oxygen isotope records. *Earth and Planetary Science Letters* 141:227–36.

Charles CD, Rind D, Jouzel J, Koster RD, Fairbanks RG. 1994. Glacial-interglacial changes in moisture sources for Greenland: influences on the ice core record of climate. *Science* 263:508–11.

Chauvin A, Duncan RA, Bonhommet N, Levi S. 1989. Paleointensity of the earth's magnetic field and K-Ar dating of the Louchadiere volcanic flow (central France): new evidence for the Laschamp excursion. *Geophyscial Research Letters* 16(10):1189–92.

Cortijo E, Labeyrie L, Vidal L, Vautravers M, Chapman M, Duplessy J-C, Elliot M, Arnold M, Turon J-L, Auffret G. 1997. Changes in sea surface hydrology associated with Heinrich Event 4 in the North Atlanticm-Ocean between 40°N and 60°N. *Earth and Planetary Science Letters* 146:29–45.

Domack EW, Jull AJT, Anderson JB, Linick TW, Williams CR. 1989. Application of tandem accelerator mass-spectrometer dating to late Pleistocene-Holocene sediments of the East Antarctic continental shelf. *Quaternary Research* 31:277–87.

Dokken TM, Jansen E. 1999. Rapid changes in the mechanism of ocean convection during the last glacial cycle. *Nature* 401:458–61.

Duplessy JC, Labeyrie L, Blanc PL. 1988. Norwegian Sea deepwater variations over the last climatic cycle: paleo-oceanographical implications. In: Wanner H, Siegenthaler X, editors. *Long and short term variability of climate.* Heidelberg: Springer Verlag. p 83–116.

Geyh MA, Schlüchter C. 1998. Calibration of the $^{14}C$ time scale beyond 22,000 BP. *Radiocarbon* 40(1):475–82.

Gonzalez S, Sherwood G, Böhnel H, Schnepp E. 1997. Palaeosecular variation in Central Mexico over the last 30,000 years: the record from lavas. *Geophysical Journal International* 130:201–19.

Goslar T, Arnold M, Bard E, Kuc T, Pazdur MF, Ralska-Jasiewiczowa M, Rozanski K, Tisnerat N, Walanus A, Wicik B, Wieckowski K. 1995. High concentration of atmospheric $^{14}C$ during the Younger Dryas cold episode. *Nature* 377:414–17.

Grönvold K, Oskarsson N, Johnsen S, Clausen HB, Hammer CU, Bond G, Bard E. 1995. Ash layers from Iceland in the Greenland GRIP ice core correlated with oceanic and land sediments. *Earth and Planetary Science Letters* 135:149–55.

Grootes PM, Stuiver M, White JWC, Johnsen S, Jouzel J. 1993. Comparison of oxygen isotope records from the GISP2 and GRIP Greenland ice cores. *Nature* 366: 552–4.

Grootes PM, Stuiver M. 1997. $^{18}O/^{16}O$ variability in Greenland snow and ice with $10^{-3}$ to $10^{5}$ year time resolution. *Journal of Geophysical Research* 102(C12): 26,455–70.

Haflidason H, Sejrup HP, Klitgaard-Kristensen D, Johnsen S. 1995. Coupled response of the Late Glacial climatic shifts of northwest Europe reflected in Greenland ice cores: evidence from the northern North Sea. *Geology* 23(12):1059–62.

Hammer CU, Andersen KK, Clausen HB, Dahl-Jensen,D, Schøtt Hvidberg C, Iversen P. 1997. *The stratigraphic dating of the GRIP Ice Core*. Special report. University of Copenhagen, Denmark: Geophysical Department, Niels Bohr Institute for Astronomic Physics and Geophysics. 14 p.

Hughen KA, Overpeck JT, Lehman SJ, Southon J, Kashgarian M, Peterson LC. 1997. Radiocarbon change in the Cariaco Basin. Presented. AGU 1997 Fall Meeting, San Francisco, California, 8–12 December. EOS Transactions. Fall Meeting Supplement, F338. *AGU* 78(46).

Hughen KA, Overpeck JT, Lehman SJ, Kashgarian M, Southon J, Peterson L, Alley R, Sigman DM. 1998. Deglacial changes in ocean circulation from an extended radiocarbon calibration. *Nature* 391:65–8.

Indermühle A, Monnin E, Stauffer B, Stocker TF, Wahlen M. 2000. Atmospheric $CO_2$ concentration from 60 to 20 kyr BP from the Taylor Dome ice core, Antarctica. *Geophysical Research Letters* 27(5):735–8.

Johnsen SJ, Dansgaard W, White JWC. 1989. The origin of Arctic precipitation under present and glacial conditions. *Tellus* 41B:452–68.

Johnsen SJ, Clausen HB, Dansgaard W, Fuhrer K, Gundestrup N, Hammer CU, Iversen P, Jouzel J, Stauffer B, Steffensen JP. 1992. Irregular glacial interstadials recorded in a new Greenland ice core. *Nature* 359: 311–3.

Jouzel J, Alley RB, Cuffey KM, Dansgaard W, Grootes P, Hoffmann G, Johnsen SJ, Koster RD, Peel D, Shuman CA, Stievenar, M, Stuiver M, White J. 1997. Validity of the temperature reconstruction from water isotopes in ice cores. *Journal of Geophysical Research*: 102(C12):26,471–88.

Kitagawa H, van der Plicht J. 1998a. Atmospheric radiocarbon calibration to 45,000 yr BP: Late Glacial fluctuations and cosmogenic isotope production. *Science* 279:1187–90.

Kitagawa H, van der Plicht J. 1998b. A 40,000-yr varved chronology from Lake Suigetsu, Japan: extension of the radiocarbon calibration curve. *Radiocarbon* 40(1): 505–16.

Kohfeld KE, Fairbanks RG, Smith SL, Walsh ID. 1996. *Neogloboquadrina pachyderma* (sinistral coiling) as paleoceanographic tracer in polar oceans: evidence from Northeast Water Polynya plankton twos, sediment traps, and surface sediments. *Paleoceanography* 11(6):679–99.

Laj C, Kissel C, Mazaud A, Channell JET, Beer J. 2000. North Atlantic palaeointensity stack since 75 ka (NAPIS-75) and the duration of the Laschamp Event. *Philosophical Transactions of the Royal Society London* A358:1009–25.

Lein D. 1998. Die Radiolarien-Gemeinschaften von 52 ka bis 12 ka vor heute im Sedimentkern PS2644 aus dernördlichen Dänemarkstraße. Diploma thesis. Kiel: 51 p.

Levi S, Audunsson H, Duncan RA, Kristjansson L, Gillot P-Y, Jakobsson SP. 1990. Late Pleistocene geomagntic excursion in Icelandic lavas: confirmation of the Laschamp excursion. *Earth and Planetary Science Letters* 96:443–57.

Marco S, Ron H, McWilliam, MO, Stein M. 1998. High-resolution record of geomagneticsecular variation from Late Pleistocene Lake Lisan sediments (paleo Dead Sea). *Earth and Planetary Science Letters* 161: 145–60.

Meese DA, Alley RB, Gow AJ, Grootes PM, Mayewski PA, Ram M, Taylor KC, Waddington ED, Zielinski GA. 1994. Preliminary depth-age scale of the GISP2 ice core. *CRREL Special Report 94–1.* Hanover, New Hampshire: Cold Regions Research and Engineering Laboratory. 66 p.

Meese DA, Gow AJ, Alley RB, Zielinski GA, Grootes PM, Ram M, Taylor KC, Mayewski PA, Bolzan JF. 1997. The GISP2 depth-age scale: methods and results. *Journal of Geophysical Research* 102(C12): 26,411–24.

Nadeau M-J, Grootes PM, Voelker A, Bruhn F, Duhr A, Oriwall A. Carbonate $^{14}C$ background: does it have multiple personalities? *Radiocarbon*. Submitted.

Neftel A, Oeschger H, Staffelbach T, Stauffer B. 1988. $CO_2$ record in the Byrd ice core 50,000–5,000 years BP. *Nature* 331:609–11.

Rasmussen TL, Thomsen E, Labeyrie L, van Weering TCE. 1996. Circulation changes in the Faeroe-Shetland Channel correlating with cold events during the last glacial period (58–10 ka). *Geology* 24(10):937–40.

Richards DA, Beck WJ, Donahue DJ, Edwards RL, Silverman BW, Smart PL. Atmospheric radiocarbon before 11 ka using submerged speleothems from the Bahamas. *Science.* Submitted.

Roberts AP, Lehman B, Weeks RJ, Verosub KL, Laj C. 1997. Relative paleointensity of the geomagentic field over the last 200,000 years from ODP sites 883 and 884, North Pacific Ocean. *Earth and Planetary Science Letters* 152:11–23.

Roperch P, Bonhommet N, Levi S. 1988. Paleointensity of the earth's magnetic field during the Laschamp excursion and its geomagentic implications. *Earth and Planetary Science Letters* 88:209–19.

Sachs JP, Lehman SJ. 1999. Subtropical North Atlantic temperatures 60,000 to 30,000 years ago. *Science* 286: 756–759.

Sarnthein M, Jansen E, Weinelt M, Arnold M, Duplessy J-C, Erlenkeuser H, Flatoy A, Johannessen G, Johannessen T, Jung S, Koc N, Labeyrie L, Maslin M, Pflaumann U, Schulz H. 1995. Variations in Atlantic surface ocean paleoceanography, 50–80°N: a time-slice record of the last 30,000 years. *Paleoceanography* 10(6):1063–94.

Sarnthein M, Stattegger K, Dreger D, Erlen Keuser H, Grootsep, Haupt B, Jung S, Kieter T, Kuhnt W, Pflaumann U, Schäfer-Neth C, Schulz M, Seidor D, Simstich J, van Kreveld-Alfane S, Vogelsang E, Voelker A, Wenelt M. Fundamental modes and abrupt changes in North Atlantic circulation and cliamte over the last 60 ky–numerical modelling and reconstruction. Forthcoming. In: Schäfer P, Ritzrau W, Schlüter M, Thiede J, editors. *The Northern North Atlantic: a changing environment*. Springer Verlag, Heidelberg.

Schleicher M, Grootes PM, Nadeau M-J, Schoon A. 1998. The carbonate $^{14}$C background and its components at the Leibniz AMS facility. *Radiocarbon* 40(1): 85–94.

Schmitz WJ, McCartney MS. 1993. On the North Atlantic circulation. *Reviews of Geophysics* 31(1):29–49.

Schramm A, Stein M, Goldstein SL. 2000. Calibration of the $^{14}$C time scale to >40 ka by $^{234}$U–$^{230}$Th dating of Lake Lisan sediments (last glacial Dead Sea). *Earth and Planetary Science Letters* 175:27–40.

Seidov D, Sarnthein M, Stattegger,K, Prien R, Weinelt M. 1996. North Atlantic ocean circulation during the last glacial maximum and subsequent meltwater event: a numerical model. *Journal of Geophysical Research* 10(C7):16,305–332.

Simstich J. 1999. Die ozeanische Deckschicht des Europäischen Nordmeeres im Abbild stabiler Isotope unter-schiedlicher Planktonforaminiferen. DSc dissertation, University of Kiel, Germany: Berichte-Reports Institut für Geowissenschaften, Univerität Kiel. Nr 2. 96 p.

Sowers T, Bender M, Labeyrie L, Martinson D, Jouzel J, Raynaud D, Pichon JJ, Korotkevich A. 1993. A 135,000-year Vostock-Specmap common temporal framework. *Paleoceanography* 8:737–66.

Stocker TF, Wright DG. 1996. Rapid changes in ocean circulation and atmospheric radiocarbon. *Paleoceanography* 11(6):773–95.

Stocker TF, Wright DG. 1998. Rapid changes in ocean circulation and atmospheric radiocarbon. *Radiocarbon* 40(1):359–66.

Stoner JS, Channell JET, Hillaire-Marcel C. 1995. Late Pleistocene relative geomagnetic paleo-intensity from the deep Labrador Sea: regional and global correlaions. *Earth and Planetary Science Letters* 134:237–52.

Stuiver M, Reimer PJ, Bard E, Beck JW, Burr GS, Hughen KA, Kromer B, McCormac G, van der Plicht J, Spurk M. 1998. INTCAL98 Radiocarbon age calibration, 24,000–0 cal BP. INTCAL98: calibration issue. *Radiocarbon* 40(3):1041–83.

Stuiver M, Grootes PM. 2000. GISP2 oxygen isotope ratios. *Quaternary Research* 53(3):277–84.

Trauth MH, Sarnthein M, Arnold M. 1997. Bioturbational mixing depth and carbon flux at the seafloor. *Paleoceanography* 12:517–26.

Valet J-P, Tric E, Herrero-Bervera E, Meynadier L, Lockwood JP. 1998. Absolute paleointensity from Hawaiian lavas younger than 35 ka. *Earth and Planetary Science Letters* 161:19–32.

van Kreveld S, Sarnthein M, Erlenkeuser H, Grootes PM, Jung S, Nadaeu M-J, Pflaumann U, Voelker A. 2000. Potential links between surging ice sheets, circulation changes, and the Dansgaard-Oeschger cycles in the Irminger Sea, 60-18 kyr. *Paleoceanography* 15(4): 425–42.

Voelker AHL, Sarnthein M, Grootes PM, Erlenkeuser H, Laj C, Mazaud C, Nadeau M-J, Schleicher M. 1998. Correlation of marine $^{14}$C ages from the Nordic Seas with the GISP2 isotope record: implications for $^{14}$C calibration beyond 25 ka BP. *Radiocarbon* 40(1):517–34.

Voelker AHL. 1999. Zur Deutung der Dansgaard-Oeschger Ereignisse in ultra-hochauflösenden Sedimentprofilen aus dem Europäischen Nordmeer. DSc dissertation, University of Kiel, Germany: *Berichte-Reports, Institut für Geowissenschaften, Univerität Kiel,* nr. 9:278p.

Vogel JC. 1983. $^{14}$C variations during the Upper Pleistocene. *Radiocarbon* 25(2):213–18.

Vogel JC, Kronfeld J. 1997. Calibration of radiocarbon dates for the late Pleistocene using UTh dates on stalagmites. *Radiocarbon* 39(1):27–32.

Wagner G, Beer J, Laj C, Kissel C, Masarik J, Muscheler R, Synal H-A. 2000. Chlorine-36 evidence for the Mono Lake Event in the Summit GRIP ice core. *Earth and Planetary Science Letters* 181:1–6.

Yiou F, Raisbeck GM, Baumgartner S, Beer J, Hammer C, Johnsen S, Jouzel J, Kubik PW, Lestringuez J, Stievenard M, Suter M, Yiou P. 1997. Beryllium 10 in the Greenland Ice Core Project ice core at Summit, Greenland. *Journal of Geophysical Research* 102(C12):26,783–94.

Zielinski GA, Mayewski PA, Meeker LD, Grönvold K, Germani MS, Whitlow S, Twickler MS, Taylor K. 1997. Volcanic aerosol records and tephrochronology of the Summit, Greenland, ice cores. *Journal of Geophysical Research* (Oceans) 102(C12):26,625–40.

## APPENDIX

Table 1 Marine calibration points derived from core PS2644[a]

| Composite depth[b] (cm) | Lab code (KIA-) | $^{14}C$ age $\pm 1\ \sigma$ (yr BP) | GISP2 calendar age (yr BP) | Age difference (yr) | Marine $\Delta^{14}C^{c}$ (‰) |
|---|---|---|---|---|---|
| 22 | 74 | 9980 ± 60 | 11,390 | 1410 | 145.0 |
| 65 | 802 | 14,370 ± 60 | 15,720 | 1350 | 119.3 |
| 65 (b) | 741 | 14,050 ± 90 | 15,720 | 1670 | 164.8 |
| 71 | 77 | 15,080 ± 210 | 16,040 | 960 | 65.1 |
| 71 (b) | 1649 | 14,450 ± 80 | 16,040 | 1590 | 152.0 |
| 80 | 736 | 14,890 ± 80 | 17,240 | 2350 | 261.0 |
| 80 (b) | 742 | 14,130 ± 90 | 17,240 | 3110 | 386.1 |
| 80 (b) | 743 | 14,490 ± 90 | 17,240 | 2750 | 325.3 |
| 86 | 78 | 15,210 ± 240 | 17,460 | 2250 | 244.4 |
| 86 (b) | 1650 | 14,720 + 90/–80 | 17,460 | 2740 | 322.7 |
| 91 | 79 | 15,660 + 220/–210 | 17,680 | 2020 | 208.3 |
| 95 | 737 | 15,380 ± 80 | 17,940 | 2560 | 291.2 |
| 95 (b) | 744 | 15,150 ± 90 | 17,940 | 2790 | 328.7 |
| 105 | 803 | 16,510 ± 70 | 18,100 | 1590 | 143.7 |
| 113 | 804 | 17,630 ± 90 | 18,840 | 1210 | 88.0 |
| 113 (b) | 1641 | 15,790 ± 120 | 18,840 | 3050 | 368.0 |
| 129 | 806 | 19,300 ± 90 | 21,640 | 2340 | 240.0 |
| 129 (b) | 745 | 17,740 ± 160 | 21,640 | 3900 | 505.8 |
| 134[d] | [1647/710] | 21,410 ± 180 | 24,080 | 2670 | 281.0 |
| 134 (b)[d] | [746/747] | 21,450 ± 200 | 24,080 | 2630 | 274.6 |
| 141 | 5373 | 22,140 ± 70 | 25,000 | 2860 | 307.4 |
| 141 (b) | 5374 | 21,590 ± 70 | 25,000 | 3410 | 400.1 |
| 143 | 738 | 22,780 ± 180 | 25,620 | 2840 | 301.3 |
| 163 | 739 | 25,700 + 300/–290 | 29,000 | 3300 | 361.7 |
| 176 | 81 | 27,550 + 910/–820 | 30,180 | 2630 | 247.6 |
| 180 | 740 | 27,440 + 300/–290 | 30,360 | 2920 | 292.6 |
| 199 | 758 | 28,030 + 340/–320 | 31,420 | 3390 | 365.4 |
| 206 | 82 | 29,340 + 1150/–1010 | 31,720 | 2380 | 202.8 |
| 218 | 808 | 28,470 ± 200 | 32,300 | 3830 | 437.8 |
| 229 | 809 | 29,400 ± 210 | 32,820 | 3420 | 363.7 |
| 236 | 759 | 30,190 + 440/–410 | 33,160 | 2970 | 287.9 |
| 241 | 810 | 29,130 + 230/–220 | 33,240 | 4110 | 483.9 |
| 251 | 1648 | 29,050 + 420/–400 | 33,520 | 4470 | 550.4 |
| 253 | 760 | 30,140 + 270/–260 | 33,580 | 3440 | 363.5 |
| 255 | 9856 | 29,910 + 260/–250 | 33,660 | 3750 | 416.7 |
| 258 | 9857 | 30,060 + 270/–260 | 33,780 | 3720 | 410.9 |
| 260 | 811 | 30,110 + 260/–250 | 33,860 | 3750 | 415.7 |
| 262 | 9858 | 30,490 + 290/–280 | 33,960 | 3470 | 366.8 |
| 265 | 9859 | 30,090 + 310/–290 | 34,080 | 3990 | 457.6 |
| 268 | 9860 | 31,030 + 340/–330 | 34,240 | 3210 | 321.9 |
| 270 | 812 | 31,040 + 260/–250 | 34,320 | 3280 | 333.1 |

Table 1 Marine calibration points derived from core PS2644[a] (*Continued*)

| Composite depth[b] (cm) | Lab code (KIA-) | $^{14}C$ age ± 1 σ (yr BP) | GISP2 calendar age (yr BP) | Age difference (yr) | Marine $\Delta^{14}C$[c] (‰) |
|---|---|---|---|---|---|
| 273 | 9861 | 31,170 + 340/–330 | 34,420 | 3250 | 327.7 |
| 275 | 761 | 31,580 + 500/–470 | 34,540 | 2960 | 280.1 |
| 283 | 813 | 31,800 + 270/–260 | 34,740 | 2940 | 276.0 |
| 292 | 814 | 31,950 + 280/–270 | 35,140 | 3190 | 314.5 |
| 297.5 | 75 | 32,080 + 1670/–1380 | 35,280 | 3200 | 315.5 |
| 304 | 815 | 31,930 + 280/–270 | 35,540 | 3610 | 383.1 |
| 312 | 816 | 32,550 + 290/–280 | 35,780 | 3230 | 318.1 |
| 320 | 817 | 32,410 + 330/–310 | 36,220 | 3810 | 414.6 |
| 325 | 818 | 33,140 + 330/–320 | 36,360 | 3220 | 313.7 |
| 331 | 819 | 36,160 + 360/–340 | 36,800 | 3640 | 382.1 |
| 340 | 820 | 33,430 + 320/–310 | 37,380 | 3950 | 433.6 |
| 344 | 821 | 33,920 + 350/–330 | 37,640 | 3720 | 391.8 |
| 354 | 11,257 | 32,580 + 240/–230 | 38,020 | 5440 | 721.9 |
| 357 | 11,256 | 32,650 + 270/–260 | 38,220 | 5570 | 748.7 |
| 359 | 1449 | 32,660 + 560/–520 | 38,260 | 5600 | 755.0 |
| 363 | 11,258 | 33,920 + 270/–260 | 38,580 | 4660 | 559.4 |
| 367 | 889 | 34,850 + 930/–840 | 38,800 | 3950 | 426.4 |
| 370 | 11,259 | 34,890 + 300/–290 | 39,020 | 4130 | 457.6 |
| 374 | 11,260 | 35,300 + 310/–300 | 39,320 | 4020 | 436.3 |
| 379 | 890 | 35,150 + 990/–880 | 39,920 | 4770 | 573.5 |
| 381 | 11,261 | 35,200 + 310/–300 | 40,120 | 4920 | 602.0 |
| 384 | 11,262 | 34,780 + 300/–290 | 40,200 | 5420 | 704.4 |
| 386 | 11,263 | 35,170 + 300/–290 | 40,260 | 5090 | 635.5 |
| 389 av | 1552/11,264[e] | 32,910 ± 220 | 40,440 | 7530 | 1214.6 |
| 390 | 910 | 33,250 + 770/–710 | 40,460 | 7210 | 1127.9 |
| 392 | 5375 | 34,400 + 190/–180 | 40,520 | 6120 | 857.5 |
| 394 | 5376 | 34,240 + 220/–210 | 40,560 | 6320 | 904.1 |
| 401 | 5377 | 35,330 ± 200 | 40,680 | 5350 | 686.8 |
| 403 | 5378 | 35,550 ± 200 | 40,780 | 5230 | 661.2 |
| 405 | 3347 | 36,810 + 1160/–1020 | 40,840 | 4030 | 430.4 |
| 414 | 911 | 37,450 + 1400/–1190 | 41,080 | 3630 | 359.8 |
| 414 (b) | 1644 | 37,740 + 1190/–1040 | 41,080 | 3340 | 311.5 |
| 422 | 891 | 38,990 + 1640/–1360 | 41,540 | 2550 | 186.8 |
| 435 | 912 | 39,210 + 1670/–1380 | 41,740 | 2530 | 183.0 |
| 452 | 11,265 | 40,660 + 580/–540 | 42,220 | 1560 | 46.7 |
| 460 | 913 | 39,710 + 1820/–1480 | 42,560 | 2850 | 227.5 |
| 474 av | 914/5379 | 42,350 + 390/–370 | 43,280 | 750 | –57.3 |
| 482 | 1553 | 44,140 + 2540/–1930 | 43,880 | –260 | –170.4 |
| 488 av | 1554/3975 | 42,700 + 840/–760 | 44,260 | 1560 | 39.2 |
| 492 av | 892/3976 | 43,100 + 880/–800 | 44,420 | 1720 | 59.5 |
| 503 av | 1555/4120 | 44,550 + 1080/–950 | 44,860 | 710 | –67.1 |
| 507 av | 1556/4121 | 44,340 + 990/–880 | 45,060 | 1120 | –19.0 |
| 530 av | 915/ 4151 | 45,190 + 1200/–1040 | 45,677[f] | 890 | –48.8 |

Table 1 Marine calibration points derived from core PS2644[a] (*Continued*)

| Composite depth[b] (cm) | Lab code (KIA-) | $^{14}C$ age ± 1 σ (yr BP) | GISP2 calendar age (yr BP) | Age difference (yr) | Marine $\Delta^{14}C$[c] (‰) |
|---|---|---|---|---|---|
| 535 | 4122 | 44,850 + 1180/–1030 | 45,824[g] | 1370 | 9.3 |
| 542 av | 3506/ 3696 | 46,210 + 660/–610 | 46,660 | 850 | –56.7 |
| 549 av | 3507/ 3697 | 45,920 + 650/–600 | 47,040 | 1520 | 23.9 |
| 580 av | 3509/ 3699 | 48,840 + 960/–860 | 49,220 | 780 | –73.3 |
| 627 av | 3763 | 51,180 + 1700/–1400 | 52,380 | 1600 | 14.9 |
| 657 av[f] | 3761/ 3979 | 52,470 + 1670/–1380 | 53,261 | 990 | 76.8 |
| 665 av[f] | 3764/ 3980 | 51,560 + 1480/–1250 | 53,261 | 2100 | –62.2 |

[a]Notes: $^{14}C$ ages are in Libby years ($T_{1/2}$ = 5568 yr) and not reservoir corrected. (b): ages measured on benthic foraminifera; av = weighted average (see Voelker et al. 1998 and Voelker 1999 for single dates); [b] composite depth scale resulting from core fit between giant boxcore (GKG) and gravity core (SL) is achieved by adding 6 cm to original gravity core depths (Voelker 1999).[c] not atmospheric level, because $^{14}C$ ages are not corrected for reservoir effect.[d] interpolated between $^{14}C$ ages from 133 and 137 cm (Voelker et al. 1998). [e] KIA11,264 32,850 ± 240. [f] ages for North Atlantic Ash Zone 2. [g] calendar ages based on linear interpolation between age control points (Voelker 1999).

## RADIOCARBON UPDATES

### *Retirement*

*Lloyd Currie.* "Retired" from full-time employment at NIST as of 30 June 2000, though he says it's more accurate to call it a career change. Dr Currie has been appointed Scientist Emeritus at NBS/NIST. He plans on "a new career of lecturing, writing and consulting". His future research will focus on advances in chemometrics, and the history of carbonaceous particles as recorded in ice cores. Dr Currie will fill his "spare" time with his most important loves: family, music, and skiing.

### *Conferences and Meetings*

*Fourth International Radiocarbon Intercomparison (FIRI) Workshop.* Following the end of the first phase of FIRI, a participants' workshop will be held in Edinburgh, Scotland to discuss the results. The meeting will be held on 22–23 March 2001. This first meeting is restricted to intercomparison participants only, but a summary of the meeting will be made available. Contact Marian Scott for details: marian@stats.gla.ac.uk.

*LSC 2001.* The Liquid Scintillation Spectrometry 2001 Conference will be held 7–11 May 2001 at the Center for Advanced Technological and Environmental Training (FTU), which is part of Forschungszentrum Karlsruhe (FZK), Germany. LSC 2001 continues the series of conferences most recently held in Gatlinburg, Tennessee in 1989, in Vienna in 1992, and in Glasgow in 1994. The conference will provide a forum for radioanalysts to discuss their most recent findings and future work either as oral lectures, including both invited and contributed papers, or as posters. For details, see http://www.ftu.fzk.de/LSC2001, or the announcement at the back of this issue.

*Methods of Absolute Chronology Conference.* The 7th International Conference will be held 23–26 April 2001 in Ustrón, Poland, hosted by the Department of Radioisotopes Radiocarbon Laboratory at the Institute of Physics, Silesian University of Technology. The organizing committee chairperson is Anna Pazdur. Abstracts (in English) must be submitted by 15 February 2001. For more information, see www.polsl.gliwice.pl/~chronos, or email chronos@polsl.gliwice.pl.

### *Calibration Program and Database*

*CALIB 4.3 for Windows.* Paula Reimer announces the release of the latest version of the radiocarbon calibration program CALIB 4.3 for Windows. The program can now handle up to 3000 samples. Printing of the graphics has also been simplified. The program can be downloaded from our Internet site http://www.calib.org. Please follow the CALIB link to the downloadable versions and note the instructions for downloading and decompressing the Windows version there. A Macintosh version for G3/G4 platforms is also available.

*Marine Reservoir Correction Database.* A marine reservoir correction database has been developed and funded by the Institute for Aegean Prehistory. The URL is http://www.calib.org. The database is intended for use with radiocarbon calibration programs.

RADIOCARBON, Vol 42, Nr 3, 2000, p 455–478 

# RADIOCARBON LABORATORIES

This is *Radiocarbon*'s annual list of active radiocarbon laboratories and personnel known to us. Conventional beta-counting facilities are listed in Part I, and accelerator mass spectrometry (AMS) facilities in Part II. Laboratory code designations, used to identify published dates, are given to the left of the listing. (See p 476 ff. for a complete list of past and present lab codes.)

Please notify us of any changes in staff, addresses, or other contact information.

## *I. CONVENTIONAL $^{14}$C COUNTING FACILITIES*

### ARGENTINA

AC
Héctor Osvaldo Panarello
Pabellón INGEIS
Ciudad Universitaria
1428 Buenos Aires, Argentina
Tel: +54 11 4783 3021/23; Fax: +54 11 4783 3024
Email: hector@ingeis.uba.ar

LP
Aníbal Juan Figini
Laboratorio de Tritio y Radiocarbono-LATYR
Facultad de Ciencias Naturales y Museo-UNLP
Paseo del Bosque S/N°
1900 La Plata, Argentina
Tel/Fax: +54 21 270648

### AUSTRALIA

ANU
Rainer Grün
Quaternary Dating Research Centre
Australian National University
Research School of Pacific Studies
Canberra ACT 0200 Australia
Tel: +61 6 249 3122; Fax: +61 6 249 0315
Email: rainer.grun@anu.edu.au

SUA
Mike Barbetti
The NWG Macintosh Centre for Quaternary Dating
Madsen Building F09
The University of Sydney
NSW 2006 Australia
Tel: +61 2 9351 3993; Fax: +61 2 9351 4499
Email: m.barbetti@emu.usyd.edu.au

### AUSTRIA

VRI
Edwin Pak
Institut für Radiumforschung und Kernphysik
Universität Wien
Boltzmanngasse 3
A-1090 Vienna, Austria
Tel: +43 1 4277 51764; Fax: +43 1 4277 51752
Email: pak@ap.univie.ac.at

Franz Schönhofer
Federal Institute for Food Control and Research
Kinderspitalgasse 15
A-1090 Vienna, Austria
Tel: +43 1 40491 520; Fax: +43 1 40491 540

IAEA Manfred Gröning
International Atomic Energy Agency (IAEA)
Isotope Hydrology Laboratory
Wagramerstrasse 5
P.O. Box 100
A-1400 Vienna, Austria
Tel: +43 1 2600 21740/21766; Fax: +43 1 20607
Email: M.Groening@iaea.org

Roland Tesch
Austrian Research and Testing Centre Arsenal
Environment Division
Faradaygasse 3
A-1030 Vienna, Austria
Tel: +43 1 79747 516
Fax: +43 1 79747 587
Email: tesch.r@arsenal.ac.at

**BELGIUM**

ANTW R. Vanhoorne
Department of General Botany
State University Centre Antwerp
Groenenborgerlaan 171
B-2020 Antwerp, Belgium

IRPA M. Van Strydonck
Royal Institute for Cultural Heritage
Jubelpark 1
B-1000 Brussels, Belgium
Tel: +32 2 739 67 11 (institute), +32 2 739 67 02 (lab)
Fax: +32 2 732 01 05
Email: mark.vanstrydonck@kikirpa.be

LAR Jean Govaerts
Lab. d'Application des Radioéléments
Chimie B6, Sart Tilman
Liège, Belgium

**BELARUS**

IGSB N. D. Michailov
Institute of Geological Sciences of the
National Academy of Sciences of Belarus
Kuprevich Street 7
Minsk 220141 Belarus
Tel: +375 0172 63 81 13; Fax: +375 0172 63 63 98
Email: mihailov@ns.igs.ac.by

**BRAZIL**

FZ M. F. Santiago
Departamento de Física - UFC
Campus do Pici - Cx. Postal 6030
60455-760 Fortaleza-CE, Brazil
Tel: +55 85 288 9913; Fax: +55 85 287 4138
Email: marlucia@fisica.ufc.br

CENA Luiz Carlos Ruiz Pessenda
Radiocarbon Laboratory
Centro de Energia Nuclear na Agricultura
Universidade de São Paulo
Avenida Centenario 303
Caixa Postal 96 – CEP 13400-970
Piracicaba, São Paulo, Brazil
Tel: +55 19 429 4656; Fax: +55 19 429 4610
Email: lcrpesse@pira.cena.usp.br

**CANADA**

GSC Roger N. McNeely
Radiocarbon Dating Laboratory
Geological Survey of Canada
601 Booth Street
Ottawa, Ontario K1A 0E8 Canada
Tel: +1 613 995 4241; Fax: +1 613 992 6653
Email: mcneely@gsc.nrcan.gc.ca

BGS Howard Melville
Department of Earth Sciences
Brock University
St. Catharines, Ontario L2S 3A1 Canada
Tel: +1 905 688 5550 ext. 3522; Fax: +1 905 682 9020
Email: hmelvill@spartan.ac.BrockU.ca

WAT Robert J. Drimmie
Department of Earth Sciences
Environmental Isotope Laboratory
University of Waterloo
Waterloo, Ontario N2L 3G1 Canada
Tel: +1 519 888 4567 ext. 2580; Fax: +1 519 746 0183
Email: rdrimmie@sciborg.uwaterloo.ca

UQ Serge Occhietti and Pierre Pichet
Radiocarbon Laboratory
GEOTOP
University of Québec at Montréal
P.O. Box 8888, Succursale Centre Ville
Montréal, Québec H3C 3P8 Canada
Tel: +1 514 987 4080; Fax: +1 514 987 3635
Email: occhietti.serge@uqam.ca

**CHINA**

CG Yijian Chen and G. Peng
Radiocarbon Laboratory
Institute of Geology
State Seismological Bureau
P.O. Box 634
Beijing 100029 China
Tlx: 6347

HLYunzhang Yue
Second Institute of Oceanography
State Oceanic Adminstration
P.O. Box 1207
Hangzhou, Zheijiang 310012 China
Tel: +86 571 8076924 ext. 328; Fax: +86 571 8071539
Tlx: 35035 NBOHZ CN; Cable: 3152

Dai Kaimei
Department of Physics
Nanjing University
Nanjing 210093 China
Tel: +86 25 3596746
Fax: +86 25 307965; Tlx: 34151 PRCNU CN
Email: postphys@nju.edu.cn

XLLQ Zhou Weijian
Institute of Earth Environment
XiYing Lu 22-2
Xi'an 710054, Shaanxi, China
Tel: +86 29 5512264 (work); 86 29 5256429 (home); Fax: +86 29 5522566
Email: weijian@loess.llqg.ac.cn; weijian@public.xa.sn.cn

## CROATIA

Z Drs. Bogomil Obelić and Nada Horvatinčić
Ruđer Bošković Institute
P.O.B. 1016, Bijenička 54
10001 Zagreb, Croatia
Tel: +385 1 4680 219; Fax: +385 1 4680 239
Email: Bogomil.Obelic@irb.hr and Nada.Horvatincic@irb.hr
WWW: http://www.irb.hr/zef/c14-lab/

## CZECH REPUBLIC

CU Jan Šilar
Department of Hydrogeology
Charles University
Albertov 6
CZ-12843 Prague 2 Czech Republic
Tel: +42 2 21952139 or +42 2 21951111
Fax: +42 2 21952180
Email: silar@prfdec.natur.cuni.cz

## DENMARK

K Kaare Lund Rasmussen
$^{14}C$ Dating Laboratory
National Museum
Ny Vestergade 11
DK-1471 Copenhagen K, Denmark
Tel: +45 33 47 3176; Fax: +45 33 47 3310
Email: kaare.lund.rasmussen@natmus.dk

## ESTONIA

Tln Enn Kaup
Radiocarbon Laboratory
Institute of Geology at Tallinn Technical University
Estonia pst 7
10143 Tallinn, Estonia
Tel: +372 645 4679; Fax: +372 631 2074
Email: kaup@gi.ee; rajamae@isogeo.gi.ee

Ta Volli Kalm and Arvi Liiva
Radiocarbon Laboratory
Institute of Geology
University of Tartu
Vanemuise St. 46
51014 Tartu, Estonia
Tel/Fax: +372 7 375 836
Email: geol@ut.ee

## FINLAND

Su Tuovi Kankainen
Geological Survey of Finland
P.O. Box 96
FIN-02151 Espoo, Finland
Tel: +358 205 50 11; Fax: +358 205 50 12
Email: tuovi.kankainen@gsf.fi

Hel Högne Jungner
Dating Laboratory
P.O. Box 11, Snellmaninkatu 3
FIN-00014 Helsinki University, Finland
Tel: +358 9 191 23436; Fax: +358 9 191 23466
Email: hogne.jungner@helsinki.fi

**FRANCE**

Gif Michel Fontugne
Centre des Faibles Radioactivités
Laboratoire mixte CNRS-CEA
F-91198 Gif sur Yvette, Cedex, France
Tel: +33 1 69 82 35 25; Fax: +33 1 69 82 35 68
Email: Michel.Fontugne@cfr.cnrs-gif.fr
*and*
Laboratoire Souterrain de Modane
Laboratoire mixte IN2I 3-CNRS/DSM-CEA
90, Rue Polset
F-73500 Modane, France

Ly Jacques Evin
CDRC - Centre de Datation par le RadioCarbone
Université Claude Bernard Lyon I, Batiment 217
43, Boulevard du 11 Novembre 1918
F-69622 Villeurbanne Cedex, France
Tel: +33 472 44 82 57; Fax: +33 472 43 13 17
Email: jacques.evin@cismsun.univ-lyon1.fr

**GEORGIA**

TB S. Pagava
Radiocarbon Laboratory
I.Javakhishvili Tbilisi State University
I.Chavchavadze av., 3
Tbilisi 380008 Georgia
Tel: +995 32 222105
Email: spagava@access.sanet.ge

**GERMANY**

Bln Jochen Görsdorf
Deutsches Archäologisches Institut
Eurasien-Abteilung
Postfach 330014
14191 Berlin, Germany
Tel: +49 30 203 77 275: Fax: +49 30 203 77 275
Email: goerc14@zedat.fu-berlin.de

Fra Reiner Protsch von Zieten
Radiocarbon Laboratory
J. W. Goethe-Universität
Siesmayerstrasse 70
60323 Frankfurt am Main, Germany
Tel: +49 69 798 24764 / 24767; Fax: +49 69 798 24728

Fr Detlef Hebert
Institut für Angewandte Physik
Technische Universität Bergakademie Freiberg
09596 Freiberg/Sa., Germany
Tel: +49 3731 39 2371 / 2594; Fax: +49 3731 39 4004
Email: hebert@tu-freiberg.de

HAM Peter Becker-Heidmann
Institut für Bodenkunde
Universität Hamburg
Allende-Platz 2
20146 Hamburg, Germany
Tel: +49 40 42838 2003; Fax: +49 40 42838 2024
Email: PBeckerH@Uni-Hamburg.de
WWW: http://www.geowiss.uni-hamburg.de/i-boden/tt14c.htm

Hv
M. A. Geyh
Niedersächsisches Landesamt für Bodenforschung
Postfach 510153
30655 Hannover-Stillweg 2, Germany
Tel: +49 511 643 2537; Fax: +49 511 643 2304
Email: Mebus.Geyh@BGR.de

Hd
Bernd Kromer
Heidelberger Akademie der Wissenschaften
c/o Institut für Umweltphysik
Universität Heidelberg
Im Neuenheimer Feld 229
69120 Heidelberg, Germany
Tel: +49 6221 5 46 357; Fax: +49 6221 5 46 405
Email: Bernd.Kromer@iup.uni-heidelberg.de

KI
Helmut Erlenkeuser and Pieter M. Grootes
Leibniz-Labor
Christian-Albrechts-Universität
Max-Eyth-Str. 11
24118 Kiel, Germany
Tel: +49 431 880 3894 (P.M.G.); +49 431 880 3896 (H.E.)
Fax: +49 431 880 3356
Email: pgrootes@leibniz.uni-kiel.de; herlenkeuser@leibniz.uni-kiel.de
WWW: http://www.uni-kiel.de:8080/leibniz/indexe.htm

KN
Bernhard Weninger
Labor für $^{14}$C-Datierung
Institut für Ur-und Frühgeschichte
Universität zu Köln
Weyertal 125
50923 Köln, Germany
Tel: +49 221 470 2880 / 2881; Fax: +49 221 470 4892

LZ
Achim Hiller
UFZ-Umweltforschungszentrum Leipzig-Halle GmbH
Sektion Hydrogeologie
Arbeitsgruppe Paläoklimatologie
Theodor-Lieser-Strasse 4
06120 Halle, Germany
Tel: +49 345 5585 226; Fax: +49 345 5585 559
Email: hiller@hdg.ufz.de

## GREECE

DEM
Yannis Maniatis
Laboratory of Archaeometry
Institute of Materials Science
National Centre for Scientific Research "Demokritos"
153 10 Aghia Paraskevi Attikis
Greece
Tel: +30 1 6503389 or +30 1 6524821; Fax: +30 1 6519430
Email: maniatis@ims.demokritos.gr
WWW: http://www.ims.demokritos.gr/archae

LIH
Nicolaos Zouridakis
Laboratory of Isotope Hydrology
Institute of Physical Chemistry
National Centre for Scientific Research "Demokritos"
153 10 Aghia Paraskevi Attikis
POB 60228
Greece
Tel: +30 1 6503969; Fax: +30 1 6511766
Email: nizouri@cyclades.nrcps.ariadne-t.gr

**HUNGARY**

Deb Zsusa Szanto
Institute of Nuclear Research of the Hungarian Academy of Sciences
H-4026 Bem tér 18/c,
P.O. Box 51
H-4001 Debrecen, Hungary
Tel: +36 52 417266; Fax: +36 52 416181
Email: aszanto@moon.atomki.hu

**ICELAND**

Páll Theodórsson
Science Institute
University of Iceland
Dunhaga 3
IS-107 Reykjavík, Iceland
Tel: +354 525 4800; Fax: +354 552 8911
Email: pth@raunvis.hi.is

**INDIA**

PRLCH R. Bhushan, S. Krishnaswami and B. L. K. Somayajulu
Physical Research Laboratory
Chemistry Department
Oceanography and Climatic Studies Area
Navrangpura
Ahmedabad 380 009 India
Tel: +91 79 6462129; Fax: +91 79 6560502
Email: bhushan@prl.ernet.in; swami@prl.ernet.in; soma@prl.ernet.in

PRL M. G. Yadava
Radiocarbon Dating Research Unit
Oceanography and Climate Studies Area
Earth Sciences and Solar System Division
Physical Research Laboratory
Navrangpura
Ahmedabad 380 009 India
Tel: +91 79 462129; Fax: +91 79 6560502
Telegram: "Research"
Email: myadava@prl.ernet.in

JUBR S. D. Chatterjee, R. C. Sastri and Haradhan De
Biren Roy Research Laboratory for Archaeological Dating
Department of Physics
Jadavpur University
Calcutta 700 032 India
Tel: +91 33 473 4044; Fax: +91 33 473 4266; Tlx: 21-4160 (VC JU IN)

BS G. Rajagopalan
Radiocarbon Laboratory
Birbal Sahni Institute Palaeobotany
PO Box 106, 53 University Road
Lucknow 226 007 India
Tel: +91 522 32 4291; Fax: +91 522 37 4528, +91 522 38 1948
Email: bsip@bsip.sirnetd.ernet.in

**IRELAND**

UCD Peter I. Mitchell and Edward McGee
UCD Radiocarbon Laboratory
Department of Experimental Physics
University College Dublin
Belfield, Dublin 4, Ireland
Tel: +353 1 706 2220 / 2225 / 2222
Fax: +353 1 283 7275
Email: Peter.Mitchell@ucd.ie; Edward.Mcgee@ucd.ie
WWW: http://www.ucd.ie/~radphys

### ISRAEL

RT Israel Carmi, Elisabetta Boaretto
Department of Environmental Sciences and Energy Research
Weizmann Institute of Science
76100 Rehovot, Israel
Tel: +972 8 342544; Fax: +972 8 344124
Email: cicarmii@wis.weizmann.ac.il; elisa@wis.weizmann.ac.il

### ITALY

ENEA Agostino Salomoni
ENEA Radiocarbon Laboratory
Via dei Colli, 16
I-40136 Bologna, Italy
Tel: +39 51 6098168; Fax: +39 51 6098187

R Salvatore Improta
Dipartimento di Fisica
Università "La Sapienza"
Piazzale Aldo Moro, 2
I-00185 Rome, Italy
Tel: +39 6 49914208
Fax: +39 6 4957697
Email: Salvatore.Improta@roma1.infn.it
*and*
Giorgio Belluomini
Radiocarbon Laboratory
Istituto per le Tecnologie Applicate ai Beni Culturali
Consiglio Nazionale delle Ricerche
Area della Ricerca di Roma
CP 10 – Via Salaria Km 29,300
I-00016 Monterotondo St., Rome, Italy
Tel: +39 06 90672469; Fax: +39 06 90672373
Email: belluomi@mlib.cnr..it

Rome Gilberto Calderoni
Department of Earth Sciences
University of Rome "La Sapienza"
Piazzale Aldo Moro, 5
I-00185 Rome, Italy
Tel: +39 6 499 14580; Fax: +39 6 499 14578
Email: calderoni@axrma.uniroma1.it

UD Piero Anichini, Valerio Barbina, per.ind. Ennio Virgili
Azienda Speciale Servizi Laboratorio e CRAD
Via Nazionale, 33
I-33040 Pradamano UD, Italy
Tel: +39 432671061; Fax: +39 432671176
Email: laboratorio@azservizi.cciaa-ud.xnet.it

### JAPAN

KEEA Yoshimasa Takashima
Kyushu Environmental Evaluation Association
1-10-1, Matsukadai, Higashiku
Fukuoka 813-0004, Japan
Tel: +81 92 662 0410; Fax: +81 92 662 0990
Email: kawamura@keea.or.jp

Yasuo Nagashima
Tandem Accelerator Center
University of Tsukuba
Tennoudai 1-1-1, Tsukuba
Ibaraki, 305-8577, Japan
Tel: +81 298 53 2565; Fax: +81 298 53 4461
Email: nagashima@tac.tsukuba.ac.jp
http://www.tac.tsukuba.ac.jp (in Japanese)

KSU Osamu Yamada
Faculty of Science
Kyoto Sangyo University
Kita-ku, Kyoto 603 Japan

OR Setsuko Shibata
Research Center of Radioisotopes
Research Institute for Advanced Science and Technology
University of Osaka Prefecture
1-2, Gakuen-cho, Sakai, Japan
Tel: +81 722 36 2221; Fax: +81 722 54 9938
Email: shibata@riast.osakafu-u-ac.jp

GaK Kunihiko Kigoshi
Radiocarbon Laboratory
Gakushuin University
Mejiro Toshima-ku, 1-5-1, Faculty of Science
Tokyo 171, Japan
Tel: +81 3 3986 0221 ext. 6482; Fax: +81 3 5992 1029
Email: kunihiko.kigoshi@gakushuin.ac.jp

PAL Shigemoto Tokunaga
Radiocarbon Laboratory
Palynosurvery Co.
Nissan Edobashi Bld.
1-10-5 Honcho, Nihonbashi
Chuoku, Tokyo, Japan
Tel (office): +81 3 3241 4566; (lab) +81 274 42 8129
Fax: +81 3 3241 4597
Email: palynoa@blue.ocn.ne.jp

TK Kunio Yoshida
C-14 Dating Laboratory
The University Museum
The University of Tokyo
7-3-1 Hongo, Bunkyo-ku
Tokyo 113 Japan
Tel: +81 3 3812 2111
Fax: +81 3 3814 4291
Email: gara@um.u-tokyo.ac.jp

NU Kunio Omoto
Radiocarbon Dating Laboratory
Department of Geography
College of Humanities and Science
Nihon University
25-40, 3 Chome, Sakurajosui
Setagaya-ku, Tokyo 156 Japan
Tel: +81 35317 9273 *or* +81 33303 1691
Fax: +81 35317 9429 *or* +81 33303 9899
Email: omoto@chs.nihon-u.ac.jp

JGS Hajime Kayanne
Department of Geography
University of Tokyo
Mongo 113-0033, Tokyo, Japan
Tel: +81 3-5841-4573
Fax: +81 3-3814-6358
kayanne@geogr.s.u-tokyo.ac.jp

PLD Hideki Yamagata
Paleo Labo Co., Ltd.
63, Shima 5-chome Oguma-cho
Hashima, Gifu 501-6264 Japan
Email: pal@usiwakamaru.or.jp

**KOREA**

Jung Sun Ahn
Advanced Atomic Energy Research Institute
150, Duk-Jin Dong, Seo-Ku
Daejeon, Chung Nam, Korea

KCP Hyung Tae Kang and Kyung Yim Nah
Archaeological Studies Division
National Cultural Property Research Institute
1-57 Sejongno Chongno-gu
Seoul, Korea 110 050
Tel: +82 2 735 5281 ext. 323; Fax: +82 2 735 6889
Email: vvyckht1@chollian.net

**LATVIA**

Riga V. S. Veksler and A. A. Kristin
Institute of Science - Application Research
Riga 50 Merkelya 11
Riga 226 050, Latvia
Tel: +371 7 212 501 *or* +371 7 213 636

**MONACO**

IAEA-MEL Pavel Povinec (*see also* Slovakia)
International Atomic Energy Agency
Marine Environmental Laboratory
4 Quai Antoine 1er
MC-98012 Monaco
Tel: +377 979 77216; Fax: +377 979 77273
Email: p.povinec@iaea.org

**THE NETHERLANDS**

GrN J. van der Plicht
Centre for Isotope Research
University of Groningen
Nijenborgh 4
NL-9747 AG Groningen, The Netherlands
Tel: +31 50 3634760; Fax: +31 50 3634738
Email: plicht@phys.rug.nl

**NEW ZEALAND**

Wk A. G. Hogg and T. F. G. Higham
Radiocarbon Laboratory
University of Waikato
Private Bag
Hamilton, New Zealand
Tel: +64 7 838 4278; Fax: +64 7 838 4192
Email: ahogg@waikato.ac.nz, *or* thigham@waikato.ac.nz
http://www.radiocarbondating.com

NZ Rodger Sparks
Rafter Radiocarbon Laboratory
Institute of Geological and Nuclear Sciences, Ltd.
P.O. Box 31-312
Lower Hutt, New Zealand
Tel: +64 4 570 4671; Fax: +64 4 570 4657
Email: R.Sparks@gns.cri.nz

**NORWAY**

T Steinar Gulliksen
Radiological Dating Laboratory
Norwegian University of Science and Technology
N-7491 Trondheim, Norway
Tel: +47 73 593310; Fax: +47 73 593383
Email: Steinar.Gulliksen@vm.ntnu.no

**POLAND**

Gd Anna Pazdur and Tomasz Goslar
Radiocarbon Laboratory
Silesian University of Technology
Institute of Physics
Krzywoustego 2
PL-44-100 Gliwice, Poland
Tel: +48 32 2372254; Fax: +48 32 2372488
Email: pazdur@zeus.polsl.gliwice.pl

KR Tadeusz Kuc
Krakow Radiocarbon Laboratory
Environmental Physics Department
University of Mining and Metallurgy
PL-30-059 Krakow, Poland
Tel: +48 12 6172979 *or* 6333740; Fax: +48 12 6340010
Tlx: 0322203 agh pl
Email: kuc@novell.ftj.agh.edu.pl

LOD Paweł Trzeciak and Ireneusz Borowiec
Radiochemical Laboratory
Archaeological and Ethnographical Museum in Lódz
Pl. Wolnšci 14
PL-91-415 Lódz, Poland
Tel: +48 42 6328440 *or* +48 42 6334307
Fax: +48 42 6329714
Email: jotmol@krysia.uni.lodz.pl

**PORTUGAL**

Sac A. M. Monge Soares
Laboratório de Isótopos Ambientais
Instituto Tecnológico e Nuclear
Estrada Nacional 10
P-2686 Sacavém Codex, Portugal
Tel: +351 1 9550021; Fax: +351 1 9441455
Email: amsoares@itn1.itn.pt

**REPUBLIC OF CHINA**

NTU Tsung-Kwei Liu
Department of Geology
National Taiwan University
245 Choushan Road
Taipei, Taiwan, Republic of China
Tel/Fax: +886 2 3657380
Email: liutk@ccms.ntu.edu.tw

**RUSSIA**

MAG Anatoly V. Lozhkin
Quaternary Geology and Geochronology Laboratory
Northeast Interdisciplinary Scientific Research Institute
Russian Academy of Sciences, Far East Branch
16 Portovaya St
Magadan 685000 Russia
Email: lozhkin@neisri.magadan.su

GIN L. D. Sulerzhitsky
Geological Institute
Russian Academy of Sciences
Pyzhevsky 7
Moscow 109017 Russia
Tel: +7 095 230 8136
Email: suler@geo.tv-sign.ru, suler@ginran.msk.su

IEMAE L. Dinesman
Institute of Ecology and Evolution
Russian Academy of Sciences
Leninsky Prospect 33
Moscow 117071 Russia
Fax: +7 095 954 5534
Email: sevin@sovamsu.sovusa.com

IGAN O. A. Chichagova
Institute of Geography
Russian Academy of Sciences
Staromonetnyi 29
Moscow 109017 Russia
Tel: +7 095 230 8366; Fax: +7 095 959 0033
Email: ochichag@mtu-net.ru

IORAN V. Kuptsov, Chief of Isotope Group
P.P. Shirshov Institute of Oceanology
Russian Academy of Sciences
Nakhimovsky Prospekt, 23
Moscow 117851 Russia
Fax: +7 095 1245983

IWP Yu. A. Karpytchev
Isotope Laboratory
Institute of Water Problems
Russian Academy of Sciences
13/3 Sadovo-Tschernogryazskaya
Moscow 103064 Russia
Tel: +7 095 208 5471

MSU P. A. Kaplin and O. B. Parunin
Laboratory of Recent Sediments and Pleistocene Paleogeography
Moscow State University
Vorobyovy Gory
Moscow 119899 Russia
Email: g1706@mail.ru

SOAN L. Orlova
United Institute of Geology, Geophysics and Minerology (UIGGM SB RAS)
Universitetsky pr. 3
630090 Novosibirsk 90 Russia
Tel: +7 3832 352 654; +7 3832 357 363; Fax: +7 3832 352 692
Email: vitaly@uiggm.nsc.ru; Tlx: 133 123 KORA SU

IVAN O. A. Braitseva, S. N. Litasova
I. V. Melekestev and V. N. Ponomareva
Institute of Volcanology
Bul Piipa 9
Petropavlovsk-Kamchatsky 683006 Russia
Tel: +7 5 91 94

LE Ganna Zaitseva
Institute of the History of Material Culture
Russian Academy of Sciences
Dvortsovaya Naberezhnaya, 18
191186 St. Petersburg, Russia
Tel: +7 812 311 8156; Fax: +7 812 311 6271
Email: ganna@mail.wplus.net

LU Kh. A. Arslanov
Geographical Research Institute
St. Petersburg State University
Sredniy Prospect 41
St. Petersburg 193004 Russia
Tel/Fax: +7 812 218 7904
Email: kozyrev@mail.nevalink.ru

**SLOVAKIA**

Ba Pavel Povinec (*see also* Monaco)
Department of Nuclear Physics
Comenius University
Mlynská dolina F1
842 15 Bratislava, Slovakia
Fax: +42 7 725882

**SOUTH AFRICA**

Pta S. Woodborne
Quaternary Research Dating Unit (QUADRU)
c/o Enviromentek, CSIR
P.O. Box 395
0001 Pretoria, South Africa
Tel: +27 12 841 3380; Fax: +27 12 349 1170
Email: swoodbor@CSIR.co.za

**SPAIN**

UBAR Gemma Rauret and Joan S. Mestres
Laboratori de Datació per Radiocarboni
Departament de Química Analítica
Universitat de Barcelona
Facultat de Química, 3a. Planta
C/. Martí i Franquès, 1-11/Avda. Diagonal, 647
E-08028 Barcelona, Spain
Tel: +34 3 402 1281; Fax: +34 3 402 1233
Email: jmestres@d3.ub.es

UGRA M. Purificación Sánchez and Elena Villafranca
Laboratorio de Datación por C-14
Centro de Instrumentación Científica
Campus Fuentenueva, Ed. Mecenas
Universidad de Granada
E-18071 Granada, Spain
Tel: +34 58 244229; Fax: +34 58 243391
Email: mpsansan@goliat.urg.es *and* jlazuen@goliat.urg.es

CSIC Fernán Alonso and Antonio Rubinos
Geochronology Laboratory
Instituto de Química-Física Rocasolano - CSIC
Serrano, 119
28006 Madrid, Spain
Phone: +34 91 561 9400
Fax: +34 91 564 2431
Email: f.alonso@iqfr.csic.es or rubinos@iqfr.csic.es

**SWEDEN**

Lu Göran Skog
Radiocarbon Dating Laboratory
University of Lund
Tornavägen 13
SE-223 63 Lund,
Tel: +46 46 222 7885; Fax: +46 46 222 4830
Email: Goran.Skog@c14lab.lu.se

U Ingrid U. Olsson
Department of Physics
Uppsala University
Box 530
SE-751 21 Uppsala, Sweden
Tel: +46 18 4713571; Fax: +46 18 4713524
Email: ingrid.olsson@fysik.uu.se

**SWITZERLAND**

B Thomas Stocker
Climate and Environmental Physics
Physics Institute
Sidlerstrasse 5
CH-3012 Bern, Switzerland
Tel: +41 31 631 44 64; Fax: +41 31 631 44 05
Email: stocker@climate.unibe.ch
http://www.climate.unibe.ch

**TURKEY**

METU Mustafa Özbakan
Radiocarbon Dating Laboratory
Middle East Technical University
Department of Physics
06531 Ankara, Turkey
Tel: +90 312 210 32 76; Fax: +90 312 210 12 81
Email: ozbakan@metu.edu.tr

**UKRAINE**

Ki Nikolai N. Kovalyukh and Vadim V. Skripkin
National Academy of Sciences and Ministry of Extraordinary Situation of Ukraine
State Scientific Centre of Environmental Radiogeochemistry
Kyiv Radiocarbon Laboratory
Palladin 34
Kyiv-142
252680 Ukraine
Tel/Fax: +38 0 44 444 0060
Fax: +38 0 44 444 1465
Email: kyiv14c@radgeo.freenet.kiev.ua

URCRM Michael Buzinny
Ukrainian Research Center for Radiation Medicine
Academy of Medical Sciences of Ukraine
04050, Melnikova str. 53
Kiev, Ukraine
Tel: +380 44 2445874; Fax: +380 44 2137202
Fax: +1 413 473-3008
Email: buzinny@bigfoot.com; buzinny@hotmail.com
http://bigfoot.com/~buzinny

**UNITED KINGDOM**

Birm R. E. G. Williams
Department of Geological Sciences
P.O. Box 363
University of Birmingham
Birmingham B15 2TT England

Q Roy Switsur
Cambridge Radiocarbon Dating Research Laboratory
Environmental Sciences Research Centre
East Road
Cambridge CB1 1PT England
Tel: +44 1223 363271 x2594
Email: vrs1@cam.ac.uk

RCD R. L. Otlet / A. J. Walker
RCD – Radiocarbon Dating
The Old Stables
East Lockinge, Wantage
Oxon OX12 8QY England
Tel/Fax: +44 1235 833667

| | |
|---|---|
| UB | Gerry McCormac<br>Radiocarbon Dating Laboratory<br>School of Archaeology and Palaeoecology<br>The Queen's University of Belfast<br>Belfast BT7 1NN Northern Ireland<br>Tel: +44 2890 335141; Fax: +44 2890 315779<br>Email: f.mccormac@qub.ac.uk<br>http://www.qub.ac.uk/arcpal |
| GU | G. T. Cook<br>SURRC Radiocarbon Dating Laboratory<br>Scottish Universities Research & Reactor Centre<br>Scottish Enterprise Technology Park<br>East Kilbride G75 0QF Scotland<br>Tel: +44 13552 23332 or +44 13552 70136; Fax: +44 13552 29898<br>Email: g.cook@surrc.gla.ac.uk |
| SRR | Professor A. E. Fallick<br>NERC Radiocarbon Laboratory<br>Scottish Enterprise Technology Park<br>Rankine Avenue<br>East Kilbride, Glasgow G75 0QF Scotland<br>Tel: +44 1355 260037; Fax: +44 1355 229829<br>Email: radiocarbon@nercrcl.gla.ac.uk<br>http://www.gla.ac.uk/nercrcl |
| | E. M. Scott<br>Department of Statistics<br>University Gardens<br>University of Glasgow<br>Glasgow, G12 8QW, Scotland<br>Tel: +44 141 330 5125; Fax: +44 141 330 4814<br>Email: marian@stats.gla.ac.uk |
| SWAN | Quentin Dresser<br>Department of Geography<br>University of Wales, Swansea<br>Singleton Park, Swansea<br>West Glamorgan SA2 8PP Wales<br>Tel: +44 1792 295148; Fax: +44 1792 295955<br>Email: P.Q.Dresser@swansea.ac.uk |

**UNITED STATES**

| | |
|---|---|
| A | Austin Long<br>Laboratory of Isotope Geochemistry<br>Geosciences Department<br>The University of Arizona<br>Tucson, Arizona 85721 USA<br>Tel: +1 520 621 8888; Fax: +1 520 621 2672<br>Email: along@geo.arizona.edu |
| UCI | Ellen Druffel and Sheila Griffin<br>Radiocarbon Laboratory<br>Department of Earth System Science<br>University of California, Irvine<br>PSRF 207<br>Irvine, California 92697-3100 USA<br>Tel (Druffel/office): +1 949 824 2116<br>Fax: +1 949 824 3256; Email edruffel@uci.edu |
| UCLA | Rainer Berger<br>Institute of Geophysics and Planetary Physics<br>University of California<br>Los Angeles, California 90024 USA<br>Tel: +1 310 825 4169; Fax: +1 310 206 3051 |

UCR R. E. Taylor
Radiocarbon Laboratory
Department of Anthropology
Institute of Geophysics and Planetary Physics
University of California, Riverside
Riverside, California 92512 USA
Tel: +1 909 787 5521; Fax: +1 909 787 5409
Email: retaylor@citrus.ucr.edu

Beta M. A. Tamers and D. G. Hood
Beta Analytic Inc.
4985 SW 74 Court
Miami, Florida 33155 USA
Tel: +1 305 667 5167; Fax: +1 305 663 0964
Email: beta@radiocarbon.com

UGA John E. Noakes
Center for Applied Isotope Studies
The University of Georgia
120 Riverbend Road
Athens, Georgia 30602-4702 USA
Tel: +1 706 542 1395; Fax: +1 706 542 6106

ISGS Chao-li Liu and Hong Wang
Isotope Geochemistry Section
Illinois State Geological Survey
615 E. Peabody Drive
Urbana, Illinois 61820 USA
Tel: +1 217 333 9083; Fax: +1 217 244 7004
Email: jliu@geoserv.isgs.uiuc.edu

NIST Lloyd A. Currie and George A. Klouda
Atmospheric Chemistry Group
National Institute of Standards and Technology

*Currie:*
100 Bureau Dr., Stop 8370
Gaithersburg, Maryland 20899-8370 USA
Tel: +1 301 975 3919; Fax: +1 301 216-1134
Email: Lloyd.Currie@nist.gov

*Klouda:*
100 Bureau Dr., Stop 8372
Gaithersburg, MD 20899-8372 USA
Tel: +1 301 975 3931; Fax: +1 301 216-1134
Email: George.Klouda@nist.gov

GX Alexander Cherkinsky
Geochron Laboratories, a division of
Krueger Enterprises, Inc.
711 Concord Avenue
Cambridge, Massachusetts 02138 USA
Tel: +1 617 876 3691; Fax: +1 617 661 0148
Email: acherkinsky@geochronlabs.com

I James Buckley
Teledyne Brown Engineering Environmental Services
50 Van Buren Avenue
Westwood, New Jersey 07675 USA
Tel: +1 201 664 7070; Fax: +1 201 664 5586
Tlx: 134474

QL Emeritus Minze Stuiver
Quaternary Isotope Laboratory
Box 351360
Quaternary Research Center
University of Washington
Seattle, Washington 98195-1360 USA
Tel: +1 206 685 1735; Fax: +1 206 543 3836
Email: minze@u.washington.edu

WIS David M. McJunkin
Center for Climatic Research
University of Wisconsin-Madison
1225 W. Dayton Street
Madison, Wisconsin 53706 USA
Tel: +1 608 262 7328; Fax: +1 608 262 5964
Email: mcj@facstaff.wisc.edu

**URUGUAY**

URU Cristina Ures and Roberto Bracco
Laboratorio de $^{14}C$
Facultad de Química
Universidad de la República
Gral. Flores 2124
Montevideo, Uruguay
Tel: +598 2 924 8571; Fax: +598 2 924 1906
Email: radquim@bilbo.edu.uy

## *II. $^{14}C$ ACCELERATOR FACILITIES (AMS)*

**AUSTRALIA**

ANSTO Ewan Lawson
ANTARES AMS Centre
Physics Division
Australian Nuclear Science and Technology Organisation (ANSTO)
New Illawarra Road
Lucas Heights, NSW 2234 Australia
Tel: +61 2 9717 3025; Fax: +61 2 9717 3257
Email: eml@ansto.gov.au

ANUA L. Keith Fifield
Department of Nuclear Physics, RSPhysSE
Australian National University
Canberra, ACT 0200 Australia
Tel: +61 2 6249 2095; Fax: +61 2 6249 0748
Email: keith.fifield@anu.edu.au

**AUSTRIA**

VERA Walter Kutschera
VERA-Laboratorium
Institut für Radiumforschung und Kernphysik
Universität Wien
Währingerstrasse 17
A-1090 Vienna, Austria
Tel: +43 1 4277 51700; Fax: +43 1 4277 9517
Email: Walter.Kutschera@univie.ac.at

**CANADA**

TO Roelf P. Beukens
IsoTrace Laboratory
University of Toronto
60 St. George Street
Toronto, Ontario, Canada M5S 1A7
Tel: +1 416 978 4628; Fax: +1 416 978 4711
Email: isotrace.lab@utoronto.ca
http://www.physics.utoronto.ca/~isotrace

**CHINA**

PKU Kun Li and Zhiyu Guo
Department of Technical Physics
Institute for Heavy Ion Physics
Peking University
Beijing 100871 China
Tel: +86 10 2501881 or +86 10 62501875
Fax: +86 10 2501873 or +86 10 62501875
Email: puihip@sun.ihep.ac.cn

**DENMARK**

AAR Jan Heinemeier and Niels Rud
AMS $^{14}$C Dating Laboratory
Institute of Physics and Astronomy
University of Aarhus
DK-8000 Aarhus C, Denmark
Tel: +45 8942 3718; Fax: +45 8612 0740
Email: jh@dfi.aau.dk
http://www.c14.dk

**FRANCE**

Gif A GDR Tandetron
Domaine du CNRS
Avenue de la Terrasse, Bat. 30
F-91198 Gif sur Yvette Cedex, France
Tel: +33 1 69 82 39 15; Fax: +33 1 69 82 36 70

Jean-Claude Duplessy, director
Centre des Faibles Radioactivités
Laboratoire mixte CNRS-CEA
F-91198 Gif sur Yvette Cedex, France
Tel: +33 1 69 82 35 26; Fax: +33 1 69 82 35 68
Email: Jean-Claude.Duplessy@cfr.cnrs-gif.fr

*AMS $^{14}$C*
Maurice Arnold
Centre des Faibles Radioactivités (CEA-CNRS)
Tandetron
Avenue de la Terrasse
BP 1
F-91198 Gif sur Yvette Cedex, France
Tel: +33 1 69 82 35 63; Fax: +33 1 69 82 36 70
Email: Maurice.Arnold@cfr.cnrs-gif.fr

*AMS $^{10}$Be, $^{126}$Al, $^{129}$I*
Françoise Yiou and Grant Raisbeck
CSNSM Bat. 108
F-91405 Campus Orsay Cedex, France
Tel: +33 1 69 15 52 64; Fax: +33 1 69 15 52 68
Email: yiou@csnsm.in2p3.fr; raisbeck@csnsm.in2p3.fr

**GERMANY**

Wolfgang Kretschmer
Physikalisches Institut
Universität Erlangen-Nürnberg
Erwin-Rommel-Str. 1
91054 Erlangen, Germany
Tel: +49 9131 857075; Fax: +49 9131 15249
Email: kretschmer@physik.uni-erlangen.de

J
Gert Jaap van Klinken
$^{14}C$ AMS Laboratory
Max-Planck-Institut für Biogeochemie
PO Box 10 01 64
07701 Jena, Germany
Tel: +49 3641 643708/3806; Fax: +49 3641 643710
Email: vklinken@bgc-jena.mpg.de
http://www.bgc-jena.mpg.de

KIA
Pieter M. Grootes, Marie-Josee Nadeau
Leibniz-Labor
Christian Albrechts Universität
Max-Eyth-Str. 11
24118 Kiel, Germany
Tel: +49 431 880 3894 (P.M.G.); +49 431 880 7373 (M.-J.N., M.S.)
Fax: +49 431 880 3356
Email: pgrootes@leibniz.uni-kiel.de (P.M.G.)
http://www.uni-kiel.de:8080/leibniz/indexe.htm

**KOREA**

SNU
Jong Chan Kim
The Inter-University Center for National Science Research Facility
Seoul National University
Seoul 151-742 Korea
Tel: +82 2 880 5774; Fax: +82 2 884 3002
Email: jckim@phya.snu.ac.kr
http://npl3.snu.ac.kr

**JAPAN**

Takafumi Aramaki
Marine Research Laboratory
Japan Atomic Energy Research Institute (JAERI-MRL)
4-24 Minato-machi, Mutsu
Aomori, 035-0064, Japan
Tel: +81 175 28 2614; Fax: +81 175 22 4213
Email: mrl@popsvr.tokai.jaeri.go.jp
Webpage in preparation

NUTA
Toshio Nakamura
Tandetron AMS Laboratory
Dating and Materials Research Center
Nagoya University
Chikusa, Nagoya 464-8602 Japan
Tel: +81 52 789 2578; Fax: +81 52 789 3095
Email: g44466a@nucc.cc.nagoya-u.ac.jp

**THE NETHERLANDS**

GrA
J. van der Plicht
Centre for Isotope Research
University of Groningen
Nijenborgh 4
NL-9747 AG Groningen, The Netherlands
Tel: +31 50 3634760; Fax: +31 50 3634738
Email: plicht@phys.rug.nl

UtC K. van der Borg
R. J. van de Graaff Laboratorium
Universiteit Utrecht
Princetonplein 5
P.O. Box 80.000
3508 TA Utrecht, The Netherlands
Tel: +31 30 53 2238 or +31 30 53 1492
Fax: +31 30 2532532; Email: k.vanderborg@fys.ruu.nl

**NEW ZEALAND**

NZA Rodger Sparks
Rafter Radiocarbon Laboratory
Institute of Geological and Nuclear Sciences, Ltd.
P.O. Box 31-312
Lower Hutt, New Zealand
Tel: +64 4 570 4671; Fax: +64 4 570 4657
Email: R.Sparks@gns.cri.nz
http://www.gns.cri.nz/atom/rafter/rafter.htm

**SWEDEN**

LuA Göran Skog
Radiocarbon Dating Laboratory
University of Lund
Tornavägen 13
SE-223 63 Lund, Sweden
Tel: +46 46 222 7885; Fax: +46 46 222 4830
Email: Goran.Skog@C14lab.lu.se

Ua Göran Possnert
Tandem Laboratory
University of Uppsala
Box 533
SE-751 21 Uppsala, Sweden
Tel: +46 18 4713059; Fax: +46 18 555736
Email: possnert@material.uu.se

**SWITZERLAND**

ETH Georges Bonani
ETH/AMS Facility
Institut für Teilchenphysik
Eidgenössische Technische Hochschule Hönggerberg
CH-8093 Zürich, Switzerland
Tel: +41 1 633 2041; Fax: +41 1 633 1067
Email: bonani@particle.phys.ethz.ch

**UNITED KINGDOM**

OxA R. E. M. Hedges / C. Bronk Ramsey
Oxford Radiocarbon Accelerator Unit
Research Laboratory for Archaeology and the History of Art
Oxford University
6 Keble Road
Oxford OX1 3QJ England
Tel: +44 1865 273939; Fax: +44 1865 273932
Email: orau@rlaha.ox.ac.uk
http://www.rlaha.ox.ac.uk

**UNITED STATES**

AA D. J. Donahue, P. E. Damon and A. J. T. Jull
NSF-Arizona AMS Facility
PO Box 210081
The University of Arizona
Tucson, Arizona 85721-0081 USA
Tel: +1 520 621 6810; Fax: +1 520 621 9619
Email: ams@physics.arizona.edu
http://www.physics.arizona.edu/ams

CAMS John Knezovich
Center for Accelerator Mass Spectrometry
Lawrence Livermore National Laboratory
P.O. Box 808, L-397
Livermore, California 94550 USA
Tel: +1 510 422 4520; Fax: +1 510 423 7884
Email: knezovich1@llnl.gov

NSRL Scott Lehman
INSTAAR Laboratory for AMS Radiocarbon Preparation and Research (NSRL)
CU-Boulder
1560 30th St.
Campus Box 450
Boulder, Colorado 80309-0450
Telephone: +1 303 492-0362 Fax: +1 303 492-6388
Email: Scott.Lehman@colorado.edu
http://www.Colorado.EDU/INSTAAR/RadiocarbonDatingLab

BETA M. A. Tamers and D. G. Hood
Beta Analytic, Inc.
Professional Radiocarbon Dating Services
4985 SW 74 Court
Miami, Florida 33155 USA
Tel: +1 305 667 5167; Fax: +1 305 663 0964
Email: beta@radiocarbon.com
http://www.radiocarbon.com/

BIOCAMS Ronald Hatfield and Darden Hood, directors
BIOCAMS International, Inc.
AMS for Art and Antiquities
13020 SW 120 Street
Miami, Florida 33186 USA
Tel: +1 305 992 3635; Fax: +1 305 631 3434
Email: director@biocams.com
http://www.biocams.com/

PL David Elmore
Purdue Rare Isotope Measurement Laboratory
Purdue University
1396 Physics Building
West Lafayette, Indiana 47907-1396 USA
Tel: +1 765 494 6516; Fax: +1 765 494 0706
Email: elmore@primelab.physics.purdue.edu
http://primelab.physics.purdue.edu

WHAMS John M. Hayes
National Ocean Sciences AMS Facility
Woods Hole Oceanographic Institution
McLean Laboratory, Mail Stop #8
Woods Hole, Massachusetts 02543-1539 USA
Tel: +1 508 289 2649; Fax: +1 508 457 2183
Email: shandwork@whoi.edu
http://nosams.whoi.edu

**LABORATORIES – CODE DESIGNATIONS***

| | | |
|---|---|---|
| A | Arizona | USA |
| AA | NSF-Ariz. AMS Facility | USA |
| AAR | University of Aarhus | Denmark |
| AC | Ingeis | Argentina |
| AECV | Alberta Environmental Center of Vegreville | Canada |
| AERIK* | Atomic Energy Res. Inst. | Korea |
| ALG* | Algiers | Algeria |
| ANL* | Argonne Nat. Lab., Ill. | USA |
| ANTW | Antwerp | Belgium |
| ANU | Australian National University | Australia |
| ANUA | ANU Accelerator | Australia |
| AU* | University of Alaska | USA |
| B | Bern | Switzerland |
| Ba | Bratislava | Slovakia |
| BC* | Brooklyn College | USA |
| Beta | Beta Analytic | USA |
| Birm | Birmingham | UK |
| Bln | Berlin | Germany |
| BM | British Museum | England |
| BONN* | Universität Bonn | Germany |
| BS | Birbal Sahni Institute | India |
| BSG | Brock University | Canada |
| C* | Chicago | USA |
| CAMS | Center for Accelerator Mass Spectrometry | USA |
| CAR* | Univ. College, Cardiff | Wales |
| CENA | Centro Energia Nuclear na Agricultura | Brazil |
| CG | Institute of Geology | China |
| CH | Chemistry Laboratory | India |
| CRCA | Cairo | Egypt |
| CSIC | Geochronology Lab, IQFR-CSIC, Madrid | Spain |
| CSM* | Cosmochemistry Lab. USSR Academy of Sciences | USSR |
| CT* | Caltech, Calif. Inst. Tech. | USA |
| CU | Charles University | Czech Republic |
| D* | Dublin, Trinity College | Ireland |
| Dak* | Univ. de Dakar | République du Sénégal |
| DAL* | Dalhousie University | Canada |
| DE* | USGS, Denver | USA |
| Deb | Debrecen | Hungary |
| DEM | NCSR Demokritos | Greece |
| DIC* | Dicar Corp and Dicarb Radioisotope Company | USA |
| DRI* | Desert Research Institute | USA |
| ENEA | ENEA, Bologna | Italy |
| ETH | ETH/AMS Facility | Switzerland |
| F | Florence | Italy |
| Fr | Freiberg | Germany |
| Fra | Frankfurt | Germany |
| FSU* | Florida State University | USA |
| FZ | Fortaleza | Brazil |
| G* | Göteborg | Sweden |
| GAK | Gakushuin University | Japan |
| Gd | Gliwice | Poland |
| GD* | Gdansk | Poland |
| Gif | Gif sur Yvette | France |
| Gif A | Gif sur Yvette and Orsay | France |
| GIN | Geological Institute | Russia |
| GL* | Geochronological Lab. | England |
| Gro* | Groningen | The Netherlands |
| GrN | Groningen | The Netherlands |
| GrA | Groningen AMS | The Netherlands |
| GSC | Geological Survey | Canada |
| GU | Scottish Universities Research & Reactor Centre (formerly Glasgow University) | Scotland |
| GX | Geochron Laboratories | USA |
| H* | Heidelberg | West Germany |
| HAM | Hamburg | Germany |
| HAR* | Harwell | England |
| Hd | Heidelberg | Germany |
| Hel | Helsinki | Finland |
| HIG* | Hawaii Inst. of Geophys. | USA |
| HL | Second Institute of Oceanography | China |
| HNS* | Hasleton-Nuclear, Palo Alto, California | USA |
| Hv | Hannover | Germany |
| I | Teledyne Isotopes | USA |
| IAEA | International Atomic Energy Agency | Austria |
| IAEA-MEL | Marine Environmental Laboratory | Monaco |
| ICEN | Instituto Tecnológico e Nuclear | Portugal |
| IEMAE | Institute of Evolutionary Morphology and Animal Ecology | Russia |
| IGAN | Institute of Geography | Russia |
| IGS* | Inst. of Geological Sci., | Sweden |
| II* | Isotopes, Inc., Palo Alto | USA |
| IOAN | Institute of Oceanography | Russia |
| IORAN | Institute of Oceanology | Russia |
| IRPA | Royal Institute of Cultural Heritage | Belgium |
| ISGS* | Illinois State Geological Survey | USA |
| IVAN | Institute of Volcanology | Ukraine |
| IVIC* | Caracas | Venezuela |
| IWP | Institute of Water Problems | Russia |

*Indicates laboratories that are closed, no longer measuring $^{14}C$, or operating under a different code designation.

| | | |
|---|---|---|
| J | Max-Planck-Institut für Biogeochemie, Jena | Germany |
| JGS | Geological Survey of Japan | Japan |
| JUBR | Biren Roy Research Laboratory | India |
| K | National Museum | Denmark |
| KAERI* | Korean Atomic Energy Research Institute | Korea |
| KCP | National Cultural Property Research Institute | Korea |
| KEEA | Kyushu Environmental Evaluation Association | Japan |
| KI | Kiel | Germany |
| KIA | Kiel AMS | Germany |
| Ki (KIEV) | Institute of Radio-Geochemistry of the Environment | Ukraine |
| KN | Köln | Germany |
| KR | Krakow | Poland |
| KRIL | Krasnoyarsk Institute | Russia |
| KSU | Kyoto Sangyo University | Japan |
| L* | Lamont-Doherty | USA |
| LAR | Liège State University | Belgium |
| LE | St. Petersburg | Russia |
| LIH | NCSR Demokritos | Greece |
| LJ* | Scripps (UCSD) La Jolla | USA |
| LOD | Lodz | Poland |
| LP | La Plata | Argentina |
| Lu | Lund | Sweden |
| LU | St. Petersburg State Univesity | Russia |
| Lv* | Louvain-la-Neuve | Belgium |
| Ly | University of Lyon | France |
| LZ | Umweltforschungs-zentrum Leipzig-Halle | Germany |
| M* | University of Michigan | USA |
| Ma* | University of Winnepeg | Canada |
| MAG | Quaternary Geology and Geochronology Laboratory | Russia |
| MC* | Centre Scientifique de Monaco | Monaco |
| METU | Middle East Technical University | Turkey |
| ML* | Miami | USA |
| Mo* | Verdanski Inst. of Geochemistry, Moscow | USSR |
| MOC* | Archaeological Institute, Czechoslovak Acad. of Sci. | Czechoslovakia |
| MP* | Magnolia Petroleum | USA |
| MRRI* | Marine Resources Research Institute | USA |
| MSU | Moscow | Russia |
| N | Nishina Memorial | Japan |
| NIST | National Institute of Standards and Technology | USA |
| NPL* | National Physical Laboratory, Middlesex | England |
| NS* | Nova Scotia Research Foundation | Canada |
| NSRL | INSTAAR – University of Colorado | USA |
| NSTF* | Nuclear Science and Technology Facility, State Univ. of New York | USA |
| NSW* | U. of New South Wales | Australia |
| NTU | National Taiwan University | Republic of China |
| NU | Nihon University | Japan |
| Ny* | Nancy, Centre de Recherches Radiogéologiques | France |
| NZ | New Zealand | New Zealand |
| NZA | New Zealand | New Zealand |
| O* | Humble Oil & Refining | USA |
| OBDY | ORSTOM Bondy | France |
| ORINS* | Oak Ridge Institute of Nuclear Studies | USA |
| OWU* | Ohio Wesleyan Univ. | USA |
| OX* | USDA Oxford, Mississippi | USA |
| OxA | Oxford Radiocarbon Accelerator Unit | England |
| P* | Univ. of Pennsylvania | USA |
| Pi* | Pisa | Italy |
| PI | Permafrost Institute | Russia |
| PIC* | Packard | USA |
| PITT* | University of Pittsburgh | USA |
| Pr* | Prague | Czechoslovakia |
| PSU* | Pennsylvania State Univ. | USA |
| PKU | Peking University | China |
| PL | Purdue Rare Isotope Measurement Laboratory | USA |
| PRL | Physical Research Laboratory | India |
| Pta | Pretoria | South Africa |
| Q | Cambridge | England |
| QL* | Quaternary Isotope Laboratory | USA |
| QC* | Queens College | USA |
| QU* | Centre de Recherches Minérales, Québec | Canada |
| R | Rome | Italy |
| RCD | Radiocarbon Dating | England |
| RI* | Radiochemistry, Inc. | USA |
| RIDDL* | Simon Fraser Univ. | Canada |
| Riga | Institute of Science | Latvia |
| RL* | Radiocarbon, Ltd. | USA |
| Rome | Department of Earth Sciences, Rome | Italy |
| RT | Rehovot | Israel |
| RU* | Rice University | USA |
| S* | Saskatchewan | Canada |
| Sa* | Saclay, Gif-sur-Yvette | France |

| | | |
|---|---|---|
| Sac | Instituto Tecnológico e Nuclear | Portugal |
| SFU* | Simon Fraser Univ. | Canada |
| Sh* | Shell Development Co. | USA |
| SI* | Smithsonian Institution | USA |
| SL* | Sharp Laboratories | USA |
| SM* | Mobil Oil Corp., Dallas (formerly Magnolia & Socony Mobil Oil) | USA |
| SMU* | Southern Methodist Univ. | USA |
| SNU | Seoul National Univ. | Korea |
| SOAN | Institute of Geology and Geophysics | Russia |
| SR* | Salisbury, Rhodesia | Rhodesia |
| SRR | NERC Radiocarbon Laboratory | Scotland |
| St* | Stockholm | Sweden |
| Su | Finland | Finland |
| SUA | Sydney University | Australia |
| SWA | Swansea | Wales |
| T | Trondheim | Norway |
| TA | Tartu | Estonia |
| TAM* | Texas A & M University | USA |
| TB | Tblisi | Georgia |
| TBNC* | Kaman Instruments (formerly Texas-Bio-Nuclear) | USA |
| TEM* | Temple University | USA |
| TF* | Tata Institute of Fundamental Research | India |
| TK | University of Tokyo | Japan |
| TKU | Turku | Finland |
| Tln | Tallinn | Estonia |
| TO | IsoTrace Laboratory | Canada |
| TUNC* | Tehran University Nuclear Centre | Iran |
| Tx* | Texas | USA |
| U | Uppsala | Sweden |
| Ua | Uppsala AMS | Sweden |
| UB | Belfast | Northern Ireland |
| UBAR | University of Barcelona | Spain |
| UCD | University College, Dublin | Ireland |
| UCI | University of California, Irvine | USA |
| UCLA | University of California, Los Angeles | USA |
| UCR | University of California, Riverside | USA |
| UD | Udine | Italy |
| UGa | University of Georgia | USA |
| UGRA | University of Granada | Spain |
| UM* | University of Miami | USA |
| UQ | University of Quebec at Montreal | Canada |
| URCRM | Ukrainian Research Ctr. for Radiation Medicine | Ukraine |
| URU | University of Uruguay | Uruguay |
| USGS* | USGS, Menlo Park | USA |
| UtC | Utrecht van de Graaff Laboratorium | The Netherlands |
| UW* | University of Washington | USA |
| V* | Melbourne, Victoria | Australia |
| VRI | Vienna Radium Institute | Austria |
| W* | USGS, National Center | USA |
| WAT | University of Waterloo | Canada |
| WHAMS | National Ocean Sciences AMS Facility | USA |
| WIS | Wisconsin | USA |
| Wk | University of Waikato | New Zealand |
| WRD* | USGS Washington, D.C. Water Resources Division | USA |
| WSU* | Washington State Univ. | USA |
| XLLQ | Xian Laboratory of Loess and Quaternary Geology | China |
| X* | Whitworth College | USA |
| Y* | Yale University | USA |
| Ya* | Yale University | USA |
| Z | Zagreb | Croatia |

# AUTHOR INDEX
# VOLUME 42, 2000

## SUBJECT INDEX
## VOLUME 42, 2000

**14C** ***RADIOCARBON***

# $5 Back Issues Clearance Sale

**We found hundreds of copies in an old shed! Priced to move.**

| YEAR | VOL. | Write in the number of copies desired for each issue | | | | | |
|---|---|---|---|---|---|---|---|
| | | NR 1 | NR 2 | NR 2A | NR 2B | NR 3 | NR 4 |
| 1980 | 22 | | | | | | |
| 1981 | 23 | | | | | | |
| 1982 | 24 | | | | | | |
| 1983 | 25 | | | | | | |
| 1984 | 26 | | | | | | |
| 1985 | 27 | | | | | | |
| 1986 | 28 | | | | | | |
| 1987 | 29 | | | | | | |
| 1988 | 30 | | | | | | |
| 1989 | 31 | | | | | | |
| 1990 | 32 | | | | | | |
| 1991 | 33 | | | | | | |
| 1992 | 34 | | | | | | |

### Calculate Payment

____ copies × $5 ea. = $________

**Subtotal:** $________

**Shipping via surface mail:**
(Contact us for other shipping methods)
Add $2 ea. book for US
Add $3 ea. book outside US

___ copies × $____ea. = $________

**Shipping total:** $________

**Total due:** $________

## Payment & Shipping Address

❑ MasterCard ❑ Visa
❑ Check enclosed ❑ Please bill me

Name:

Address:

Fax: E-mail:

**For Credit-Card Orders**

Card number: Expiration date:

Signature: Phone:

**For online Contents see:** `http://www.radiocarbon.org/Pubs/contents.html`

**Prices good while supplies last. Mail or fax this form to:**

RADIOCARBON, 4717 East Fort Lowell Road, Room 104, Tucson, Arizona 85712-1201 USA
Phone: +1 520 881-0857; Fax: +1 520 881-0554; orders@radiocarbon.org

# LSC 2001

## International Conference on Advances in Liquid Scintillation Spectrometry

7–11 May 2001, Karlsruhe, Germany

**LSC 2001** continues the series of conferences most recently held in Gatlinburg, Tennessee, USA in 1989, Vienna, Austria in 1992, and Glasgow, Scotland in 1994.

Liquid scintillation, with its recent developments in low-level counting and $\alpha/\beta$-discrimination, has become a key technique in radiation counting and $\beta$-spectrometry. This conference will provide a forum for radioanalysts to discuss their most recent findings and future work, either as oral lectures including both invited and contributed papers, or as posters. Poster authors will have the opportunity to give a short presentation before each poster session. The conference will be held in English.

The conference site will be Karlsruhe, Germany, a beautiful historical city at the northern edge of the legendary Black Forest, near the city of Heidelberg with its famous castle and the lovely Neckar valley. Sightseeing tours will be offered to participants and accompanying persons.

The conference fee will be approximately US$ 400 for active participants. This includes a welcome reception, coffee during session breaks, excursion fees (Heidelberg, boat tour on the Neckar river), the conference dinner, and snacks during poster sessions. A reduction for students is foreseen. To receive the next circular, please register on our website.

### Call for Papers

One-page (A4) abstracts were due by 1 October 2000. See our website for more information.

### Conference Topics

- New Instrumentation
- Environmental Applications and Analysis
- Bioscience Applications and Medicine
- Health Physics Applications
- Natural Radioactivity with Special Emphasis on Radon
- Alpha Counting
- Cerenkov and Luminescence Counting
- Sample Preparation and Cocktails
- Other Scintillation Techniques

(The list of topics is certainly not exhaustive and is for informative purpose only.)

### Conference Website

`http://www.ftu.fzk.de/lsc2001/`

### Conference Secretariat

Siegurd Möbius
Forschungszentrum Karlsruhe GmbH
FTU
Postfach 3640
D-76021 Karlsruhe, Germany

Tel: +49 7247 823791
Fax: +49 7247 824857
E-mail: LSC2001@ftu.fzk.de